National University of Science and Technology
POLITEHNICA Bucharest

Faculty of Industrial Engineering and Robotics

Journal of Industrial Engineering and Robotics

2024, Volume 8, Issue 3

BUILDING AN EDUCATIONAL ENTERTAINMENT ROBOT FOR PREUNIVERSITY ACTIVITIES VIA ADDITIVE MANUFACTURING

ȘELARU Carmen-Cristina-Ioana[1], HANGA Mihail[2] and CAZACU Carmen-Cristiana[3]

[1]Faculty: Industrial Engineering and Robotics, Robotics Specialization, Year of study: II, e-mail: selaru.carmen.ioana@gmail.com
[2]Faculty: Industrial Engineering and Robotics, Applied Informatics in Industrial Engineering Specialization,
[3]Faculty: Industrial Engineering and Robotics, Department: Robots and Production Systems

ABSTRACT: This article aims to present a robot in an industry that is still developing, a robot made through additive manufacturing, whose role is to influence children from the pre-university environment. The robot is an international symbol, present in the First tech challenge competition, a launching pad for the STEAM community and for all those who want to pursue a career in this field.

KEYWORDS: STEAM, First Tech Challenge, Entertainment robot, 3D printing, Axon Programming

1. Introduction

Entertainment can be defined as an activity or performance that aims to amuse, entertain, or relax, or anything that produces pleasure, satisfaction, or joy. Watching a movie or show, listening to music, reading a book or magazine, playing a game, attending a sporting or cultural event, and spending time with friends or family are all forms of common entertainment that all people need due to the benefits they offer. The impact of entertainment is another very important topic to discuss as entertainment can have a positive impact on mental and physical health, reduce stress, anxiety and depression, increase creativity and happiness, or improve social relationships and a sense of belonging.

A robot is a programmable machine that can imitate human actions or operate autonomously in a predefined environment. There are several important points to highlight in the definition of a robot:

1. *Programmable machine* - Robots are not living entities with their own intelligence. They are machines controlled by software programs that dictate their behaviour. These programs can be simple or complex, depending on the capabilities of the robot.
2. *Imitation of human actions* - Some robots are humanoid, meaning they resemble humans in appearance and movement. They can perform tasks similar to humans, such as walking, manipulating objects, or even interacting with the surrounding environment.
3. *Autonomous operation* - Not all robots are remote controlled by humans. Some robots can operate autonomously, which means they can make their own decisions within the limits of their programming. They use sensors to perceive their surroundings and take action based on the information received.
4. *Different purposes*- it can be used for a variety of purposes, including:
   - *Industrial work* - it can perform repetitive and dangerous work in factories.
   - *Space exploration* - it can be sent into space to explore planets and other celestial bodies.
   - *Medical surgery* - it can assist surgeons in performing delicate operations.
   - *Household activities* - it can be used for cleaning, mowing the lawn, or other household chores.

Entertainment Robots

Robots can be used for entertainment purposes, such as playing games or participating in shows.

Entertainment robots are a special category of robots whose main purpose is to entertain, amuse, and captivate the audience. Unlike industrial or medical robots, which have specific functional purposes, entertainment robots rely on creative interactions, captivating performances, and unique experiences to create memorable moments.

Defining characteristics of entertainment robots:

- *Artistic abilities:* Entertainment robots can dance, sing, play music, paint, sculpt, or even write. They can be programmed with a wide range of artistic skills to deliver stunning and interactive performances.
- *Audience interaction:* Entertainment robots can interact with the audience in real time, creating a personalized and engaging experience. They can recognize gestures, voices, and facial expressions, adapting their behaviour to the reactions of the spectators.
- *Humour and comedy:* Some entertainment robots can be programmed with a fine sense of humour or even stand-up comedy skills. They can tell jokes, anecdotes, and funny stories to make the audience laugh.
- *Captivating personality:* Entertainment robots can have unique and memorable personalities, designed to connect with the audience on an emotional level. They can be friendly, funny, serious, or even eccentric, depending on the context of the performance.
- *Advanced technology:* Entertainment robots use a wide range of advanced technologies, including artificial intelligence, advanced robotics, sophisticated sensors, and 3D animation systems. This combination of technologies allows them to perform fluid movements, realistic facial expressions, and complex interactions with the audience.

Benefits and Importance

The use of entertainment robots in educational activities within pre-university settings offers a multitude of significant benefits for students, teachers, and the education system as a whole. Here are some compelling reasons why their implementation is crucial:

1. *Stimulates Interest and Motivation:* Entertainment robots can serve as captivating tools that spark students' curiosity in various fields, including science, technology, engineering, art, and mathematics (STEAM). Their playful and interactive nature can motivate students to explore complex concepts and actively engage in the learning process.
2. *Facilitates Personalized Learning:* Entertainment robots can be tailored to the individual needs of each student, providing a personalized and flexible learning environment. Students can progress at their own pace, receiving individualized feedback and tailored support.
3. *Promotes Inclusion:* Robots can be employed to create a more inclusive learning environment, offering equal opportunities for participation for all students, regardless of their abilities or disabilities.
4. *Ensures an Engaging Learning Experience:* Entertainment robots can make learning more fun and engaging, transforming lessons into interactive and memorable experiences. Students will enjoy the learning process and be more likely to retain information.
5. *Develops Social and Emotional Skills:* Interacting with robots can help students develop their social and emotional skills, such as empathy, compassion, and responsibility. It can also teach them to manage difficult emotions and resolve conflicts.
6. *Nurtures Creativity and Imagination:* Robots can be used as tools to explore new ideas, create original projects, and develop innovative solutions. Students can unleash their imaginations and experiment with different possibilities in a safe and fun environment.
7. *Prepares Students for STEAM Careers:* Students exposed to STEAM concepts at an early age can develop a passion for these fields and acquire the necessary skills to pursue successful careers in robotics or technology in general. Integrating arts into the STEAM curriculum helps students approach problems with creativity and innovation, essential skills for the 21st-century workforce.

2. PLOWIE the Robot

Plowie has been a symbol of the FIRST Tech Challenge (FTC) competition since 2008 when it first appeared in the opening animation for the new season, introducing the game theme and exemplifying the tasks required to score points and penalties for behaviour that contradicts the core idea of the international competition.

The FTC competition offers an immense opportunity to all young people around the world through the annual challenge of building a robot capable of fulfilling a set of objectives without breaking the established rules. Everyone involved in the competition develops a wonderful list of skills in the STEAM field.

3. Robot Design

The model is a public resource that can be easily found in the Onshape program. The 3D model is presented in fig. 1 (a, b).

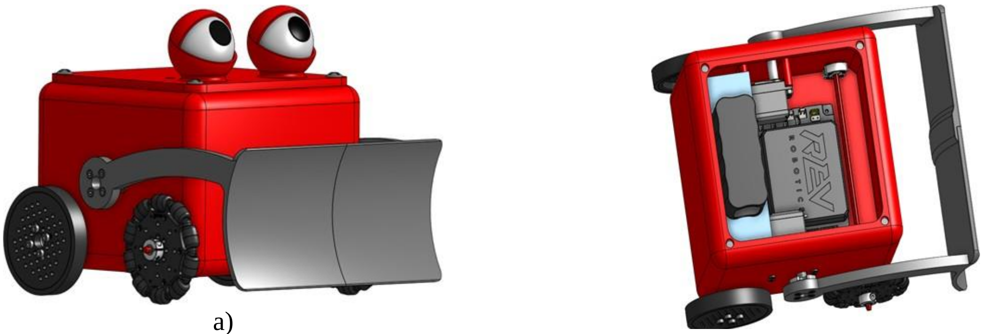

a) b)

Fig. 1. The 3D model

4. PLOWIE the Robot: Technical Details

PLOWIE is a versatile robot capable of a variety of movements and actions, including walking, rotating, moving its bucket, and even moving its eyes. These capabilities make it well-suited for the challenges of the FIRST Tech Challenge competition.

Adaptations and Improvements

The PLOWIE robot design has undergone several adaptations and improvements to enhance its functionality and performance. These modifications include:

1. *Battery Holder:* A two-part battery holder has been implemented to facilitate easier manipulation within the robot's main frame (Figure 2, a). This design allows for quick and convenient battery changes during competitions.
2. *Omni Wheel Alignment Axis:* An alignment axis has been introduced to ensure precise alignment of the front omni wheels (Figure 2, b). This alignment is crucial for smooth and stable movement of the robot.
3. *Synchronized Eye Movement Mechanism:* A synchronized eye movement mechanism has been developed to control the movement of both eyes simultaneously (Figure 3). This mechanism utilizes a guide and a servo motor to achieve precise and coordinated eye movements.

a) b)

Fig. 2. Parts 3D design

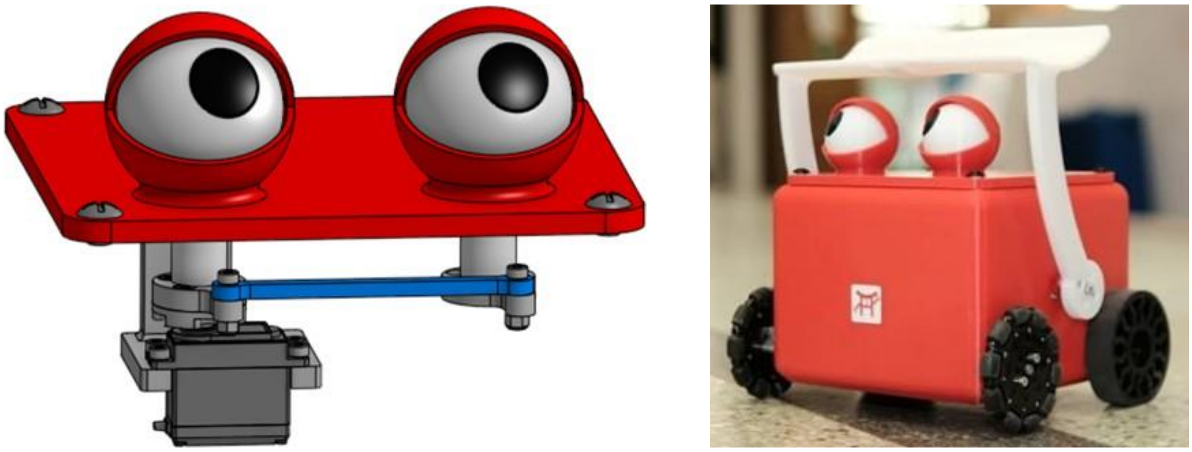

a) b)

Fig. 3. Synchronized Eye Movement Mechanism(3)

Printing Parameters

The PLOWIE robot can be printed using both PLA+ and PETG filaments. The recommended printing parameters for each material are as follows:

PLA+ Printing Parameters:

- Nozzle Temperature: 210°C
- Nozzle size: 0.4 mm
- Bed Temperature: 60°C
- Print Speed: 100 mm/s
- Retraction Distance: 0.5 mm
- Cooling Fan Speed: 100%

PETG Printing Parameters:

- Nozzle Temperature: 245°C
- Nozzle size: 0.4 mm
- Bed Temperature: 90°C
- Print Speed: 100 mm/s
- Retraction Distance: 0.5 mm
- Cooling Fan Speed: 70%

These parameters serve as a starting point for achieving high-quality prints. Adjustments may be necessary depending on the specific printer and filament being used.

5. Programming PLOWIE the Robot: Control and Communication

The PLOWIE robot's movements and actions are controlled by a combination of hardware and software components. The hardware consists of five Axon MAX servo motors, each responsible for a specific function:

- *Wheels:* Two servo motors control the rotation of the front and rear wheels, enabling the robot to move forward, backward, and turn.
- *Bucket:* Two servo motors control the tilting and emptying of the bucket, allowing the robot to manipulate objects and perform various tasks.
- *Eyes:* One servo motor controls the movement of the robot's eyes, adding a playful and expressive element.

The software component responsible for controlling these servo motors is a Java program developed using a specialized servo programmer. This program communicates with the Control Hub, the robot's "brain," provided by REV Robotics. The Control Hub (figure 4, a) features an embedded Android system and a network card (figure 4, b) that creates its own Wi-Fi network, enabling connection from another device (1, 2).

a) b)

Fig. 4. The Control Hub

The program assigns specific ports to each servo motor:

- **Ports 0 and 5:** Control the wheels
- **Ports 1 and 4:** Control the bucket
- **Port 3:** Controls the eyes

All servo motors are programmed to operate in a continuous rotation mode with a range of 360 degrees. The movement of the bucket is calculated based on the sum of values to ensure optimal power distribution and prevent overloading the servo motors. The wheels are set to operate at 90% of the Axon Max servo motor's total power, while the eye movements are limited to 35%. All control parameters are visible in Figure 5.

Fig. 5. Control Parameters

6. The current state

Plowie is completely printed, assembled and programmed, he has already participated in numerous activities in a pre-university environment, where he caught the eyes of fascinated children.

7. Conclusion: Robots and the Future of Entertainment and Education

The world of entertainment is on the verge of transformation, and robots are poised to play a pivotal role in this revolution. Entertainment robots, with their captivating abilities and interactive nature, are set to redefine the way we experience entertainment, making it more engaging, immersive, and personalized.

In the realm of pre-university education, robots offer a transformative approach to learning, fostering interest in STEAM fields and preparing students for future careers in technology and innovation. Educational activities involving entertainment robots can spark curiosity, promote active participation, and enhance the learning process, making it more enjoyable and effective.

PLOWIE the Robot, a well-known symbol in the FIRST Tech Challenge competitions, serves as an exemplary model for encouraging new generations of children to explore the world of robotics and STEM. With its versatility and engaging features, PLOWIE demonstrates the potential of robots to inspire and educate young minds.

As we look towards the future, further advancements in robotics technology will undoubtedly lead to even more sophisticated and immersive entertainment experiences. Potential improvements for PLOWIE the Robot include enhancing its mobility with better rear wheels for smoother movement, adding LED lights for a more captivating appearance, and incorporating an LCD screen for its mouth to express emotions and enhance communication.

The convergence of entertainment and education through robots holds immense promise for shaping the future, igniting imaginations, and nurturing the next generation of innovators and problem solvers.

8. Bibliography

[1]https://www.google.com/url?sa=i&url=https%3A%2F%2Faxon-robotics.com%2Fproducts%2Faxon-servo-pr ogrammer&psig=AOvVaw3DdNly_cgsDJNVgmDzr0C-&ust=1715191915987000&source=images&cd=vfe&opi=89978449&ved=0CBIQjRxqFwoTCIi01PiR_IUDFQAAAAAdAAAAABAE (accessed on 05-03-2024)
[2]https://ftc-docs.firstinspires.org/en/latest/control_hard_compon/rc_components/hub/ports/ch-ports.html (accessed on 05-07-2024)
[3]https://www.instagram.com/p/C55-y8uqBJO/?utm_source=ig_web_copy_link&igsh=MzRlODBiNWFlZA== (accessed on 05-08-2024)

DESIGNING A ROBOT FOR DISTRIBUTING ADVERTISING MATERIALS USING ADDITIVE MANUFACTURING

CULA Ștefan[1], BURGHIU Liviu-Mihai[2], CAZACU Carmen-Cristiana[3]
[1]Faculty: Industrial Engineering and Robotics, Robotics Specialization, Year of study: IV, e-mail: stefanncula@gmail.com
[2]Faculty: Mechanical Engineering and Mechatronics, Year of study: III
[3]Faculty: Industrial Engineering and Robotics, Department: Robots and Production Systems

ABSTRACT: This project focuses on developing a robot equipped with an oscillating arm and a specialised end-effector for handling and delivering advertising leaflets. By designing a modular system, we aimed to enhance the robot's flexibility and adaptability across various environments and use cases. The development of the oscillating arm involved optimising the design for efficiency and precision in manipulation tasks. Performance evaluation was conducted to validate the robot's capability to deliver leaflets accurately, swiftly, and reliably, thus meeting the project's objectives. This integrated approach resulted in a robust and versatile robotic system tailored to the specific needs of advertising material distribution.

KEYWORDS: Additive Manufacturing, Mobile Robot, Modular System

1. Introduction

This project focuses on developing a practical robot for distributing advertising materials, specifically designed for use in our academic environment. While not aiming for groundbreaking innovation, our goal is to create a functional solution using a modular design approach. The robot features an oscillating arm and a specialised end-effector for leaflet handling. Through performance evaluations, we aim to ensure its reliability and accuracy for leaflet delivery tasks.

2. Current Stage

The robot prototype, designed for efficient leaflet distribution within our academic environment, is now complete. The next crucial step involves rigorous performance testing to evaluate its reliability and accuracy in delivering leaflets throughout various designated locations.

Fig. 1. Final model of the robot

3. Design

Modular Aluminum Construction (Tetrix): Tetrix aluminium channels, known for their modularity and ease of assembly.

Quadrupedal Drive Train (4x Motors): four high torque (60:1 gear ratio) Torquenado motors, providing powerful and efficient traction.

Omnidirectional Mobility: implementation of two omni wheels, enabling the robot to travel laterally in addition to forward and backward movements.

Traction Wheels: two traction wheels providing grip and stability during manoeuvres.

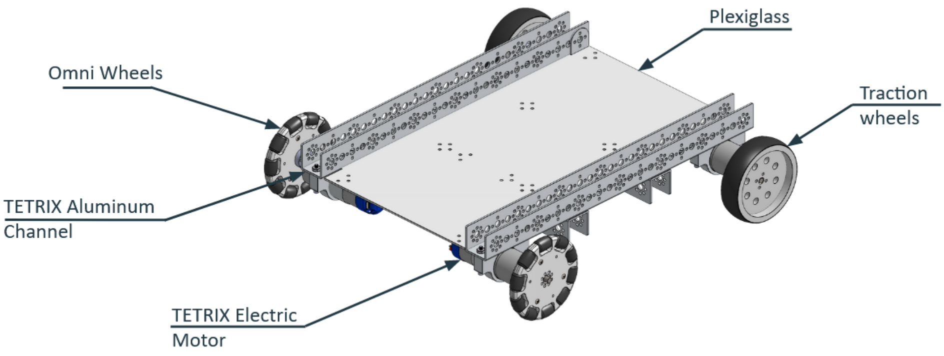

Fig. 2. Chassis overview

Oscillating Arm Design: an arm that rotates back and forth.

Bevel Gear Drive: bevel gears and a high torque motor for precise and powerful arm movement.

Modular Construction: implemented a modular design that in the future can bring attachments of additional components

Rigid Intermediate Plate: a rigid intermediate plate where the motor is fixed, providing stability and support for the entire mechanism.

Plastic Cover (Optional): the plastic cover serves a specific purpose (e.g., protecting the gears or enhancing aesthetics)

Motion Range: approximative 90 degrees of movement

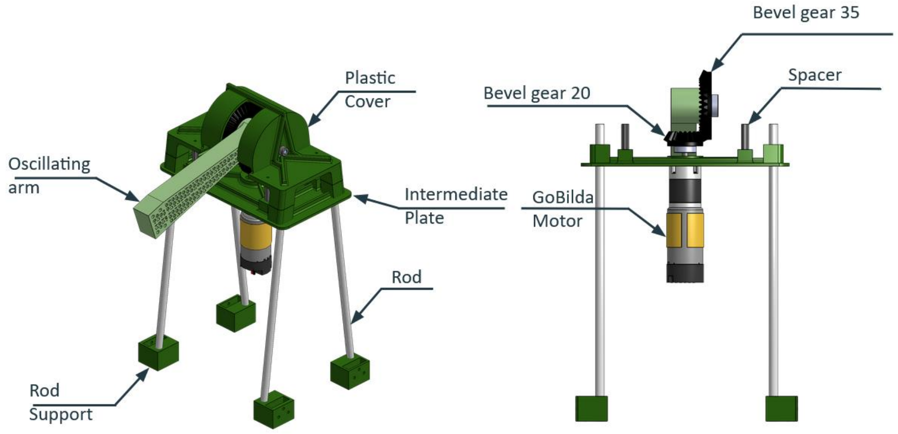

Fig. 3. Oscillating arm turret overview

Servo-Driven Leaflet Gripper: This emphasises the functionality, mentions the servo as the driving force, and highlights the efficiency of the design.

Dual Gear Covers for Protection: This mentions the gear covers and their purpose of protecting the gears.

Herringbone Gear Transmission: Using herringbone gears for their high driving force, the advantage of using herringbone gears they reduce the axial thrust on the shaft compared to helical gears.

Quad-Wheel Gripping Mechanism: The leaflet-grasping mechanism comprises four wheels: two front wheels made of Thermoplastic Polyurethane (TPU) for rigidity, and two rear wheels made of corn starch with silicone cast in a Polylactic Acid (PLA) mould for flexibility.

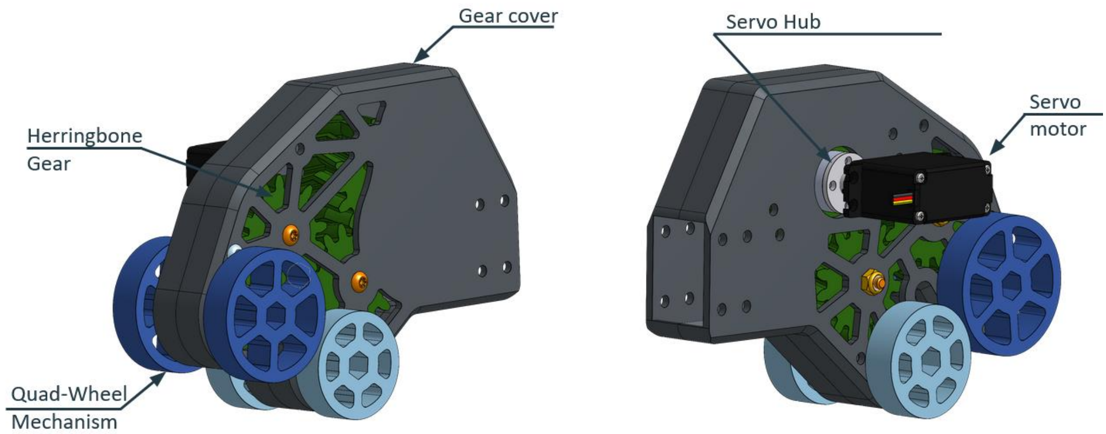

Fig. 4. Gripping mechanism

The leaflet holder is specifically tailored to accommodate A5 leaflets securely, ensuring they are effectively presented during distribution tasks. The optional adapter for ⅓ of A4 size leaflets adds versatility, allowing the robot to handle different promotional materials as needed. Its design includes a base that can be quickly removed for maintenance or replacement, streamlining operational efficiency. The incorporation of a back support not only enhances stability during transport but also reinforces the holder's overall durability, contributing to long-term reliability during usage.

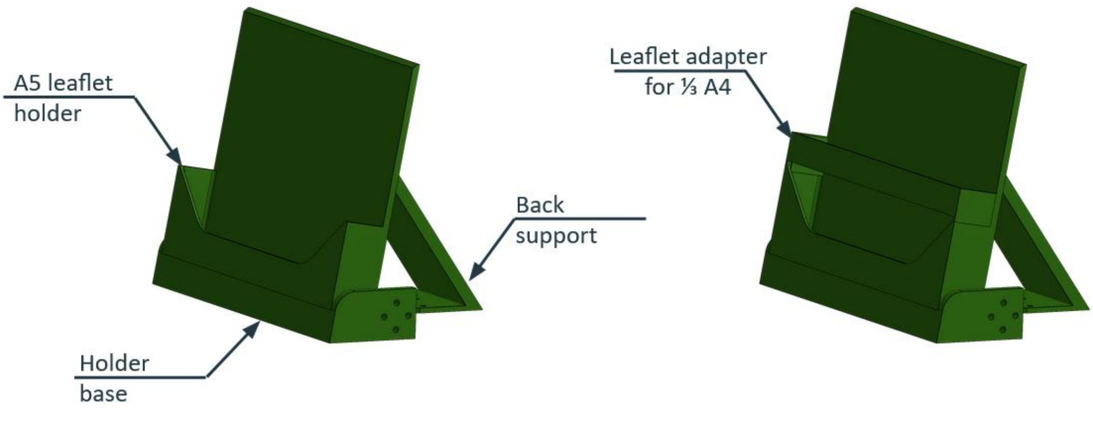

Fig. 5. Leaflet holder and adapter

The chassis aesthetics include four side panels that cover the aluminium channels, designed to attract attention and encourage people to take leaflets. The arm turret features three side panels displaying the faculty logo, the modelling program used, and the team's symbol that built it. Additionally, there is a back door for easy access to the electrical components, battery, and wiring.

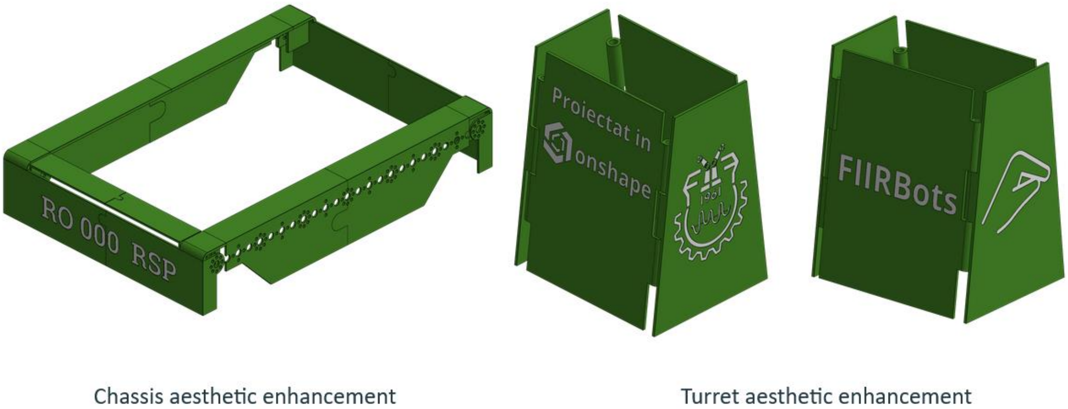

Fig. 6. Aesthetic improvements

Fig.7 Overview of the robot in real life

4. Manufacturing properties of 3D printed parts

For parts that are used in a mechanical way, we printed them in PETG using its properties for having a better material strength and higher elasticity. PETG offers excellent material strength, ensuring durability and resistance to deformation, while its higher elasticity allows the parts to flex without breaking, absorbing mechanical stress effectively. Additionally, PETG's chemical resistance makes it suitable for applications where exposure to solvents or other corrosive substances is expected.

- PETG printing properties: Layer height: 0.2 mm; Nozzle size: 0.4 mm @ 245°C

Bed temperature: 90°C; Max print speed: 180 mm/s ; Max acceleration: 2500 mm/s^2

Most of the decorative parts used PLA/PLA+ for printing faster and being easy to print material. PLA and PLA+ are known for their ease of printing, requiring lower printing temperatures and less specialised equipment, simplifying the printing process and reducing the likelihood of printing errors. Their faster print speeds make them ideal for rapid prototyping or large-scale manufacturing, ensuring efficiency in production.

- PLA/PLA+ printing properties: Layer height: 0.2 mm; Nozzle size: 0.4 mm @ 210°C;

Bed temperature: 60°C; Max print speed: 200 mm/s; Max acceleration: 1500 mm/s^2

For other parts that needed strength but didn’t use them in mechanical parts, we used PLA Tough. PLA Tough is engineered to offer higher impact resistance and durability compared to standard PLA, striking a balance between strength and flexibility. This choice ensures that the parts maintain toughness without sacrificing too much on flexibility, ensuring reliable performance even under stress or impact.

- PLA Tough printing properties: Layer height: 0.2 mm; Nozzle size: 0.4 mm @ 215°C;

Bed temperature: 60°C; Max print speed: 200 mm/s; Max acceleration: 1500 mm/s^2

For mechanical parts requiring flexibility and impact resistance, TPU can be a suitable choice due to its elastomeric properties. Its ability to flex without breaking makes it ideal for components subjected to repetitive stress or shock loads. Printing with TPU allows for the creation of parts that can absorb mechanical energy, reducing the risk of damage or failure.

- TPU 95A printing properties: Layer height: 0.2 mm; Nozzle size: 0.4 mm @ 235°C;

Bed temperature: 60°C; Max print speed: 100 mm/s; Max acceleration: 1000 mm/s^2

For the leaflet gripper wheels, we used 4 wheels printed in TPU95A, and 2 wheels had a cornstarch-combined silicone layer, forming a mould.

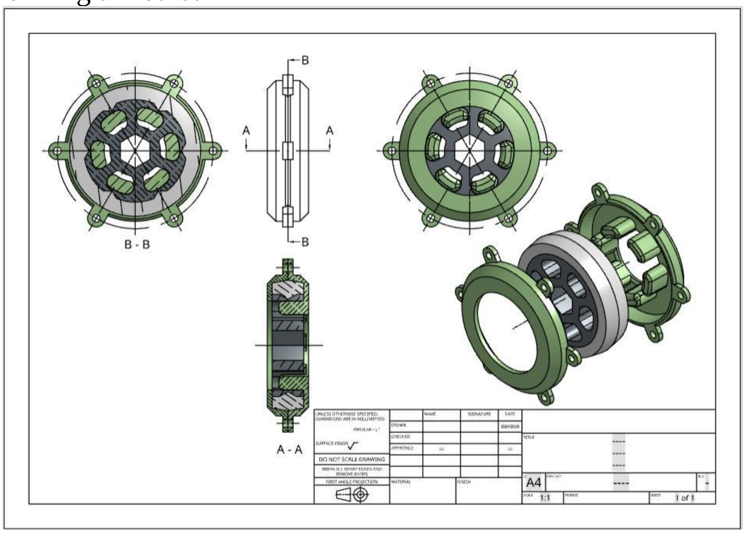

Fig. 8 Wheel mould

5. Design validation

Motor sizing calculations were carried out to guarantee the consistent and uninterrupted rotation of the oscillating arm. These calculations involved assessing key factors such as the mass and centre of mass of both the end effector and the arm, in relation to the bevel gears. By multiplying these masses by the gear ratio and applying a safety factor of 1.2, we determined the torque requirement for the motor. This thorough analysis ensured that the selected motor had sufficient power to drive the oscillating arm smoothly and reliably under various operational conditions, thereby optimising the performance and longevity of the robotic system.

$$(m_{effector} * g * l_{arm} + m_{arm} * g * \frac{l_{arm}}{2}) * \frac{7}{4} * 1.2 < J_{motor} \quad (1)$$

Where $m_{effector}$ is approximately 500 g (determined from Onshape mass calculator), m_{arm} is 109 g (determined from Onshape mass calculator), l_{arm} is 200 mm (determined from Onshape mass calculator), g is 9.81 m/s^2 and J_{motor} is 133.2 kg·cm (from Gobilda motor data sheet)

$$(500g * 9.81\frac{m}{s^2} * 200mm + 109g * 9.81\frac{m}{s^2} * \frac{200mm}{2}) * \frac{7}{4} * 1.2 < 133.2kg \cdot cm \quad (2)$$

$$2.2656\ Nm < 13.062Nm \quad (3)$$

The motor is sufficient, albeit oversized. Due to component availability, there wasn’t another option to use a motor that would strictly meet the requirements for oscillating the arm, considering the possible speed of the arm, ensuring it remains slow.

Finite Element Analysis (FEA) was conducted to validate the arm of the robot's ability to withstand the weight of the end effector assembly. A force of 6.672 N is applied to the tip of the arm, while the other end is treated as a fixed support due to its attachment to the bevel gear.

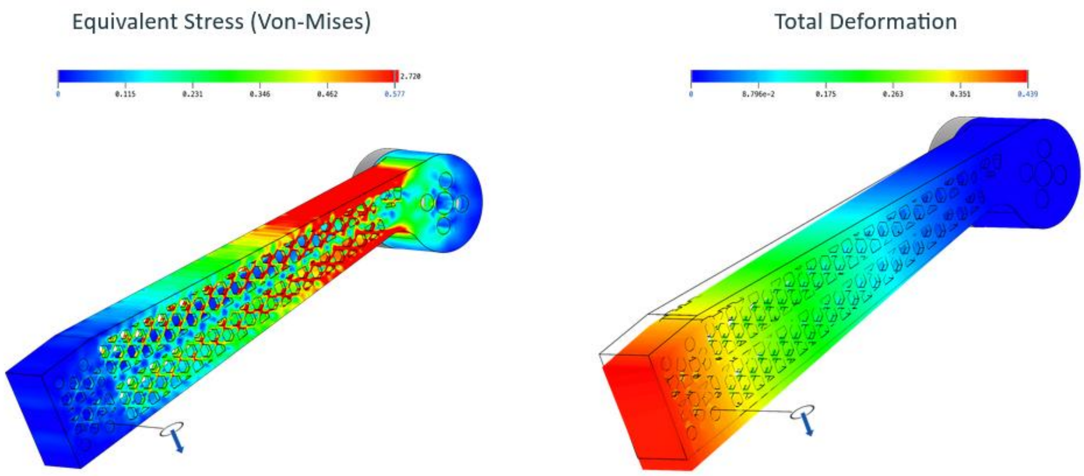

Fig. 9. Equivalent Stress and Total Stress

The analysis indicates a maximum stress of 2.72 MPa at the arm's base, well within safe operational limits for this application. Furthermore, the maximum deformation of 0.439 mm at the arm's tip falls within acceptable parameters given the material properties and operating conditions. Therefore, the conclusion drawn is that the arm can withstand the applied loads effectively.

6. Functionality

The main movement capabilities of the robot encompass both translational and rotational motions, providing versatility in its operational capabilities. The forward and backward translation motions are facilitated by the chassis motors, enabling the robot to navigate various environments. Additionally, the rotational movements around the midpoint of the rear part of the robot enhance its manoeuvrability, allowing it to pivot and align for precise positioning during leaflet distribution tasks. This combined movement system ensures efficient and effective performance, contributing to the robot's overall functionality in advertising material distribution scenarios.

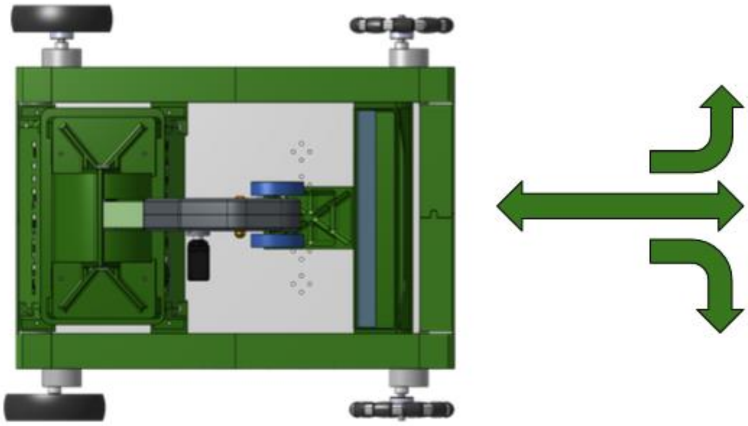

Fig. 10. Movement of the robot

The movement of the oscillating arm is achieved by operating the turret motor with the help of a bevel gear set with a power ratio of 4:7.

The movement of the wheels on the end-effector occurs at the arm's limit points, enabling an intake motion to grasp the leaflet, followed by an outtake motion to release the leaflet.

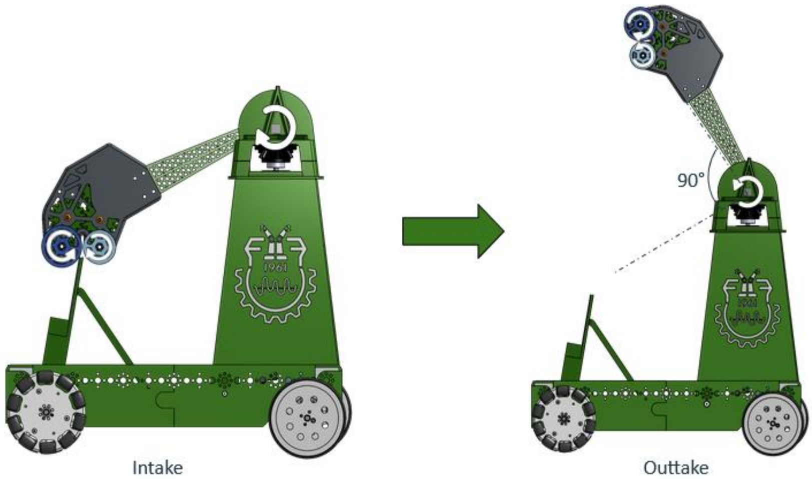

Fig. 11. Movement of the arm and end-effector

7. Conclusions

In conclusion, the developed robot for distributing advertising materials integrates various key features and design elements to fulfil its intended functions effectively. The use of additive manufacturing techniques allowed for the creation of custom components such as the leaflet holder and arm mechanisms. The modular design approach ensures flexibility and ease of maintenance, while the incorporation of herringbone gears and finite element analysis ensures robustness and reliability in operation. The analysis results confirm that the robot can withstand applied loads and perform its tasks within safe operational limits. Overall, the combination of mechanical design, material selection, and functional testing demonstrates a successful integration of engineering principles to create a functional and efficient advertising material distribution robot.

8. Future plans

Looking ahead, there are exciting prospects for the advertising material distribution robot:

- Enhanced Automation: Integrating advanced sensors and machine learning can enable autonomous navigation and adaptive advertising strategies.
- Multi-Purpose Functionality: Expanding capabilities beyond leaflet distribution to include interactive customer engagement can increase the robot's utility.
- Environmental Sustainability: Using sustainable materials and energy-efficient designs can align with eco-friendly initiatives.
- Modular Upgrades: Designing with modular components allows for easy upgrades and customization for different campaigns.
- Collaborative Robotics: Exploring human-robot collaboration can combine automation with human creativity.

9. Bibliography

[1]"Onshape Learning Center," *learn.onshape.com*. https://learn.onshape.com/

[2]"REV DUO | Documentation," *Revrobotics.com*, Jan. 04, 2024. https://docs.revrobotics.com/docs/rev-duo

[3]"REPREZENTAREA ȘI COTAREA ROȚILOR DINȚATE ȘI ANGRENAJELOR." Available: https://desen.utcluj.ro/curs/roti%20dintate%20+%20angrenaje.pdf

[4]"Shop Pitsco | TETRIX Robotics," *www.pitsco.com*. https://www.pitsco.com/Shop/TETRIX-Robotics/&TXredir=1

[5]"MOTION - Motors - Yellow Jacket Planetary Gear Motors - goBILDA®," *www.gobilda.com*. https://www.gobilda.com/yellow-jacket-planetary-gear-motors

[6] Pupaza C. – Inginerie Asistata de Calculator 1, note de curs si aplicatii, UPB, 2023

[7] Pupaza C. – Inginerie Asistata de Calculator 2, note de curs si aplicatii, UPB, 2023

DESIGNING AND PROGRAMMING HEXAPOD ROBOTS AND POSSIBLE USES

DOBRESCU Diana- Maria[1], MUTULEASA Razvan- Mihai[2] and CAZACU Carmen-Cristiana[3]

[1]Faculty: Industrial Engineering and Robotics, Industrial IT Specialization, Year of study: I, e-mail: diana.maria.do@gmail.com

[2]Faculty: Industrial Engineering and Robotics, Machine Construction Technology Specialization

[3]Faculty: Industrial Engineering and Robotics, Department: Robots and Production Systems

ABSTRACT: The following pages detail the process of designing, building and programming of a hexapod robot. From a simple concept on paper, to a sketch in AutoCAD, to a functional 3D printed prototype to prove the forementioned concept using Arduino.

KEYWORDS: hexapod, programming, CAD, Arduino

1. Introduction

From more advanced creations like Spot® by Boston Dynamics, Inc. to simpler robots posted on the internet, interest in multi-legged robots skyrocketed in the past years. This is why we also decided to make our own polypod companion in the form of a hexapod robot. The following paper focuses on designing and programming such robots.

The intent of the project is to build a robot using Arduino that can move smoothly on multiple surfaces varying in texture, with the only limitation being the incline of the plane on which it moves. In the future, a possible improvement could be the ability to navigate an obstacle course efficiently and autonomously.

2. State of the art

At the moment the project is a work in progress, as we lacked certain necessary materials such as servo motors (MG996R) [1] and other electronic components. However, despite these inconveniences, we managed to bring proof for concept to the presentation in the form of one of the legs of the hexapod. It utilizes three servos to move and the way they work shall be described in the pages that follow.

3. Designing the hexapod

We shall start by explaining the progression and thought process behind our final design. To finalize the design we used the following apps: AutoCAD, Onshape, SolidEdge, Fusion360 and Unity (for a simulation).

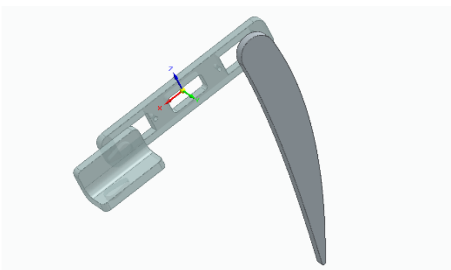

Fig. 1. First iteration of the leg mechanism

In the first phase of the project, we did a minimalistic iteration of a leg as seen in the images above (Fig. 1), it is a functional design, however, it is neither elegant nor resistant, that is why we moved on to the next two variations, one for the augmented version below (Fig. 2) (in order to better show the mechanisms behind the robot we made a larger version of the leg) and one for the complete hexapod (Fig. 3&4) (which is built in a way that the MG996R servos can support its weight).

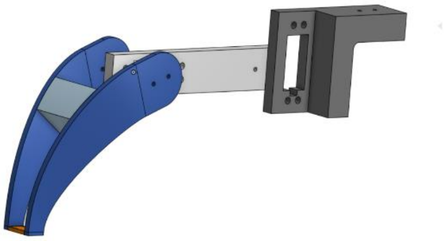

Fig. 2. Final model for the augmented leg

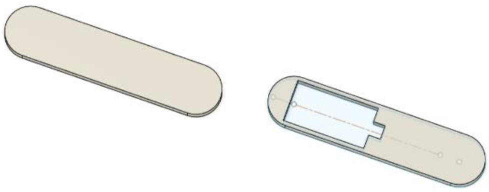

Fig. 3. Final model for the femur of the complete hexapod

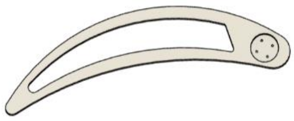

Fig. 4. Final model for the tibia of the complete hexapod

Other concerns during the design of the robot appeared when we had to choose measurements for the end of the leg, our supposed tibia. The length of it was chosen not to risk damaging the battery (which rests under the robot) and to give the hexapod an esthetic look in its rest position. To solve this issue a quick 3D sketch was created in AutoCAD (Fig. 5) and it helped solve any other dilemmas we had about the design and the dimensions.

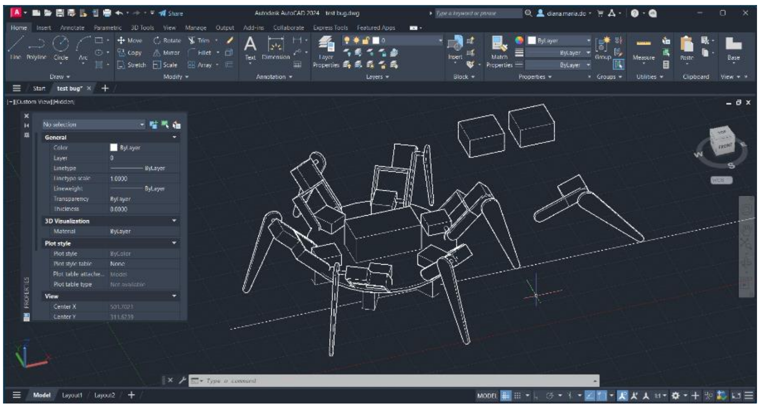

Fig. 5. Concept of complete hexapod in AutoCAD

4. Programming

As far as programming goes, we shall present the code behind the simulation in Unity [2] (Fig. 6& 7), which helped us understand the exact movement of the legs, when to synchronize them and when to move them individually, giving its steps a more natural flow and better accuracy.

```
Spider.cs
Miscellaneous Files                                   Spider

    int nMovePhase = 0;

    // Update is called once per frame

    float fCurrMoveTime = 0;
    const float fTargetMoveTime = 1; // sec to move in one direction

    const float fBodyMove = 5;// not sure what measuring unit this is?!
    const float fHipMoveAngle = 15;// degrees
    const float fFemurMoveAngle = 15;// degrees
    const float fTibiaMoveAngle = 30;// degrees
    float[] fCurrRotHip = { 0, 0, 0, 0, 0, 0 };
    float[] fCurrRotFemur = { 0, 0, 0, 0, 0, 0 };
    float[] fCurrRotTibia = { 0, 0, 0, 0, 0, 0 };

    // In the first implementation I will consider a fixed direction
    // I will only move to the right, along the dir of leg 0
    void MoveLeg(int nIdx)
    {
        switch (nIdx)
        {
            case 0:
                ExtendRetractLeg(0, true);
                break;
            case 1:
                MoveSidewaysLeg(1, false, false);
                break;
            case 2:
                MoveSidewaysLeg(2, true, false);
                break;
            case 3:
                ExtendRetractLeg(3, false);
                break;
            case 4:
                MoveSidewaysLeg(4, true, true);
                break;
            case 5:
                MoveSidewaysLeg(5, false, true);
                break;
            default:
                break;
        }
    }
```

Fig. 6. Unity sample code showing movement in a fixed direction

```
Spider.cs
Miscellaneous Files                                   Spider
        // I want to create 6x femur & tibia and spread them around the bug somehow

        Vector3 vMainBodyCenter = _rigidbody.transform.position;
        Quaternion qMainBodyRot = _rigidbody.transform.rotation;
        Quaternion qFemurRot = Quaternion.Euler(0, -45, 0);
        Quaternion qTibiaRot = Quaternion.Euler(0, 0, 45);

        for (int i = 0; i < 6; i++)
        {
            Quaternion rot = Quaternion.Euler(90, fLegsPosAngle * i, 0);

            _femurs[i] = Instantiate(femurTemplate);
            _femurs[i].transform.position = rot * vOffLeg + vMainBodyCenter;
            _femurs[i].transform.rotation = rot * qMainBodyRot;

            Transform trfChildFemur = _femurs[i].transform.Find("FemurAssembly").transform;
            trfChildFemur.localRotation = qFemurRot * trfChildFemur.localRotation;
            trfChildFemur.localPosition = new Vector3(0, 0, -2);

            Transform trfChildMotor = _femurs[i].transform.Find("Motor").transform;
            trfChildMotor.localPosition = new Vector3(0, 0, -2) + trfChildMotor.localPosition;

            int nChildren = trfChildFemur.childCount;
            Transform trf = trfChildFemur.Find("Join1");
            trf = trf.Find("Join2");

            _tibia[i] = Instantiate(tibiaTemplate);
            _tibia[i].transform.parent = trf;
            _tibia[i].transform.localPosition = Vector3.zero;
            _tibia[i].transform.localRotation = Quaternion.Euler(-90, 90, 0);
        }
    }

    //
    // I plan for 4 movement phases:
    // 0: no movement
    // 1: 3 legs (1) raise and move to new space position
    // 2: 3 legs (1) above move back (touching the ground to move spidr forward)
    //    3 legs (2)(the rest) move also touching the ground to that they basically
    //    stay in place as the spider moves forward
    // 3: 3 legs (2) raise and move back to their previous position
    // from one movement set to another we could switch the set of legs

    int nMovePhase = 0;
87 %    No issues found
```

Fig. 7. Unity sample code showing thought process behind movement

In the case of the augmented leg, the code shows movement based on angles that can be calculated easily [3] (Fig.9). As for the math behind the movement, it is shown below (Fig. 10) and it represents the base for reverse cinematics which contributes to the smoothness of the movement done by the leg. There is also a segment of code provided below to show the applied calculations [4] mentioned above (Fig. 11).

```
void ServoWritePos(float Target_a1, float Target_a2, float Target_a3)
{
  float Current_a1 = s1.read();
  float Current_a2 = s2.read();
  float Current_a3 = s3.read();
  float Delta_a1 = Target_a1 - Current_a1;
  float Delta_a2 = Target_a2 - Current_a2;
  float Delta_a3 = Target_a3 - Current_a3;
  p1 = Delta_a1 / nrp;
  p2 = Delta_a2 /nrp;
  p3 = Delta_a3 / nrp;
  for(int i = 1;  i<=nrp; i++)
  {
    Current_a1 += p1;
    Current_a2 += p2;
    Current_a3 += p3;
    s1.write(Current_a1);
    s2.write(Current_a2);
    s3.write(Current_a3);
    delay(25);
  }
}
```

Fig. 9. Sample code for servo movement based on angles

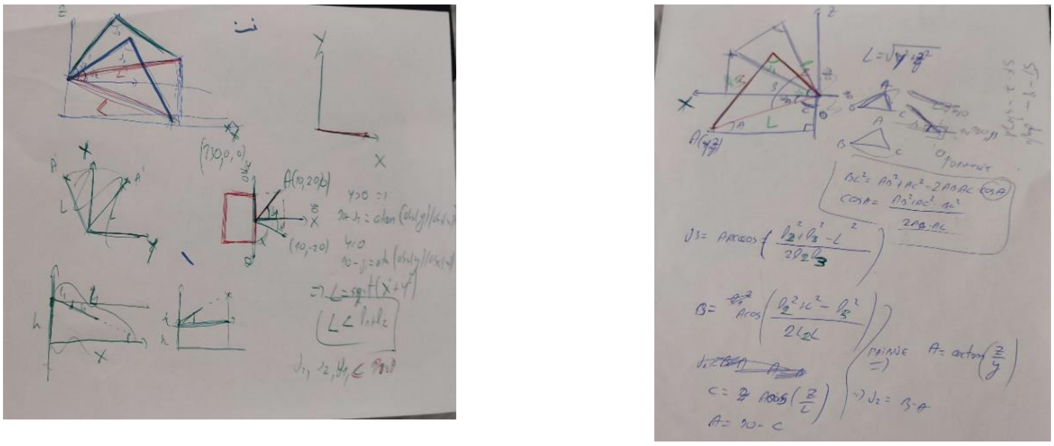

Fig. 10. Calculations for reverse cinematics

```
int ServoAng(double posy, double posx, double *test)
{

  L = sqrt( posx*posx + posy*posy);

  j3 = (180.00/M_PI) * acos( (l1*l1 + l2*l2 - L*L) / (2*l1*l2));
  Serial.println("J3 este:");Serial.println(j3);
  ST.write(90 - j3);


  j2 = ((180.00/M_PI) * acos(( l1*l1 + L*L - l2*l2) / (2*l1*l2))) - ((180.00/M_PI) * atan(abs(posy)/abs(posx)));
  Serial.println("J2 este:");Serial.println(j2);
  SF.write(90 - j2);

  return j2;
  *test = j3;

}
```

Fig. 11. Reverse cinematics code written based on Fig. 10

5. Conclusions

Throughout the process of completing this project many issues were discovered that we would like to fix for future versions of the robot. To start with, our intent is to fully build the hexapod once we acquire all the materials necessary such all 18 servo motors. Furthermore, we would like to complete the code and eventually configure the robot in a way so it can be controlled with a console controller such a PS4 or XBOX ONE/360.

Another improvement worth mentioning is fixing the rough and imprecise movement of the legs, as it is both imprecise and inaesthetic. To fix this issue we should learn how to apply interpolation in our code.

With future development in mind, we would like to add supports on top of the body such as a camera support, with the intent of using the mechanism to navigate spaces that are difficult for humans to reach.

6. Bibliography

[1].https://www.optimusdigital.ro/en/servomotors/1160-servomotor-metalic-digital-mg996.html?search_query=servo+996&results=5&HTTP_REFERER=https%3A%2F

[2]. https://play.unity.com/mg/other/webgl-builds-406887

[3]. https://youtu.be/1-FJhmey7vk?si=4GmUK9MMw5b-muES

[4]. https://youtu.be/pcfJJxv6q1s?si=hLK55uFVILLW1Pj0

DEMONSTRATIVE MODEL OF AN AUTOMATED GREENHOUSE

LIȘIȚĂ DANIEL-CONSTANTIN, CHEBĂRUȘ ANDREI-NICOLAE, IVAN ANDREI MARIO
Faculty of Industrial Engineering and Robotics, Specialization: Robotics, Year of Study: I
Email: hello.daniellys@gmail.com

ABSTRACT: The project presents the development of a demonstrative model for an automated greenhouse using the open-source platform Arduino. Currently, the greenhouse includes three automation systems - an automatic irrigation system, a system for monitoring environmental parameters such as temperature and humidity, and a crankshaft mechanism for opening the roof. The goal of this initiative is to offer an accessible and efficient solution for both small farmers and home gardeners. Through this project, we aim to demonstrate how technology can be used to improve agricultural efficiency and sustainability, providing an accessible solution for both small farmers and home gardeners.

KEYWORDS: greenhouse, automation, Arduino

1. Introduction

In a rapidly developing world, access to quality food has become increasingly expensive. BIO products, which should be a healthy and accessible solution, have often become just another profitable business. To meet the growing emand for food and to protect the environment, it is necessary to maximize agricultural production without resorting to destructive methods such as deforestation. A viable solution is optimizing traditional greenhouses to ensure ideal growing conditions for plants in an automated manner.

Greenhouses are specially designed structures for growing plants in a controlled environment, protected from extreme weather conditions and pests. They are constructed from transparent materials (glass or transparent polymer - plastic) that allow sunlight to penetrate while maintaining a constant temperature inside. The operation of greenhouses is based on the natural greenhouse effect, where solar radiation heats the soil and air inside, and the heat is retained, creating a favorable environment for plant growth.

This project focuses on developing a demonstrative model of an automated greenhouse using accessible technologies such as the Arduino platform. The greenhouse automation includes automatic irrigation systems, environmental parameter monitoring, and automatic ventilation, all aimed at creating an optimal environment for plant growth. Through this project, we aim to demonstrate how technology can be used to improve agricultural efficiency and sustainability, providing an accessible solution for both small farmers and home gardeners.

2. Project Objectives

- ✓ **Sustainability:** Creating an automated system that optimizes the use of natural resources, reducing water and energy waste, and minimizing environmental impact.

- ✓ **Efficiency:** Reducing maintenance costs and human effort required to manage the greenhouse by implementing a fully automated system for irrigation, monitoring, and ventilation.

- ✓ **Accessibility:** Offering an economical and easy-to-implement solution for small farmers and home gardeners using affordable components and open-source software.

3. Current Status

The development project of an automated greenhouse is currently in an early stage (in the third stage of development). From a construction standpoint, it features the use of recycled wood and manual construction. The structure allows for improvements in terms of sealing.

Functionally, three automation systems have been implemented - an automatic irrigation system, an environmental parameter monitoring system (such as temperature and humidity), and a crankshaft mechanism for roof opening. These systems help maintain a favorable climate for plant development. Additionally, the automatic adjustment of temperature and humidity based on plant needs remains a viable development option.

4. Project Implementation

Like any ambitious project, our greenhouse went through several development stages. We informed ourselves about what a greenhouse is and how it works to provide people thinking about growing their own aromatic plants an answer to the question, "Is it worth investing in an automated greenhouse?"

We began by designing the greenhouse itself. After its construction, we implemented the automation systems.

a. Greenhouse Design and Costruction

We started by sketching the project (Fig. 1) using AutoCAD software at a two-dimensional level. After creating the model, we proceeded to build it (Fig. 2). The greenhouse structure is mainly made from recycled wood - leftover materials from building a desk. The walls were made from rigid transparent polymer (plastic) film with a thickness of approximately 0.5 mm.

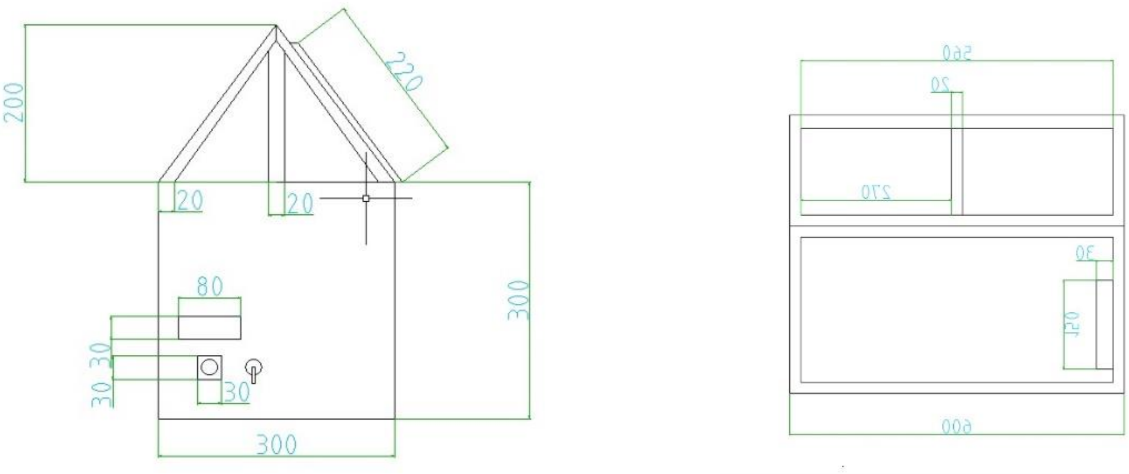

Fig. 1 Project Sketch

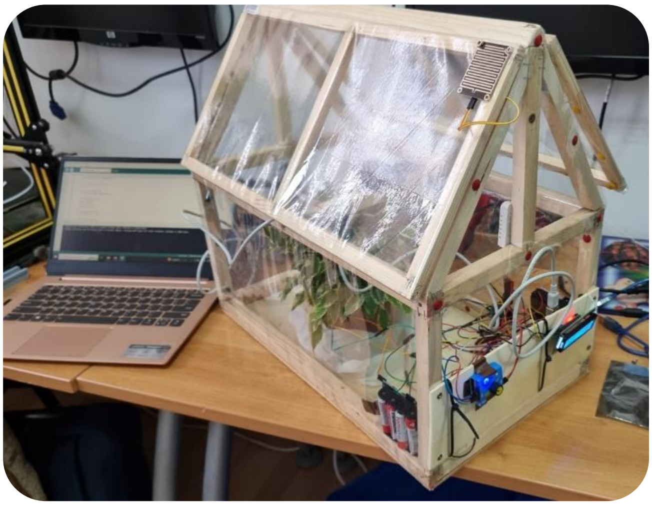

Fig. 2 Stage two: Development

b. Hardware

The project is developed on an ARDUINO UNO R3 DEVELOPMENT BOARD. Our current demonstrative model of the greenhouse comprises three systems:

1. <u>Automatic Plant Watering System</u>
   a. Functionality

The irrigation system is the centerpiece of any crop. We implemented an automatic system (Fig. 3) that starts the pump when the soil moisture drops below a certain percentage (using a soil moisture sensor plus a comparison module).

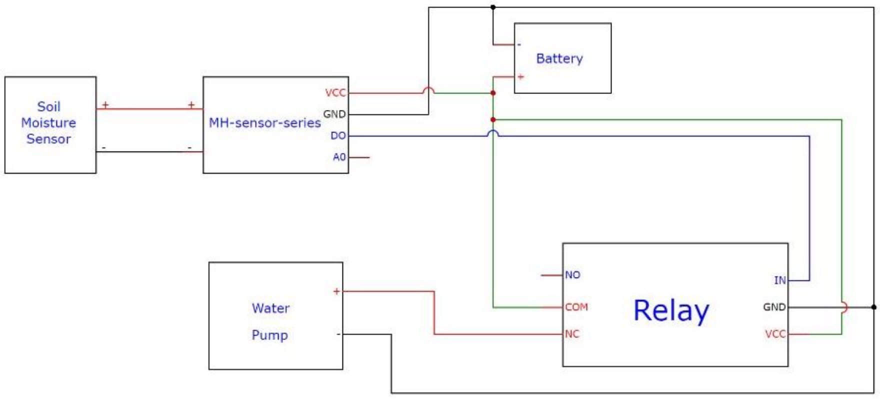

Fig. 3 Principle Schematic of the Irrigation System

b. Components used

- ✓ Irrigation pump
- ✓ 80cm water hose & reservoir
- ✓ Soil moisture probe + comparison module
- ✓ 5V relay module for irrigation control

2. Environmental Parameter Monitoring System

a. *Functionality*

Monitoring environmental parameters (humidity, temperature, etc.) is one of the main requirements when designing a greenhouse. Currently, we have integrated a sensor that measures temperature and humidity, placed slightly above the greenhouse (Fig. 4). We connected an LCD display and programmed it to display data transmitted by the sensor.

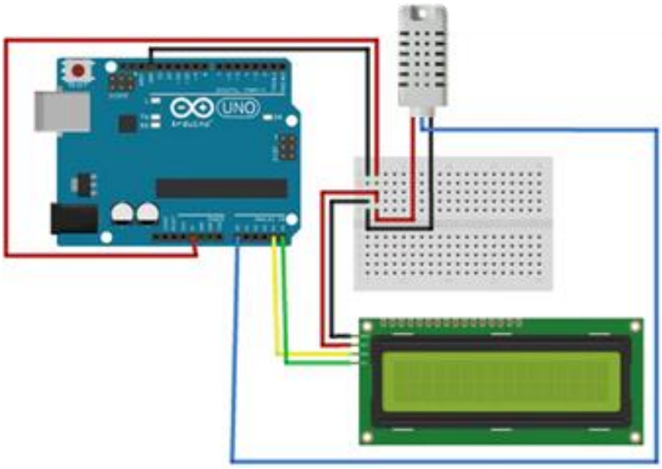

Fig. 4 Principle Schematic of the Monitoring System

b. *Components Used*

- ✓ 1602 LCD SCREEN WITH I2C ICC MODULE
- ✓ Temperature and Humidity Sensor DHT22/AM2302B

3. Roof Opening System

a. *Functionality*

The roof opening system plays a crucial role in ventilation, given the chosen construction solution -allowing air circulation between the interior and exterior. We opted for a hybrid solution (Fig. 5) that includes the possibility of manually operating the servomotor with a potentiometer as well as automatically. The automated actuation solution is based on using a rain sensor so that the roof flap closes when it rains.

Fig. 5 Crankshaft Mechanism for Roof Opening

b. *Components used*

- ✓ Servomotor MG996 (90°)
- ✓ Direction device for servomotor
- ✓ Aluminum strips, screws, and nuts
- ✓ Potentiometer and rain sensor module

c. Software (The programming part was implemented using the Arduino IDE application)

```
#include <DHT.h>;
#include <LiquidCrystal_I2C.h>
#include <Wire.h>

LiquidCrystal_I2C lcd(0x27,16,2); // set the LCD address to 0x27 for a 16 chars and 2 line display

//Constants
#define DHTPIN 7     // what pin we're connected to
#define DHTTYPE DHT22   // DHT 22
DHT dht(DHTPIN, DHTTYPE); //// Initialize DHT sensor for normal 16mhz Arduino
//Variables
//int chk;
int h;  //Stores humidity value
int t; //Stores temperature value
int motorPin = 3; // pin that turns on the motor
int blinkPin = 13; // pin that turns on the LED
int watertime = 2; // how long it will be watering (in seconds)
int waittime = 2; // how long to wait between watering (in minutes)

void setup()
{
  pinMode(motorPin, OUTPUT); // set Pin 3 to an output
  pinMode(blinkPin, OUTPUT); // set pin 13 to an output
  Serial.begin(9600);
  Serial.println("Temperature and Humidity Sensor Test");
    dht.begin();
    lcd.init(); //initialize the lcd
    lcd.backlight(); //open the backlight
}

void loop()
{
  h = dht.readHumidity();
    t = dht.readTemperature();

    //Print temp and humidity values to serial monitor
    Serial.print("Humidity: ");
    Serial.print(h);
    Serial.print(" %, Temp: ");
    Serial.print(t);
    Serial.println(" ° Celsius");

// set the cursor to (0,0):
// print from 0 to 9:

    lcd.setCursor(0, 0);
    lcd.println("Now Temperature ");

    lcd.setCursor(1, 1);
    lcd.print("T:");
    lcd.print(t);
    lcd.print("C");

    lcd.setCursor(6, 1);
    lcd.println("    ");

    lcd.setCursor(10, 1);
    lcd.print("H:");
    lcd.print(h);
    lcd.print("%");

  delay(1000); //Delay 1 sec.

  int moisturePin = analogRead(A0); //read analog value of moisture sensor
  int moisture = ( 100 - ( (moisturePin / 1023.00) * 100 ) ); //convert analog value to percentage
  Serial.println(moisture);
  if (moisture < 40) { //change the moisture threshold level based on your calibration values
    digitalWrite(motorPin, HIGH); // turn on the motor
    digitalWrite(blinkPin, HIGH); // turn on the LED
    delay(watertime * 1000);      // multiply by 1000 to translate seconds to milliseconds
  }
  else {
    digitalWrite(motorPin, LOW);  // turn off the motor
    digitalWrite(blinkPin, LOW);  // turn off the LED
    delay(waittime * 60000);      // multiply by 60000 to translate minutes to milliseconds
  }

}
```

5. Problem Solving

Throughout the project, we encountered various situations that complicated development, serving as valuable learning opportunities.

1. LCD Interface Issues

During the implementation of the environmental parameter monitoring system, we had difficulties connecting the LCD display. Due to a mistake, the displayed data was reversed. We discovered that the data was correctly retrieved and displayed, but the informational messages (Temp and Humidity) were swapped.
The issue was easily resolved but taught us to pay attention to details. Additionally, we burned out about three LCDs during the process.

2. Synchronization Issues with Rain Sensor and Servomotor

This problem was due to the poor distribution of available ports in the early stages of the project. Since all three systems share certain ports, we had to use a Breadboard. Eventually, we managed to connect the rain sensor. It worked during tests but not at the project's first presentation in a faculty lab, likely due to a low-quality sensor.

6. Conclusions

Implementing automation solutions at the greenhouse level, even at a demonstrative level, represents a significant step towards improving agricultural processes by bringing technology to the forefront of food production. Although it was a complex and challenging project, the results are promising and relevant for the future of sustainable agriculture.

The implementation of three automation systems - automatic irrigation, environmental parameter monitoring, and roof opening - demonstrates that technology can optimize agricultural processes, reducing resource consumption and creating a favorable environment for plant growth. The accessibility and low costs make this project a viable option for small farmers and home gardeners, thus contributing to the democratization of technology in agriculture.

However, there is still room for improvements and innovations. Transitioning to more advanced platforms such as ESP32 microcontrollers could bring additional functionalities and greater efficiency in greenhouse management. Furthermore, adding additional sensors and implementing an artificial intelligence system could optimize the growing environment for plants and contribute to more sustainable and efficient agricultural production.

7. References

[1]. Arduino Automatic Plant Watering System
[2]. Automatic Irrigation System using an Arduino Uno
[3]. Automatic Plant Watering with Arduino
[4]. Arduino Water Sensor and Servo
[6]. Rain Drop Sensor With Servo Motor
[5]. How to Use I2C LCD with Arduino
[7]. Project Hub Arduino
[8]. Arduino Forum

MOBILE ROBOT FOR „FOOTBALL” COMPETITIONS

GEORGESCU Gabriel[1], OBREJA Alexandru-Valentin[2], ȚENESCU Mihai-Matei[3], IVAN Andrei Mario

[1] Faculty: Industrial Engineering and Robotics, Specialization: Industrial Informatics, Year: I, e-mail: gabriel.georgescu04@stud.fiir.upb.ro
[2] Faculty: Industrial Engineering and Robotics, Specialization: Robotics in English, Year: I, e-mail: alexandru.obreja@stud.fiir.upb.ro
[3] Faculty: Industrial Engineering and Robotics, Specialization: Robotics in Romanian, Year: I, e-mail: matei_mihai.tenescu@stud.fiir.upb.ro

ABSTRACT: For The Minoan Robotsports Competition Global Olympiad 2024 that took place in Stadium "2 Aorakia" Neas Alikarnassou, Crete, Greece, on April 27- 29 2024 we had decided to partake in the Football (Soccer) Section for which we were required to build small car-like robot nicknamed "Hagi" for competing against other likewise robots in alliances. For that, we had designed a Raspberry Pi Pico microcontroller car-like robot, controlled from laptop via Bluetooth, featuring 2 wheels spun by 2 DC motors, a rotating ball on the back for balance and a rectangular-shaped header with a gap that allows the game ball to be centered in the header before being propelled by the header using a oscillating spring forced by a mechanism with another DC motor.

KEYWORDS: ROBOTICS, BALL-GAME, COMPETITION, OLYMPIAD, MECHATRONICS

1. Introduction

a. The General Description of the Football Game

The competition consists of a tournament of alliances made of 3 robotics teams. Each match of the tournament takes place on a small 236.2 x 114.3 [cm] football field with a playing area of 197.34 x 98.42 [cm]. The football gates are with a length of 35 [cm], a height of 12 [cm] and a depth of 8 [cm] (Fig. 1) with two alliances (one alliance being formed by 3 participating robotics teams) competing against each other per match with the robots each team had built. The alliance scores a goal if one robot of that alliance shoots the ball in the football gate or if the ball touches a robot whose parts are inside the football gate. Each match lasts 7 minutes with no half-time and no pause. The alliance that scores the most goals in a match advances in the next one. If there is a tie, additional time is given for more goals to be scored. The alliance that goes through all matches wins the whole competition.

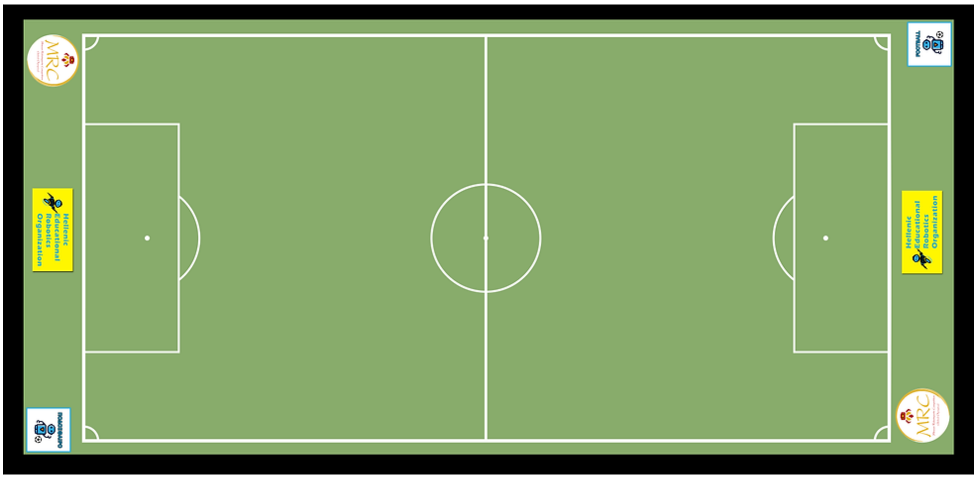

Fig 1. The Football Field

b. The Requirements of the Robots

The robots competing in The Minoan Robotsports Competition Global Olympiad 2024 needed to meet some requirements posted by the Competition Committee on their official website [1]:

- The Robot Football Player must be remote-controlled with a program made on a computer – laptop.
- The use of a remote control is only allowed if it is programmed to connect to the Robot Soccer Player.
- Off-the-shelf remote-control apps that were not programmed by the team to operate the Robot Soccer Player are prohibited.
- Wi-Fi connection to the stadium network is not allowed for participating teams and visitors.
- The maximum dimensions of the Robot Football Player must be 20cm Width x 20cm Length.
- To confirm the specifications listed above, the Robot Football Player will be weighed and must comfortably fit in a control box.
- The control box measures 20 x 20 [cm] plus two (2) [mm] tolerance.
- The Robot Football Player should be placed in the control box without applying pressure.
- The Robot Football Player must not wear or damage the pitch or pose a threat to spectators in any way.
- The Robot Football Player should have a shooting mechanism.
- Each Robot Football Player is allowed a maximum of 4 motors and 1 single microprocessor.
- The Robot Football Player must have a start and stop button.
- The maximum weight of the robot must be 700 grams.
- For Football ball will be used LEGO Mindstorms ball – Part Number 41250 (diameter 52mm) red or blue color.
- The Robot Football Players of an alliance should bring in a visible place of their construction some "signature" that the alliance should have agreed on in advance, for example a flag, label, color combination, etc., so that one is immediately recognized by the referee in which alliance belongs.
- A Robot Football Player should not hold the ball in any way.
- The ball may not penetrate more than 2 [cm] in any part of the Robot Football Player construction.
- A Robot Football Player is not allowed to pick up the ball by placing it on his body in any way.
- A Robot Football Player is not allowed to pick up the ball by placing it under his body.

2. The Robot and Its Current Status

Our robot nicknamed "*Hagi"* after the great Romanian football player Gheorghe Hagi, had been designed to meet the requirements mentioned above and it had participated in the competition, winning first prize with other robots in Alliance 49. It is made from a 3D printed encasing which is suited to fit the whole electric circuit with 3 DC Motors and the header for scooping the ball and launching it (Fig 2). The full specifications for the hardware and the software of the robot shall be provided in the following paragraphs.

Fig 2. Hagi the Robot Football Player.

3.1. Hardware Implementation Details

a. <u>The Robot's Casing</u>

Hagi's 3D printed case is made from (insert material here) with a bronze and shiny look. It was designed on Fusion 360 with a length of 112 [mm], a width of 145 [mm] and a height of 62 [mm], with the name of our team "sySTEMatic" and other decorations to give it a nice look. (Fig 3)

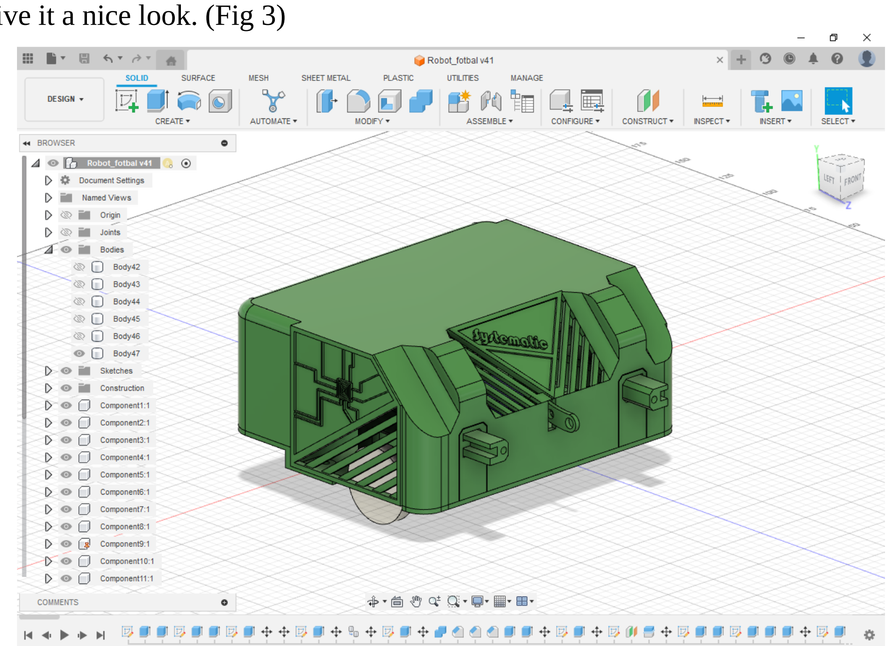

Fig. 3. Robot's Casing Designed on Fusion 365.

b. The Robot’s Circuit and Control System

The Circuit comprises of a Microcontroller, 3 DC motors with 25:1 gear reducers connected to their afferent drivers and a battery.

The robot’s control system is based on a GroundStudio Marble Pico development board (a Raspberry Pi Pico clone), which features an ARM Cortex M0+ dual-core microcontroller, with 264kB RAM and 8MB flash memory on-board [2]. This development board was chosen because it provides flexibility, supporting various programming languages, including Python and C++. Its dual-core architecture allows future expansion by enabling processing commands and running various algorithms simultaneously.

The system uses a Bluetooth module to communicate with a computer. Bluetooth was chosen because of its universal compatibility with most laptops, smartphones and other devices. On the other hand, because the protocol uses the widely popular 2.4 GHz ISM (Industrial, Scientific and Medical) band, it is prone to interference in extremely busy areas, as other technologies such as Wi-Fi share the same radio spectrum.

A motor controller is used to drive the main motors – the ones that have one wheel attached to each – while an N-MOSFET is used for the header motor. The system is powered from a 2-cell Lithium-Polymer battery, featuring a nominal voltage of 7,4 [V]. The control electronics are powered by a 5 [V] supply generated by a step-down regulator.

c. The Robot’s Header and Propulsion System

The header is designed in such a way as to center the ball for a more precise launch thanks to its central gap (Fig. 4).

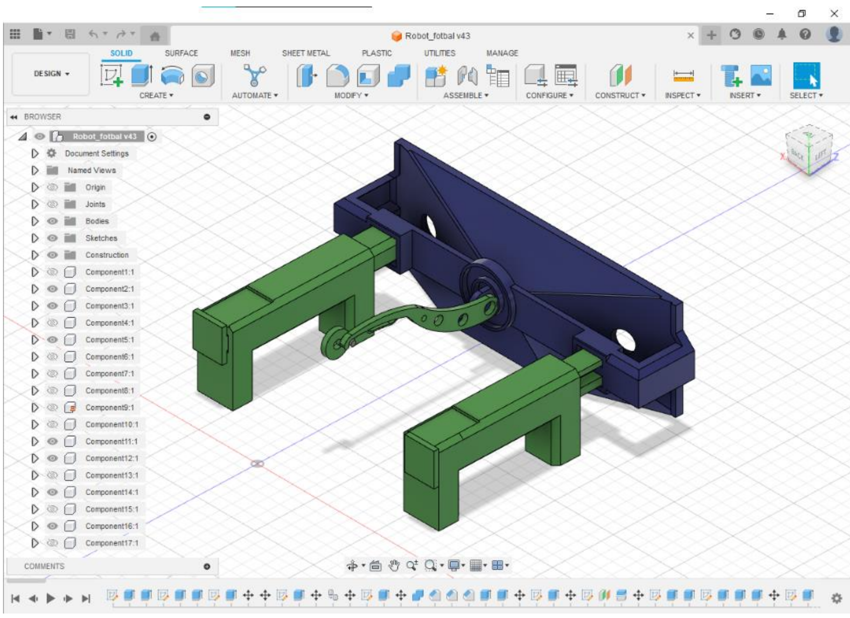

Fig. 4. The header of the Robot viewed from the front.

On the back it is connected to its rotating propulsion motor via a long curved coupling which pulls and releases the header as the motor rotates (Fig. 5). When the header is released, the compressed spring which is attached between the circular support on the back of the header and the main body pushes the header back to its original position with a high force which knocks and pushes the ball with a high speed.

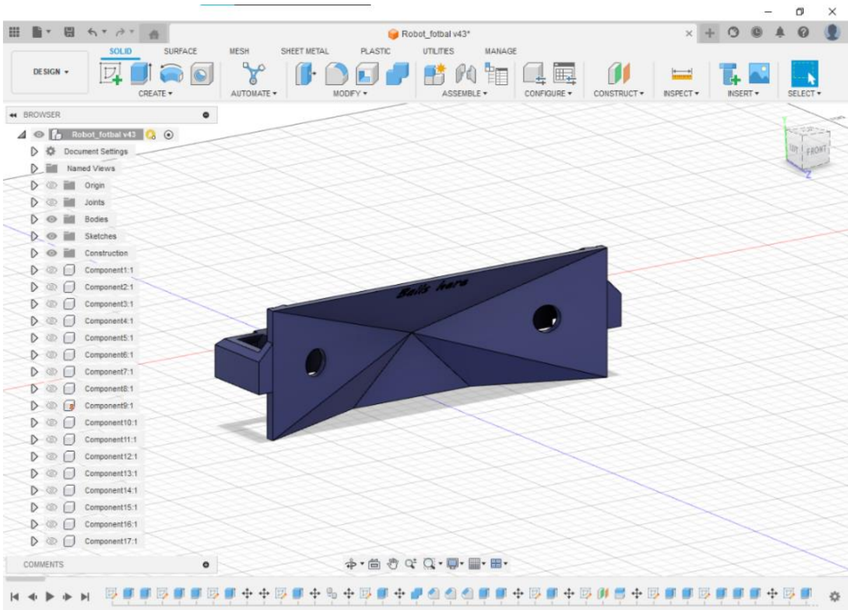

F ig. 5. The Header with its curved coupling and supporing beams (back view).

3.2. Software Implementation Details

The robot's firmware was written in the Python programming language, running on the MicroPython platform, which allows running Python on various microcontroller platforms, such as the Raspberry Pico-based development board used in this project.

The development board communicates with the Bluetooth module using the UART (Universal Asynchronous Receiver Transmitter) (Fig 6.1.).

The robot is controlled by transmitting a series of characters through the serial connection (Fig 6.2).

```
cmd = cmd.strip(" \n\r\t")
if cmd == "s":
    motor_l_bw.duty_u16(spd)
    motor_r_bw.duty_u16(spd)
    print("S")
if cmd == "d":
    motor_l_fw.duty_u16(spd_steer)
    print("d")
if cmd == "w":
    motor_l_fw.duty_u16(spd)
    motor_r_fw.duty_u16(spd)
    go_fw = True
    print("W")
if cmd == "a":
    motor_r_fw.duty_u16(spd_steer)
    print("a")
if cmd == "e":
    motor_goal.duty_u16(spd)
    print("E")
```

Fig. 6.2. Control algorithm.

```
while True:
    if uart.any():
        char = uart.readline()
        if char == b'\n':
            print(command)
            execute_cmd(command)
            command = ""
        command += char.decode("utf-8")
```

Fig. 6.1. Software implementation of communication

The received command is decoded and the corresponding motors are turned on and configured to the required speed using PWM (Pulse Width Modulation).

The commands are sent from a PC connected via Bluetooth. Another Python program is running on the control computer, registering key-down and key-up events and sending the corresponding commands to the robot (Fig. 7).

```
def show(key):
    if key == Key.delete:
        # Stop listener
        return False
    try:
        if not key_pressed[key.char]:
            if key.char == "w":
                port.write(b"w\n")
            if key.char == "a":
                port.write(b"a\n")
            if key.char == "s":
                port.write(b"s\n")
            if key.char == "d":
                port.write(b"d\n")
            if key.char == "e":
                port.write(b"e\n")
            if key.char == "t":
                port.write(b"t\n")

            key_pressed[key.char] = True
            print("[info] Key {} was pressed".format(key.char))
    except:
        pass
```

Fig. 7. Function detecting key-down events.

4. Improvement Possibilities

The current control system is based on pressing keys on the computer keyboard. A significant improvement would consist in using an off-the-shelf controller used in game consoles (such as an Xbox or PlayStation controller), allowing precise control of motor speed and movement direction.

The header can be improved by having a larger surface area, thus making it easier to “catch” the ball. Maneuverability can be improved with various mechanical design changes, and higher speeds can be obtained by changing the motor gearbox ratio to 10:1.

5. Conclusions

While the football player robot *Hagi* has been a fine success for our team at the competition with its compact and simple design, it still has room for improvement so it can become better at what he was made to do. We are looking forward to expanding and empowering its functionalities as more opportunities for participating in football competitions for robots appear.

6. Bibliography

[1]. MRC GLOBAL OLYMPIAD | ΠΟΔΟΣΦΑΙΡΟ - FOOTBALL (he-ro.gr)
[2]. https://ardushop.ro/ro/home/2652-marble-pico.html

PROGRAMMING AND OFFLINE SIMULATION OF A ROBOTIC CELL FOR PALLETIZING USING PROCESS SIMULATE ENVIRONMENT

CICÎRÎC Diana-Maria, PUPĂZĂ Cristina

Faculty: Industrial Engineering and Robotics, Specialization: Robotics, Mster student, Year of study: 1
e-mail: diana_maria.ciciric@stud.fiir.upb.ro

ABSTRACT: This research encompasses the virtual prototype of a robotic cell designed for palletizing parallelepiped boxes containing milk cardboard boxes, integrating two articulated arm industrial robots with six numerically controlled axes and equipped with two poly-functional effectors. This study is a continuation of the bachelor thesis and it is focused on the signal-based simulation of the cell employing Siemens Process Simulate environment.

KEYWORDS: palletizing, sensor, Process Simulate.

1. Introduction

This study is a continuation of the bachelor thesis, containing a robotic cell which model is based on an internet video supporting the project theme. The work is focused on a signal-based simulation of the functioning of the cell in the Siemens Process Simulate environment.

The main goals of a signal-based simulation are the reduction of the development time and the increase of the precision and reliability - the working cycles of the robots are tested, the operating parameters can be changed without needing to turn off the production in real time and possible collisions between equipments are visualized and eliminated. It is a fundamental step towards Virtual Commissioning.

The source cell involves the palletizing and transport process of milk packages, arranged in parallelepiped cardboard boxes that present two distinct dimensional variants. Two industrial robots and a fully automatic pallet entry and exit system are also included (Fig. 1).

Fig.1 Overview of the palletizing cell [1]

The boxes enter in the cell (Fig. 2) on the main entrance conveyor, equipped with sensors that detect the type of the two boxes to be handled, and a selection and redistribution of them to the designated industrial robot is carried out (Fig. 3). The objects are picked up by the robot with the help of the effector and placed on a pallet generated by the automatic feeding system. The completed pallet starts on the exit conveyor to the wrapper and then leaves the cell.

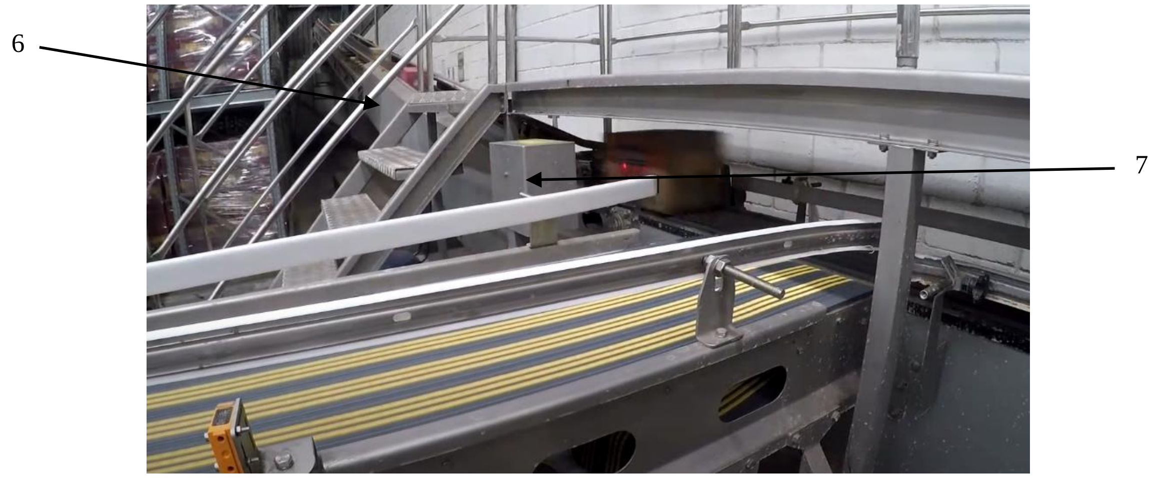

Fig. 2 Main entry conveyor and sorting of objects [1]

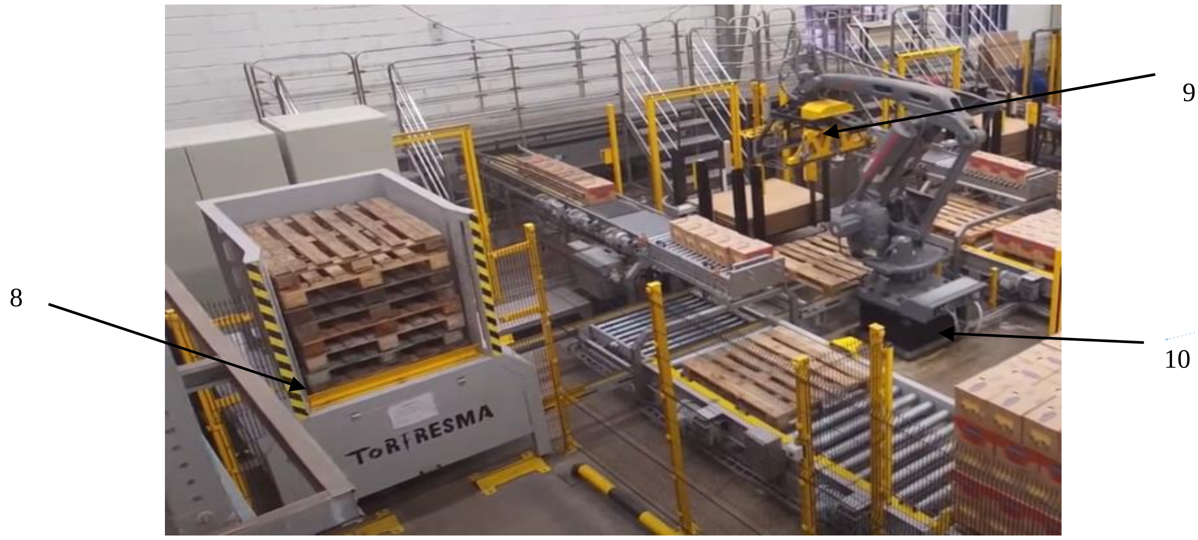

Fig. 3 Additional view of the cell [1]

The cell contains the following components: 1 - informational units, 2 - two industrial robots ABB IRB 660-250/3.15, 3 - mobile transport system of completed pallets, 4 – wrapper, 5 - protective fence, 6 - system entry conveyor of boxes before sorting, 7 - photoelectric sorting sensor, 8 - automatic pallet feeding system, 9 – effector, 10 - support for robot.

2. Development of the virtual prototype of the robotic cell in Siemens Process Simulate environment

Siemens Process Simulate is a digital manufacturing solution employed to verify the manufacturing processes in a three-dimensional environment and virtually check the designed workflows throughout their entire lifecycle.

The mechanisms of the subsystems were created in the Process Simulate environment in order to support the simulation of the component movements for the palletizing cell, that were already chosen in the bachelor thesis.

Examples of such mechanisms are shown in Fig.4 and Fig.5. Rotational kinematics are illustrated by black arrows and translational ones by blue.

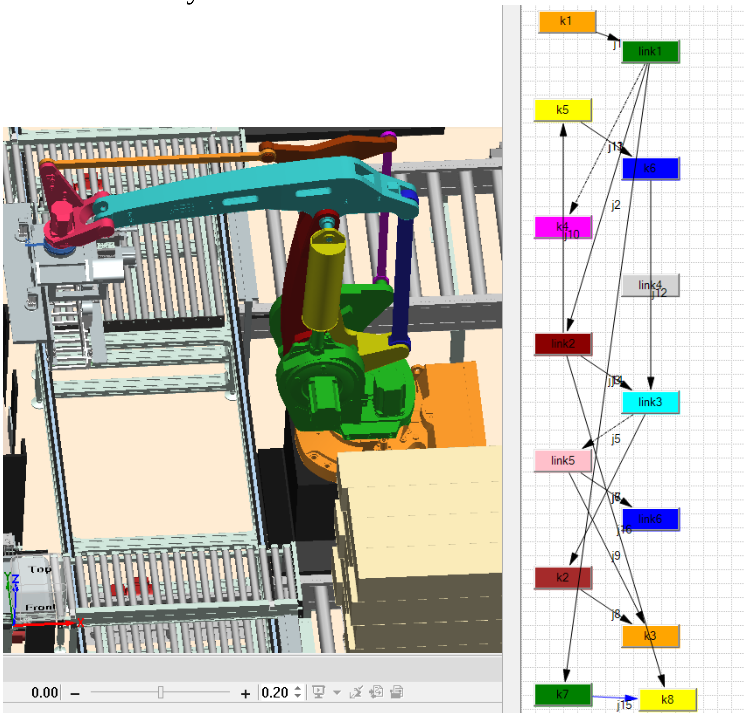

Fig. 4 Kinematics of the industrial robot [1]

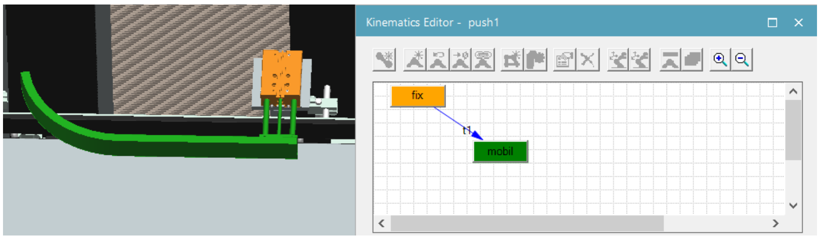

Fig. 5 Kinematics of pneumatic piston with retractable rod for box reorientation

The positions of the component systems in the cell assembly were also defined. In fig.6 is presented an example of the effector and its defined positions: initial (base position), fetch carton dividers and fetch boxes.

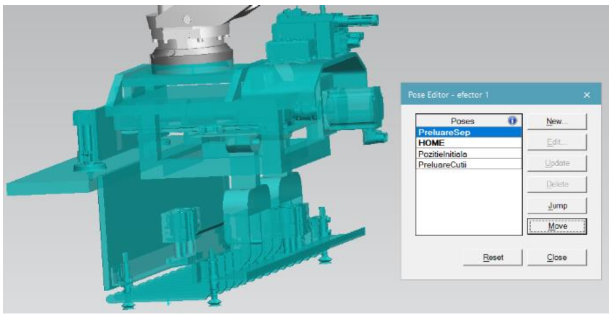

Fig.6 The position of the effector to pick-up a cardboard box divider (suction cups lowered)

The last step to realize the simulation of the robotic cell illustrated in Fig. 7 is to create processes, that are of several types, depending on the type of movement and of the mobile element. "Object Flow" operations are employed to move parallelepipedal box-type objects on conveyors; objects palletized by industrial robots equipped with effectors require "Pick and Place" type operations, and "Device Operation" is used for the mechanisms and to change their position.

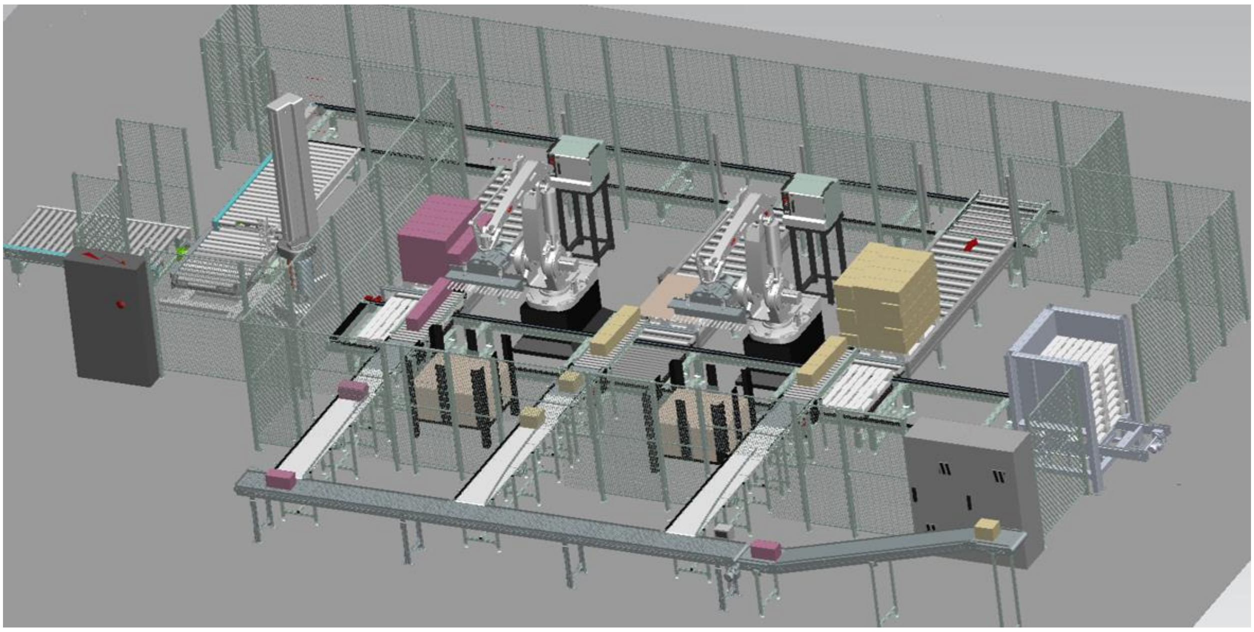

Fig. 7 Overview of the robotic cell developed in the Process Simulate environment [1]

3. The flowchart detailing all the processes, events and signals specific to the operation of the robotic application

In the analyzed application, the boxes are introduced into the cell by an slanting entrance conveyor, and their presence is sensed by a photoelectric sensor. The inclined conveyor is followed by a roller conveyor with interchangeable orientation, equipped with photoelectric sensors that detect the type of the two boxes to be handled. They are then selected and redistributed to the designated industrial robot, through a sequence of belt conveyors (accumulating, accelerating and changing the orientation of the boxes). The boxes are counted by the signals transmitted by the photoelectric sensors positioned at the entrance on the three conveyors, to the information unit. Once the desired number is reached the change of the orientation of the boxes is performed with the help of a pneumatic piston with an adjustable curved rod.

The boxes advance on a roller conveyor, equipped with two photoelectric sensors (next to the position of the first and last box to be picked up respectively, in order to comply with the imposed palletizing scheme), and are picked up after the stopping action of the industrial robot with the bifunctional effector, compatible with the spaces between the rolls. The boxes are placed on a pallet.

The pallets are generated by the automatic feeding system. A photoelectric actuator senses the presence of the pallets and they are transported on a chain conveyor to the lift module, within the range of the reflective photoelectric sensors. The lifting module transfers the pallets to the roller conveyor on which they are filled. The pallets stop in the palletizing area, the position being indicated by the diffusion photoelectric sensors placed at the end. The robot places a cardboard divider from the designated storage on the surface of the pallet.

The complete pallet advances on the roller conveyor on which the palletization was done up to the light barrier and is taken over by a transport module, consisting of a chain conveyor and a roller conveyor, equipped with photoelectric sensors with reflection that transmit information about the picking and positioning points of the pallet on the roller conveyor.

The complete pallet goes, through the light barrier, on the exit roller conveyor. In front of this conveyor there is a safety light barrier, to identify the presence of the human operator in the transfer space to the wrapper and to stop the process during the reception of signals for operator presence. The full pallet is transported to the rotary table enwrapper, equipped with photoelectric sensors, and then leaves the cell via another roller conveyor to the last light barrier which signals that the pallet is ready to be picked up by the human operator.

This logical operation process is also presented in Fig.8, in the application's functional organization chart (flowchart).

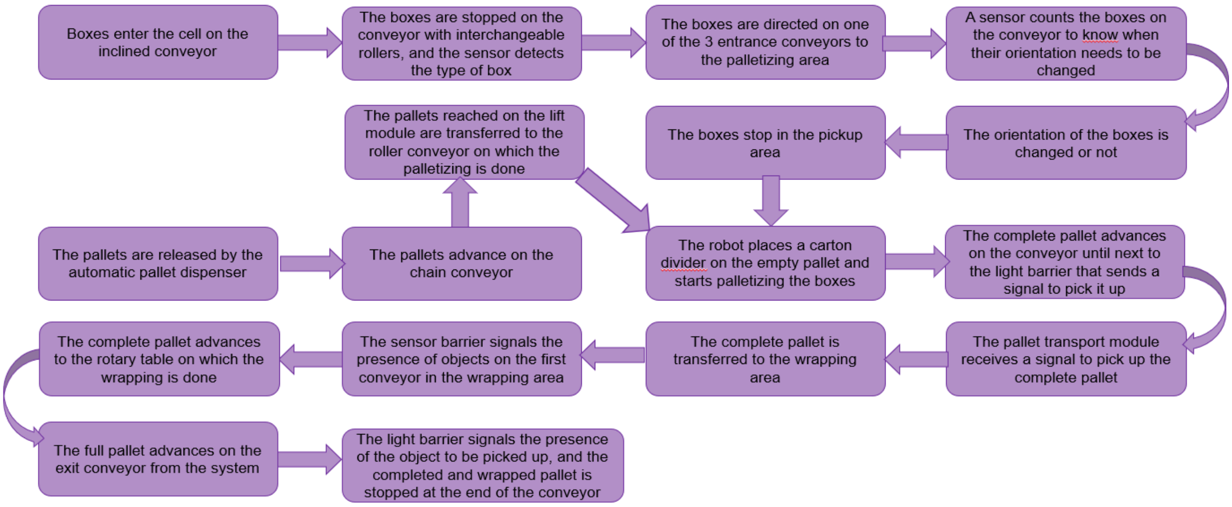

Fig. 8 Functional flowchart of the robotic cell

Different types of signals and sensors are used in the virtual robotic cell: signals from and to the informational unit (digital inputs and outputs), photoelectric sensors with diffusion, photoelectric sensors with reflection and light barrier type sensors.

Photoelectric sensors detect changes in the light intensity. A photoelectric sensor consists of a light source (emitter), a phototransistor (receiver), an amplifier and a signal converter. When the emitted light is interrupted or reflected by the detected object, the amount of light reaching the receiver varies. The phototransistor analyzes the incoming light, checks that it comes from the emitter, and through the amplifier and converter, the optical signal (light) is converted into an electrical signal. These electrical signals represent in the present robotic cell various digital inputs or outputs to the system information unit.

Light barrier sensors (Fig. 9) contain the transmitter and the receiver as two separate entities, and the connection between them is done by light rays. When an object passes through the light rays, the connection between the transmitter and the receiver is interrupted, and the photoelectric sensor detects the respective object. This type of detection is not dependent on the shape of the object, its color or the material it is made of.

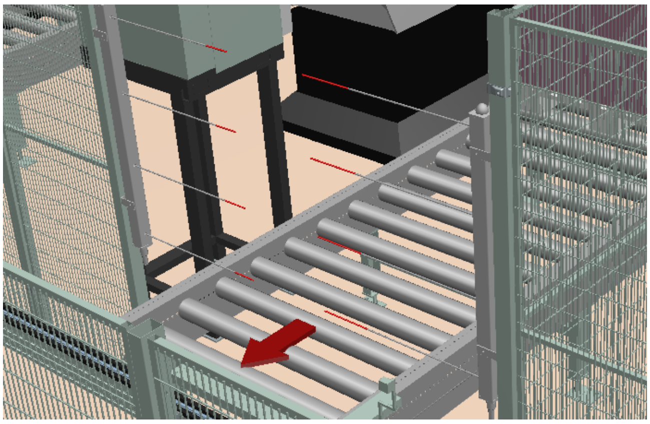

Fig.9 Light barrier present in the robotic cell

Diffusion photoelectric sensors contain the light emitter and receiver in a single housing, and mounting and the wiring is done in one side. The light beam is reflected in the receiver by the surface of the object to be detected. The operation of diffusion sensors is influenced by the color of the object, so the presence of a sensitivity adjustment potentiometer is necessary.

The third type of sensors present in the robotic cell are photoelectric sensors with reflection (retroreflective). Like diffuse sensors, both the transmitter and receiver are in the same housing, but the light beam from the transmitter reaches the receiver through a reflective element.

The location of the sensors in the robotic cell is illustrated in Fig. 9 and Fig. 10. The presence of the safety barriers is marked with red, the photoelectric sensors with diffusion with yellow, and the photoelectric sensors with reflection with green.

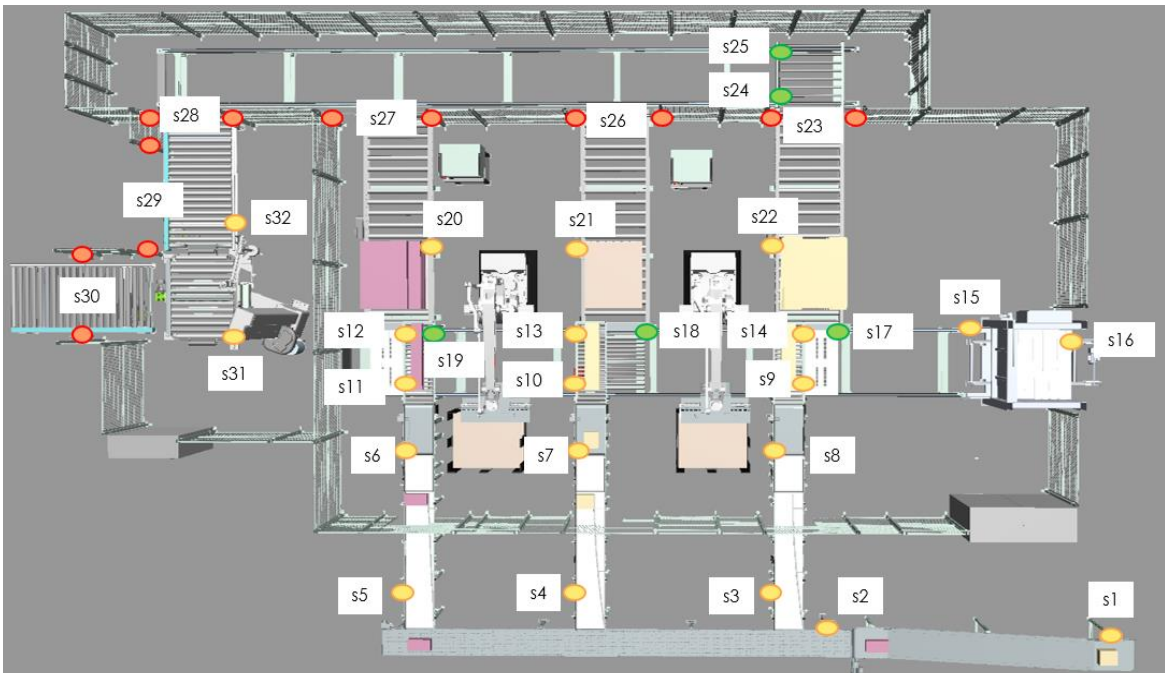

Fig. 9 Location of the sensors in the robotic cell

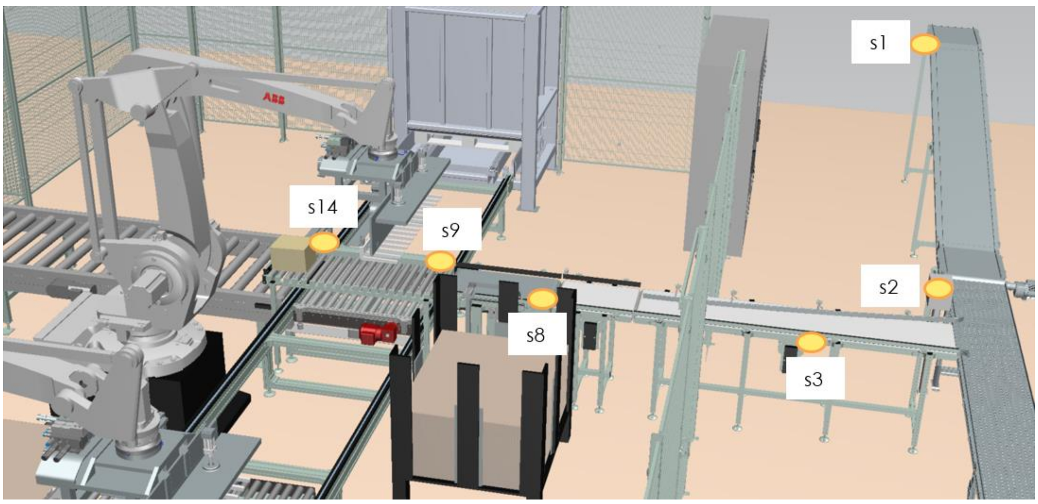

Fig.10 Location of the sensors on one of the entry conveyor for boxes to the palletizing area

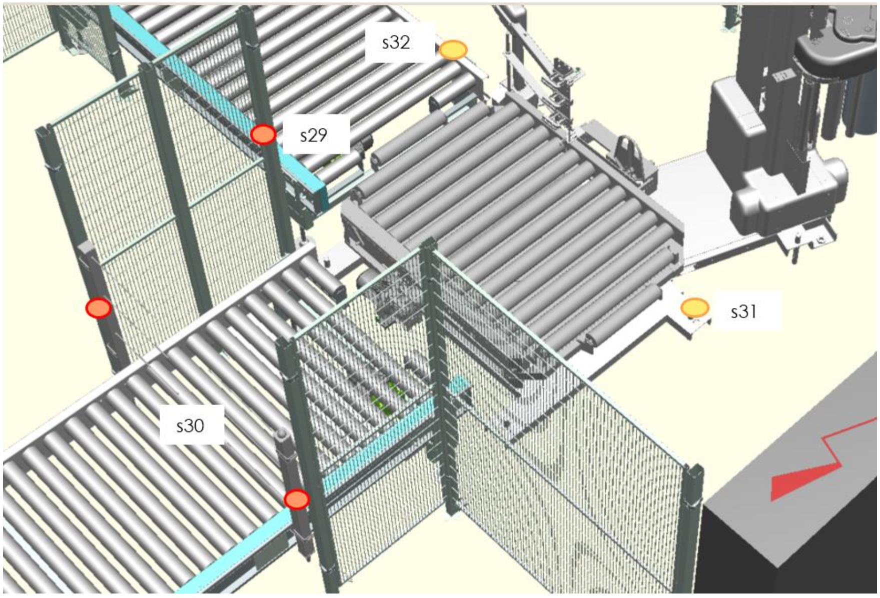

Fig. 11 Location of the sensors in the wrapping area

Table 1 includes the categories of sensors required in the robotic cell, the signals provided and the functional conditions imposed to the cell operation.

Table 1 Characteristics of sensors identified in the robotic cell

Number	Sensor type	Signal type	Functional role	Interconditionings
s1	Photoelectric sensor with diffusion	Digital	Box detection	The conveyor is moving while the boxes are detected
s2	Photoelectric sensor with diffusion	Digital	Sorting boxes	The boxes are routed on one of the 3 conveyors
s3, s4, s5	Photoelectric sensor with diffusion	Digital	Counting boxes	After a certain number, the orientation of the boxes will change
s6, s7, s8	Photoelectric sensor with diffusion	Digital	Box detection	Depending on the box number, the reorientation rod will be actuated
s9, s10, s11, s12, s13, s14	Photoelectric sensor with diffusion	Digital	Detection of boxes to be picked up by the industrial robot	After the optimal number of boxes is reached, they are picked up by the effector
s15	Photoelectric sensor with diffusion	Digital	Pallet detection in the pallet dispenser	A pallet is lowered if at least one is present in the dispenser
s16	Photoelectric sensor with diffusion	Digital	Pallet detection at the end of the conveyor	Pallet at the end of the storage conveyor; pick up by chain conveyor
s17, s18, s19	Photoelectric sensors with reflection	Digital	Pallet detection; command generation to the lift module	The presence of the pallet on the chain conveyor, above the lift module
s20, s21, s22	Photoelectric sensor with diffusion	Digital	Pallet detection	The presence of the pallet in addition on the conveyor

s23, s26, s27	Safety light barriers	Digital	Complete pallet presence detection	Pickup of the complete pallet by the transport module
s24	Photoelectric sensors with reflection	Digital	Pallet start detection (when entering)	The presence of the complete pallet
s25	Photoelectric sensors with reflection	Digital	Pallet end detection (when entering)	The presence of the complete pallet
s28	Safety light barriers	Digital	Complete pallet presence detection	The complete pallet starts to the wrapper
s29	Safety light barriers	Digital	Human operator presence detection	Stop in case of human operator interference
s30	Safety light barriers	Digital	Detection of the presence of a human operator/pallet towards the system exit	Start conveyor complete to exit the system; takeover by human operator
s31	Photoelectric sensor with diffusion	Digital	Pallet detection in wrapping area	The pallet advances to the rotary table; beginning of foiling
s32	Photoelectric sensor with diffusion	Digital	Sends wrap completion signal	Complete pallet to the last conveyor, rotary table stop

4. Conclusion

The main original contributions of this research are:

- the new employment of Siemens Process Simulate environment for developing the mechanisms, positions and operations for the process simulation of the robotic cell designed in Siemens NX environment;
- elaboration of the flowchart detailing all the processes, events and signals specific to each operation from the robotic cell;
- identification of the used signals and their interconditionings with other components of the virtual prototype of the robotic cell.

Future work will focus on fully programming the robotic cell.

5. References

[1]. Diana-Maria Cicîrîc – Practică de cercetare 2 (2024)

OFF-LINE PROGRAMMING AND SIMULATION OF A FLEXIBLE PAINTING CELL WITH TWO ARTICULATED ARM INDUSTRIAL ROBOTS

DRAGOMIRESCU Alin-Marian, Cristina PUPĂZĂ

Facultatea: Inginerie Industrială și Robotică, Specializarea: Robotică, Anul de studii: II,
e-mail:dragomirescu.alin.marian@gmail.com
Conducător ştiinţific: Prof.dr.ing.

ABSTRACT: The purpose of the application is to reduce the painting time of a car body and to increase the uniformity of the paint layers
KEYWORDS: simulation, painting, robots, cell, sensors

1. Introduction

The purpose of the application is to reduce the painting time of a car body and to increase the uniformity of the paint layers. The car is lifted by means of 4 jacks, each being fixed under a wheel. While the car is raised, the transport system is positioned under it and the operator fixes the jack mounted on the trolley in special places on the car body. The trolley is handled by the human operator, being positioned in the cell; later the operator evacuates the cell.

Fig. 1 Robotics cell

After the door is closed, the first robot starts the whistling between the 2 robots where there is a gap, not to hit the middle area of the car. The painting trajectories are linear in zigzag, plane parallel to the ground.

The car is painted in 4 stages: frontal area (Hood+front bar); ceiling; rear area (luggage rack and rear bar); the side area (doors together with the wings of the car).

2. The simulation

The first step in the painting process is to prepare the car. This essential stage consists of a series of activities designed to ensure a quality and sustainable end result. Specifically, machine preparation involves the following operations:

-- Cleaning the machine from dust and oil: A thorough cleaning of the machine surface is carried out to remove any traces of dust, dirt or grease. This can be done with the help of specialized cleaning solutions and appropriate utensils such as cloths or brushes.

-- Covering areas that we don't want to be painted: To protect certain areas of the car that don't need to be painted, such as windows, headlights or other delicate elements, masking materials such as masking foil or masking tape are used . These materials are carefully applied to ensure effective paint protection.

-- Removal of elements so that they are not at risk of being painted: Elements that do not need to be painted or that could be affected by paint, such as exterior trim, grilles or emblems, are carefully removed. This allows access to the surfaces that require painting and prevents possible damage or damage during the painting process. The second stage is the transport on a special trolley to a painting cell.

In order to be able to start painting, the operator must close the cell doors and press a button, which is outside the painting cell, which confirms the fulfillment of his duties. When the operator pressed the button, the sensors under the car must detect the car to start painting.

The robots start painting the car. When the car is painted, the doors will be unlocked and the centering and fixing equipment will be withdrawn.

The car will be evacuated from the painting room and will be left in the drying cell where the protective elements of the car will be removed.

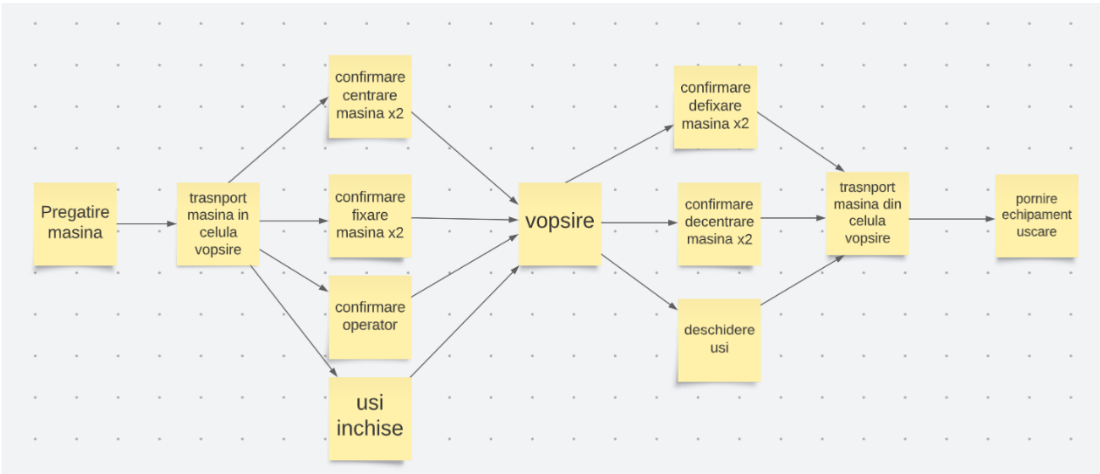

Fig. 2 Flow Chart

After designing the cell and importing the standardized elements into Siemens NX [1], all components were successfully exported and integrated into the Siemens Process Simulate software [2], [3]. Later, kinematics was created for all elements of the cell [4].

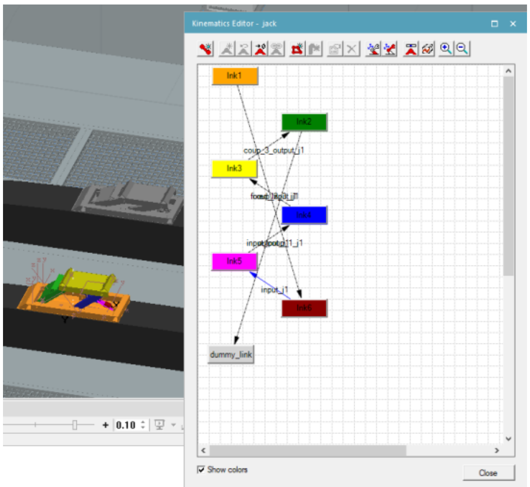

Fig. 3 Kinematics for the 4 cricks

To achieve the kinematics for the 4 jacks mounted on the trolley, the Crank command was used, as the traditional method was not viable. This was necessary to set up the complex movements of the jacks in a precise and efficient way. The Crank command allowed the appropriate definition and control of jack movements according to the specific requirements of the application.

To achieve this kinematics, the program was used to insert the required elements, which included 8 rotational motions and one translational motion related to the associated hydraulic cylinder. These elements were automatically integrated into the simulation system, allowing precise configuration of jack movements according to technical and functional requirements.

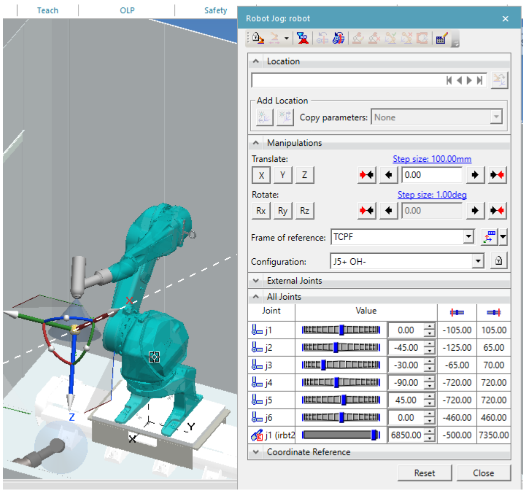

Fig. 4 Kinematics for the Robot

In Fig. 4 the ABB IRB 5510 Robot was added with an additional ground translation axis and the robot's kinematics was tested by moving the robot from the TCP to the effector mounted on the robot.

A capacitive proximity sensor from SICK, model CM30-25NAP-KW1 was used to detect the trolley in the cell. The positions of these sensors can be found also in Fig. 4, in the front and rear ends of the stroller. The sensor will be mounted on a system consisting of rectangular bars.

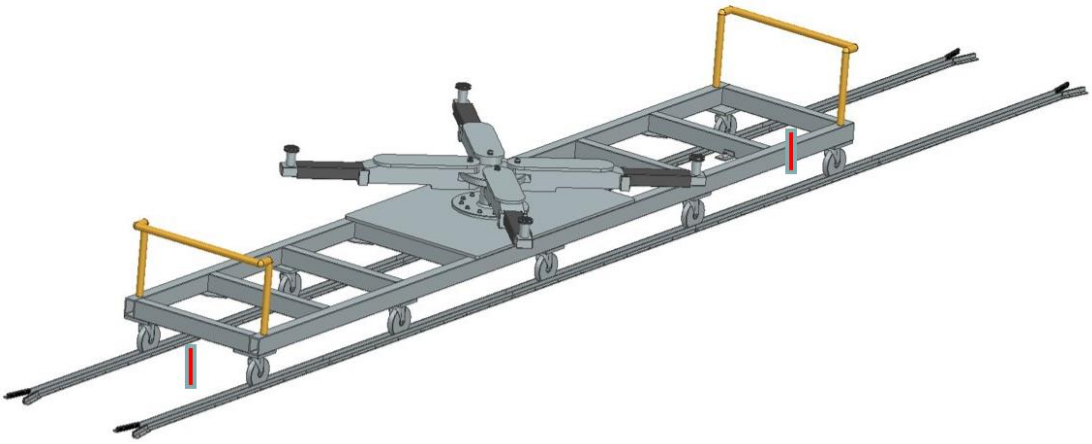

Fig. 5 The position of the sensors in the Cell layout

Fig. 6 CM30-25NAP-KW1

The connection cables for the sensors and the pneumatic elements of the fixing equipment from TUENKERS are connected directly to the CPX, which in turn communicates with the central PLC of the application [5].

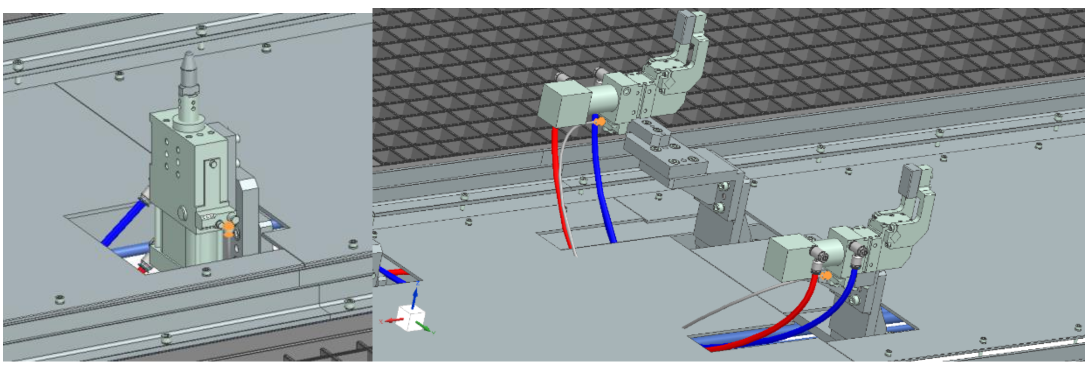

Fig.7 Pneumatic equipment

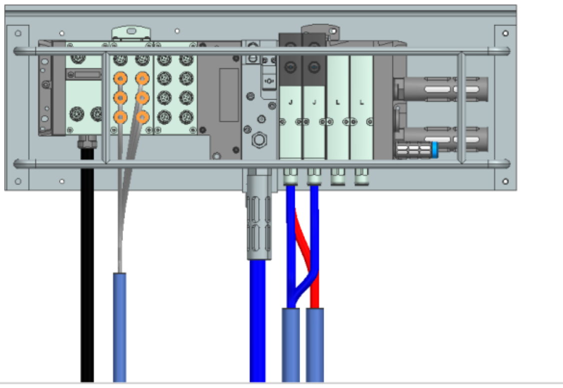

Fig. 8 CPX

By creating device operation & signals within the system, the generation of the necessary signals for the automatic movement and positioning of the devices in the cell can be realized. This command allows to define operations and signals associated with the devices, which will allow to automate and control the movements durinhg the production process of the selected device.

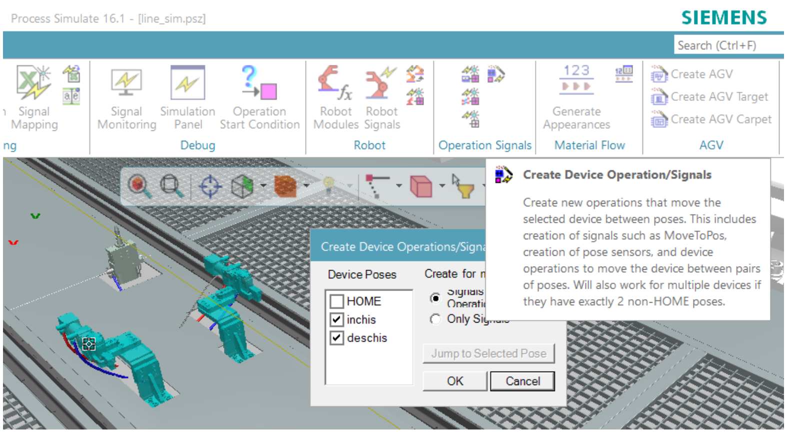

Fig. 9 Signals generation

Sensors can be added from the tab Control > Sensors > choose the sensor it belongs to. This sensor is used in 2 chambers: in the painting cell to detect the correct position and at the same time the presence of the trolley in the cell and in the drying cell to detect the trolley and to activate the painting devices [6]

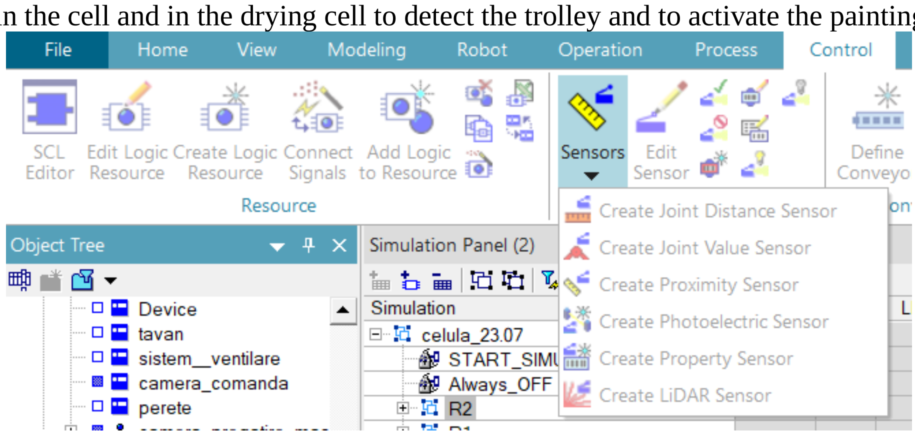

Fig.10 Sensors definition

Signal Name	Memory	Type	Robot Signal Nar	Address	IEC Format	PLC Connec	External Connect	Resource	Comment
Conveyer Position		REAL		No Address	I	✓		Conveyer	
DESCHIDERE POARTA 3 end		BOOL		No Address	I			usa 3	
intrare masina end		BOOL		No Address	I				
DESCHIDERE JACKS1 end		BOOL		No Address	I			jack	
DESCHIDERE JACKS1 end 1		BOOL		No Address	I			jack 1	
DESCHIDERE JACKS1 end 2		BOOL		No Address	I			jack 2	
DESCHIDERE JACKS1 end 3		BOOL		No Address	I			jack 1 1	
DESCHIDERE POARTA 2 end		BOOL		No Address	I			usa 1	
sistem transport masina Op end		BOOL		No Address	I				
DESCHIDERE X-JACK MASINA end		BOOL		No Address	I			X	
Op sistem centrare d end		BOOL		No Address	I			sistem ce	
Op sistem centrare p end		BOOL		No Address	I			sistem ce	
Op1 sistem fixare end		BOOL		No Address	I			sistem fix	
Op2 sistem fixare end		BOOL		No Address	I			sistem fix	
Inchidere usa 3 end		BOOL		No Address	I			usa 3	
Inchidere usa 1 end		BOOL		No Address	I			usa 1	
Paint Robotic Op mirrored mirrored e		BOOL		No Address	I				
Paint Robotic Op end		BOOL		No Address	I				
Cont Robotic Op end		BOOL		No Address	I				
Paint Robotic Op2 end		BOOL		No Address	I				
Paint Robotic Op end 1 1		BOOL		No Address	I				
Paint Robotic Op mirrored end		BOOL		No Address	I				
Cont Robotic Op mirrored end		BOOL		No Address	I				
Paint Robotic Op mirrored mirrored m		BOOL		No Address	I				
Paint Robotic Op2 mirrored end		BOOL		No Address	I				
Paint Robotic Op end 1 1		BOOL		No Address	I				
Deschidere usa 3 end		BOOL		No Address	I			usa 2	
Evacuare masina end		BOOL		No Address	I				
Op inchidere sistem centrare p end		BOOL		No Address	I			sistem ce	
Op inchidere sistem centrare d end		BOOL		No Address	I			sistem ce	
Op deschidere sistem fixare end		BOOL		No Address	I			sistem fix	
Op deschidere sistem fixare 2 end		BOOL		No Address	I			sistem fix	
Walk to WalkLoc2 end		BOOL		No Address	I				
Walk to WalkLoc4 end		BOOL		No Address	I				
TSB Simulation 1 end		BOOL		No Address	I				
Use Device carucior Jack end		BOOL		No Address	I				
Pose end		BOOL		No Address	I				

Fig.11 Signals

In the Module editor, many rules for signals have been added. The first signal is forced to be ON when the simulation starts, because the automation and the simulation of the process cell are considered to be generated when the operators have finished their duties. The second signal becomes positive when the signal from the positive sensor is active. The conveyor speed for the third example can also be set.

To initiate the activation of the two robots, this relies on the closed position of the door and the clamping system to start the painting process. For this purpose, the first program available in the program library of the robot's computer was employied to perform the painting, according to the predefined parameters and instructions.

Module Editor - START

Result Signal	Expression / Called Module
Conveyer_Start	RE(START_SIMULARE)
usa_1_to_inchis	SR(RE(TON(light_sensor,1)),usa_1_at_inchis)
Conveyer_speed	30000
usa_1_to_deshis	SR(RE(TON (START_SIMULARE,1)),usa_1_at_deshis)

Fig. 12 Module editor

In the Robots Editor Module, the first robot program to be number 1 was elected. Afterwards, a program for each robot was created, named r1_door_closed2 and R2_door_closed, to be activated 10 seconds after the cell door was closed.

Module Editor - Robots

Result Signal	Expression / Called Module
R1_programNumber	1
r1_door_closed2	SR(RE(usa_1_at_inchis),TON (usa_1_at_inchis,10))
R2_door_closed	SR(RE(usa_1_at_inchis),TON (usa_1_at_inchis,10))
R2_programNumber	1

Fig. 13 Module editor

After the sensor in the paint cell detects the passage of the conveyor, both the centering and clamping systems are initiated simultaneously. In this initiative, the centering system is the first to come into operation, starting its activity 1 second after the sensor detects the conveyor. This system works to ensure the precise positioning of the part or object on the conveyor by properly centering it.

After the centering system completes its movement and is in the correct centering position, the clamping system is activated. This activation happens one second after the centering system has completed its movement and settled into the correct position. The clamping system is responsible for ensuring the stability and security of the part or object on the conveyor, avoiding any unwanted movement or displacement during transport or the subsequent painting process. Thus, the precise and coordinated sequence of actions between the centering and clamping system ensures an efficient and reliable process within the production line.

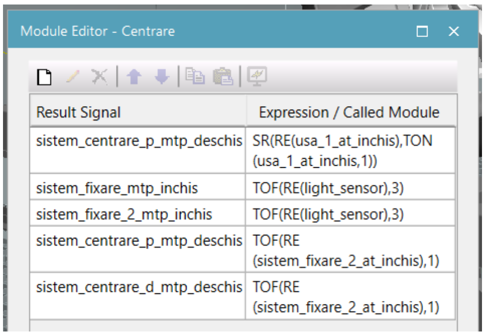

Fig. 14 Module editor

4. Comparrison of the painting robots

In Table 1 a comparative analysis was done with the help of a table in which the parameters of painting robots are highlighted and compared from the largest manufacturers of Industrial Robots on the market. First, an important factor in choosing the robot was the accessibility of a JT format to do an offline simulation of the cell operation in the Process Simulate environment. On this criterion, the only manufacturer that provided this service was ABB. In this sense, the Robots from ABB were chosen, namely model IRB 5510 and IRB 5400.

Table 1. Robots

Robot	P-50iA	EPX2750	IRB 5400	IRB 5510
NR. OF AXES	6	6	6	6
Axa 1	±137.5°; 160°/s	± 150°; 124°/s	± 300°; 137°/s	± 105°; 100°/s
Axa 2	±135°/-65°; 160°/s	-40°/-+90°; 127°/s	±160°; 137°/s	+125°/-65°; 100°/s
Axa 3	±147°; 160°/s	+10° /-+90°; 112°/s	±160°; 137°/s	+65°/-70°; 100°/s
Axa 4	±540s; 460°/s	±260°; 360°/s	Fără limită; 465°/s	465°/s ; +/-720°
Axa 5	±540s; 480°/s	±270°; 360°/s	Fără limită; 350°/s	350°/s; +/-720°
Axa 6	±540s; 600°/s	±260°; 360°/s	Fără limită; 535°/s	535°/s; +/-460°
Repeatability	0.2 mm	0.5 mm	0.15 mm	0.15 mm
MoUNTING	Podea	Podea	Podea	Podea, Perete, Invers
The maximum load added to the wrist	7.5 kg	10 kg	10 kg	13 kg
Protecţion	IP66	IP66	IP67	IP66
Footprint	451x451 mm	750x580 mm	750x580 mm	581x717.5 mm

From the point of view of the bearing load, the ABB IRB 5510 robot was chosen, over the IRB 5400 model, because it is a newer generation and has a higher maximum wrist load of 13 kg, compared to only 10 kg of the older model.

From the point of view of the mounting possibility, the robot model from ABB IRB 5510 is the most reliable, because it can be mounted in 3 ways: floor, wall and vice versa. The other robots can only be mounted on the floor and cannot be mounted differently

Following the analysis of the above functional characteristics, it was decided to choose the ABB IRB 5510 robot to be integrated into the robotic painting cell.

5. Conclusions

The Cell layout is automated to eliminate the repetitive work of operators, to increase productivity and product quality. The originality of the work is represented by the design of the cell in the NX 12 environment and the novel simulation of the process in Process Simulate. Regarding the simulation of the process, a new achievement was the use of the OLP commands and the operator module, with an operator being introduced to transport the car. By developing the simulation and off-line programming in the proposed virtual cell it is was possible to demonstrate the usefulness and importance of such a process of verification and preparation in a virtual environment at an industrial scale, intended to bring benefits such as:

• The possibility of realizing the spatial layout of the machinery and equipment in the factory in an optimal and efficient way from the point of view of the painting process;

• The possibility of checking the compliance with safety and ergonomics standards regarding the human operator;

• The possibility of checking the feasibility of equipment location solutions and robots;

• The possibility of creating trajectories and robot programs that can be downloaded and uploaded directly to the physical robots in the hall;

• The possibility of predicting collision or interference situations in the virtual space between machines and/or robots and solving them before they cause material damage in the real environment;

All these benefits of using simulation and off-line programming of a robotic application in the industrial environment help manufacturing companies to save material resources and time in the process of developing new products aimed at making people's lives easier. Through the robotization of the painting cell, the operator no longer has to stay in a toxic environment and the painting is done faster.

In conclusion, the objective of designing, modeling, simulating and validating a robotic cell integrating two articulated arm type robots, with the role of painting the car body in an automated service mode was demonstrated.

6. References

[1]. Dobrescu T. – Bazele Cinematicii Robotilor Industriali, Ed. Bren, ISBN-973-9427-02-2, Bucureşti, 1998

[2]. Nicolescu A., Coman C. - Robotica 2, note de curs si aplicatii, UPB, 2017

[3]. Nicolescu A., Coman C. - Robotica 3, note de curs si aplicatii, UPB, 2018

[4]. Nicolescu, A., Cristoiu C. – NX CAD Basic – Proiectare asistat de calculator, Editura Politehnica Press, ISBN 978-606-515-914-3, 2020, Bucuresti

[5]. Nicolescu A., Conceptia si Exploatarea Robotilor Industriali, Editura Politehnica Press, 473 pag., ISBN 978-606-515-916-7, 2020, Bucuresti

[6]. Silvestru C. – Bazele Programarii Off-line a Robotilor Industriali, note de curs si suport aplicatii, UPB 2020

OFF-LINE PROGRAMMING AND SIMULATION OF A ROBOT CELL FOR PLASTIC BOTTLE PALLETIZATION USING "PROCESS SIMULATE" SOFTWARE. PROGRAMMING BASED ON SIGNALS

GIURCAN Andreea-Loredana, Cristina PUPĂZĂ

Faculty: Industrial Engineering and Robotics, Speciality: Robotics, Year: 2,
e-mail: andreeagiurcan@outlook.com

ABSTRACT: The paper consists in the continuation of the diploma work by carrying out the off-line programming and simulation of a robotic cell for palletizing bottle sets with plastic bottles and cardboard separators, integrating an industrial robot, MOTOMAN GP180 type of articulated arm with 6 numerically controlled axes, which is equipped with an effector with pneumatically actuated jaws and a vacuum subsystem. The simulation is performed based on the signals in Process Simulate software

1. Introduction

The paper consists in the continuation of the diploma work, by carrying out the off-line programming and simulation, based on the signals in the Process Simulate work environment, of a robotic cell for palletizing bottle sets with plastic bottles and cardboard separators. The cell was made as part of the thesis based on a foundation film, and later improved to eliminate the need for human operators, thus making the cell safe and automated.

Fig.1.1. The selected robotic cell starts in the foundation film with the pallet dispenser. [1]

Fig.1.2. The main action in the chosen robot cell. [1]

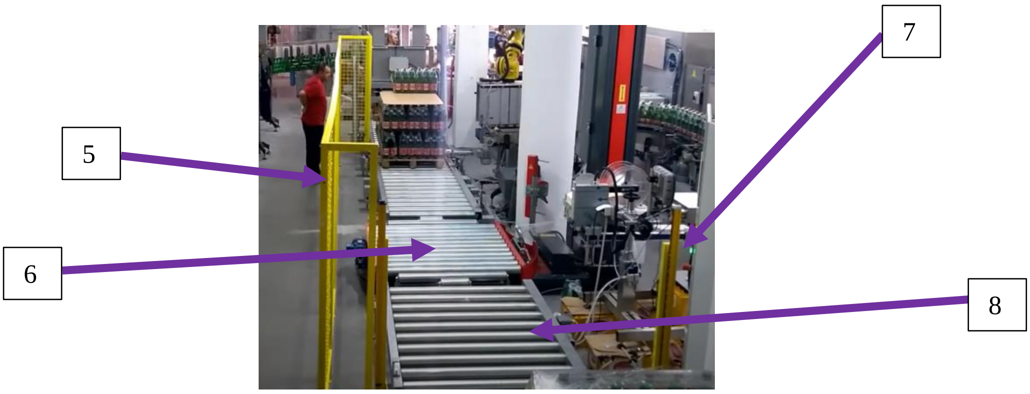

Fig.1.3. The end part of the cell is observed. [1]

Legend: [1]

1. Pneumatically operated piston for centering the pallet;
2. Roller conveyor that brings empty pallets to the robot;
3. Support of cardboard separators;
4. Modular belt conveyor that transports the bottle sets with 2 liter plastic beer bottles;
5. The protective fence surrounding the cell;
6. Vertical wrapping machine with rotating base;
7. Barrier-type sensor for exiting the cell of the full stack;
8. Roller conveyor for the evacuation of the complete stack.

2. Types of sensors used in the designed cell

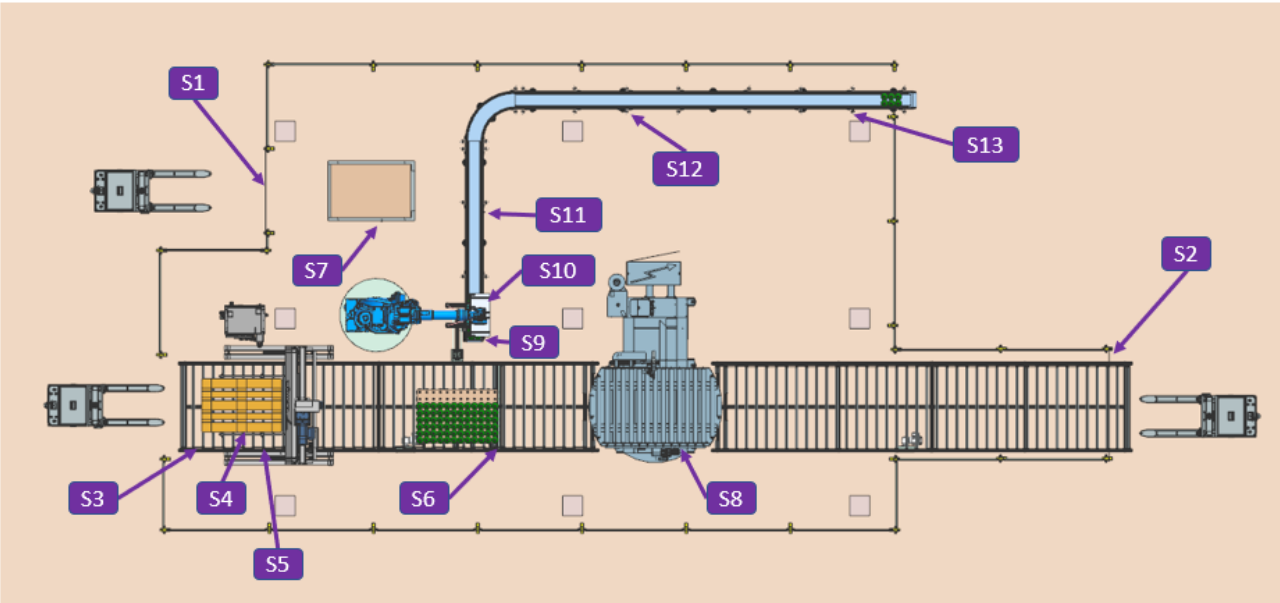

Fig.2.1. Top view with positioning of all sensors. [1]

Table 1. Specific details of each sensor used in the cell *[1]*

Specifications	Sensor type	Function
S1, S2	Barrier type sensors (these are used in pairs)	It detects the supply of the cell with cardboard separators and the evacuation of full stacks.
S3 → S13	Photoelectric sensors	Detects objects carried in the cell.

3. Signal-based simulation performed in the Process Simulate work environment

The simulation continues with the robot picking up a separator, when the pallet has been stopped and fixed in the appropriate position. [1]

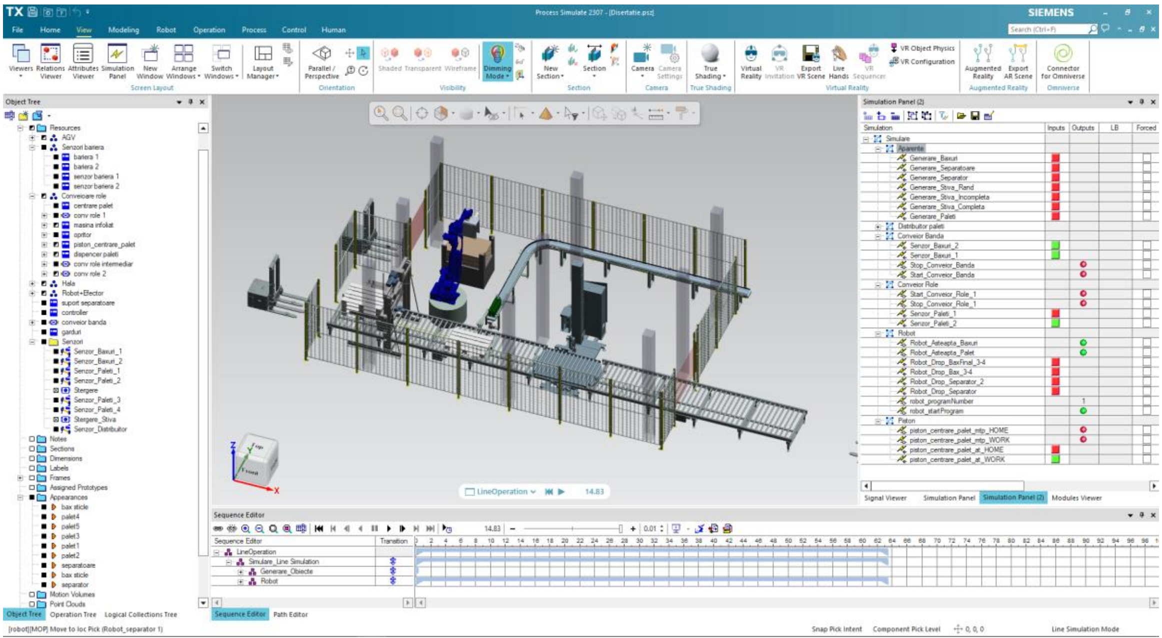

Fig.3.1. The robot takes the first separator [1]

Further, the two bottle sets are detected near the robot, and it picks them up, then places them on the pallet. [1]

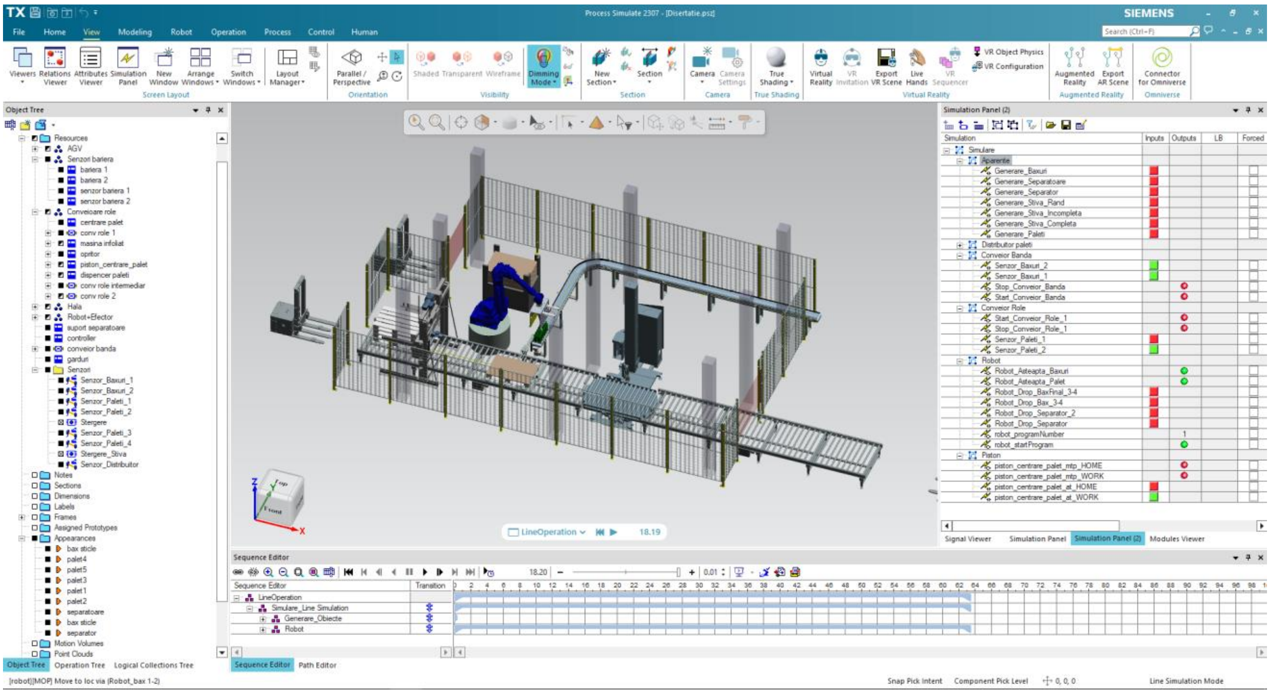

Fig.3.2. The separator is placed on the pallet, and the robot takes the bottle sets from the belt conveyor [1]

After the first sets of bottles are deposited, two new sets of bottles are waiting at the end of the belt conveyor. This is checked with the help of the two conveniently positioned sensors. [1]

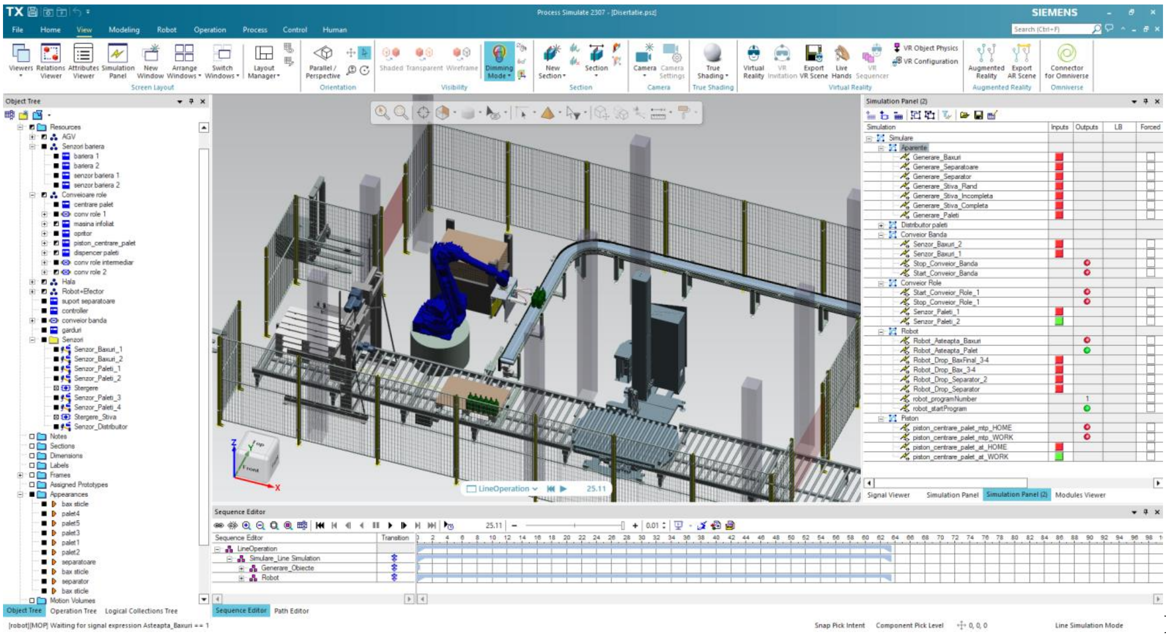

Fig.3.3. The first sets of bottles is deposited and the robot waits for the next one set [1]

After the second round of bottle sets has been deposited, the appearances at the deposit point are replaced by an appearance consisting of a pallet, a separator and the first row of bottle sets, and the robot then takes over the second separator. [1]

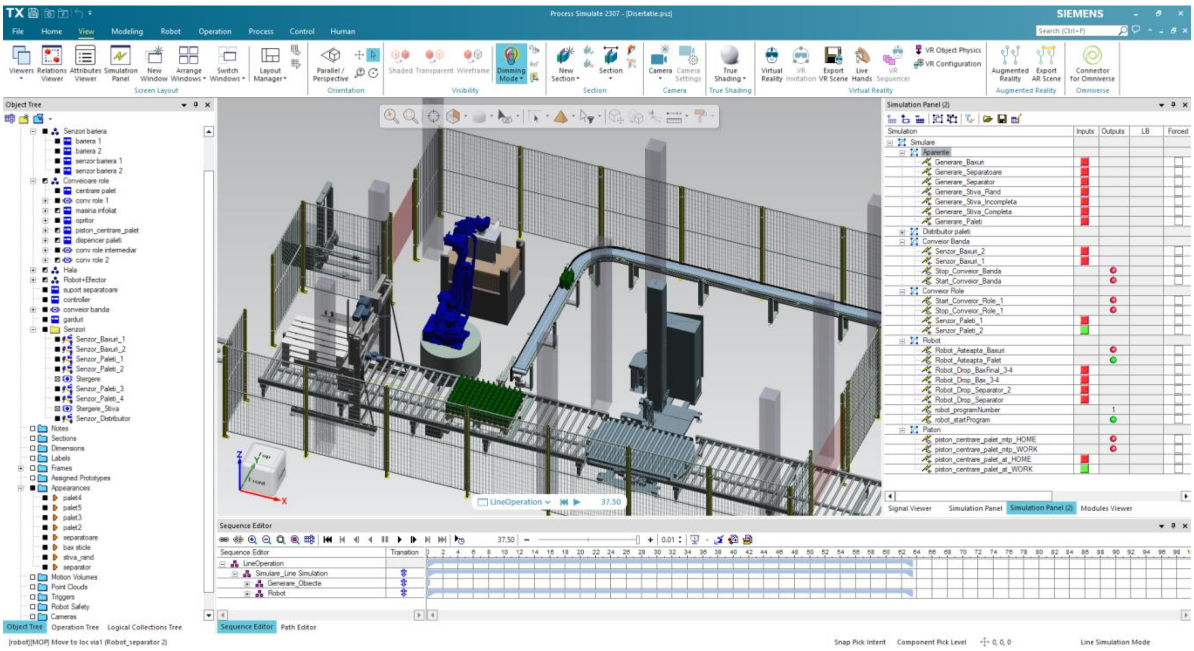

Fig.3.4. Displaying the first row of sets of bottles on the pallet and picking up the second separator [1]

After the second separator has been deposited, the appearances are again replaced with an appearance of an incomplete stack, and the robot is about to pick up the last round of bottle sets. [1]

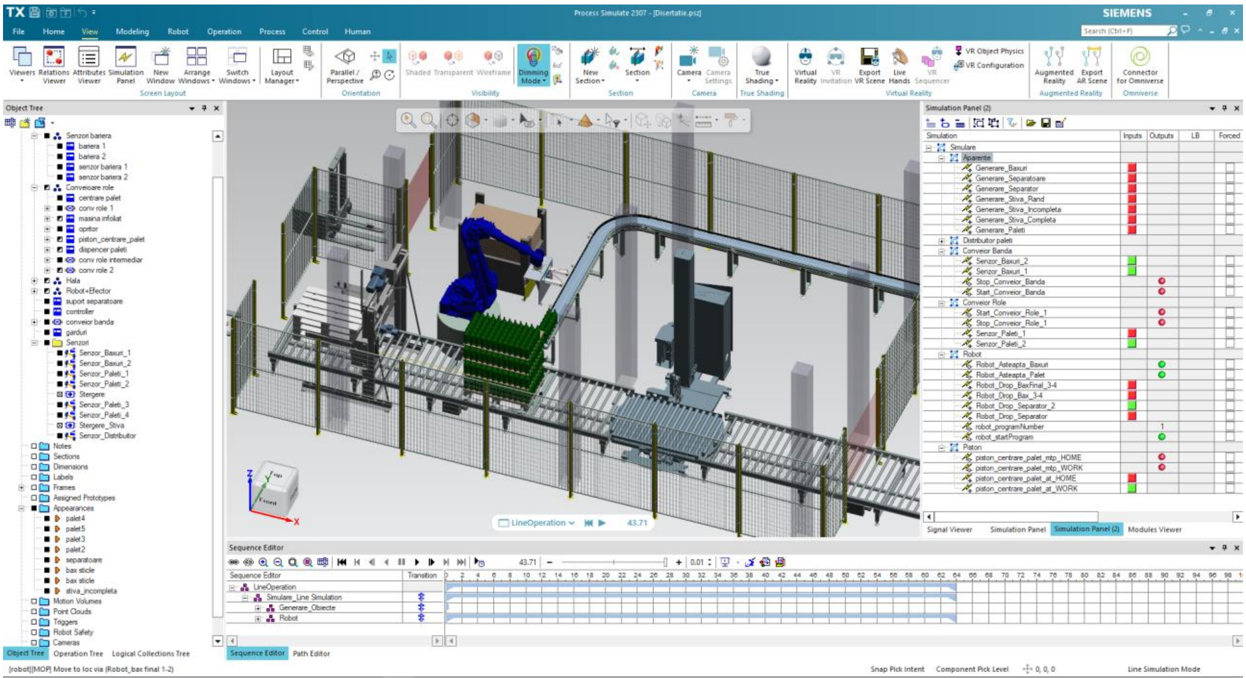

Fig.3.5. Displaying an incomplete stack [1]

After the robot deposits 2 more sets of bottles, the appearances are replaced with another appearance of a full stack, and now it waits for the plunger to retract for the pallet to continue its path. [1]

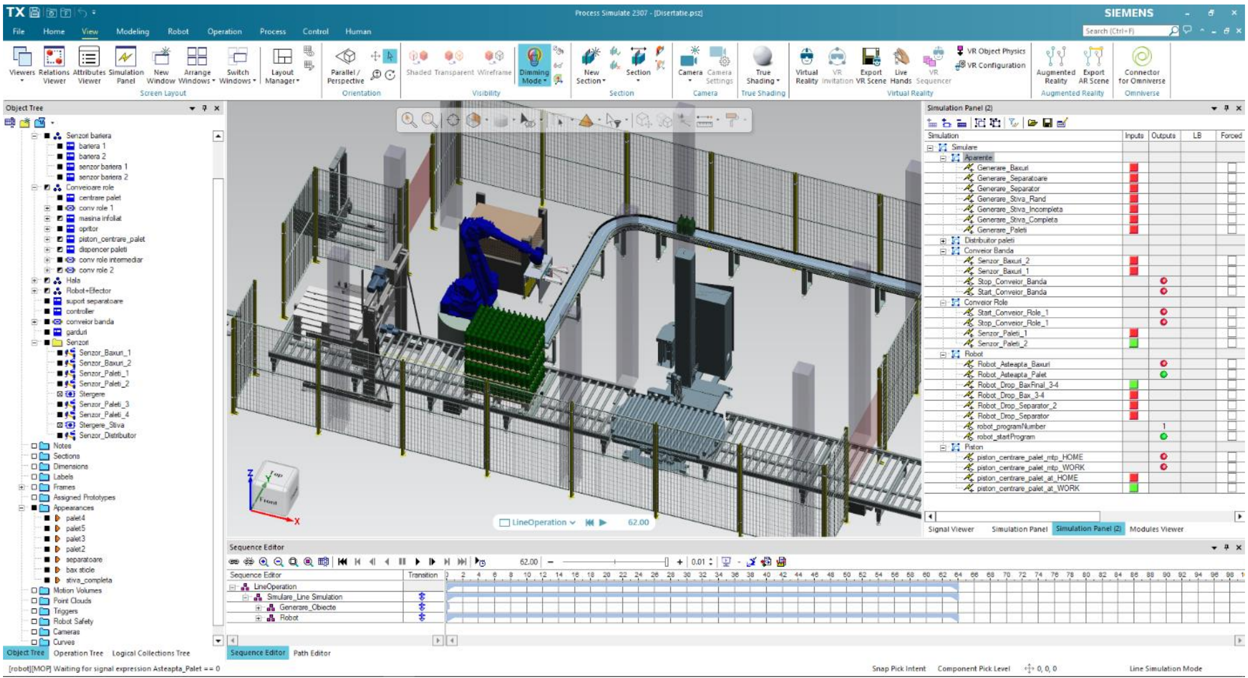

Fig.3.6. Replacing appearances with the full stack [1]

The stack then continues its path until it is stopped at the wrapping system. [1]

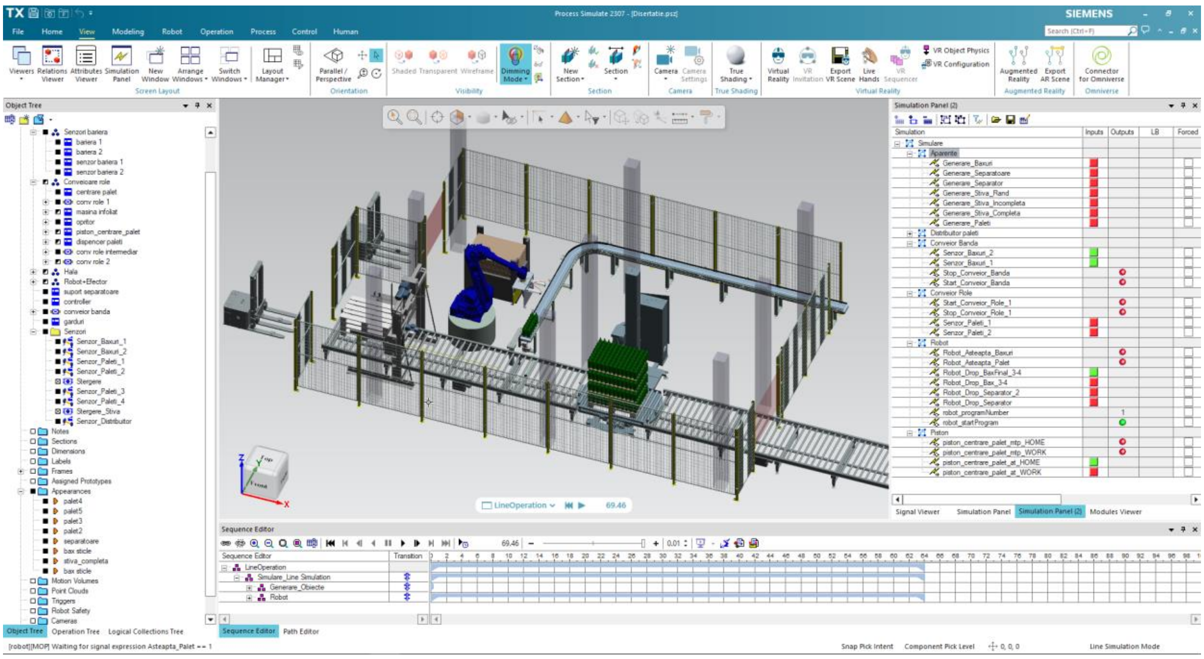

Fig.3.7. The stack is stopped at the level of the wrapping system [1]

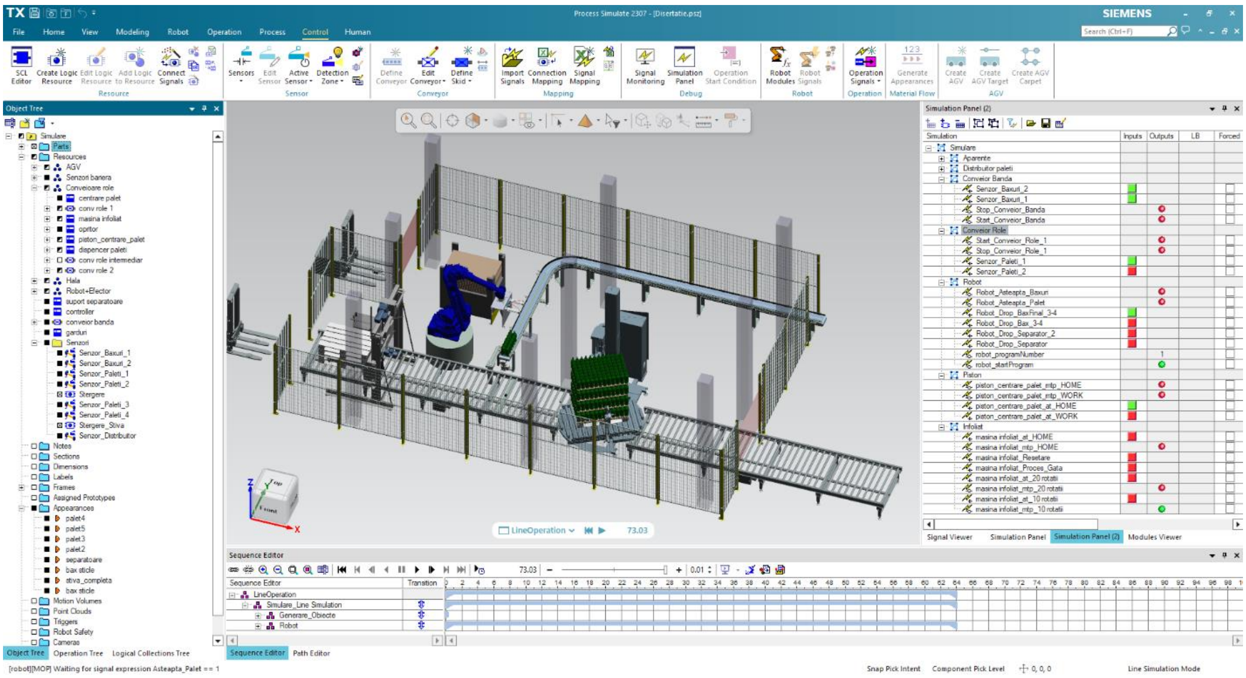

Fig.3.8. Wrapping simulation [1]

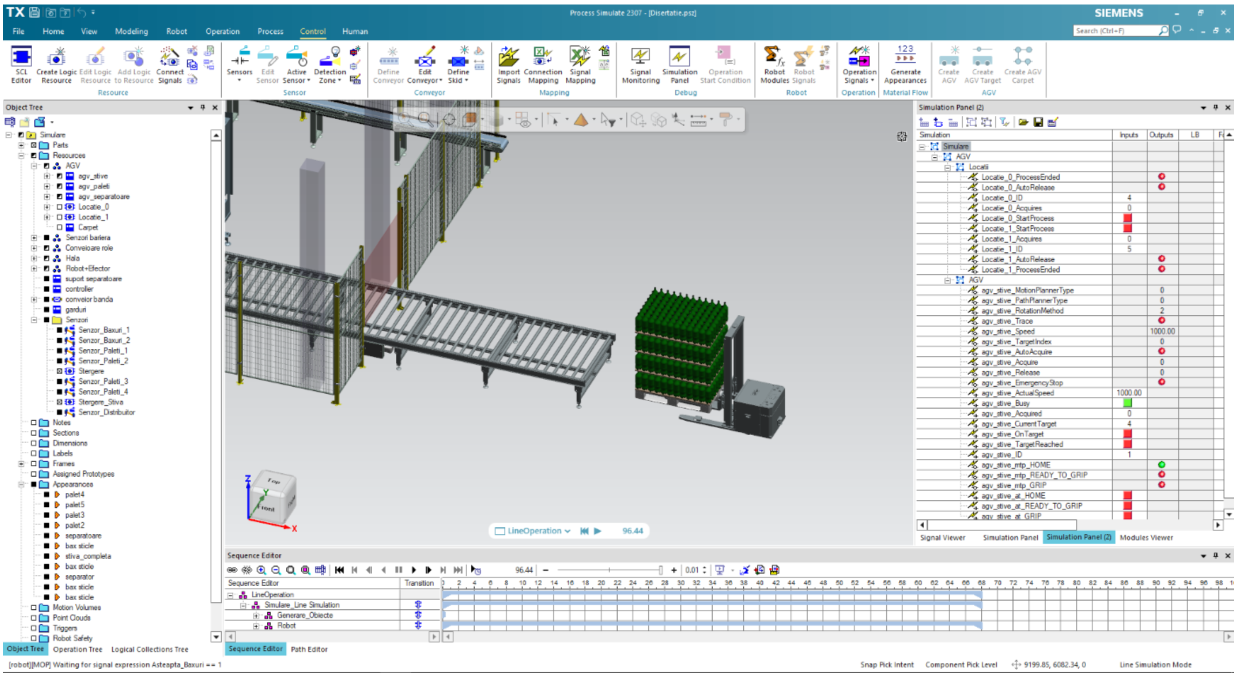

Fig.3.9. Picking up the complete stack with the help of the automatic guided vehicle [1]

4. Conclusions

After the simulation was completed the following changes were done:

- The necessary photoelectric sensors were added to the cell
- Automated guided vehicles were employed to eliminate the need for human operators

5. Bibliography

[1] Andreea-Loredana Giurcan – Cercetare științifică și practică 4 (2024)

STUDY AND 3D PRINTING OF AN INNOVATIVE JOINT FOR THE EFFICIENT ASSEMBLING OF WOODWORK

CODREANU Irina-Maria, PUPĂZĂ Cristina

Faculty: Industrial Engineering and Robotics, Study Programme: Industrial Engineering,
Year of Study: 4, e-mail: irina.codreanu01@gmail.com

ABSTRACT: The present study introduces a concept of an innovative joint which aims to fundamentally transform the process of furniture assembling. In a period of fast-paced industrial developments and an increasing interest in new technologies, sustainable materials and practices, the simple notion of a joint for furniture assembling can be upgraded in such a way that it may renew the whole industrial process. This study presents the main key steps in the development of such a product. First the review of what is already on the market is presented. Then the design of multiple variants, additive manufacturing procedures to obtain the joint and its versatility are described. The structural analysis of the assembly and an optimization attempt of the production system are also included. These viewport is intended to help in the development of time and cost-effective product development that also follows recent sustainability recommendations.

KEYWORDS: innovation, furniture, sustainability, additive manufacturing, optimization

1. Introduction

The drive to develop innovative products has always been a fundamental aspect of human nature. Innovation, through the evolving needs of people, has led to progress in many different domains. The field of furniture assembly and manufacturing is one of the vastest ones as well as one of the most popular for young people. It is hard to see furniture as an indispensable item when everyone is focused mainly on technological gadgets, but the need for furniture was, is and will always be present.

Ever since the start of building structures and objects from wood, there has been a need to find innovative ways of putting the pieces together. This is what led to the development of joinery – a collection of methods which use shapes, hardware, and bindings to hold pieces of wood together. In ancient times, carpenters used only crafted wood pieces that would be joined without any additional tools or solutions [1].

In Fig. 1.1 some complex joints can be compared, which have been used since the very beginning in furniture manufacturing. In Fig. 1.2 some contemporary hard pieces for joining the furniture are illustrated.

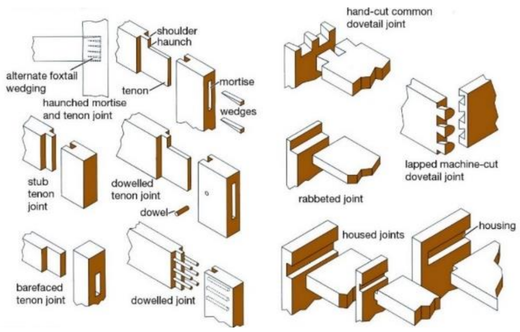

Fig. 1.1 - Basic timber joints [2]


Fig. 1.2 - Basic woodworking hardware [3]

The joints introduced aim to provide ease of use, flexibility, modularity, and sustainability, compared to traditional methods. Although traditional joints have been used since antiquity and their efficiency is not contested, nowadays, there is a tremendous amount of material loss in many industrial processes, such as screws, dowels, hinges and so on. Additionally, even though these methods are tried and true, they require specialized tools, skills and instructions, while the joint developed in the present study will not need any additional features. The concept of additive manufacturing is focused on how to add only the necessary material, and not remove any, leading to less waste [4]. Applications of additive manufacturing in the development of furniture are an emerging field of study. The possibility of 3D printing enables the design engineer to create models with no limits of shape, size, additional features or colour. Additionally, the versatility of the 3D printers allows for numerous materials to be used for different products [5].

In this research, main key steps in the development of the 3D printed joint are analyzed. To ascertain the need for the product and how it should behave, a brief analysis of the market is conducted, and several concepts are generated. Designs for other products, two similar joints which aid to assembly the bookshelf are then shaped. Static analysis is also performed on an assembly to test how the joints will behave under specific loads and to see if the material can be removed and if the joint can be reshaped for mass reduction. After the static analysis a topology optimization is performed to establish if further modifications can be done to the initial design of the joints. Lastly, the manufacturing system of the final product is developed, analysed and optimized, to ensure its efficiency.

2. Development of the joint

To better understand the type of product that is created, a short study was conducted on potential customers. Through this, there were established clear requirements for the product, as can be seen in Table 1. Each requirement is assigned a score of relative importance.

Table 2.1 – Ranking of customers' requirements

Customers' requirements	Relative importance
Stability	5
Ease of handling	4
Safe	5
Fit	4
Modularity	3
Sustainability	3

The general function of the furniture joint can be considered as "joining of complex furniture structures". This function can very well be split into three critical functions as follows:

- joining of furniture pieces
- holding of the furniture pieces
- stability to furniture assembly.

The critical functions of a product are tasked with keeping the development of important features of the product in line with the actual purpose of the product. In this manner, several possible partial solutions were introduced. These solutions were the result of general effects of the critical functions. In Table 2 are illustrated the critical functions and their possible partial solutions.

Table 2.2 – Possible partial solutions

Function No.	Name of the critical function	Possible partial solutions
1.	Joining furniture pieces (Ø2)	S1. Cap-like joint S4a. Two piece joint with screws S4b. Puzzle-like joint
2.	Holding of the furniture piece (Ø3)	S1. Self-contracting joint S3. Claw-like edges S5. Adhesive coating
3.	Stability to furniture assembly (Ø7)	S1a. Different infill density of 3D print S1b. Different infill pattern of 3D print S5a. Use a denser material

Of all the above solutions, a few were retained for each critical function and were ordered in Table 3 to generate concepts.

Table 2.3 – Solutions for concepts

Critical function Ø2: Joining furniture pieces	Critical function Ø3: Holding of the furniture piece	Critical function Ø7: Stability to furniture assembly
Two-piece joint with screws	Self-contracting joint	Better infill density of 3D print
Puzzle-like joint	Claw-like edges	Better infill pattern of 3D print
Cap-like joint	Adhesive coating	Denser material

In Table 4 simplified sketches of main concepts from Table 2.4 are presented.

Table 2.4 - Concepts

Concept	Sketch	Description
C1	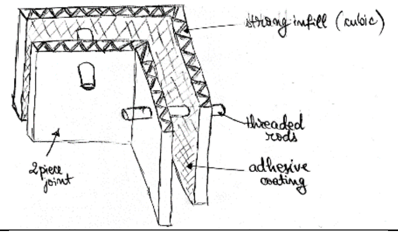	A two-piece joint, fastened through threaded rods. For added support, the inner walls of the joint are coated with an adhesive. The infill pattern of the joint is cubic, one of the strongest infill patterns.
C2	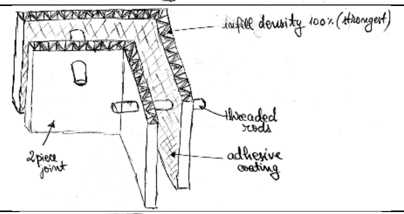	A two-piece joint, fastened through threaded rods. For added support, the inner walls of the joint are coated with an adhesive. The infill density of the joint is 100%.
C3	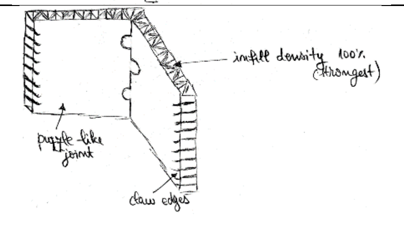	A two-piece joint that connects like a puzzle. Small claw like pins pierce the wood for added support. The infill density is 100%.
C4	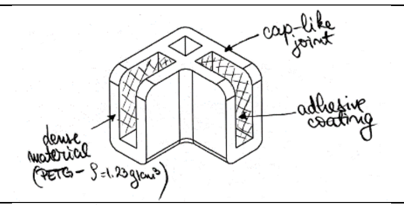	A joint that caps the wood pieces. For added support, the inner walls of the joint are coated with an adhesive. The material is PETG (ρ = 1.23 g/cm^3), the densest filament material.
C5	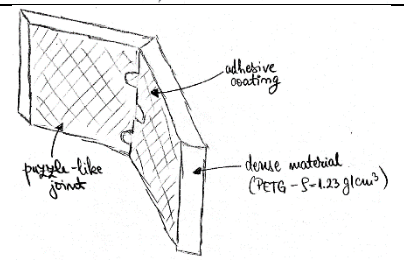	A two-piece joint that connects like a puzzle. For added support, the inner walls of the joint are coated with an adhesive. The material is PETG (ρ = 1.23 g/cm^3), the densest filament material.

After the comparison of all the concepts it was decided that the best one would be C4. The design of this concept will be further developed.

3. Design and manufacturing of the joint

Following the initial concept, two joints were designed in a similar style, to be used in the assembly of a bookshelf. In Fig. 3.1 a joint resembling an "L" shape is illustrated, while in Fig. 3.2 the "T" joint can be seen.

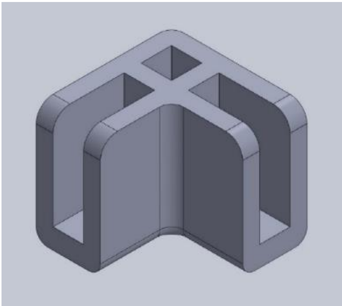

Fig. 3.1 – "L" joint

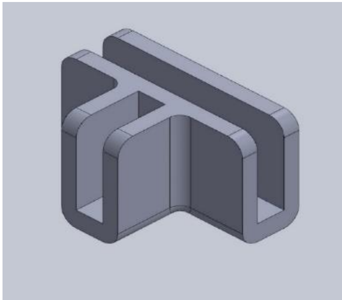

Fig. 3.2 - "T" joint

The "L" joint is used in the corners of the assembly, whereas the "T" joint can be found linking the corner of a wood board with the length of another one. In Fig. 3.3 the assembly of the bookshelf, modelled in SolidWorks is presented. The assembly contains 10 "L" joints, 12 "T" joints and 8 wood boards of different dimensions. This design of bookshelf was chosen because it is rather complex, and the quantity of joints used facilitates a comprehensive result in a future analysis of the assembly.

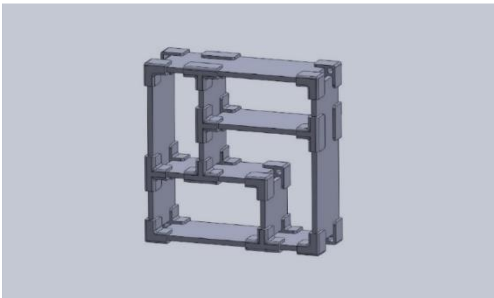

Fig. 3.3 – Assembly model

The manufacturing method chosen for this product is additive manufacturing, more specifically fused deposition modelling. This is a 3D printing process in which a part is created by the deposition of layers of material. Performing this operation is a gantry robot with an extruder which moves in X, Y and Z directions. The filament is heated to a specific temperature and then extruded through a nozzle on the build plate. The layers are built up one by one to create the product. Once the part is finished, it can be detached from the build plate [6].

In Fig. 3.4 a schematic view of the 3D printer can be seen with its most important parts: the extruder, the hot end and how the axes of the printers move for the product to be manufactured.

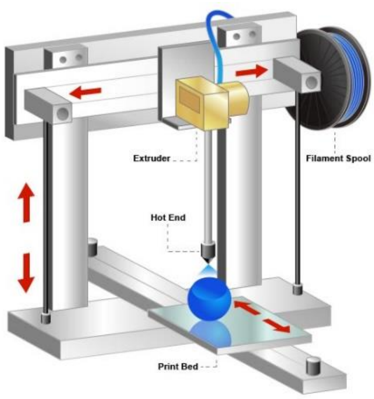

Fig. 3.4 – 3D printer and 3D printing process [7]

3D printing steps:

1. Design preparation for 3D printing – The product is created using a computer–aided design (CAD) software and then translated into the format that is understandable for the 3D printer.
2. Slicing – An .stl file is introduced into a slicing software. This type of software is used to create instructions for the 3D printer. These instructions are generated as G-Code.
3. 3D printing – The 3D printer reads instructions from the sliced file and builds the part layer by layer.
4. Post-processing – After printing, the product might need minor modifications.

Considering the overall characteristics and price of the different materials used in fused deposition modelling, the one chosen for these products is PLA [8].

PLA, also known as Polylactic Acid, is the a well-known and most used material for 3D printing. It is a type of polyester made from fermented plant starch. PLA's material qualities allow it to be employed for biodegradable medical equipments (such as screws, pins, plates, and rods that are intended to biodegrade in six to twelve months), plastic films, and bottles [9].

The manufacturing of PLA produces 68% fewer carbon emissions, requires 65% less energy than created conventional polymers, and is toxin-free. Should the appropriate end-of-life scenario be adhered to, it can also continue to be environmentally friendly [9].

In Table 3.1 the properties of this material are specified for the analysis of the parts.

Table 3.1 – Properties of PLA [10]

Properties	
Density	1250 kg/m^3
Young's Modulus	2222,9 MPa
Poisson's Ratio	0,3
Tensile Strength, Ultimate	20,0 – 100 MPa
Tensile Strength, Yield	28,3 – 101 MPa

After the completion of the CAD model the first important step towards 3D printing is the choice of the file format. While the standard file format for SolidWorks files is .sldprt, in order to start the 3D printing process, the model has to be saved in an .stl format. This format allows for the model to be imported in a 3D printing slicing software, such as UltiMaker CURA.

The joints are opened in the new software and then different parameters are modified to obtain the fastest and most accurate 3D printed part. There are many characteristics of a part which can be modified, but in this case, the only ones that are of interest are the infill density and the infill pattern. Due to the limited time and material costs, the actual parts were printed with an infill of 20%.

In Fig. 3.5 the "L" joint il illustrated and its parameters in UltiMaker CURA, as well as the "T" joint are described in Fig. 3.6.

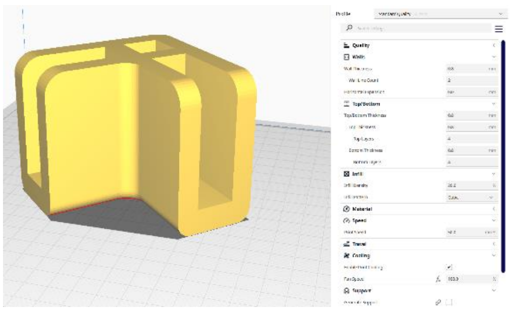

Fig. 3.5 – "L" joint parameters

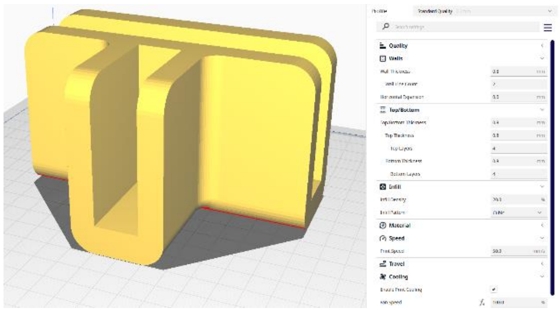

Fig. 3.6 – "T" joint parameters

The 3D printing process is then started. In a 3D printing machine, the filament is inserted, and then the printing can begin. In Fig. 3.7 and Fig. 3.8 the final parts manufactured are illustrated.

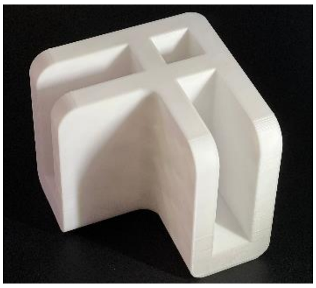

Fig. 3.7 – Final "L" joint

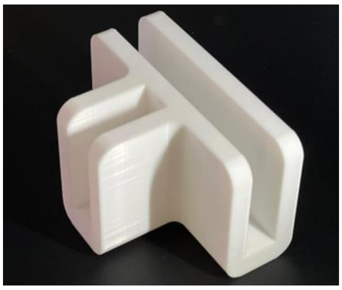

Fig. 3.8 – Final "T" joint

4. Analysis of the assembly

Computer Aided Engineering (CAE) is a tool which helps in the design, analysis, and manufacturing of the products. CAE software enables the simulation of different phenomena, as well as optimization of design for products and processes. The Computer Aided process usually follows three steps: pre-processing, solving and post-processing.

Additive manufacturing is advantageous in the development of furniture not only because it offers the possibility of creating comples shapes, but also because of the significant reduction in production times as well as the material wasted is enabled. This is where Computer Aided Engineering comes in handy. With the tools provided by the CAE software the design of any product can be optimized: lengths can be shortened, walls can be thinned and infills can be changed.

The purpose of the study is to analyse and improve the design of the new joint for furniture the assemblying. In this regard, an analysis of the loads that the joint can withstand is performed to ascertain the critical points of the product, followed by a topology optimization. To better understand the concept of Computer Aided Engineering through this specific product, the steps of the analysis and optimization will be followed, starting from the assignment of material, the discretization of the geometry, the application of loads and restraints, solving procedures and reading of the results, as well as the post-processing processes, in this case a topology optimization.

In Fig. 4.1 and Fig. 4.2 the assembly of the bookshelf in SolidWorks as well as in Workbench 19.0 environment are represented.

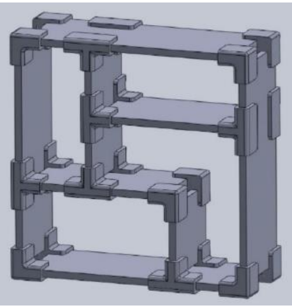

Fig. 4.1 – Assembly in SolidWorks

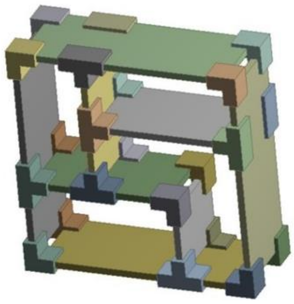

Fig. 4.2 – Assembly in ANSYS Design Modeler 19.0

The boards of the shelf are made by wood, and the joints are manufactured employing PLA, one of the most employed 3D printing materials. Although PLA is not the stiffest and most durable 3D printed material, it is the easiest to find on the market. The purpose of the CAE simulation is to determine if this material is appropriate for longer usage as an assembly joint, and if the dimensions are suitable for the studied arrangement.

For the static analysis of the assembly, the needed material properties are the density, the Young's Modulus and the Poisson's Ratio. The wood was assumed to be an orthotropic material.

In Fig. 4.3 the properties of PLA are specified as they are defined in the Engineering Data module and in Fig. 4.4 the properties of the wood are also set.

Material Field Variables	Table	
Density	1250	kg m^-3
Isotropic Elasticity		
Derive from	Young's Modulus and Poisson's ...	
Young's Modulus	2222,9	MPa
Poisson's Ratio	0,3	
Bulk Modulus	1,8524E+09	Pa
Shear Modulus	8,5496E+08	Pa

Fig. 4.3 – Properties of PLA

Material Field Variables	Table	
Density	660	kg m^-3
Orthotropic Elasticity		
Young's Modulus X direction	11000	MPa
Young's Modulus Y direction	2000	MPa
Young's Modulus Z direction	2000	MPa
Poisson's Ratio XY	0.3	
Poisson's Ratio YZ	0.3	
Poisson's Ratio XZ	0.3	
Shear Modulus XY	6.9E+08	MPa
Shear Modulus YZ	6.9E+08	MPa
Shear Modulus XZ	6.9E+08	MPa

Fig. 4.4 – Properties of the wood

The CAE analysis of this assembly was be performed in three stages. First, the static structural analysis of the assembly is done to ascertain the critical areas of the joints and to identify if the material can be removed from some areas of the joints to decrease the total mass and, subsequently, the assembly weight. After the material removal from the “L” joint, another static structural analysis must be run, to verify the stress and displacement changes, as well as to compare the mass of the initial assembly with the current mass. Therefore a Topology Optimization procedure can then be accessed for further material removal from the joints.

The first analysis is a Static Structural one. Through this analysis, it is expected to understand the behaviour of the assembly when the forces are applied. In this regard, the initial assembly, with the filled joints is subjected to forces up to 100 N evenly distributed on every wood board to simulate the loads applied by different objects which would normally sit on the bookshelf.

In the scheme below the progress of the analysis steps is represented. Firstly, the mesh of the assembly is generated. This mesh is a rather simple one, because the geometries of the parts comprising the assembly are defeatured. Then, the loads and boundary conditions were applied to the assembly: a fixed support on the bottom of a wood board and a force of 100 N on each horizontal shelf. After the definition of the loads, the solving procedure was completed. The main results were considered the Total Deformation of the assembly, as well as The Equivalent von Mises Stress. The Total Deformation proves a maximum value of 0,0081 mm and indicates that the deformation of the whole assembly is small and does not create a distorted shape. The Equivalent Stress, with a maximum value of 0,067 MPa, shows that the impact of these loads on each joint individually is small and a topology optimization of the joint can be performed further to decrease the total mass.

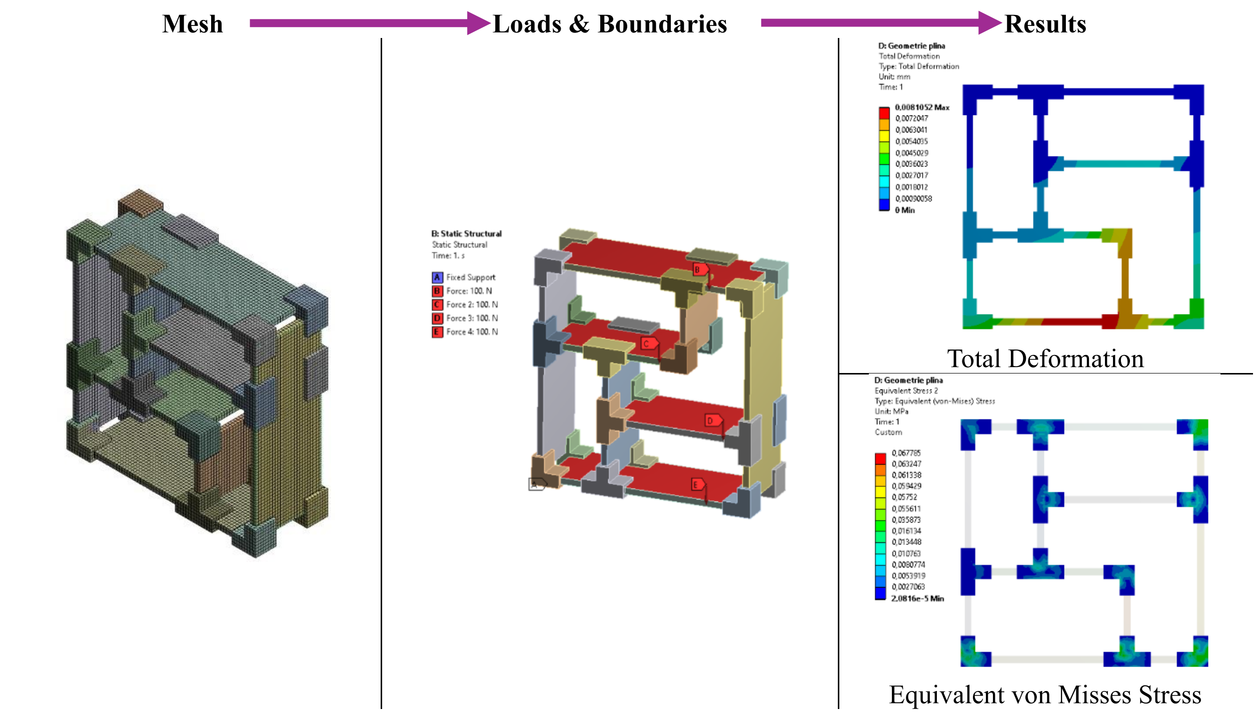

As can be seen from the Equivalent von Mises Stress plot, the stresses seem to be centred on the filled area of the “L” joints, so the material removal can be performed and elements that are not in the displacements or stress path may be removed in such a way that the joint will still ensure the required stiffness.

The second static analysis was performed to ascertain the difference a hole in the joints makes when talking it into account and recalculating the stresses and the deformations of the assembly. The “L” joints have been hollowed to manually reduce the material.

In Fig. 4.5 and 4.6 the filled joint as well as the hollowed one are illustrated.

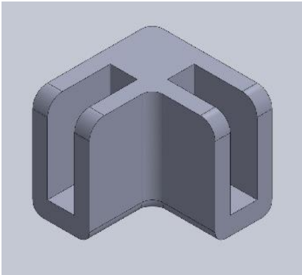

Fig. 4.5 – Filled "L" joint

Fig. 4.6 – Hollow "L" joint

The mesh of the assembly does not change much from the previous analysis. The only feature added in the assembly is the hole in the "L" joint, which does not interfere with the initial mesh, due to its squared shape. The shelf is still fixed on the bottom board to simulate the other furniture elements that can be placed on. On each horizontal shelf a force pointing downwards was applied, each of 100 N. The computation was performed similarly. The Total Deformation plot shows a maximum value of 0,0076 mm and represents the maximum deformation of the whole assembly, while the Equivalent von Mises Stress has a maximum value of 0,065 MPa. This second design proved to be also appropriate, but there are still resources for mass reduction.

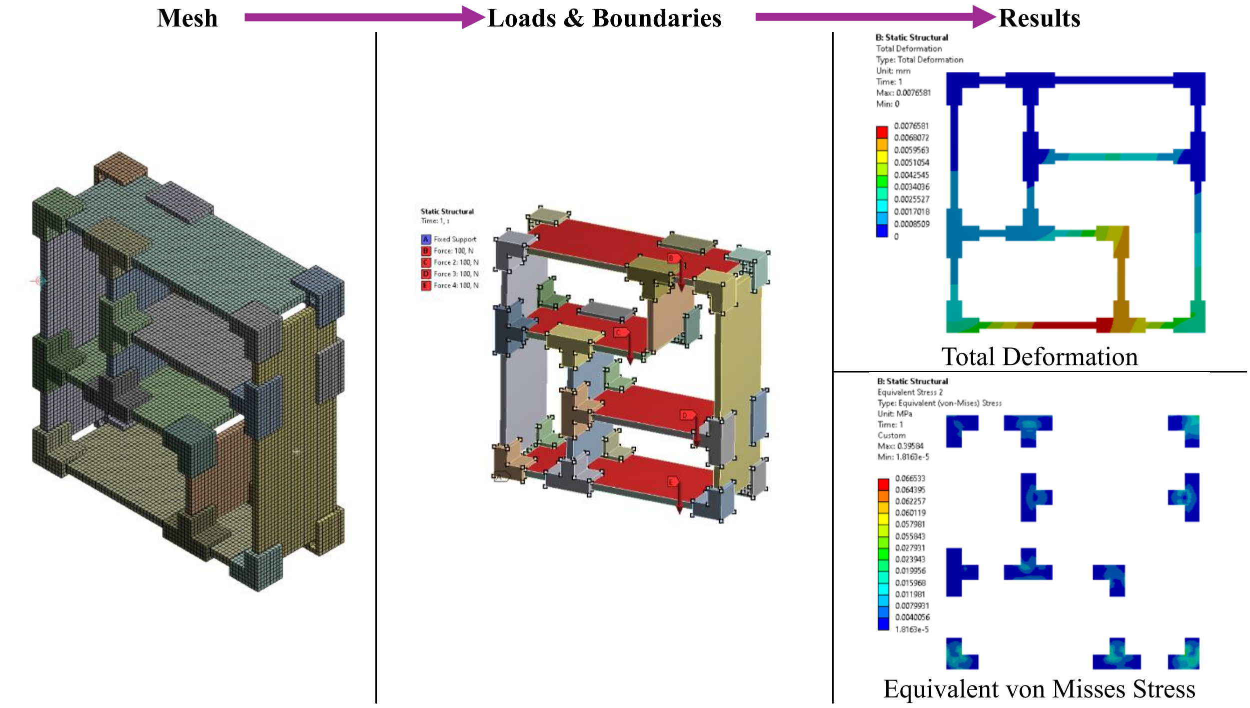

Topology Optimization is a non-parametrical procedure that seeks the minimum weight of a part, by progressively reducing the structural compliance energy. These kind of procedures are inspired from genetic algorithms. The procedure removes material from the defined design space until the target weight is reached. Topology optimization then distributes the remaining material in the most favourable way, given the restrictions and loads applied to the assembly. Some of the advantages of the topology optimization are that it can precede the prototyping stage, it deletes elements which are not in the load flow of the product, it does not require a parametric model and it abruptely changes the shape of the product, leading to an innovative solution.

The parts selected for the optimization are only the joints. The wood shelves are exclusion regions. The solver has removed different amounts of material from each joint, where the stresses, strains and deformations were low. As can be seen the shape of the joints didn't change, but the dimensions were reduced accordingly, in respect with the orientation and the location of the joint.

Optimization region → Joint designs after optimization

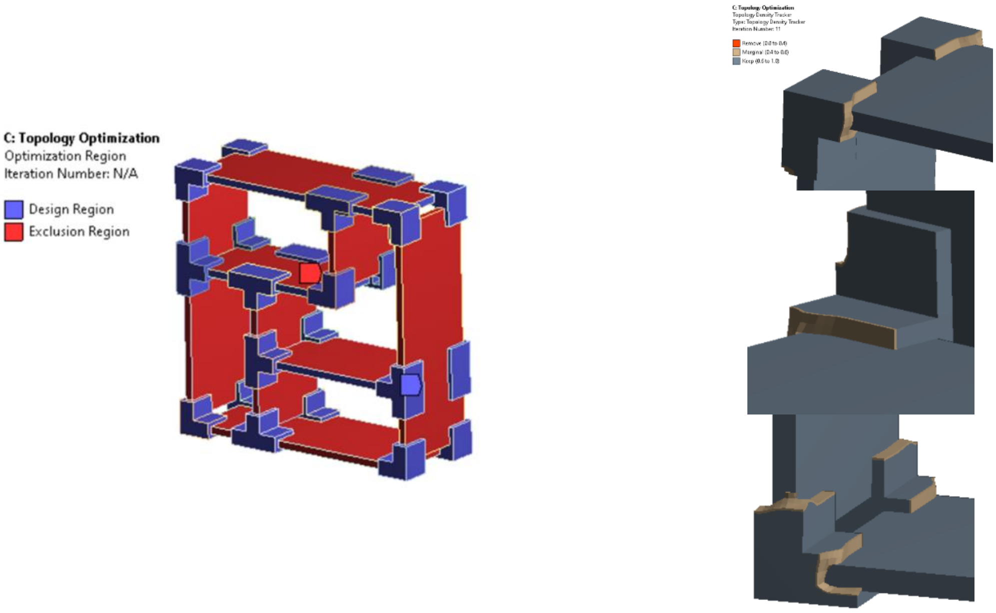

5. Integrated production system of the assembly

The system designed has the purpose of manufacturing a shelf. The assembly is made up of multiple panels of wood and 3D printed joints, which keep the wood in place. The joints are printed on 3D printers. The wood is cut on a cutting machine and then either treated in a treating machine or painted in a painting system. The assemblies are done at assembling stations.

Through this system, the efficiency of the manufacturing process of the assembly can be studied. Although 3D printing is a slow process which might hinder the production, the aim is to optimize the whole system in such a way that it would be favourable in a real-life setting.

Three variations of the same production system were analysed: the preliminary system and the two remodelled systems, the functional and the technological one. The preliminary system is characterized by the original Inter Arrival Times and Cycle Times in the system and the minimum number of machines. During the functional remodelling, the times in the system were altered, to obtain higher productivity. Lastly, during the technological remodelling, one more assembling station was added to the system. In Table 4.1 the systems and their parameters as well as the productivity of each system are summarized.

Table 4.1. – Production systems

System	Parameters	Productivity
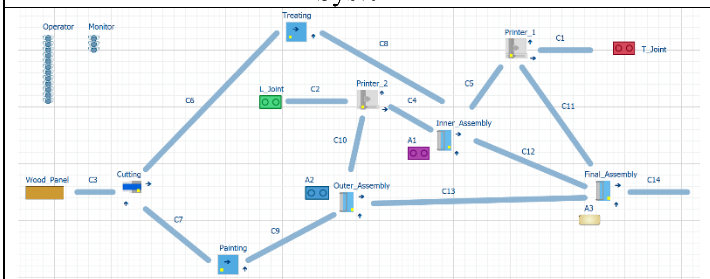	Preliminary system: Wood Panel – *Inter Arrival Time:* 10 min Machine Treating – *Cycle Time:* 60 min Machine Painting – *Cycle Time:* 60 min Machine Inner_Assembly – *Cycle Time:* 5 min Machine Outer_Assembly – *Cycle Time:* 5 min Machine Final_Assembly – *Cycle Time:* 5 min	9,5%

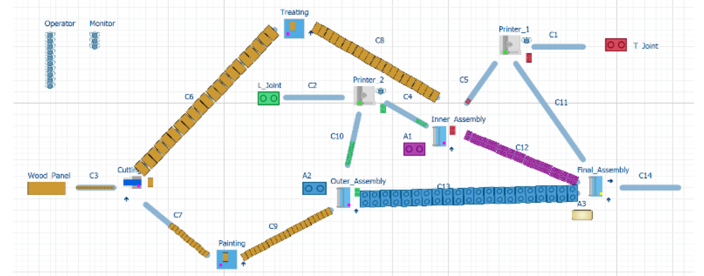	Functional remodelling: Wood Panel – Inter Arrival Time: 10 → 29 min Machine Treating – Cycle Time: 60 → 90 min Machine Painting – Cycle Time: 60 → 120 min Machine Inner_Assembly – Cycle Time: 5 → 60 min Machine Outer_Assembly – Cycle Time: 5 → 100 min Machine Final_Assembly – Cycle Time: 5 → 3.5 min	11,6%
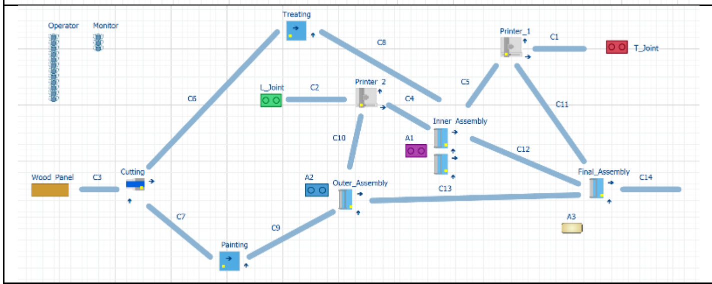	Technological remodelling: Machine Inner_Assembly – Quantity: 1 → 2 T_Joint – Inter Arrival Time: 90 → 52 min L_Joint – Inter Arrival Time: 68 → 42 min	9%

6. Conclusions

- The optimization of the constructive solution reduces the material, while keeping the assembly strong and stiff.
- Topology optimization paved the way for a future Multicriteria Optimization procedure, as well as the integration of other different optimization procedures, such as local shape optimization.
- The optimization of the production system leads to shorter production times and a more efficient use of the system.
- The manufacturing method makes possible and easier the testing of a prototype.

7. Bibliography

[1] Poole, M. (2019, August 21). Antique Joints and Joinery Techniques - Antique HQ. Antique HQ., available at https://www.antique-hq.com/antique-joints-and-joinery-techniques-2533/, accessed November 2023

[2] The Editors of Encyclopaedia Britannica. (1998, July 20). Joint | Woodworking, Mortise & Tenon. Encyclopedia Britannica., available at https://www.britannica.com/technology/joint-carpentry, accessed November 2023

[3] Staff, W. M. (2021, January 3). Choosing and using knockdown hardware. WOOD Magazine., available at https://www.woodmagazine.com/wood-supplies/fasteners-hardware/choosing-and-using-knockdown-hardware-0, accessed November 2023

[4] Hajdarevic, S., Kuzman, M. K., Obucina, M., Vratuša, S., Kušar, T., & Kariž, M. (2022). Strength and stiffness of 3D-printed connectors compared with the wooden mortise and tenon joints for chairs. Wood Material Science & Engineering, 18(3), 870–883. https://doi.org/10.1080/17480272.2022.2086065

[5] Nicolau, A., Pop, M. A., & Coşereanu, C. (2022). 3D printing application in wood furniture components assembling. Materials, 15(8), 2907. https://doi.org/10.3390/ma15082907

[6] Chennakesava, P.; Narayan, Y.S. Fused deposition modeling-insights. In Proceedings of the International Conference on Advances in Design and Manufacturing ICAD&M, Tamil Nadu, India, 5–7 December 2014; p. 1345.

[7] Linkyosms. (2014, April 9). Beginner's guide to 3D Printing., available at https://blog.supermediastore.com/article/nitty-gritty-3d-printing, accessed April 2024

[8] Simplify3D Software. (2022, November 22). Ultimate 3D Printing Material Properties Table., available at https://www.simplify3d.com/resources/materials-guide/properties-table/?filas=abs,pla,hips,petg,nylon,asa,polycarbonate,pva, accessed November 2023

[9] What is PLA? (Everything You Need To Know). (n.d.)., available at https://www.twi-global.com/technical-knowledge/faqs/what-is-pla#HowisitMade, accessed June 2024

[10] Overview of materials for Polylactic Acid (PLA) Biopolymer. (n.d.)., available at https://www.matweb.com/search/DataSheet.aspx?MatGUID=ab96a4c0655c4018a8785ac4031b9278&ckck=1, accessed June 2024

ROBOT ASSEMBLY APPLICATION ON CONVEYOR; SORTING OF PARALLELIPIPEDAL OBJECTS

VLAD Sorina, SOFIAN Bogdan, BĂNICĂ Iulian and CRISTEA Cosmin, VERDETE Bogdan-Marian
Facultatea: FIIR Specializarea: Robotică, Anul de studii: I, e-mail: vladsorina14@gmail.com

ABSTRACT: The application involves the assembly on a conveyor system, incorporating the sorting and introduction of objects based on their colors. This process includes the systematic arrangement of parallelepiped-shaped objects. The process is executed by three articulated arm robots positioned at the beginning, middle, and end of the conveyor.

KEYWORDS: robot, conveyor, assembly, sorting

1. Introduction

The application of filing - sorting by color - inserting parallelepiped objects into boxes by industrial robots is a complex application, based on two well-defined processes: pick and place and sorting - inserting objects into boxes by color. The processes underlying this application are very often used in the pharmaceutical industry. The paper aims to detail the realization of a small-scale application like the one described above, starting from some CAD models for the industrial robots used and the knowledge acquired in the 1st year of the Robotics Specialization. The boxes, objects, barriers, and respectively the robots were made by 3D printing, the band was made of wood, a piece of material, and two pieces of PPR pipe engaged by two DC motors. Also used: an Arduino board, a Breadboard, 12 servomotors, two DC motors and 4 buttons. In the end, they were all positioned and assembled on a wooden bench.

2. Actual stage

Schematically, our application is presented as in (Fig.1 Application scheme), and in reality, as in (Fig.2 The application).

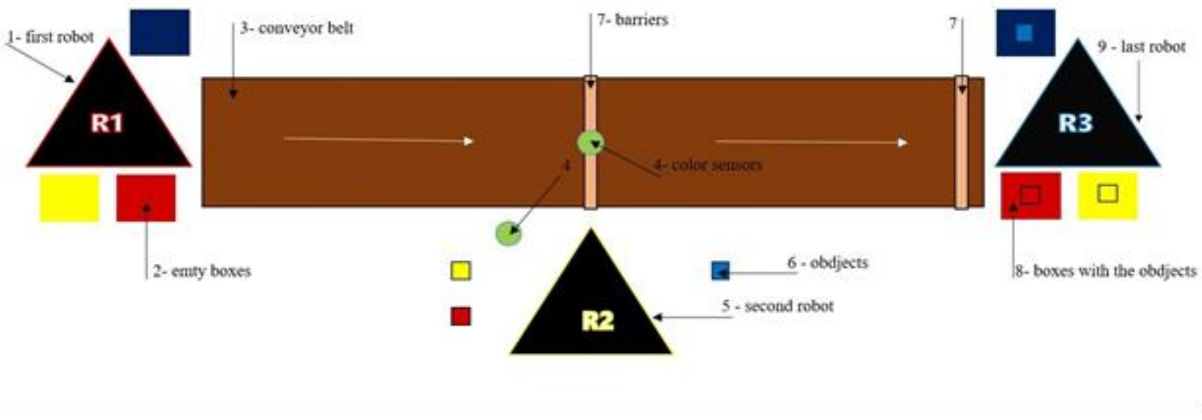

Fig.1 Application scheme

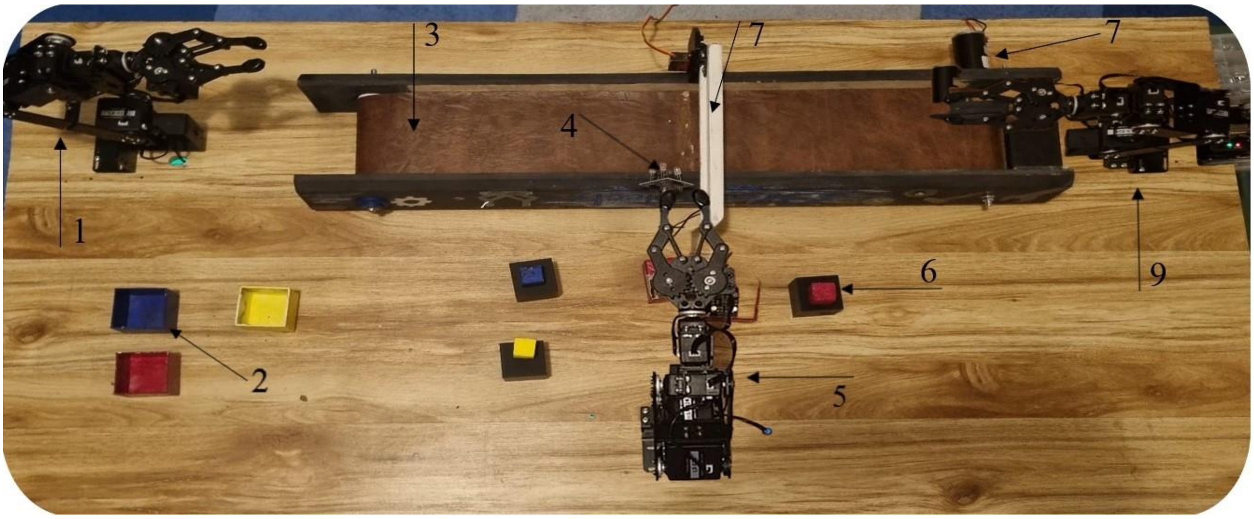

Fig.2 The application:

The process initiates with three boxes strategically placed beside the initial robot (Fig.2 The application), each set to be picked up at specific intervals and systematically arranged along the conveyor belt. In the journey from R1 to R3 on the conveyor, each box encounters a primary barrier and a color marker positioned midway along the route (Fig.4 R2).

Fig.3 R1

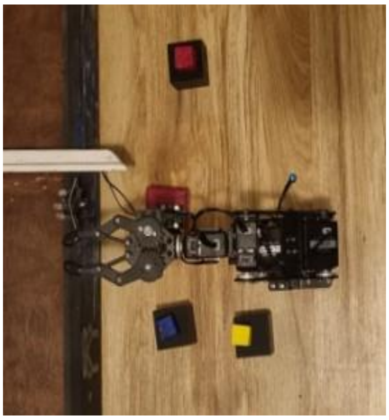

Fig.4 R2

Fig.5 R3

Adjacent to the second robot lies an array of randomly positioned objects, accompanied by an additional color sensor (Fig.4 R2). This configuration enables the objects to be efficiently sorted based on color, ensuring precise placement into the designated box. The box, now laden with its respective item, progresses uninterrupted towards R3. Upon arrival, it faces a second barrier that momentarily holds its position until the final robot gracefully lifts it and deposits it into a predefined space (Fig.5 R3). Throughout the entire circuit, the conveyor belt maintains a fluid, unbroken movement, seamlessly orchestrating the intricate process with precision and efficiency.

The three robots exhibit a general architecture characterized by a closed kinematic arm and an open kinematic chain. They operate in the Cartesian coordinate system by calculating the degrees of each axis using inverse kinematics. With the help of the set_arm function that contains the necessary mathematical operations. Both the 3D models of the robots and the end effectors were sourced online and subsequently modified by us to the desired dimensions using AutoCAD. The grinding and assembly processes were also completed entirely by our team. The conveyor belt is constructed from wood and is rotated by two pieces of PPR pipe, each connected to a motor at either end. (Tabel 1. The components).

Tabel 1. The components

Robot components	Name	Conveyor components	Name
	Arduino board uno black		Speed controller for dc motor
	SERVOMOTOR_MG90S		DC Motor band 12V 8000RPM
	Coupling device for servomotors		Screws M5
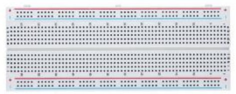	Breadboard 830 points MB 102		PPR pipe 4 m x 32 mm x 5.4 mm
	3 Position Switch		Battery support 3,7V 18650
	Switch KCD1-11-2P		Bearing 606RS 6x17x6 mm
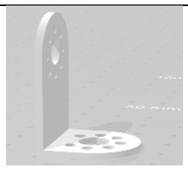	Bracket-L		Color sensor

Table with the parts used in building the 3 robots and the conveyor.

The three sorting boxes were constructed entirely from cardboard and hand painted. The corresponding objects used for sorting, are made from polystyrene. The large base on which the entire assembly is mounted consists of six parquet pieces, three wooden boards, and two plexiglass sheets. This design allows for the observation of the electrical system. The plexiglass sheets are set in grooves, facilitating movement and access around the electrical system. The programming for this robotic application involves the control and initialization of all electronic parts, including sensors, motors, and assembled units (Table 1. The components). Each robot operates under its specific program, with all the robots utilizing an Arduino board to control the motors and execute program logic. Communication between the first and third robots is established through serial communication to maintain order in the industrial process. This fact can also be observed from the electrical diagram of the assembly (Fig.6 Wiring diagram).

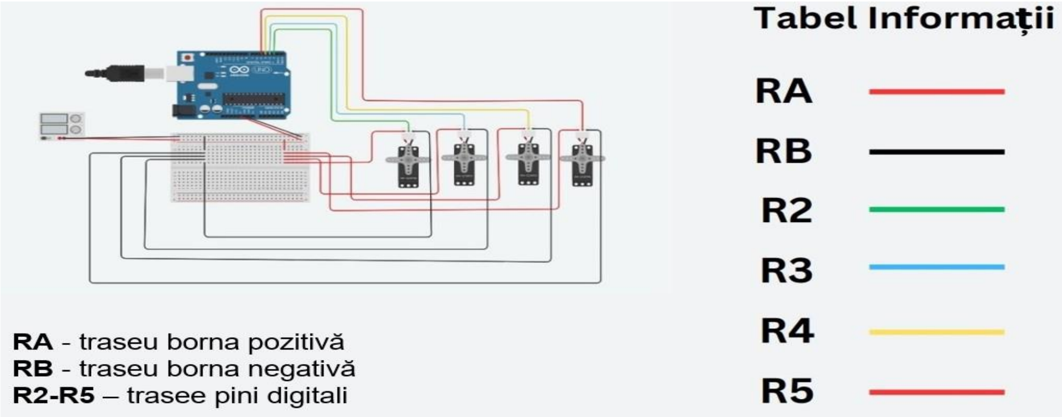

Fig.6 Wiring diagram

To ensure consistent operation, the first robot coordinates with the third robot to maintain a continuous flow of loading and unloading on the automated conveyor belt. Specifically, the first robot loads a new object each time the third robot unloads one. This procedure is crucial for the proper functioning of the application. Both the first and second robots are capable of handling the central stop on the automatic lane. This feature acts as an additional safety measure, ensuring that if an unexpected situation arises after a box loaded with objects leaves the second robot's area, the stop can be properly engaged.

3. Conclusions

Our application, which is currently in the initial stage of development, manages to fulfill what we originally set out to do. The three robots handle the boxes in the way we proposed, managing to load them with the properly sorted objects, and then transport and place them in a well-defined place, thus carrying out the processes of pick and place and sorting-introduction of the objects in color boxes. Our long-term objective is to enable continuous operation similar to an industrial cell. To achieve this, we plan to integrate an additional conveyor belt that will carry boxes and stop when the items are depleted. In addition, we aim to increase the efficiency of object sorting by equipping robots with cameras. We also plan to improve the kinematics of the robots to reduce the time and increase the speed at which they complete their tasks.

4. Bibliography

[1] https://www.youtube.com/watch?v=o7VVmtX7SKs&t=453s
[2] https://www.youtube.com/watch?v=FNFmIbqV8nc
https://www.thingiverse.com/thing:2302957
[3] https://www.printables.com/en/model/411239-robot-arm-alien3d-ufo-feb-2023
[4] https://www.youtube.com/watch?v=2B336Bt_rog
[5] https://www.youtube.com/watch?v=EVD-Q9lxwaI
[6] https://www.youtube.com/watch?v=IalkWUN6wvE
https://cults3d.com/en/3d-model/gadget/servo-gripper-for-robotic-arm-sg90-servo-gripper

THE ANALYSIS OF THE ORTHOGONAL TURNING PROCESS OF PUMP BODIES IN THE OIL INDUSTRY

MUREŞAN Ştefan-Claudiu[1] , ALEXANDRU Tudor-George, PUPĂZĂ Cristina

[1]Facultatea: IIR, Specializarea: Robotică, Anul de studii: IV, e-mail: stefanclaudiu2812@gmail.com

ABSTRACT: The research focuses on understanding and optimizing the machining process through orthogonal turning, specifically applied to pump components used in the oil industry. This machining process is essential for manufacturing precise and durable components required in the oil industry. The main objective of the study is to evaluate the influence of various cutting parameters and tool geometry on the results obtained in the orthogonal turning process. These parameters include cutting speed, depth of cut, and tool feed, each having a significant impact on the quality of the machined surface, cutting forces, and tool wear. Additionally, the tool geometry, such as the cutting angle and the shape of the cutting edge, plays a crucial role in determining the efficiency and stability of the turning process.

KEYWORDS: Turning, CAE, Steinberg-Guinan, AL1100O.

1. Introduction

The work delves into the critical machining process of orthogonal turning, which is fundamental for producing accurate and durable pump components employed in the oil industry. By focusing on understanding and optimizing this process, the work aims to evaluate how various cutting parameters, such as cutting speed, depth of cut, and tool feed, along with tool geometry, influence the quality of the machined surface, cutting forces, and tool wear. This analysis is vital for improving the efficiency, stability, and overall performance of the manufacturing process, thereby enhancing the reliability and lifespan of essential oil industry equipment.

2. Current state

In recent years, significant technological advancements have been made in the field of orthogonal turning, particularly in the oil industry. High-precision CNC (Computer Numerical Control) machines have become more prevalent, offering greater control over the cutting parameters and tool movements. These machines have improved the accuracy and repeatability of the turning process, essential for producing high-quality pump components. Extensive research has been conducted to optimize the cutting parameters for orthogonal turning [1]. Studies have focused on determining the ideal cutting speed, depth of cut, and feed rate to maximize tool life and surface finish quality while minimizing machining time and costs. [2] Advanced simulation software and empirical testing have facilitated these optimizations, providing manufacturers with precise data to inform their machining strategies. [3] The geometry of the cutting tools has been a major research and development area [4]. Innovations in tool design, such as improved cutting angles, chip breakers, and edge preparation techniques and have significantly impacted the efficiency and stability of the turning process. Custom-designed tools tailored to specific applications in the oil industry have also become more common, leading to better performance and reduced tool wear.

3. Pump and tool modelling

The part geometry was modeled in CATIA V5 software, and in the Design Modeler module, the model simplification was performed. It was necessary to consider both the starting diameter and the final diameter, as well as the length of the part, in order to subsequently input them into the calculation for selecting the cutting parameters.

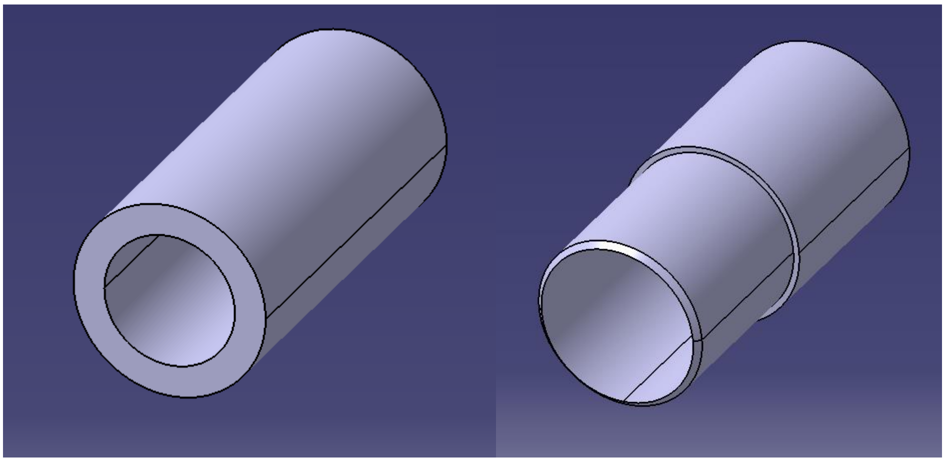

Fig. 1 Oil pump geometry

For designing the turning tool geometry, specialized literature was consulted to determine the angles and their values. Thus, the following necessary angles were identified: the rake angle - α, the clearance angle - γ, the approach angle - K, and the cutting-edge angle - ε. The values chosen for these angles are as follows: α = 6°, γ = 6°, K = 45°, ε = 90°. The design of the tool also took into account the type of operation performed and the material from which the workpiece is made. [5]

Tabela 10

Toleranțele părții active a cuțitelor

Simbol	Denumirea unghiurilor	Mărimea unghiurilor	Abateri limită
α, α_1	Unghiuri de așezare	$\alpha, \alpha_1 \leqslant 8°$ $\alpha, \alpha_1 > 8°$	± 30′ ± 1°
γ	Unghiul de degajare	$\gamma \leqslant 12°$ $\gamma > 12°$	± 1° ± 2°
$\varkappa$	Unghiul de atac principal	30, 45, 60 și 90°	± 2°
$\varkappa_1$	Unghiul de netezire (de atac secundar)	$\varkappa_1 < 5°$ $\varkappa_1 > 5°$	± 1° ± 2°
ε	Unghiul de vîrf	$\varepsilon < 100°$ $\varepsilon > 100°$	± 2° ± 3°
λ	Unghiul de înclinare a tăișului	4 ... 10°	± 1°

Fig. 2 Turning tool angles

4. Geometry simplification

For simplifying the calculation model and reducing the number of elements, the simulation was performed only on a section of the entire part, preserving only a segment of approximately 120 degrees. The turning tool was positioned adhering to the previously determined angle, while eliminating any other details that could increase model complexity and require additional processing resources.

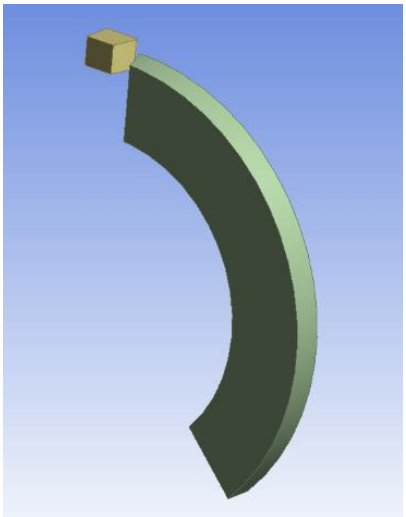

Fig. 3 Geometry simplificaton

5. Materials

For conducting the simulation, two types of materials were required: one for the turning tool and another for the workpiece. The turning tool material chosen was Structure Steel from the software material library. As for the workpiece, a material had to be created based on the specific requirements of the part. Therefore, various manufacturers of pump bodies in the oil industry were consulted. These "liners" cover the mechanisms and filters that form the pump, leading to the decision to use an aluminum alloy material.

The material chosen was AL1100-O, and its physical properties were obtained from the MatWeb digital library. In addition to traditional physical characteristics such as density, parameters like "Steinberg Guinan Strength" were incorporated for chip breakage phenomena, and "Shock EOS Linear" was included for tool-workpiece contact behavior. These parameters are crucial for accurately modeling the interaction between the tool and the workpiece in the simulation. [6]

	A	B	C	D	E
1	Property	Value	Unit		
2	Material Field Variables	Table			
3	Density	2707	kg m^-3		
4	Specific Heat, C_p	884	J kg^-1 C^-1		
5	Steinberg Guinan Strength				
6	Initial Yield Stress Y	4E+07	Pa		
7	Maximum Yield Stress Ymax	4,8E+08	Pa		
8	Hardening Constant B	400			
9	Hardening Exponent n	0,27			
10	Derivative dG/dP G'P	1,767			
11	Derivative dG/dT G'T	-1,669E+07	Pa C^-1		
12	Derivative dY/dP Y'P	0,002608			
13	Melting Temperature Tmelt	946,85	C		
14	Shear Modulus	2,71E+10	Pa		
15	Shock EOS Linear				
16	Gruneisen Coefficient	1,97			
17	Parameter C1	5386	m s^-1		
18	Parameter S1	1,339			
19	Parameter Quadratic S2	0	s m^-1		

Fig. 4 AL1100O material characteristics

6. Explanations regarding the type of analysis conducted

The purpose of the Finite Element Analysis was to examine the influence of cutting parameters and tool geometry on the orthogonal turning of rotating components. The chosen dynamic analysis was the Explicit Dynamic algorithm, which integrates differential equations of motion to solve dynamic problems.

Based on the results obtained, modifications will be made both to the cutting parameters and to the tool geometry, aiming for improved final results and dynamic behavior during the turning operation. For Explicit Dynamics simulations, various algorithms can be employed depending on the specific phenomenon: Lagrange for complex materials, Euler for gas/solid/liquid flows and shock waves, Mesh-free solver for HVI (High Velocity Impact), fracture and brittle materials, and ALE-FSI solver for fluid-structure interaction. In this case, the Eulerian algorithm was used, suitable for cases where discretization deforms and moves with the material. Unlike Lagrange, this method avoids distortion of discretization in large deformations. The solver employs an integration calculation method known as Leapfrog scheme. [7]

$$\ddot{\boldsymbol{x}}_{\boldsymbol{i}} = \boldsymbol{b}_{\boldsymbol{i}} + \frac{\boldsymbol{F}_{\boldsymbol{i}}}{\boldsymbol{m}} \quad (1)$$

7. Simulation Conditions

For conducting the analysis of the external orthogonal turning phase, it was necessary to determine the cutting parameters based on the workpiece material and the difference in diameters between the raw and semi-finished states. To determine the values of the cutting parameters, specialized literature was consulted for specific formulas, and the ToolGuide automated calculator from Sandvik Coromant, the largest manufacturer of cutting tools, was also used. Thus, the turning tool was considered stationary and positioned at the specific cutting depth, over a specific axial distance after performing four steps, while the workpiece was rotated around a cylindrical coordinate system corresponding to the axis of revolution of the lathe, with an angular value of 60 degrees, within a time interval of 0.017 seconds required for machining the respective circular arc.

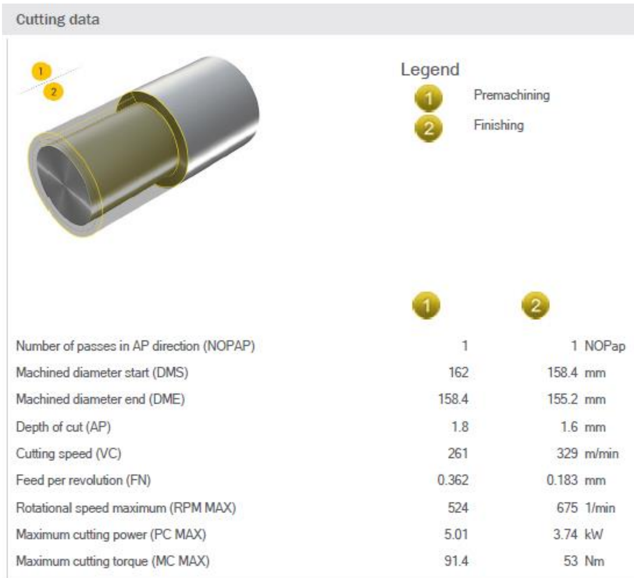

	1	2	
Number of passes in AP direction (NOPAP)	1	1	NOPap
Machined diameter start (DMS)	162	158.4	mm
Machined diameter end (DME)	158.4	155.2	mm
Depth of cut (AP)	1.8	1.6	mm
Cutting speed (VC)	261	329	m/min
Feed per revolution (FN)	0.362	0.183	mm
Rotational speed maximum (RPM MAX)	524	675	1/min
Maximum cutting power (PC MAX)	5.01	3.74	kW
Maximum cutting torque (MC MAX)	91.4	53	Nm

Fig. 5 Input parameters

8. Results

Various results were processed to analyze different parameters of the orthogonal turning process, including total displacements, equivalent stresses, elastic strain, plastic strain, internal energy, and temperature.

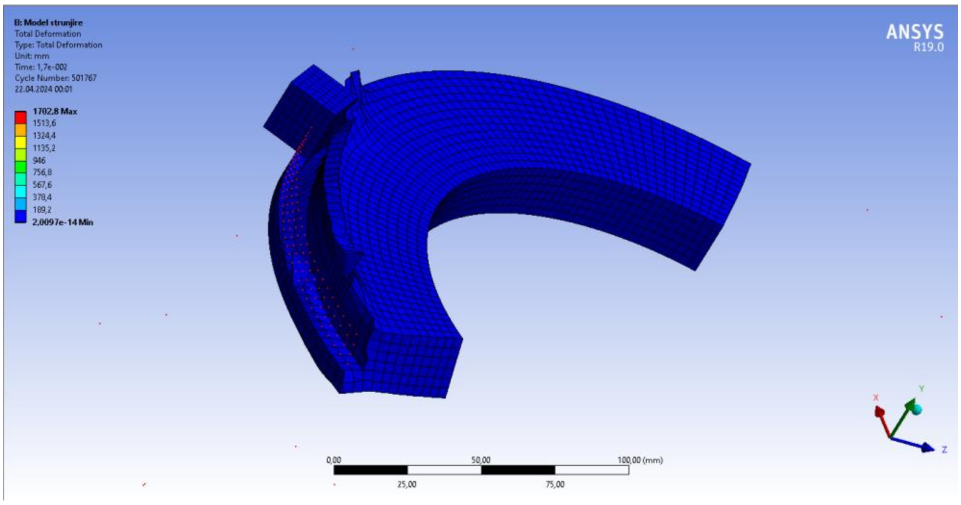

Fig. 6. Total Deformation

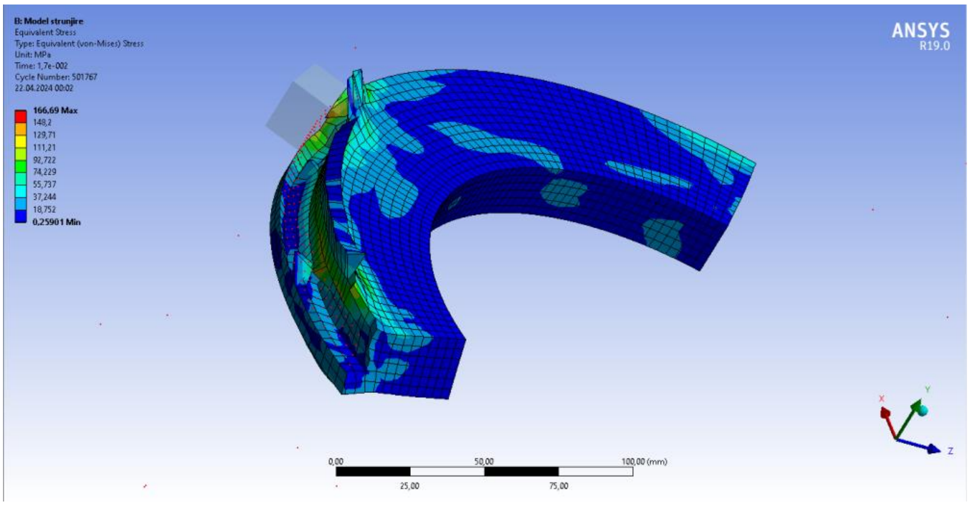

Fig. 7 Equivalent Stress

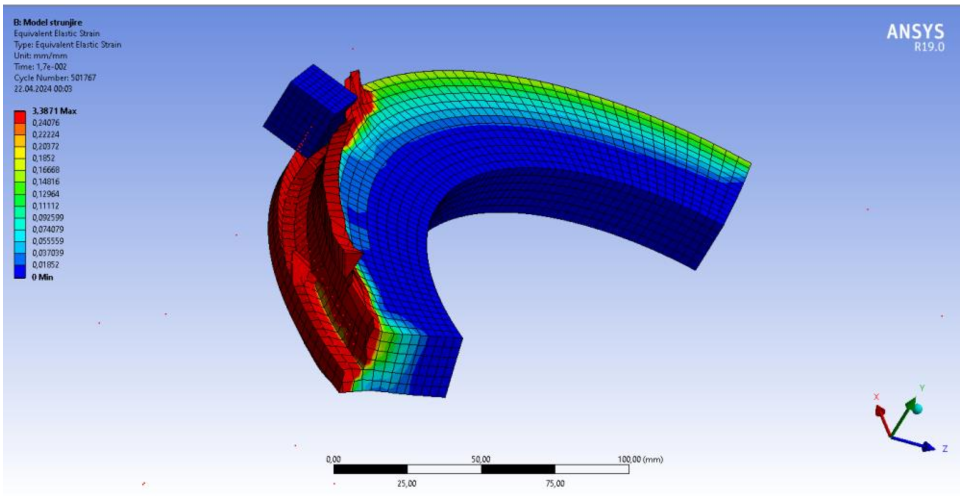

Fig. 8 Equivalent Elastic Strain

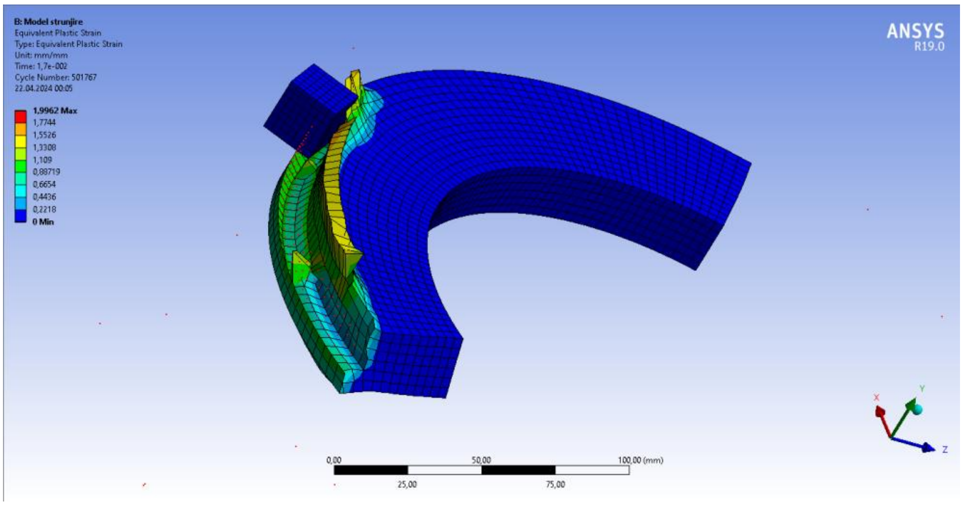

Fig. 9 Equivalent Plastic Strain

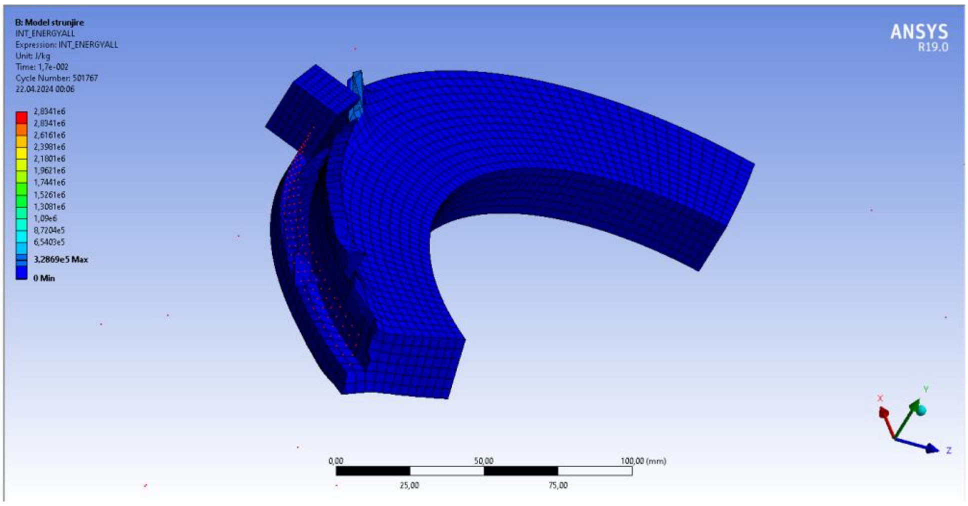

Fig. 10 Internal Energy

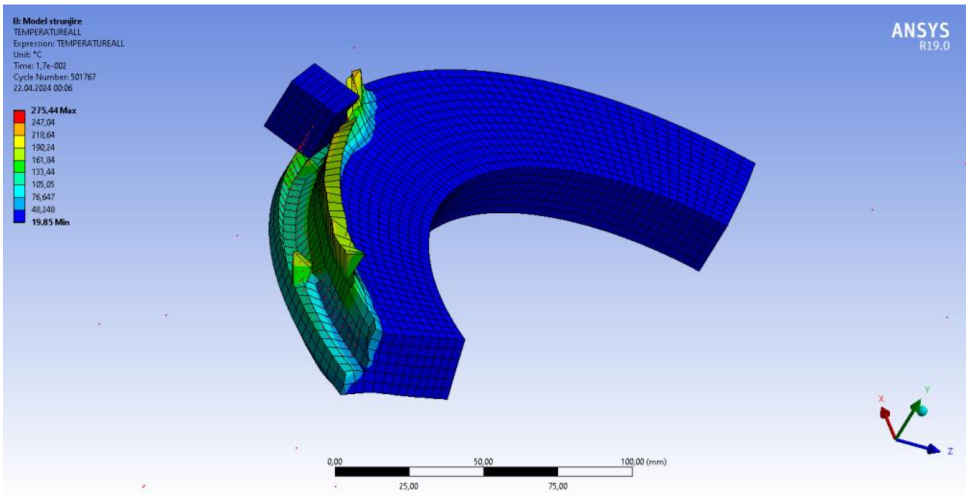

Fig. 11 Temperature

Table 1. Characteristics values ranges

Characteristic	Min. value	Max. value	Measuring unit
Total Deformation	2,00997E-14	1702,8	mm
Equivalent Stress	0,25901	166,69	MPa
Equivalent Elastic Strain	0	3,3871	mm/mm
Equivalent Plastic Strain	0	1,9962	mm/mm
Internal Energy	0	3,8341E6	J/kg
Temperature	19,85	275,44	˚C

9. Monitoring the computation procedure

During the FE computation, the evolution of energies was monitored to ensure a proper model and behavior. To ensure the correct cutting, the Hourglass energy, which represents element distortion, has to be minimized, and the breakpoints of elements be observed on the energy graph.

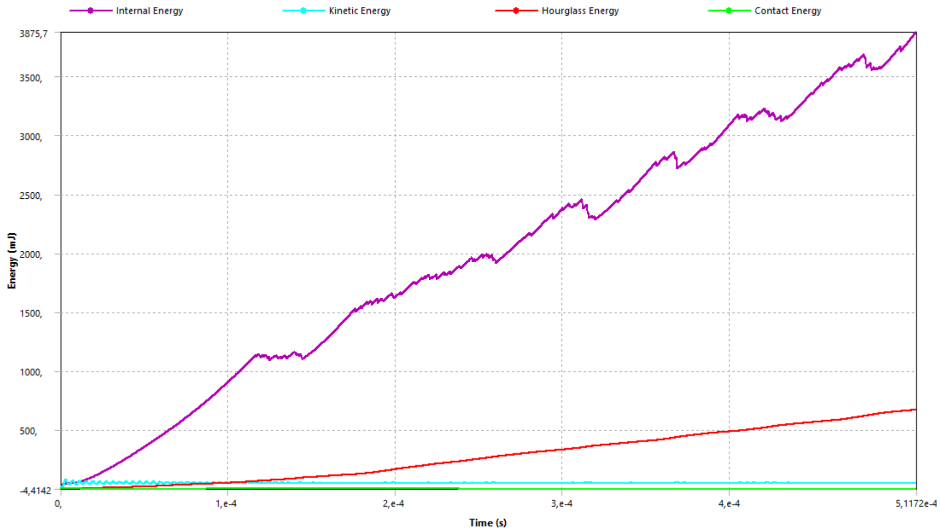

Fig. 12 Solution monitoring

10. Conclusions

The purpose of this simulation was to observe the influence of the cutting parameters and tool geometry on the manufacturing process. Initially, it was observed that an improperly designed tool geometry was employed, disregarding recommendations from the scientific literature, and also aggressive cutting parameters, leading to improper chip formation. This resulted in chip accumulation at the tool-workpiece contact zone during machining, eventually causing severe deformation of the geometry due to excessive internal energy exceeding acceptable limits.

Additionally, efforts were done to ensure that the temperature generated at the tool-workpiece contact did not exceed the material's specific flow temperature, which was maintained with a maximum temperature of 275.44 °C, without any additional forced cooling methods (such as liquid coolant or pressurized air). The specific flow temperature of the material used for the workpiece was 884 °C.

Lastly, the surface quality resulting from the orthogonal turning process was aimed to be of high quality, which visually appeared satisfactory during the final runs.

11. Bibliography

[1]. Sumesh, C.S., Venkata Roshan, M., Sakthi Balaji et.al. – Optimization of Machining parameters on Chip Thickness in Orthogonal Turning of AISI 1040 Steel, Academic Journal of Manufacturing Engineering, VOL.22, ISSUE 1/2024, pp. 92-100

[2] Bhushan, R.K.- Optimization of cutting parameters for minimizing power consumption and maximizing tool life during machining of Al alloy SiC particle composites, Journal of Cleaner Production, Volume 39, 2013, Pages 242-254

[3] Seung-Jun Shin, Jungyub Woo, Sudarsan Rachuri - Energy efficiency of milling machining: Component modeling and online optimization of cutting parameters, Journal of Cleaner Production, Volume 161, 2017, Pages 12-29, ISSN 0959-6526

[4] Astakhov, V., Davim, J. (2008). Tools (Geometry and Material) and Tool Wear. In: Machining. Springer, London. https://doi.org/10.1007/978-1-84800-213-5_2

[5]. Mihailde M., Croitoru C., Munteanu A. – Proiectarea sculelor aşchietoare – Îndrumar de laborator (2013)

[6] Steinberg, Daniel J., S. G. Cochran, and Michael W. Guinan. "A constitutive model for metals applicable at high-strain rate." *Journal of applied physics* 51.3 (1980): 1498-1504.

[7]. Pupăză C. – Computer Aided Engineering – FEM (2023-2024)

ROBOT ASSEMBLY APPLICATION ON CONVEYOR; SORTING OF PARALLELIPIPEDAL OBJECTS

VLAD Sorina, SOFIAN Bogdan, BĂNICĂ Iulian and CRISTEA Cosmin, Bogdan-Marian VERDETE

Facultatea: FIIR Specializarea: Robotică, Anul de studii: I, e-mail: vladsorina14@gmail.com

ABSTRACT: The application involves the assembly on a conveyor system, incorporating the sorting and introduction of objects based on their colors. This process includes the systematic arrangement of parallelepiped-shaped objects. The process is executed by three articulated arm robots positioned at the beginning, middle, and end of the conveyor.

KEYWORDS: robot, conveyor, assembly, sorting

1. Introduction

The application of filing - sorting by color - inserting parallelepiped objects into boxes by industrial robots is a complex application, based on two well-defined processes: pick and place and sorting - inserting objects into boxes by color. The processes underlying this application are very often used in the pharmaceutical industry. The paper aims to detail the realization of a small-scale application like the one described above, starting from some CAD models for the industrial robots used and the knowledge acquired in the 1st year of the Robotics Specialization. The boxes, objects, barriers, and respectively the robots were made by 3D printing, the band was made of wood, a piece of material, and two pieces of PPR pipe engaged by two DC motors. Also used: an Arduino board, a Breadboard, 12 servomotors, two DC motors and 4 buttons. In the end, they were all positioned and assembled on a wooden bench.

2. Actual stage

Schematically, our application is presented as in (Fig.1 Application scheme), and in reality, as in (Fig.2 The application).

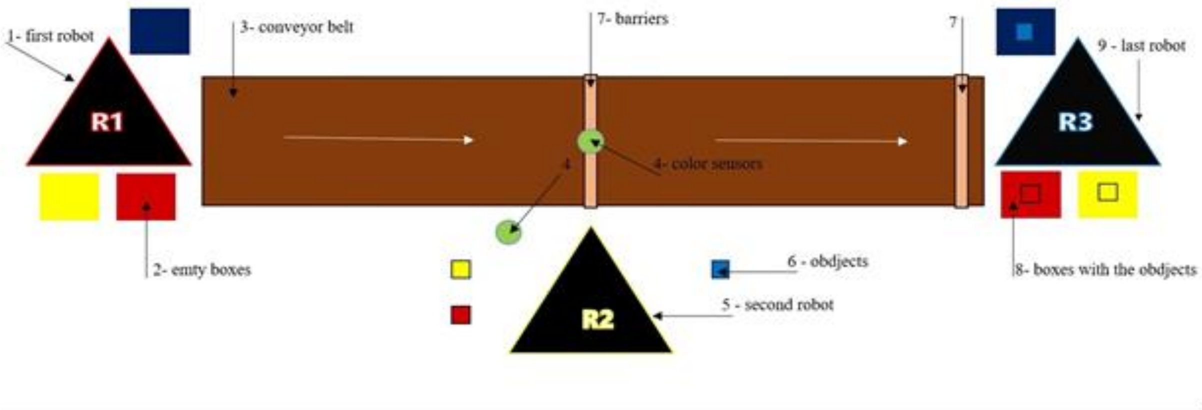

Fig.1 Application scheme

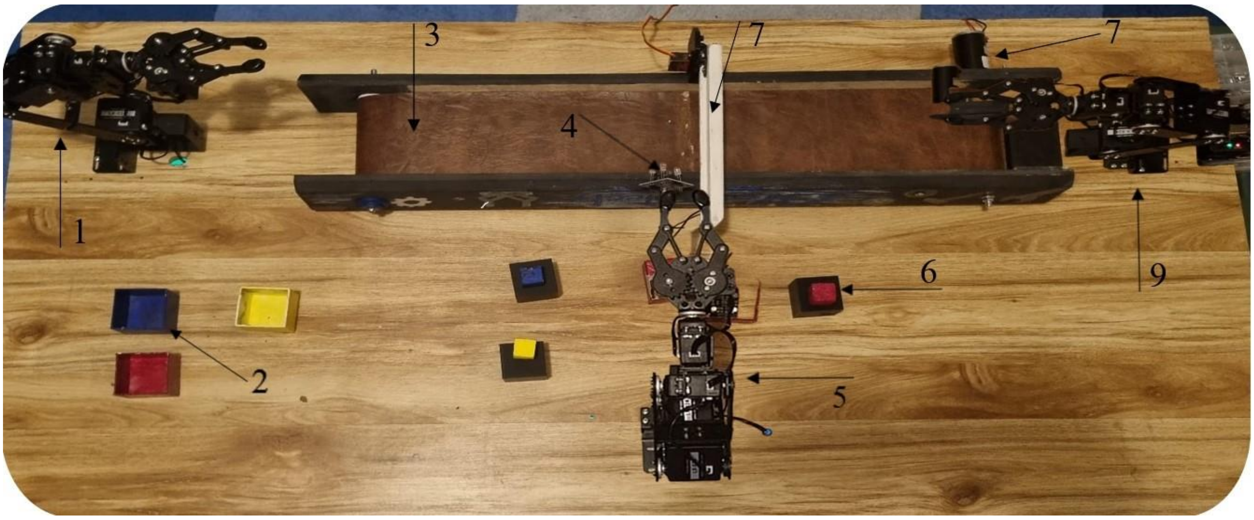

Fig.2 The application:

The process initiates with three boxes strategically placed beside the initial robot (Fig.2 The application), each set to be picked up at specific intervals and systematically arranged along the conveyor belt. In the journey from R1 to R3 on the conveyor, each box encounters a primary barrier and a color marker positioned midway along the route (Fig.4 R2).

Fig.3 R1

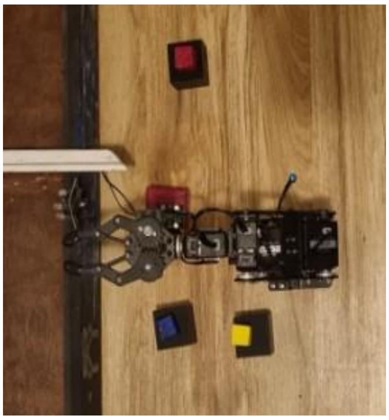

Fig.4 R2

Fig.5 R3

Adjacent to the second robot lies an array of randomly positioned objects, accompanied by an additional color sensor (Fig.4 R2). This configuration enables the objects to be efficiently sorted based on color, ensuring precise placement into the designated box. The box, now laden with its respective item, progresses uninterrupted towards R3. Upon arrival, it faces a second barrier that momentarily holds its position until the final robot gracefully lifts it and deposits it into a predefined space (Fig.5 R3). Throughout the entire circuit, the conveyor belt maintains a fluid, unbroken movement, seamlessly orchestrating the intricate process with precision and efficiency.

The three robots exhibit a general architecture characterized by a closed kinematic arm and an open kinematic chain. They operate in the Cartesian coordinate system by calculating the degrees of each axis using inverse kinematics. With the help of the set_arm function that contains the necessary mathematical operations. Both the 3D models of the robots and the end effectors were sourced online and subsequently modified by us to the desired dimensions using AutoCAD. The grinding and assembly processes were also completed entirely by our team. The conveyor belt is constructed from wood and is rotated by two pieces of PPR pipe, each connected to a motor at either end. (Tabel 1. The components).

Tabel 1. The components

Robot components	Name	Conveyor components	Name
	Arduino board uno black		Speed controller for dc motor
	SERVOMOTOR_MG90S		DC Motor band 12V 8000RPM
	Coupling device for servomotors		Screws M5
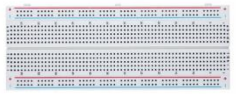	Breadboard 830 points MB 102		PPR pipe 4 m x 32 mm x 5.4 mm
	3 Position Switch		Battery support 3,7V 18650
	Switch KCD1-11-2P	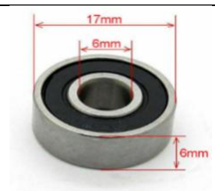	Bearing 606RS 6x17x6 mm
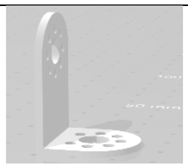	Bracket-L		Color sensor

Table with the parts used in building the 3 robots and the conveyor.

The three sorting boxes were constructed entirely from cardboard and hand painted. The corresponding objects used for sorting are made from polystyrene. The large base on which the entire assembly is mounted consists of six parquet pieces, three wooden boards, and two plexiglass sheets. This design allows for the observation of the electrical system. The plexiglass sheets are set in grooves, facilitating movement and access around the electrical system. The programming for this robotic application involves the control and initialization of all electronic parts, including sensors, motors, and assembled units (Table 1. The components). Each robot operates under its specific program, with all the robots utilizing an Arduino board to control the motors and execute program logic. Communication between the first and third robots is established through serial communication to maintain order in the industrial process. This fact can also be observed from the electrical diagram of the assembly (Fig.6 Wiring diagram).

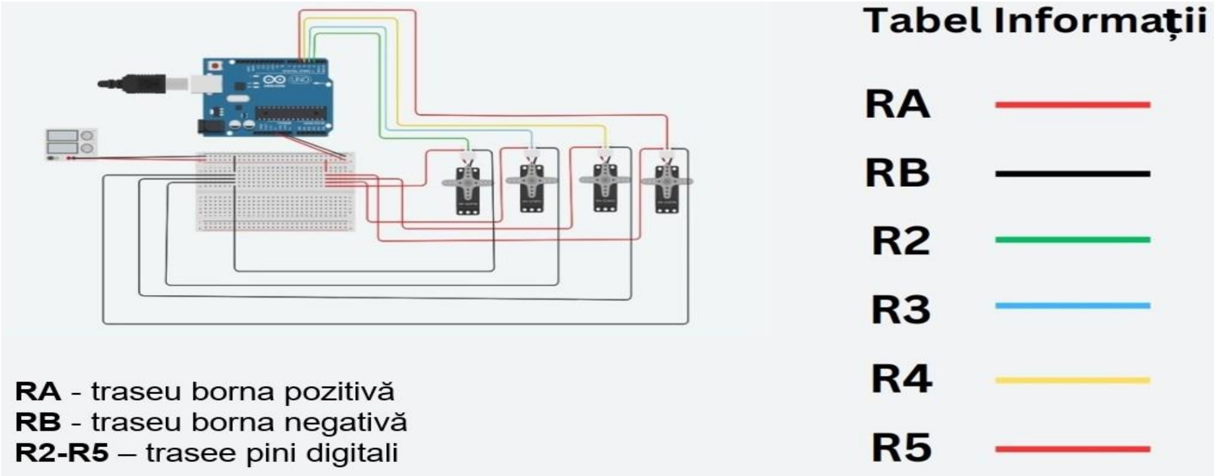

Fig.6 Wiring diagram

To ensure consistent operation, the first robot coordinates with the third robot to maintain a continuous flow of loading and unloading on the automated conveyor belt. Specifically, the first robot loads a new object each time the third robot unloads one. This procedure is crucial for the proper functioning of the application. Both the first and second robots are capable of handling the central stop on the automatic lane. This feature acts as an additional safety measure, ensuring that if an unexpected situation arises after a box loaded with objects leaves the second robot's area, the stop can be properly engaged.

3. Conclusions

Our application, which is currently in the initial stage of development, manages to fulfill what we originally set out to do. The three robots handle the boxes in the way we proposed, managing to load them with the properly sorted objects, and then transport and place them in a well-defined place, thus carrying out the processes of pick and place and sorting-introduction of the objects in color boxes. Our long-term objective is to enable continuous operation similar to an industrial cell. To achieve this, we plan to integrate an additional conveyor belt that will carry boxes and stop when the items are depleted. In addition, we aim to increase the efficiency of object sorting by equipping robots with cameras. We also plan to improve the kinematics of the robots to reduce the time and increase the speed at which they complete their tasks.

4. Bibliography

[1] https://www.youtube.com/watch?v=o7VVmtX7SKs&t=453s
[2] https://www.youtube.com/watch?v=FNFmIbqV8nc
https://www.thingiverse.com/thing:2302957
[3] https://www.printables.com/en/model/411239-robot-arm-alien3d-ufo-feb-2023
[4] https://www.youtube.com/watch?v=2B336Bt_rog
[5] https://www.youtube.com/watch?v=EVD-Q9lxwaI
[6] https://www.youtube.com/watch?v=IalkWUN6wvE
https://cults3d.com/en/3d-model/gadget/servo-gripper-for-robotic-arm-sg90-servo-gripper

RIGID-FLEXIBLE DYNAMIC ANALYSIS OF AN ELEMENT IN THE CLOSED KINEMATIC CHAIN OF THE ABB IRB660 ROBOT

ENACHE Stefan Alexandru, ALEXANDRU Tudor-George

Faculty: Industrial Engineering and Robotics, Major: Robotics, Year of study: 4, e-mail: stefan.enache1511@gmail.com

1. Introduction

The project focuses on the rigid-flexible dynamic analysis of a segment within the closed kinematic chain of the ABB IRB 660 180/3.15 industrial robot. This study aims to examine velocities, accelerations, system energy, as well as forces and moments in kinematic couplings during operation. By conducting this type of analysis, critical moments in the operation of the assembly can be identified, enabling targeted inspections and reducing the need for lengthy transient analyses. The RFBD analysis will consider forces, moments of inertia, and the centers of gravity of components throughout the process, enhancing the precision and reliability of the system's performance assessment.

2. General overview of robotic cells for palletizing operations.

Palletising is the systematic arrangement of various types of objects such as: parallelepiped-shaped cardboard boxes, bags containing bulk granular or powdered materials, and sets of pre-packaged items like bottles of water or oil, onto transport devices known as pallets. This arrangement is executed both horizontally, forming layers of uniform height, and vertically, stacking multiple layers. Pallets are standardized to optimize global logistics, handling, and transportation of goods. To ensure ISO compliance, loading criteria: maximum, half, and average, must be met.

Figure: 1 Paletizing cell examples

3. The industrial robot used in the application

Figure: 2 ABB IRB 660-180 3.15

Table 1 Robot Specifications

Robot version	IRB 660-180/3.15
Range of action	3150 mm
Payload	180 kg
Number of cycles per hour	1570
Number of axes	4
Mounting mode	La sol/podea
Protection	IP 67
Controller	IRC 5 Single Cabinet

4. Analysis type

Rigid-flexible dynamic analysis is a computational technique used to study the behavior of systems that contain both rigid and flexible components when subjected to dynamic loads or motions. In this analysis, the rigid components are those that do not deform significantly under applied loads, while the flexible components undergo deformation

Rigid Component:

Considered to have negligible deformation under the action of applied forces. Contributes to the overall structure by transmitting and distributing loads to the flexible components.Analysis of rigid components involves balances of forces and moments.

Flexible Component:

Can undergo significant deformation under loads. Responsible for absorbing and dissipating energy in the overall structure.Analysis of flexible components involves the study of deformation, tension and internal force distribution.

Finite Element Method (FEM):

Breaks down the complex structure into small elements and analyzes the behavior of each element under various loads. Used to combine rigid and flexible components into a single coherent analysis. Allows accurate simulation of the interaction between components and their cumulative effects on the overall structure.

Stiffness Matrix Method:

Uses stiffness matrices to represent the behavior of each component. Integrates stiffness and flexibility of components to assess the overall response of the structure. Effective for structures where stiff and flexible components are well defined and interact linearly.

5. Imported geometry and model simplification

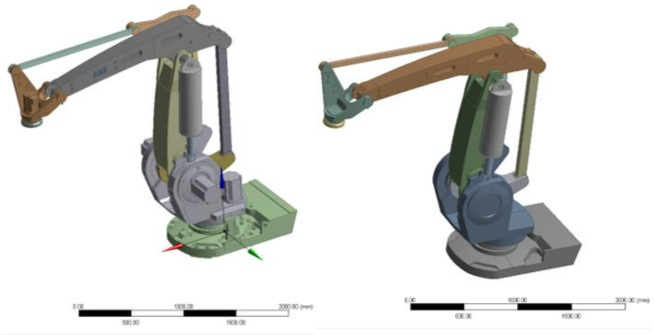

Figure: 3 Imported model and the simplified model

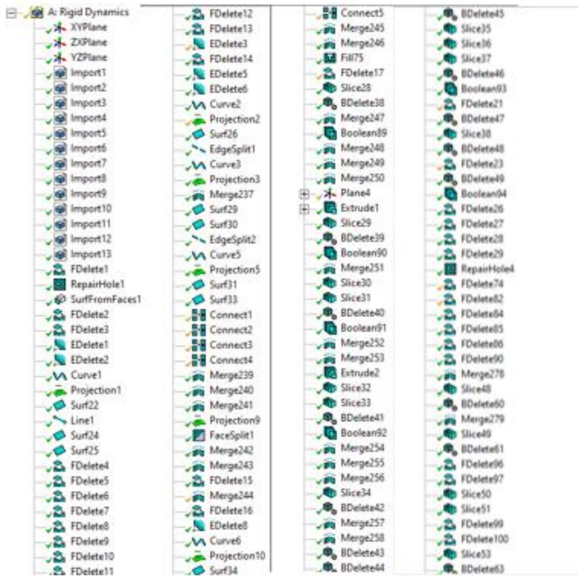

Figure: 4 Simplification commands

6. Material used

The materials used in the analysis are aluminium alloy and structural steel. Structural steel is assigned to the main elements around which the calculation models will be developed, the lower segment of the closed kinematic chain. The aluminium alloy is assigned to the remaining components of the industrial robot in order to reach a weight of 1650kg, similar to the one indicated in the technical book.

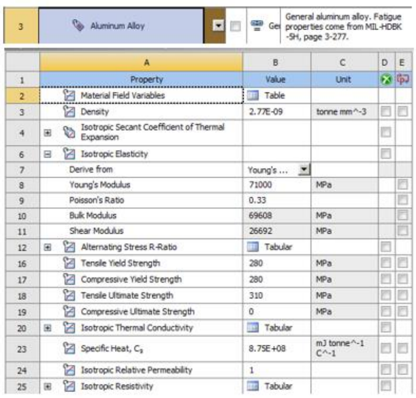

3 Aluminum Alloy — General aluminum alloy. Fatigue properties come from MIL-HDBK -5H, page 3-277.

	A	B	C	D	E
1	Property	Value	Unit		
2	Material Field Variables	Table			
3	Density	2.77E-09	tonne mm^-3		
4	Isotropic Secant Coefficient of Thermal Expansion				
6	Isotropic Elasticity				
7	Derive from	Young's ...			
8	Young's Modulus	71000	MPa		
9	Poisson's Ratio	0.33			
10	Bulk Modulus	69608	MPa		
11	Shear Modulus	26692	MPa		
12	Alternating Stress R-Ratio	Tabular			
16	Tensile Yield Strength	280	MPa		
17	Compressive Yield Strength	280	MPa		
18	Tensile Ultimate Strength	310	MPa		
19	Compressive Ultimate Strength	0	MPa		
20	Isotropic Thermal Conductivity	Tabular			
23	Specific Heat, C_p	8.75E+08	mJ tonne^-1 C^-1		
24	Isotropic Relative Permeability	1			
25	Isotropic Resistivity	Tabular			

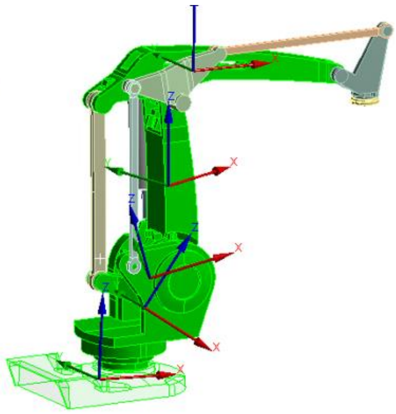

Figure: 5 Aluminum Alloy and the distribution

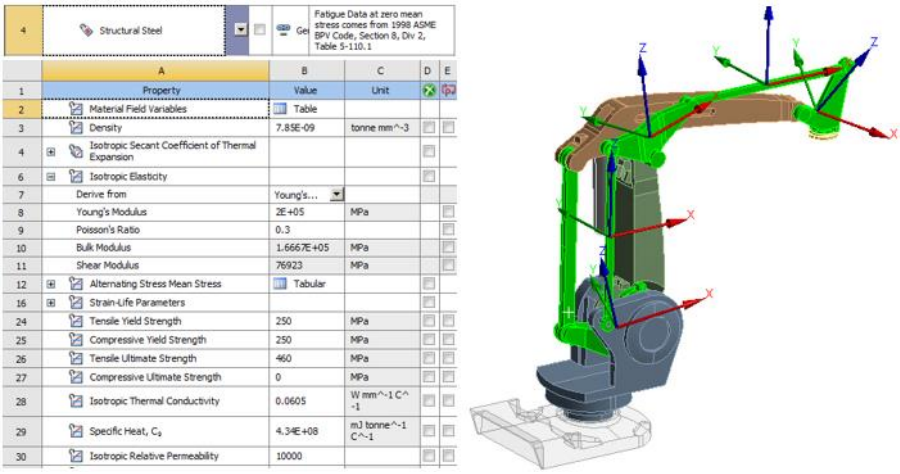

4	Structural Steel		Fatigue Data at zero mean stress comes from 1998 ASME BPV Code, Section 8, Div 2, Table 5-110.1		
	A	B	C	D	E
1	Property	Value	Unit		
2	Material Field Variables	Table			
3	Density	7.85E-09	tonne mm^-3		
4	Isotropic Secant Coefficient of Thermal Expansion				
6	Isotropic Elasticity				
7	Derive from	Young's...			
8	Young's Modulus	2E+05	MPa		
9	Poisson's Ratio	0.3			
10	Bulk Modulus	1.6667E+05	MPa		
11	Shear Modulus	76923	MPa		
12	Alternating Stress Mean Stress	Tabular			
16	Strain-Life Parameters				
24	Tensile Yield Strength	250	MPa		
25	Compressive Yield Strength	250	MPa		
26	Tensile Ultimate Strength	460	MPa		
27	Compressive Ultimate Strength	0	MPa		
28	Isotropic Thermal Conductivity	0.0605	W mm^-1 C^-1		
29	Specific Heat, C_p	4.34E+08	mJ tonne^-1 C^-1		
30	Isotropic Relative Permeability	10000			

Figure: 6 Structural Steel and the distribution

7. Discretization

In this analysis, the computational model is similar to the one used in the static analysis, except that certain components, for which simulation is desired, are considered flexible, while others may be rigid. In order to ensure convergence of the results, it is important to perform a controlled discretization, with appropriate mapping of the faces in contact. The connections between the components of the assembly can be joint, contact, spring, weld points or screws.

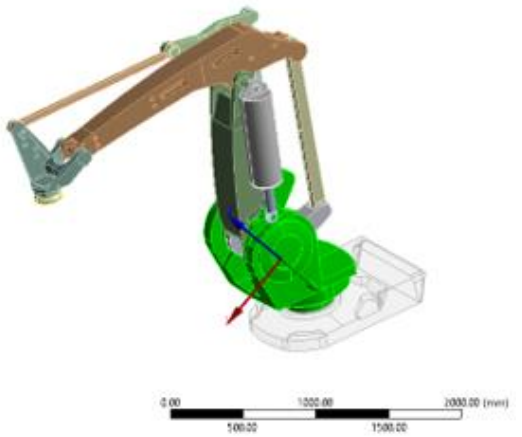

Figure:7 Rigid element

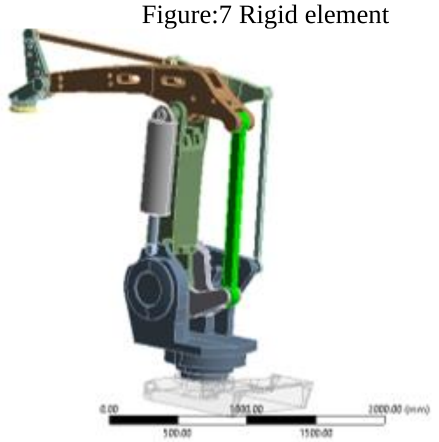

Figure:8 Flexible element

Due to the incorporation of flexible elements, the closed kinematic chain segment experiences condensed geometry, a technique aimed at simplifying dense regions of elements while preserving overall structural behavior. This involves replacing dense elements with simpler ones or applying appropriate boundary conditions. Examples include representing dense regions with condensed elements or using simplified element types that encapsulate their overall behavior. Geometry condensation leads to a notable reduction in finite elements, thereby decreasing computational time in structural analysis.

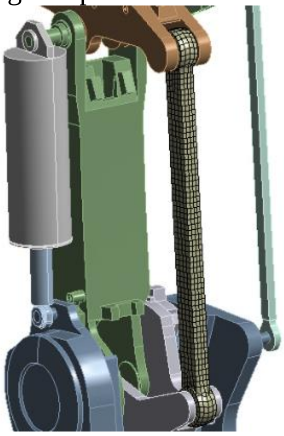

Figure:9 Element

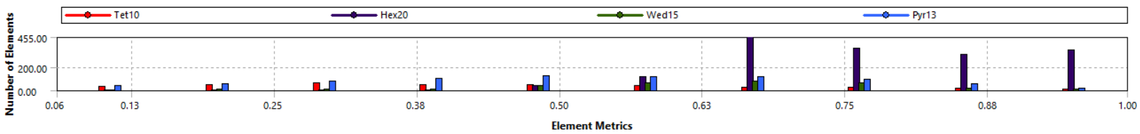

Figure:10 Element metrics

8. Simulation conditions

Kinematic couplings have been made in all axes of the industrial robot The point mass equivalent of the mass of the effector + the manipulated reference was attached.The robot motion cyclogram was extracted according to the simulation.

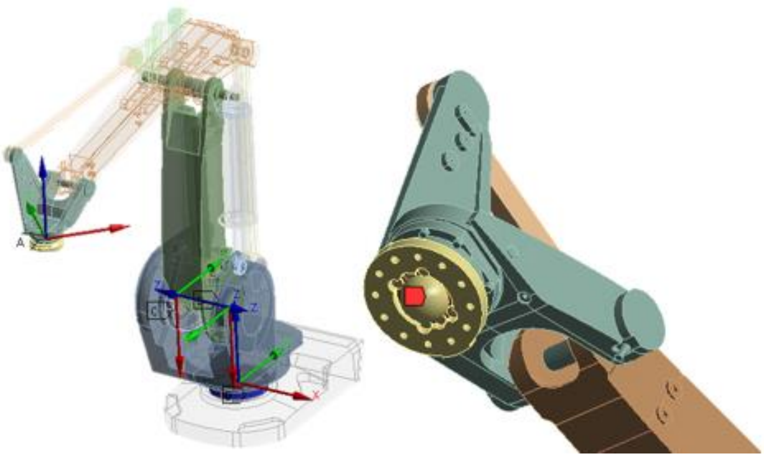

Figure:11 kinematic copling and point of mass

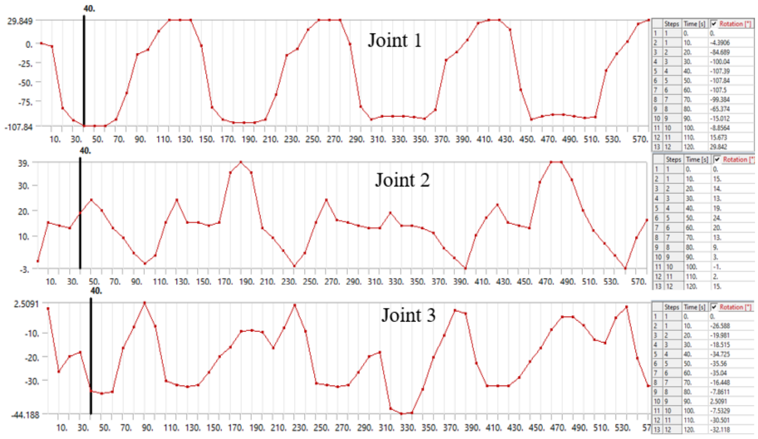

Figure:12 Joint angular speed assignment

9. Simulation Resoults

The graph of total deformation confirms the imposed kinematic cycle**.**

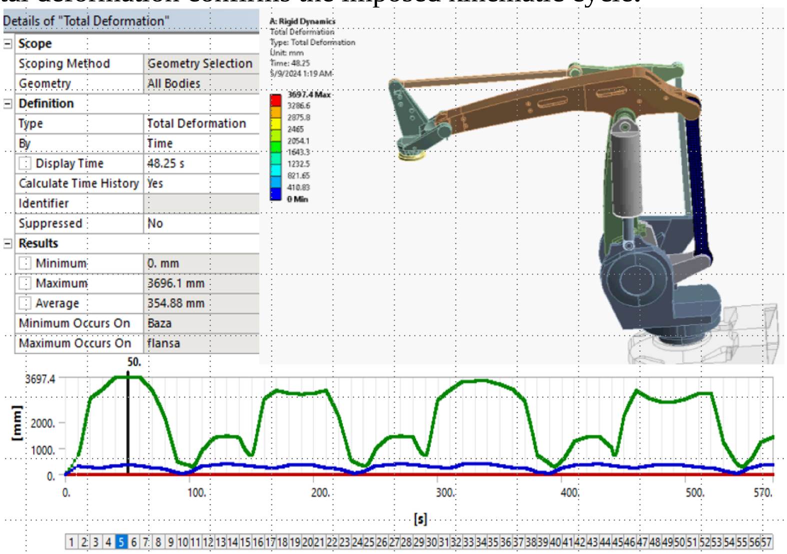

Figure:13 Total Deformation

The maximum strain value is 0.00060439%.

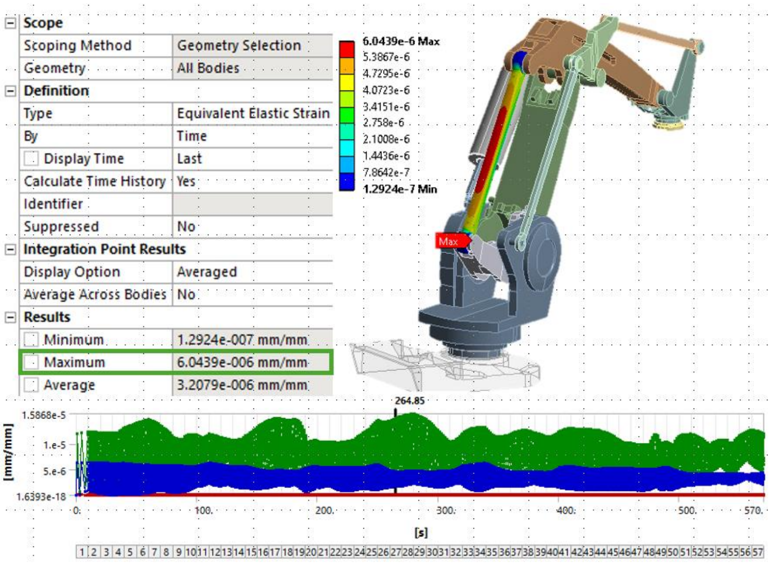

Figure:14 Equivalent elastic strain

The maximum equivalent stress has a value of 3.1736 MPa

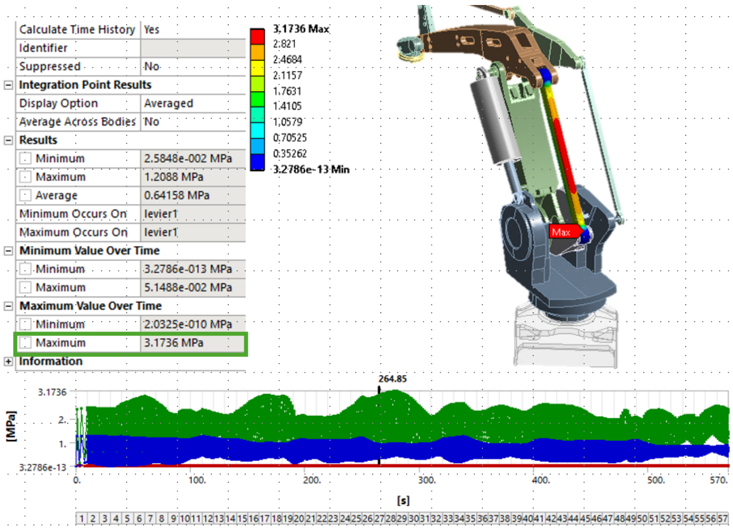

Figure:15 Equivalent stress

10. Conclusions

1) The purpose of the analysis was to capture: the full kinematic cycle, the specific stresses and strains that occur at the level of an element within the closed LC.

2) Rigid-flexible dynamic analysis was chosen to facilitate the convergence of the simulation and the reduction of the running time.

3) The results obtained confirm the structural integrity as the calculated stresses (3.1736 MPa) are well below the material yield strength (250 MPa).

4) The order of magnitude of the specific deformations (10^(-6)) confirms that the positioning accuracy of the IR is not compromised.

11. Bibliography

[1.] Pupaza C. – Inginerie Asistata de Calculator 1, note de curs si aplicatii, UPB, 2023
[2.] Pupaza C. – Inginerie Asistata de Calculator 2, note de curs si aplicatii, UPB, 2023
[3.] Pupaza C. - Curs Analiza în regim tranzitoriu (Analiză dinamică – rezolvare implicită)
[4.] Ansys inovation course - Ansys Mechanical Rigid Body Dynamics

DEVELOPMENT OF A PROTOTYPE FOR A FOUR-AXIS EDUCATIONAL ROBOT

ZAMFIROIU Mihai Alexandru, IVAN Andrei Mario

Faculty: Industrial Engineering and Robotics, Specialization: Robotics, Year of Study: I, e-mail: alexzzz2004@gmail.com

ABSTRACT: The article presents the evolution of a 4-axis palletizing robot prototype, initially developed for an elective course, utilizing 3D printing technologies with PLA material. The robot is configured with NEMA 17 motors and numerical control using Arduino and CNC Shield V3, with a gripper actuated by a Futaba S3000 servomotor.

The current configuration allows precise motion control in industrial environments, implementing equations for both forward and inverse kinematics in a Cartesian system. To enhance performance, the addition of position and speed encoders, limit switches, an efficient cooling system for the motors, as well as a command box and a physical Teach Pendant, are necessary.

These improvements will facilitate the implementation of the robot in factories, offering reliable and adaptable solutions for object handling. Thus, this palletizing robot prototype represents a promising solution for industrial automation.

KEYWORDS: Palletizing robot, 3D printing, Numerical control, Technological improvements, Industrial automation

1. Introduction

The initial idea for this robot emerged as a challenge from a professor. Initially, the concept was to develop a 5-axis modular robot, exclusively using servomotors for movements. The goal was for this robot to be able to lift 1 kg. After analysis and research, I found that NEMA 17 stepper motors are more cost-effective and offer greater precision than servomotors. Additionally, I realized that a closed kinematic chain system would be more suitable for my objective of handling 1 kg loads. This type of configuration allows for a more robust structure and can better manage larger loads while providing improved precision and control in movement.

2. The Current Stage

The current robot has 4 axes, with 3 being numerically controlled and one passive axis that maintains the flange in a vertical position. The 3 numerically controlled axes utilize NEMA 17 motors, each with a torque of 0.59Nm, controlled by an Arduino Mega board, a CNC Shield V3, and 3 DRV8825 drivers.

The 4th axis (flange) is designed for easy and quick effector changes. It is equipped with a pinion-rack architecture gripper, controlled by a Futaba S3003 servo, connected to the Arduino board.

The first axis consists of a central shaft with a smaller pinion driven by the first stepper motor. The gear ratio between the pinions is 1:4, and for smoother movement, it uses a 6006ZZ bearing.

The second axis is positioned above the first assembly and also uses a smaller pinion driven by a motor, with a larger pinion on the axis itself, maintaining the same gear ratio.

The third axis is located near the second axis, with the motors mounted end-to-end. Here, a half-cut pinion is engaged in a kinematic chain. This third axis is above the second axis and is connected to the same kinematic chain. The 4th axis is controlled by the second axis, with another kinematic chain extending from a triad on the third axis to maintain the flange in a vertical position.

All motors are powered by a 12V 5A power supply, but the effector uses a step-down module to reduce the voltage from 12V to 5V.

3. The Evolution of the Robot Over Time

Being a robot created with a low level of initial knowledge, various modifications have emerged during its development. These improvements include:

1. Replacement of the initial motors with more powerful ones, transitioning from a torque of 0.49 Nm to 0.59 Nm to ensure greater force and stability.
2. Modification of the axis attachments by replacing screws with bearings and metal profiles to reduce friction and increase reliability.
3. Enhancement of the gears by printing them from tougher materials such as nylon reinforced with carbon fiber to enhance durability.
4. Creation of an enclosure for the electrical components, centralizing and protecting the robot's control system.
5. Adoption of an Arduino Mega board instead of an Uno to leverage more memory and processing capacity.
6. Use of a CNC Shield V3 to enable the swapping of drivers during robot operation (hot-swapping).
7. Upgrading the drivers from A4988 to DRV8825 for improved performance and adding fans for their cooling, preventing overheating.

I attached below Images of the robot in the initial stage and the current stage (Fig. 1 and Fig.2).

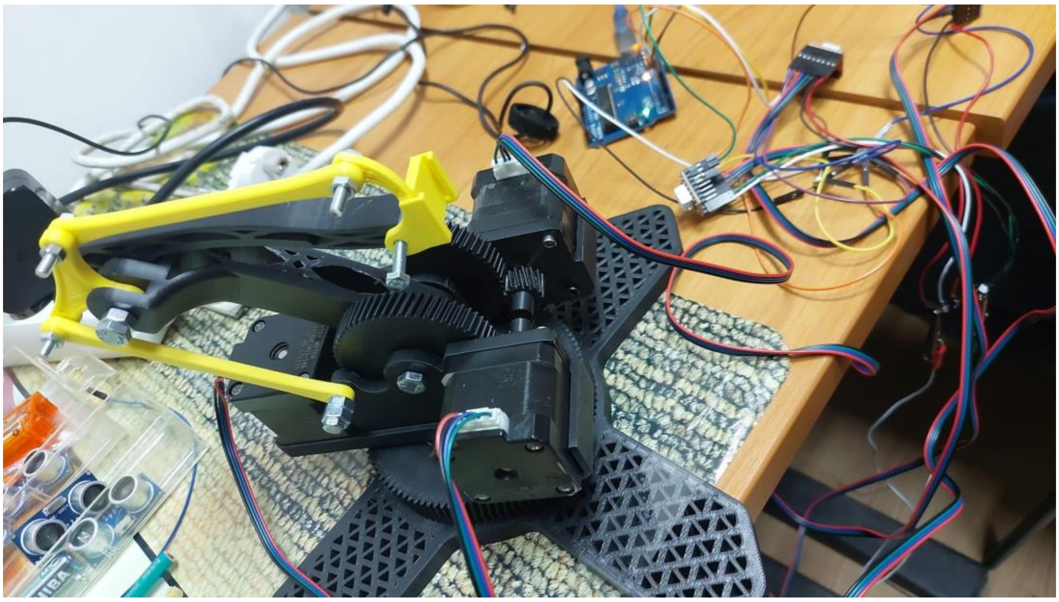

Fig.1 The initial stage of the robot

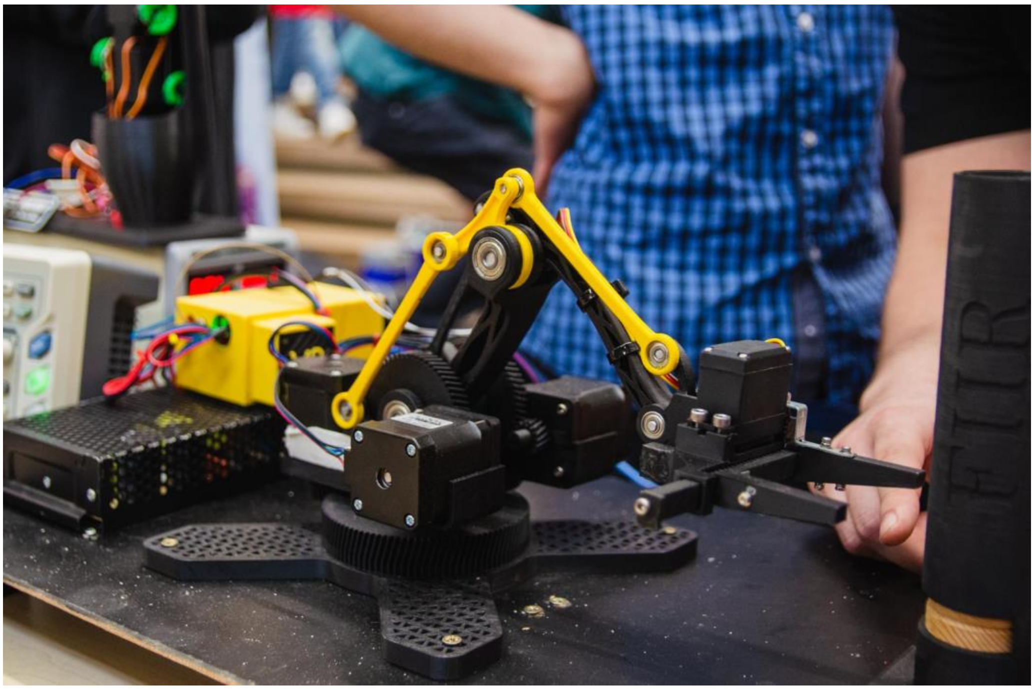

Fig.2 The current stage of the robot

4. The development of the Control System

To provide an experience closely resembling that of a teach pendant, the code was developed with this objective in mind, implemented in C++. Control of the robot on its axes is achieved using the numeric keypad. The left side represents positive rotation of the axis (+), the right side represents negative rotation (-), and the middle column allows returning to the initial position. The same system is used for controlling the robot in Cartesian space: the top line of the numeric keypad controls axis Z, the middle line controls axis Y, and the bottom line controls axis X. In both modes, pressing 0 resets the robot to the initial position (position 0).

During the robot's initialization (setup), it performs calculations using the forward kinematics to precisely determine the effector's position in Cartesian space. In the main loop, the robot calculates the angles required for each axis to move, relative to position 0, in order to control the effector in Cartesian space, using inverse kinematics.

5. The Integration of the Forward Kinematics and the Inverse Kinematics

To efficiently control the robot in a Cartesian axis system, we have implemented both the forward kinematics and inverse kinematics.

The Forward Kinematics is used to calculate the position and orientation of the effector (e.g., the tip of the effector) based on the joint values (angles or positions of the NEMA 17 motors). This model allows us to precisely determine how the robot will position and orient itself in space when specifying certain values for its motors.

The Inverse Kinematics is essential for calculating the joint values needed to place the effector in a desired position and orientation in the Cartesian coordinate system. This model allows us to solve the mathematical equations that transform the desired positions and orientations of the effector into corresponding sets of angles or motor positions, so that the robot can execute the necessary movements.

Implementing these geometric models into the robot's control system has allowed us to achieve an efficient interface for programming and controlling its movements in a Cartesian coordinate system. Thus, we can manipulate and control the robot in a predictable and precise manner, facilitating the execution of palletizing operations and other industrial applications that require controlled movements in three-dimensional space.

Forward Kinematics:

As seen in the images below, I used a YZ coordinate system to calculate the positions Z and Y' (Fig. 3). After that Y' was used in a XY coordinate system to calculate the positions X and Y (Fig. 4).

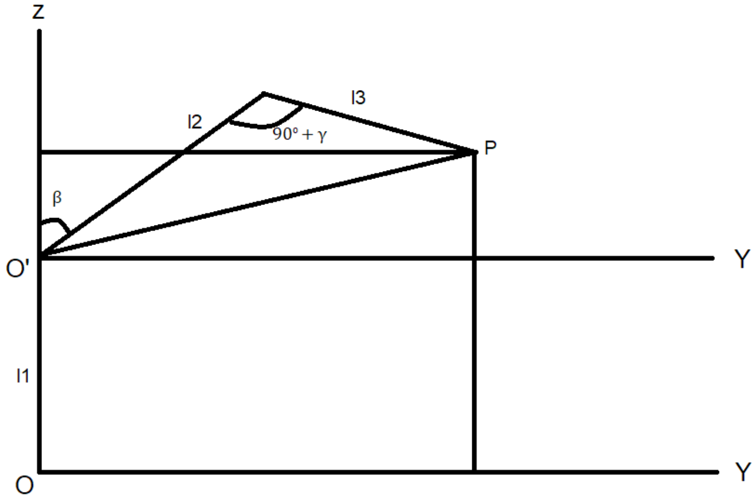

Fig. 3

$$Z = l_1 + l\ cos\,\beta\ - l_3\,cos(90° - \beta + \gamma) \quad (1)$$

$$Y' = l_2\,sin\,\beta + l_3\,sin(90 - \beta + \gamma) \quad (2)$$

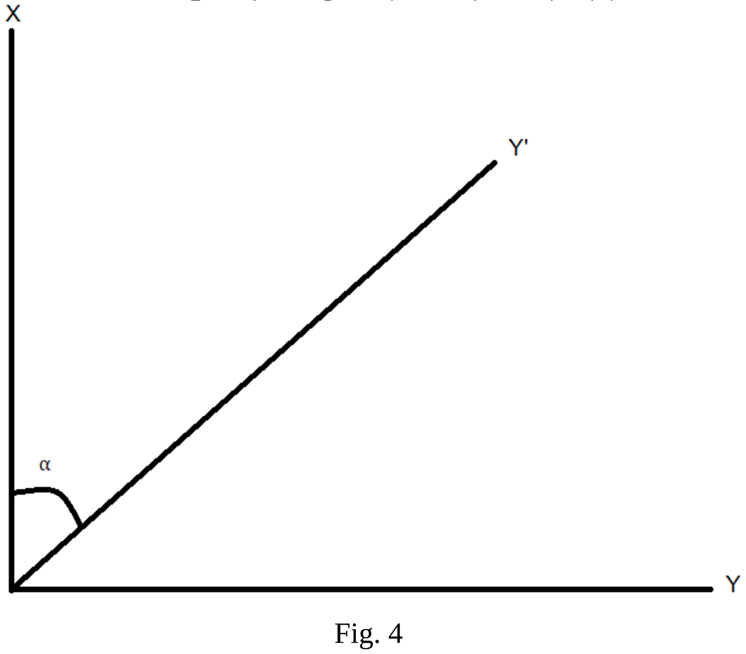

Fig. 4

$$X = \sin\alpha \cdot (l_2 \sin\beta + l_3 \sin(90 - \beta + \gamma)) \quad (3)$$

$$Y = \cos\alpha \cdot (l_2 \sin\beta + l_3 \sin(90 - \beta + \gamma)) \quad (4)$$

Inverse Kinematics:

This time instead of using 2 coordinate systems, I only used one because the architecture of the robot is restricted in moving in a linear way on the X axis and as seen below (Fig. 5), I used simple geometry to calculate the angles β and γ.

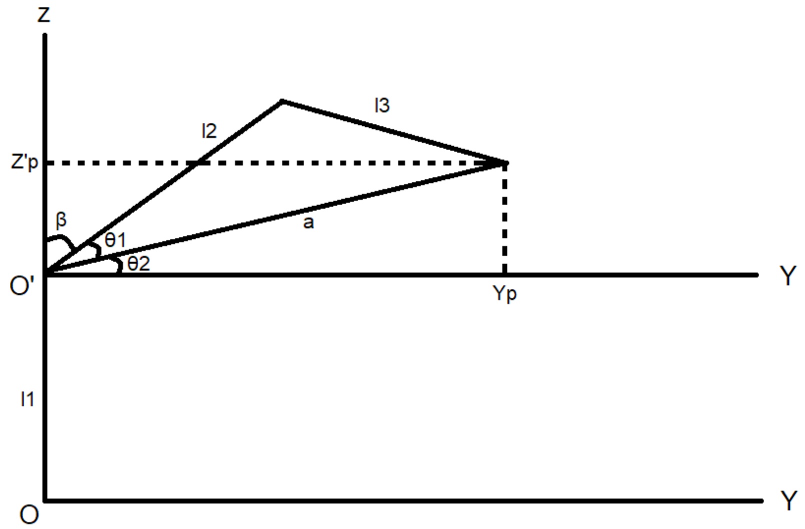

Fig. 5

$$a^2 = \sqrt{{y_p}^2 + {z'_p}^2} \quad (1)$$

$$\cos(90° + \gamma) = \frac{{l_2}^2 + {l_3}^2 + a^2}{2 \cdot l_2 \cdot l_3} \rightarrow \gamma = \cos^{-1}\frac{{l_2}^2 + {l_3}^2 - a^2}{2 \cdot l_2 \cdot l_3} - 90° \quad (2)$$

$$\beta = 90° - \theta_1 - \theta_2 \quad (3)$$

$$\cos\theta_1 = \frac{{l_2}^2 + a^2 - {l_3}^2}{2 \cdot l_2 \cdot a} \rightarrow \theta_1 = \cos^{-1}\frac{{l_2}^2 + a^2 - {l_3}^2}{2 \cdot l_2 \cdot a} \quad (4)$$

$$\tan\theta_2 = \frac{z'_p}{y_p} \rightarrow \theta_2 = \tan^{-1}\frac{z'_p}{y_p} \quad (5)$$

From (3), (4) and (5) $\rightarrow \beta = 90° - \cos^{-1}\frac{{l_2}^2 + a^2 - {l_3}^2}{2 \cdot l_2 \cdot a} - \tan^{-1}\frac{z'_p}{y_p}$ (6)

6. The 3D printing of the robot and the parts used

One of the main objectives of this project was for the robot to be largely 3D printed. Thus, except for the motors, bearings, metal profiles, and screws, all components of the robot are made of PLA, except for the pinions, which are printed from carbon fiber reinforced nylon to increase wear resistance. The robot was printed using a Bambulab A1 printer.

In terms of the parts used, to ensure low friction coefficient control and high reliability, we used aluminum bearings and metal profiles on all axes. The robot is powered by a 12V 5A power source, directly connected to a CNC Shield V3, which in turn is connected to an Arduino Mega board, over which 3 DRV8825 drivers are mounted. Two fans are powered from the same source to cool the drivers, as they tend to heat up significantly during operation. The drivers control the Nema 17 motors. To control the servo motor used in the effector, we used a step-down module to reduce the voltage from 12V to 5V, the voltage required for the servo.

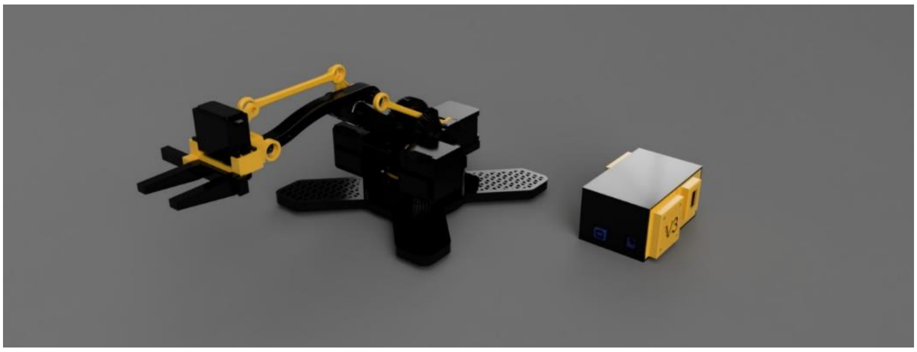

Fig. 6 Photo of the 3D model of the robot

7. Possible upgrades

Currently, the robot is in a development stage where certain components and key features are missing to enhance its performance and functionality. Here is a detailed list of the missing elements and necessary improvements:

1. Position Transducers (Encoders): The absence of position transducers affects the robot's ability to know its exact position in space in real-time. Implementing position transducers will allow precise control of each axis's position and optimize the accuracy and repeatability of movements.
2. Travel Limiters: These devices are essential to prevent movements beyond the robot's workspace, ensuring safety and preventing mechanical damage or accidents.
3. Speed Transducers: The lack of speed transducers hinders the robot's ability to monitor and adjust the speed of its movements. Integrating speed transducers will enable more precise control and optimization of movement dynamics.
4. Motor Cooling: It is important to implement an efficient cooling system for the NEMA 17 motors to prevent overheating and ensure reliable operation during long-duration operations or intense tasks.
5. Cable Channels in Axes: Integrating channels in axes for cable routing will help organize and protect power and signal cables, maintaining a secure connection and minimizing the risk of damage.

6. Integrated Control Box: An integrated control box will provide a compact and secure solution for housing electronic components and the control system, protecting them from external factors and facilitating maintenance and access.
7. Power Supply: Integrating the power supply into the control box will ensure stable and safe power supply to the entire system, avoiding issues related to electrical power.
8. Physical Teach Pendant: A physical Teach Pendant is essential for operative interaction with the robot, allowing the user to initiate and monitor the robot's movements and operations in real-time.

Implementing these improvements will significantly enhance the performance, reliability, and overall usability of the robot in industrial or experimental applications. It is important to integrate these elements to transform the robot into a complete and functional system, tailored to the specific needs and requirements of the application.

8. Conclusions

In conclusion, this palletizing robot prototype has been successfully integrated into a working cell to demonstrate its applicability in industry. Its scalability and implementation in factories are highlighted by the following aspects:

1. Easy effector changeability, allowing adaptability to various tasks and applications.

2. Implementation of intuitive control code enabling robot operation from a keyboard, similar to a Teach Pendant, for efficient and simplified interaction.

3. The simplistic design of the robot, facilitating quick part replacement in case of failures or necessary modifications.

4. The use of hot-swappable drivers, enhancing system reliability and availability in demanding industrial environments.

These essential features and functionalities demonstrate that this palletizing robot prototype is ready for extended implementation and use in factories, providing efficient and adaptable solutions for object handling in various industrial contexts.

9. Bibliography

[1]. Craig, J. J. (2004). Introduction to Robotics: Mechanics and Control (3rd ed.). Pearson Prentice Hall.
[2]. Spong, M. W., Hutchinson, S., & Vidyasagar, M. (2006). Robot Modeling and Control. Wiley.
[3]. Siciliano, B., & Khatib, O. (Eds.). (2016). Springer Handbook of Robotics (2nd ed.). Springer.
[4]. Groover, M. P. (2016). Automation, Production Systems, and Computer-Integrated Manufacturing (4th ed.). Pearson.
[5]. Niku, S. B. (2010). Introduction to Robotics: Analysis, Systems, Applications (2nd ed.). Wiley.

MOBILE PLATFORM FOR DEMONSTRATING SENSOR FUNCTIONALITY

STATE Gabriel-Marian, ACSINTE Ana-Maria, JERCĂLĂU Tiberiu Andrei, Andrei Mario IVAN

Faculty: Industrial Engineering and Robotics, Specialization: Robotics, Year of study: I, e-mail: acsinte.ana17@yahoo.com

ABSTRACT: Sensorius is our advanced robot, designed like a tank to explore and monitor dangerous or hard-to-reach places. Initially a university project, it started as a simple "car" with unreliable sensors and poor cable management.

Equipped with four sensors, Sensorius checks air quality, measures distance to hazards, detects fires, and monitors temperature. It features a screen for real-time monitoring and a Bluetooth module for remote control, enhancing its effectiveness in emergencies.

Future plans include adding tracks for better mobility, extending the structure for more equipment, and improving cable management with a protective casing. These upgrades will make Sensorius a more reliable and versatile tool for hazardous environments.

KEYWORDS: sensor, robotics, tank, autonomous, environment

1. Introduction

In today's technological world, developing robots that can explore and monitor dangerous or hard-to-reach places is increasingly important. Sensorius, our advanced robot, is designed like a tank specifically for this purpose. It is built to handle tough environments that are unsafe for humans.

Sensorius uses four different sensors to gather important information. These sensors check air quality, measure the distance to hazardous objects, detect fires, and monitor temperature. This data helps ensure that the environment is safe and that operations can continue smoothly.

Additionally, Sensorius features a screen for real-time monitoring and analysis, providing operators with immediate feedback. The robot also includes a Bluetooth module for remote control, allowing it to be operated from a safe distance. This feature makes Sensorius particularly useful in emergency situations where human presence is risky.

This essay will explore the technology behind Sensorius, focusing on its sensors, remote control capabilities, and potential uses in dangerous environments. By examining these aspects, we aim to show how Sensorius can improve safety and efficiency in hazardous situations.

2. First Stage

Our robot began as a project for an elective course at our university. In its initial stages, Sensorius was a simpler "car" equipped with fewer sensors. Many of these sensors were not very reliable and often did not function properly. The battery was not yet attached to the robot, we had no cable management, and we were using a breadboard where the wires did not stay in place very well. This made the initial version of Sensorius somewhat unstable and prone to connection issues.

Additionally, we used a car template from an Arduino kit, on which we mounted all the sensors and the Plusivo Mega board. This setup was quite basic and presented several challenges. The sensors' positions were not optimized, which affected their ability to gather accurate data. Moreover, the overall design lacked robustness, as the components were loosely connected, leading to frequent malfunctions during operation.

Unfortunately, the robot was initially controlled from a laptop, which made it less efficient and limited its usability. This setup meant that the robot's mobility and functionality were restricted by the need to stay within a certain range of the laptop, and it was cumbersome to operate in real-time, especially in emergency situations or hazardous environments. The reliance on a laptop for control also posed significant logistical issues, as it required the laptop to be constantly nearby, making it difficult to deploy the robot quickly and effectively in dynamic situations.

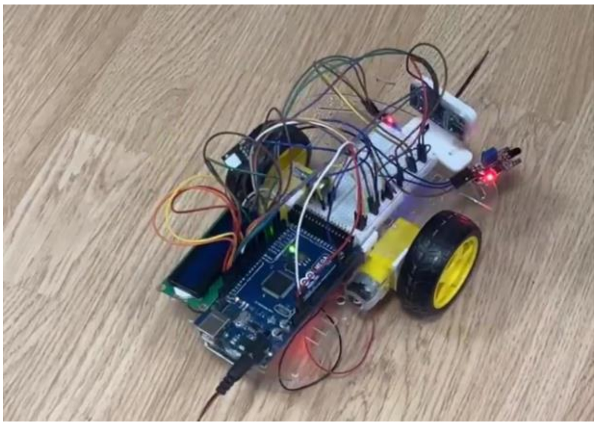

Fig. 1. How our robot looked in its initial state

3. Current Stage

Recognizing these limitations, we embarked on a series of design refinements and upgrades to improve Sensorius. We wanted to create more space for additional sensors and come up with a more innovative design. To achieve this, we replaced the Plusivo Mega board with an original Arduino Uno to ensure the robot would function optimally. We also decided to upgrade the sensors to more efficient ones.

First, we used an HC-SR04 ultrasonic distance sensor, which accurately measures the distance to nearby objects. Next, we installed an MQ-2 flame detection sensor, which identifies the presence of flames or flammable gases, providing crucial safety information. We also added a DHT11 temperature and humidity sensor to monitor the surrounding environment's temperature and humidity levels. To ensure air quality monitoring, we included an MQ-135 air quality sensor, capable of detecting pollutants like carbon monoxide, ammonia, and gasoline.

In addition to these sensor upgrades, we wanted to make the robot more efficient during critical situations by enabling remote control. To overcome the control issues we had in the first prototype, we integrated a Bluetooth module, allowing for remote operation via a custom mobile application. (Fig. 2) This significantly improved the robot's mobility and efficiency, especially in critical situations.

Additionally, for close-range operation and testing, we incorporated an LCD 1602 screen to display real-time data from the sensors. For situations where the robot is operated nearby or during testing, we added an LCD 1602 screen. This screen displays the data collected from the sensors, allowing us to easily monitor the robot’s performance and the environmental conditions it is assessing. These upgrades and improvements transformed our initial project into a more sophisticated and reliable robot, capable of performing complex tasks in hazardous environments.

Over time, we refined the design and improved its capabilities, transforming Sensorius into the advanced robot it is today. The current version of Sensorius is far more robust, reliable, and versatile, capable of performing complex tasks in hazardous environments with enhanced precision and efficiency. This evolution from a basic project to a sophisticated robot highlights the importance of iterative design and continuous improvement in engineering.

Fig. 2 .Our mobile application

4. Future improvements

One of the first things we want to change is the implementation of tracks. Our goal with this modification is to increase stability and mobility on difficult terrains. The benefits of this change are substantial. By incorporating tracks, Sensorius will be able to traverse rough or uneven surfaces with much more ease, enhancing its capability to operate in various challenging environments. This upgrade will also significantly reduce the risk of the robot tipping over or getting stuck, which is a critical improvement for ensuring reliable performance in demanding conditions.

Another priority for our development team is to extend the structure at the top of the robot. This extension is aimed at increasing the carrying capacity of Sensorius and accommodating additional functionalities. By expanding the upper structure, we can mount extra equipment, such as high-resolution cameras, specialized sensors, or manipulation tools. These enhancements are crucial for improving the robot's versatility and adaptability, allowing it to perform a broader range of tasks and operate effectively in diverse scenarios. For instance, adding a camera will enable remote visual inspections, while additional sensors can provide more comprehensive environmental data, and manipulation tools can assist in handling objects or performing specific tasks.

Beyond the technical improvements, we also want to address the design aspects of the robot. The current design of Sensorius was printed in multiple colors using different 3D printers, which resulted in an inconsistent and less professional appearance. This patchwork look not only affects the aesthetics but also compromises the structural integrity of the robot. Furthermore, the sensors were not securely attached due to the uneven print quality, leading to potential issues with sensor performance and reliability. (Fig. 3)

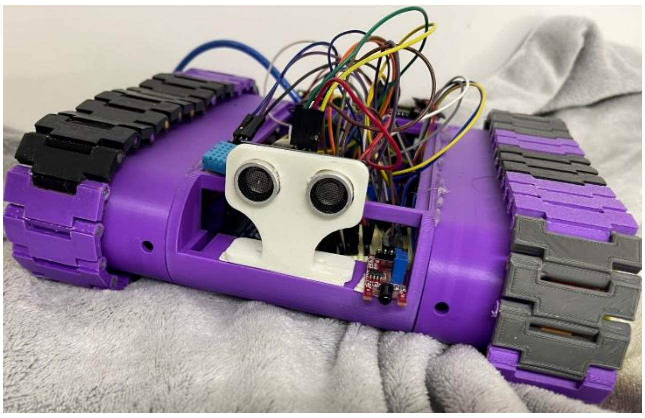
Fig. 3. How bad our print was

To overcome these design challenges, we plan to create a more refined and cohesive design for Sensorius. This involves reprinting the components using a uniform color scheme and higher-quality 3D printers to ensure a sleek and elegant appearance. By doing so, we aim to enhance the visual appeal of the robot, making it look more professional and polished. Additionally, we will ensure that all sensors and components are securely mounted, improving the overall functionality and reliability of the robot.

Implementing these modifications will transform Sensorius into a more capable, reliable, and aesthetically pleasing robot. The addition of tracks will enhance its mobility and stability, making it more effective in challenging terrains. The extended structure will increase its capacity and versatility, allowing it to perform a wider range of tasks. Finally, the improved design will not only make Sensorius look better but also ensure that all components are securely attached and function as intended. Through these comprehensive upgrades, we hope to significantly enhance the performance and usability of Sensorius, making it a more valuable tool for various applications.

At the same time, we want to implement more efficient cable management. This is crucial as we add a protective casing to shield the circuitry from water, fire, and wind. (Fig 3)

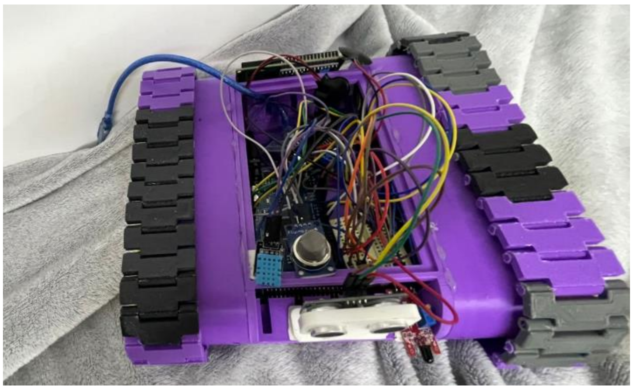

Fig. 3. How our cable management looked

Efficient cable management will help organize and secure the wires, preventing them from becoming tangled or disconnected, which can lead to malfunctions or inefficiencies in the robot's operation. Proper cable management also contributes to the overall cleanliness and maintainability of the internal components, making it easier to perform maintenance and upgrades in the future.

Adding a protective casing is another significant improvement we are planning. This casing will serve multiple purposes. First, it will protect the sensitive electronic components from environmental hazards such as water, fire, and strong winds. By safeguarding the circuitry, we can ensure that Sensorius continues to function reliably even in harsh conditions, thus extending its operational lifespan and enhancing its durability.

The protective casing will also help to enhance the robot's overall robustness and structural integrity. It will provide an additional layer of security against physical impacts and debris, which is particularly important when Sensorius is navigating through rough or hazardous terrains. With this casing, we can also improve the robot's aesthetic appeal, giving it a more polished and professional look.

5. Bibliografie

[1]. Smith, John. "Developing Robots for Hazardous Environments." Robotics Today, vol. 23, no. 4, 2023, pp. 45-59

[2]. Brown, Emily. "Advancements in Sensor Technology for Robotic Applications." Sensors Journal, vol. 15, no. 2, 2022, pp. 112-125

[3]. Patel, Rajesh. "Improving Stability and Mobility in Robotic Designs." Robotics Engineering Review, vol. 12, no. 1, 2024, pp. 30-42

THE DESIGN AND IMPLEMENTATION OF A ROBOTIC ARM WITH TWO DEGREES OF FREEDOM

POPIDAN Andrei-Cristian, POPESCU Constantin-Adrian

Faculty: Industrial Engineering and Robotics, Industrial Logistics Specialization, Year of study: I, e-mail: cpopidan@gmail.com

ABSTRACT: The document presents a control algorithm for a 2-degree-of-freedom robotic arm, utilizing inverse kinematics to calculate the joint angles required to reach the desired end-effector position. Two mathematical models are presented to determine the joint angles, based on trigonometric equations and the Pythagorean theorem. The motor control is implemented using a PID controller, which includes proportional, integral, and derivative components to reduce error, eliminate steady-state errors, and minimize the rate of change of the error. The result is a complete control system for the robotic arm.

KEYWORDS: robot, algorithm, robot programming

1. Introduction

Robotic arms are automated mechanical devices designed to perform tasks with precision and efficiency. Widely used in industries such as manufacturing, automotive, and healthcare, they enhance productivity by executing repetitive, hazardous, or complex operations that are difficult for humans. These versatile tools improve product quality, reduce labor costs, and increase workplace safety. By integrating advanced technologies like AI and machine learning, robotic arms continue to revolutionize industrial processes and drive innovation. This paper will present the design process of a robotic arm with two degrees of freedom, as well as the development process of a control program for this arm.

2. Current state

The accurate control of motion is a fundamental concern in the robot arm, where placing an object in the specific desired location with the exact possible amount of force and torque at the correct definite time is essential for efficient system operation. In other words, control of the robot arm attempts to shape the dynamic of the arm while achieving the constraints foisted by the kinematics of the arm and this has been a key research area to increase robot performance and to introduce new functionalities. In general, the control problem involves finding suitable mathematical models that describe the dynamic behaviour of the physical robot arm for designing the controller and identifying corresponding control strategies to realize the expected system response and performance [1].

3. Arm design

This type of system aims to concentrate the mass of the entire arm at its base, thereby reducing the inertial torques caused by movement. This is achieved through the innovative use of bevel gears. The transmission requires three bevel gears, two of which are identical. The identical gears are mounted on a fixed shaft so that they can rotate individually, while the third gear is mounted between the two, constrained in such a way that it has two degrees of freedom: rotation around its own central axis and rotation around the fixed shaft.

In the type of assembly presented above, by independently rotating each gear, we can achieve motion with 2 degrees of freedom. Next, I will develop the basic outline**:**

- The orange bevel gears must be "separated" from the fixed shaft by means of bearings.
- The orange bevel gears must be connected to the motors through a gear mechanism.

- A component must be designed to constrain the purple bevel gear according to the requirements.
- Addition of a gear mechanism using bevel gears to modify the axis of rotation for the second degree of freedom.
- Addition of the second arm segment.

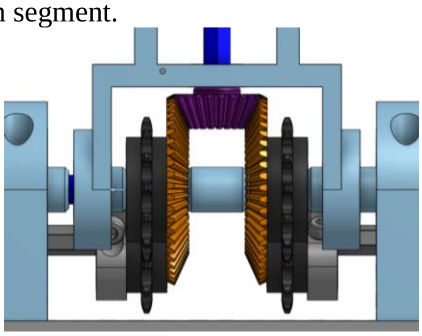

Fig. 1. CAD model of the bevel gear assembly (differential)

The arm was designed in Onshape and Fusion360.

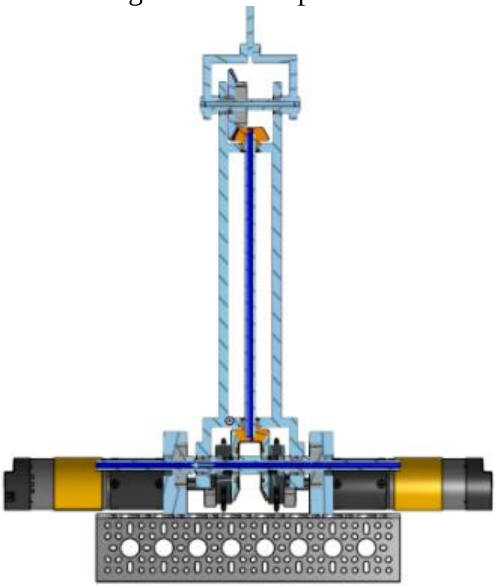

Fig. 2. Section view of the arm

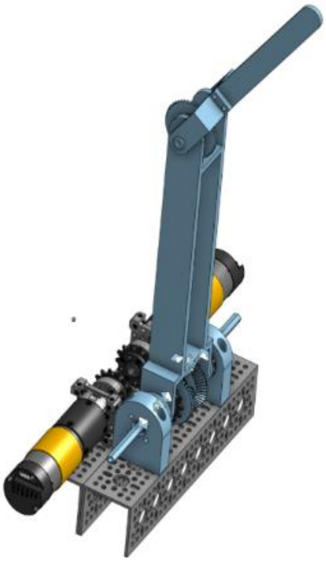

Fig.3 CAD model of the arm

4. Programming

A first step in developing a control algorithm for a system is creating a mathematical model of it.

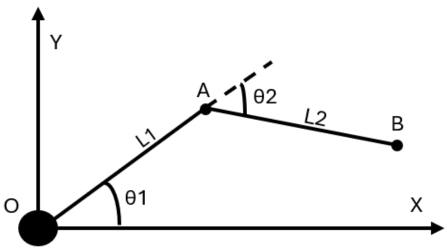

Fig. 4. System schematic

The development of the first mathematical model is presented below.

$$A_1 = \begin{pmatrix} \cos & \theta_1 & -\sin\theta_1 \\ \sin & \theta_1 & \cos\theta_1 \end{pmatrix} \; A_2 = \begin{pmatrix} \cos & \theta_2 & -\sin\theta_2 \\ \sin & \theta_2 & \cos\theta_2 \end{pmatrix} \; \bar{r} = \begin{pmatrix} x_B \\ Y_B \end{pmatrix} \tag{1}$$

A1 is the rotation matrix corresponding to the angle θ1, A2 is the rotation matrix corresponding to the angle θ2, and r is the position vector of point B (the end-effector). The column vectors with elements l1,0 and l2,0 are the polar coordinates of the ends of each segment. The following relationship exists between these matrices:

$$\bar{r} = A_1 A_2 \begin{pmatrix} l_2 \\ 0 \end{pmatrix} + A_1 \begin{pmatrix} l_1 \\ 0 \end{pmatrix} = \begin{pmatrix} l_1\cos\theta_1 + & l_2\cos(\theta_1+\theta_2) \\ l_1 \sin\theta_1 & +l_2\sin(\theta_1+\theta_2) \end{pmatrix} \tag{2}$$

With the help of this relationship, we can develop a system of equations:

$$l_1\cos\theta_1 + l_2\cos(\theta_1+\theta_2) = x_B \tag{3}$$

$$l_1\sin\theta_1 + l_2\sin(\theta_1+\theta_2) = y_B \tag{4}$$

If we move the first term of each equation to the right side of the equality, square them, and sum them up, we obtain the following equation:

$$X_B^2 + Y_B^2 + l_1^2 - l_2^2 = 2X_B l_1 \cos\theta_1 + 2Y_B l_1 \sin\theta_1 \tag{5}$$

$$A = B\cos\theta_1 + C\sin\theta_1 \tag{6}$$

A, B, and C are constants depending on the system parameters (arm lengths) and input data (desired position of the end-effector, XB and YB). To solve this equation, we will resort to a geometric method. We will divide the entire equation by $\sqrt{B^2+C^2}$. $\sqrt{B^2+C^2}$ it is equal to the length of a hypotenuse in a right triangle with legs of length B and C. Thus, we can rewrite the equation:

$$\frac{A}{\sqrt{B^2+C^2}} = \frac{B}{\sqrt{B^2+C^2}}\cos\theta_1 + \frac{C}{\sqrt{B^2+C^2}}\sin\theta_1 \tag{7}$$

$$\cos\gamma\cos\theta_1 + \sin\gamma\sin\theta_1 = \frac{A}{\sqrt{B^2+C^2}} \tag{8}$$

$$\cos(\gamma+\theta_1) = \frac{A}{\sqrt{B^2+C^2}} \tag{9}$$

The following equality results:

$$\theta_1 = \gamma \pm \arccos\left(\frac{A}{\sqrt{B^2+C^2}}\right) \tag{10}$$

$$\gamma = \arctan\left(\frac{C}{B}\right) \tag{11}$$

Thus, we can determine both valid variants for θ1. Furthermore, we will find the variants of θ2 for each θ1 by substituting, one by one, both values of θ1 into the equations that I will detail later. Below, we have the same system of equations used previously.

$$l_2\sin(\theta_1+\theta_2) = Y_B - l_1\sin\theta_1 \tag{12}$$

$$l_2\cos(\theta_1+\theta_2) = X_B - l_1\cos\theta_1 \tag{13}$$

From this, we will extract the following equality:

$$\frac{l_2\sin(\theta_1+\theta_2)}{l_2\cos(\theta_1+\theta_2)} = \frac{Y_B - l_1\sin\theta_1}{X_B - l_1\cos\theta_1} \tag{14}$$

$$\mathrm{D} = \frac{Y_B - l_1\sin\theta_1}{X_B - l_1\cos\theta_1} \tag{15}$$

With the letter D, we will denote this fraction on the right-hand side of the equality, all elements comprising it being known. Simplifying l2 by l2 and replacing sin/cos with tan, we obtain:

$$\tan(\theta_1+\theta_2) = D \Rightarrow \theta_2 = \arctan D - \theta_1 \tag{16}$$

To test this mathematical model, I translated it into a Python algorithm. This algorithm displays the angles at which the joints should be rotated in the console. To verify these angles, I also developed a "forward kinematics" algorithm where I input the data provided by the inverse kinematics.

This algorithm returns two pairs of angles (corresponding to both variants of θ1), but only one of them is correct. Unfortunately, this is unacceptable because, in most cases, one of the solutions is not physically possible (due to the physical constraints of the systems), or one of the solutions involves a considerably larger movement than the other.

In search of a solution to the problem encountered in the initial version, I found another mathematical model, simpler, which I studied more thoroughly. A major difference this variant has in approach compared to the previous one is how it begins. It first determines the angle θ2.
One first equation of this model is:

$$\theta_2 = \pi + m(\measuredangle OAB) \tag{17}$$

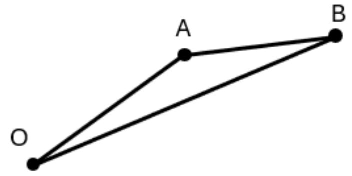

Fig. 5. The representation of triangle AOB used in calculating angle OAB

In this triangle, we apply the generalized Pythagorean theorem:

$$OB^2 = OA^2 + AB^2 + 2OA \cdot AB \cos A \tag{18}$$

$$\frac{OB^2 - OA^2 - AB^2}{2 \cdot OA \cdot AB} = \cos A \tag{19}$$

$$\frac{X^2 + Y^2 - l_1^2 - l_2^2}{2l_1 l_2} = \cos\theta_2 \tag{20}$$

$$\sin\theta_2 = \pm\sqrt{1 - \cos^2\theta_2} \tag{21}$$

$$\theta_{21} = \arctan\left(\frac{\sqrt{1 - \cos^2\theta_2}}{\cos\theta_2}\right) \tag{22}$$

$$\theta_{22} = \arctan\left(\frac{-\sqrt{1 - \cos^2\theta_2}}{\cos\theta_2}\right) \tag{23}$$

where θ_{21} and θ_{22} are the two variants of angle θ2. The next step is to find the angle θ1. To find angle θ1, we created two auxiliary angles: alpha and beta.

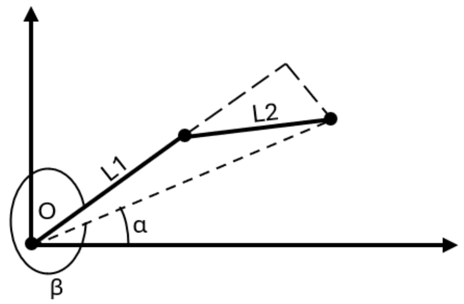

Fig. 6. The construction of the second auxiliary triangle.

These two angles are described by the following equalities:

$$\alpha = \arctan\left(\frac{Y}{X}\right) \tag{24}$$

$$\beta = \arctan\left(\frac{l_2 \sin\theta_2}{l_1 + l_2\cos\theta_2}\right) \tag{25}$$

$$\theta_1 = \alpha - \beta \tag{26}$$

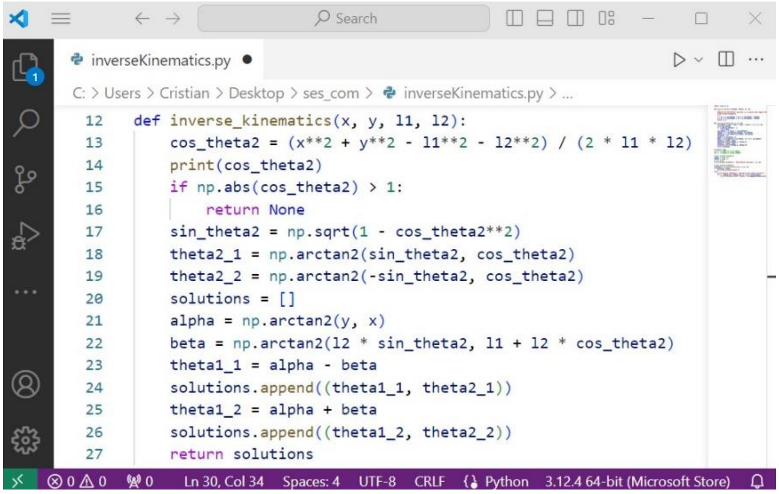

Fig. 7. The algorithm based on the second model in Python.

This time, the code returns both pairs of correct angles.

To adapt this algorithm to a differential drive robot arm, we need to transform the desired joint angles into motor rotation degrees. Considering that the total ratio between input and output wheels is 1:1, we have the following relationships:

$$\frac{m_1 + m_2}{2} = \theta_1 \tag{27}$$

$$\frac{m_1 - m_2}{2} = \theta_2 \tag{28}$$

$$m_2 = \theta_1 - \theta_2 \tag{29}$$

$$m_1 = \theta_1 + \theta_2 \tag{30}$$

Where m1 and m2 represent the rotation degrees of motors 1 and 2, respectively. The motors I'm using have integrated encoder sensors that measure the rotation of the shaft. According to the manufacturer, at a full rotation of the shaft, the encoder measures 1425 ticks (one tick is one rotation of the encoder). To control the motors and move the arm precisely, a PID controller algorithm needs to be implemented. This type of algorithm has 3 components:

1. Proportional – meant to minimize the error as much as possible
2. Integral – meant to mitigate any constraint error
3. Derivative – meant to reduce the rate of change of the error

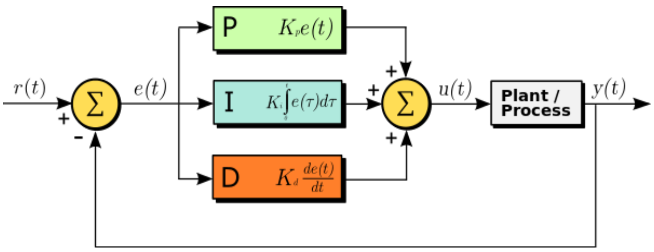

Fig. 8. PID block diagram [2]

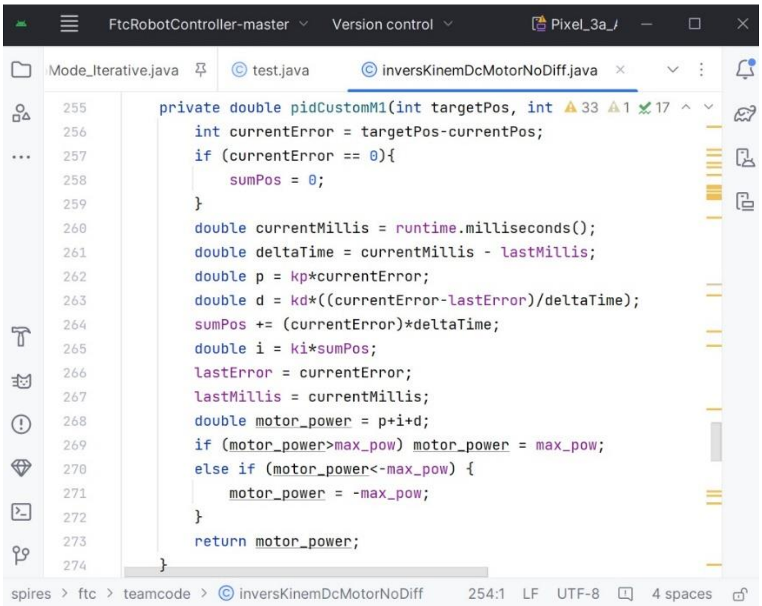

Fig. 9. PID algorithm in Java

The algorithm returns a power to be applied to the motor (the motor can receive power in the range of -1 to 1). This power is composed of 3 parts:

- The proportional part is the product of the error (the difference between the desired position and the current position) and a specific coefficient (kp).
- The derivative part is the product of the coefficient kd and the derivative of the error (the difference between the current error and the previous error divided by the difference in time between these errors).
- The integral part is the product of the coefficient ki and the integral of the error (the sum of all previous errors multiplied by the time interval between two errors).

5. Conclusion

The article discusses the development of a control algorithm for a robotic arm with two degrees of freedom. It outlines the mathematical models used for inverse kinematics to calculate the joint angles required to achieve a desired end-effector position. Additionally, it describes the implementation of a PID controller algorithm to control the motors of the robotic arm, ensuring precise movement and error reduction.

The article also highlights the importance of considering physical constraints and practical limitations when designing and implementing control algorithms for robotic systems. It emphasizes the need for accurate measurements and feedback mechanisms, such as encoder sensors, to ensure effective control and motion planning.

Overall, the article provides valuable insights into the theoretical framework and practical considerations involved in developing control algorithms for robotic arms, offering a comprehensive approach to achieving precise and efficient robotic manipulation.

6. References

[1]. Okubanjo, A. A.*, Oyetola, O. K., Osifeko, M. O., Olaluwoye, O. O. and Alao, P. O. (2017), ”Modeling of 2-DOF Robot Arm and Control”, Department of Computer and Electrical & Electronics Engineering, Olabisi Onabanjo University, Ago-Iwoye, Nigeria

[2]. https://en.wikipedia.org/wiki/Proportional%E2%80%93integral%E2%80%93derivative_controller

DESIGN OF AN AUTOMATIC WASTE SORTING AND RECYCLING SYSTEM

JELESCU Andrei, DUMITRESCU Florin-Cătălin, POPESCU Constantin-Adrian

Faculty of Industrial Engineering and Robotics, Industrial Logistics Specialization, Year II,
e-mail: jelescuandrei0102@gmail.com

ABSTRACT: The smart bin development project is an innovative initiative designed to address the challenges of urban waste management in an efficient and sustainable manner. Given the continued population growth and accelerated urbanization, it is crucial to adopt smart solutions that optimize collection processes and reduce the negative impact on the environment.

KEYWORDS: Waste, Urban, Collection, Smart, Bin.

1. Introduction

This project aims to design and present an intelligent and autonomous waste sorting and recycling device. The final product wants to have the ability to detect and separate the most common types of waste (glass, plastic, metal, paper, etc.) to then chop them up and store them in separate containers.

The intelligent "basket" aims to have a modular architecture (fig.1) by separating it into two distinct bodies (the sorting module and the recycling module) to allow the connection of several recycling modules (fig.2).

Fig.1 Assembly with a recycler

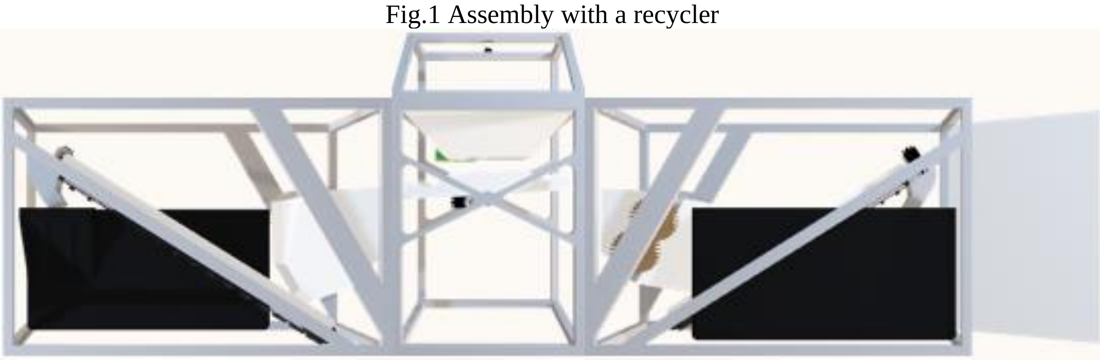

Fig.2 Assembly with two recyclers

2. The sorting module

The sorting module is the brain of the entire device. In this module, the nature of the waste is detected to send the necessary commands to the recycling bodies. From a structural point of view, the module is made up of frame, outer walls, detection chamber, microcomputer, guide funnel and pivoting tray (fig.3).

Explicitly, the frame of the device is made of construction steel (S235JR [3]) and follows the outline of a rectangular prism (plus a cover in the shape of a trapezoidal prism), plated with thin sheet metal or compact transparent polycarbonate.

The detective camera that will be used is one compatible with Raspberry Pi 4[1] (the microcomputer we intend to use), offered by the manufacturer (Raspberry Pi Module Camera 2) [2].

The swivel tray will be printed from 3D extruded plastic (PLA) and will have roughness on the upper surface (which will later be painted with a special rubberized layer to avoid slipping).

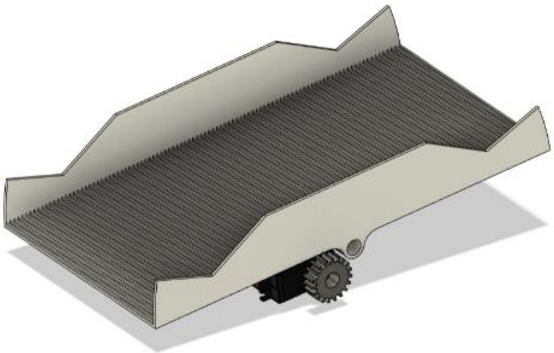

Fig. 3 Swivel tray

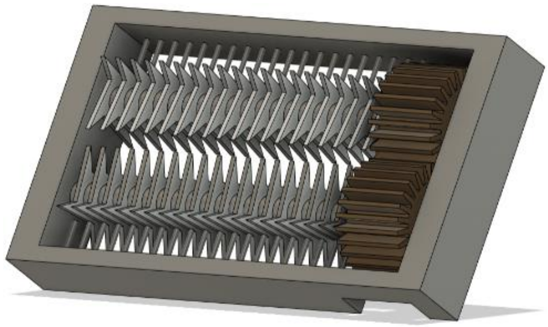

Fig. 4 Chopper

The waste path in the device follows the following critical steps:

i. Waste detection
ii. Categorization of waste
iii. Pivoting the tray

The sorting module, equipped with a microcomputer and a detection camera, will use a software model assisted by artificial intelligence.

Compared to alternatives with up to 5 distinct sensors, the program with artificial intelligence is clearly superior, being able to improve its detection capacity depending on the desired waste and the desired precision.

After the program decides what type of waste has been inserted, the pivoting tray will be tilted towards the general direction (in case of assembly with a recycling module) or to the left/right (for double assembly).

Thus, at the end of the process, the waste is removed from the sorting module in the direction decided by the program, and the route of the foreign element continues in the recycling module.

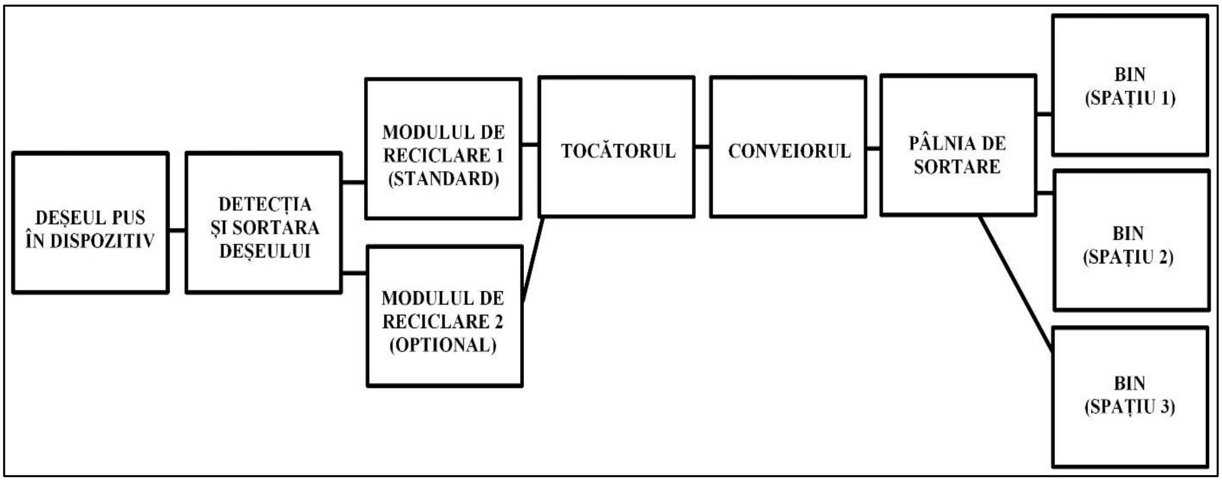

Fig. 5 The route of the waste in the sorting and recycling device

3. The recycling module

The recycling module represents the workspace of the smart device and supports all the elements that physically modify the waste. The so-called forward path of the foreign body through the recycling module follows the following main elements: input hopper, chopper (fig. 4), output hopper, conveyor (fig. 6), sorting hopper (fig. 6), sorting basket (fig, 7).

The chopper is made up of two shafts connected by toothed wheels on which shredding blades are arranged. The blades are cut and moved specifically to pull the waste inward and shred it.

The conveyor has a belt with paddles to ensure the ascent of the shredded waste to the last branch in the circuit: the sorting hopper.

The sorting hopper facilitates the final sorting between three storage compartments (which can also be used for the same type of waste where a larger volume is required.

The complete route of the waste in the device is reflected in fig 5.

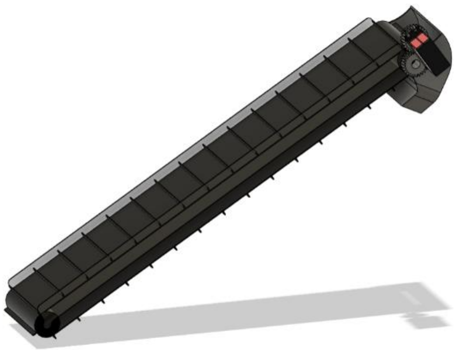
Fig. 6 Conveyor and sorting funnel

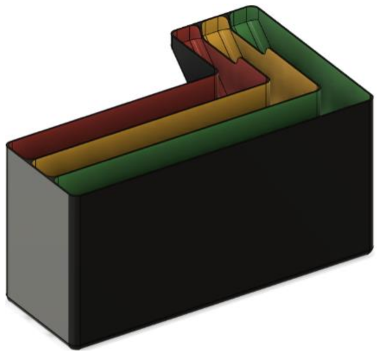
Fig. 7 Sorting basket

4. Additional features

In designing the device, we considered the following self-imposed requirements and below are the ways in which we solved each of them:

a) The provision of programmable storage spaces (to facilitate various locations with various requirements regarding the most common waste) was solved by developing a sorting bin with three storage spaces with different volumes to make efficiency possible.

b) The modular feature of the device (which also appears to expand the storage space) was made to be able to sort up to 6 different types of waste, at the buyer's choice.
c) The cleaning of the shredder through the source code of the product (which controls the entire sorting and recycling process) was optimized by successive rotations in both directions to ensure a minimum of particles mixed between the storage spaces.
d) The sorting software uses artificial intelligence to be in a continuous passive improvement and to be able to change the types of collected waste at any time, without the limitations of the sensors.

5. Status

Now, the project is at the end of the design phase, we have completely completed the waste route from a theoretical and digital point of view. From a physical point of view, the prototype is in the realization phase (the frame and the chopper are currently being built).

Among the features that we were going to achieve physically on the device, we list:

i. Obtaining and training the software with AI.
ii. Integration of some LEDs and filling sensors in the storage bin.
iii. Designing an easy-to-use entrance that does not allow hands to enter.

6. Conclusions

In summary, the sorting and recycling machine can be a useful tool in any store/mall/market/park due to its automatic nature and the novelty with which it can convince more people to recycle.

If the project is further developed and improved, we consider that our device can replace the common bins used today in public places.

Bibliography

[1] *** Buy a Raspberry Pi 4 Model B – Raspberry Pi
[2] *** Buy a Raspberry Pi Camera Module 2 – Raspberry Pi
[3] ***S235JR Material | 1.0038 Steel Equivalent, Properties, Composition (theworldmaterial.com)

STUDY ON AGV ROUTE OPTIMIZATION

STOICA David-Christian, COSTIUC Andrei-Cosmin, . Constantin-Adrian POPESCU

Faculty of Industrial Engineering and Robotics, Specialization: Industrial Logistics, Year: Licență II, email: stoicadavid12@gmail.com

ABSTRACT: *The study addresses the optimization of AGV (Automated Guided Vehicle) routes in an industrial environment, with the main objective of improving operational efficiency and reducing associated costs. By employing a variety of methods and techniques, including search and planning algorithms as well as emerging technologies like machine learning, the research proposes innovative solutions to maximize AGV performance. Using relevant input data and a rigorous evaluation of the results obtained, the study provides a clear perspective on optimal methods for AGV route optimization in a modern industrial setting. The results of this study have the potential to significantly contribute to enhancing operational efficiency and improving AGV system performance across various industries.*

1. Introduction

In a world where technology is becoming increasingly present in the industrial environment, Automated Guided Vehicles (AGVs) have become an essential component in production and logistics processes, contributing to workflow optimization and reducing operational costs [2]. They not only optimize workflows but also reduce operational costs and improve overall operational efficiency.

In this context, optimizing AGV routes becomes a crucial challenge, as routes directly influence delivery times, energy consumption, and efficient resource use in an industrial setting [1]. Therefore, this work focuses on studying and developing methods and algorithms to optimize AGV routes, considering the various variables involved.

The motivation behind this research lies in improving AGV performance in terms of response time, energy efficiency, and adaptability to changes in the work environment. The main objective of this work is to propose innovative solutions for optimizing AGV routes, with a focus on maximizing operational efficiency and minimizing associated costs.

2. Actual Study

Optimizing AGV routes reflects significant advancements in the development and implementation of technological solutions to enhance the performance of these autonomous vehicles. In recent years, researchers from various fields have explored methods and techniques to optimize AGV routes, addressing various aspects of operational efficiency and resource management [4].

Among the primary research directions are the use of search and planning algorithms, as well as the application of emerging technologies like machine learning and artificial intelligence. These approaches have enabled the development of increasingly advanced solutions that are adaptable to the specific needs of different industrial environments.

Furthermore, the current state of AGV route optimization practices reflects a rise in AGV technology adoption across industries such as manufacturing, logistics, distribution, and transportation. Companies worldwide are investing in implementing and integrating AGVs into their operational processes, recognizing the significant benefits they bring in terms of efficiency, precision, and flexibility.

However, challenges and unaddressed aspects still exist in AGV route optimization. Although considerable progress has been made, there remain opportunities for improvement and innovation in developing more efficient and adaptable solutions to meet the increasingly complex demands of the modern industrial environment.

3. Case Study

In this project, we focused on the development and implementation of an autonomous AGV (Fig.1) equipped with a towing hook, designed for the efficient handling and transport of loads in industrial environments. Our goal was to create a system capable of operating in a dynamic environment, quickly adapting to environmental changes and the specific requirements of the application.

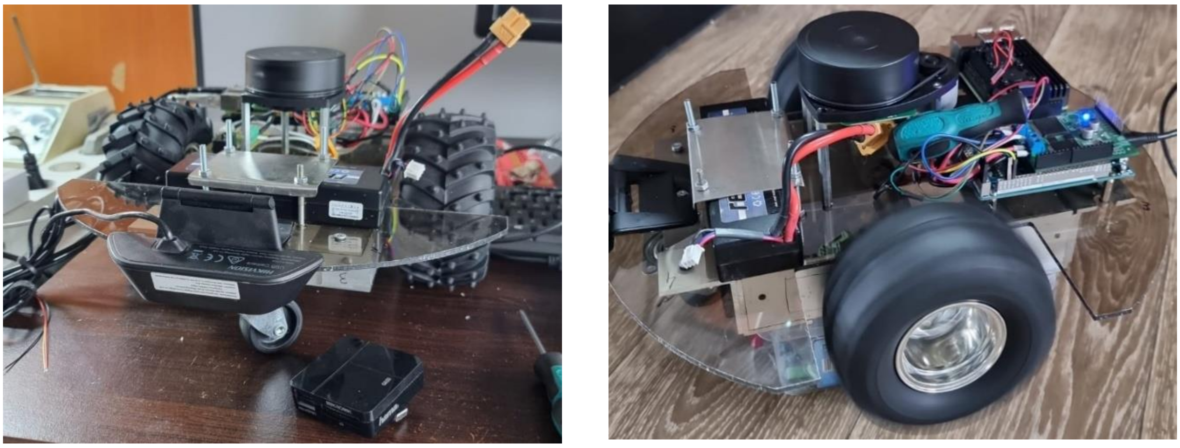

Fig. 1. AGV autonom cu carlig de remorcare

To optimize the AGV's route, we implemented an innovative method using a 360-degree lidar sensor (Fig. 2) for continuous environmental analysis. This sensor performs complete scans of the surroundings, providing detailed data about obstacles and other elements in the AGV's path [5].

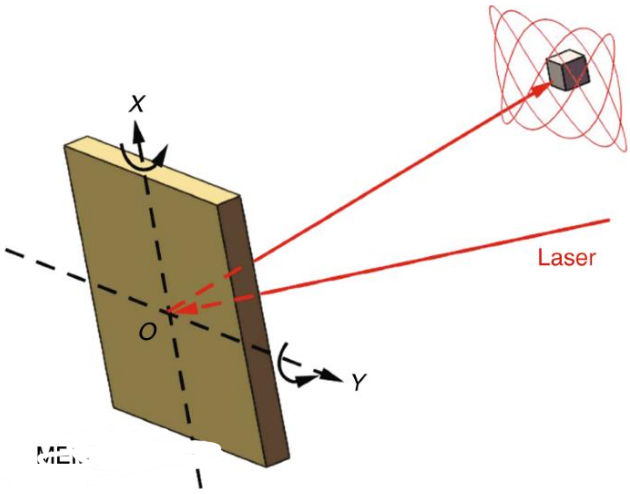

Fig. 2. Schema Lidar 360 [4]

When the lidar detects an obstacle in front of the AGV, an integrated algorithm automatically initiates a stop to prevent collisions and ensure operational safety. Simultaneously, the AGV follows a line marked on the ground or work surface, using line-tracking techniques to maintain its direction and navigate efficiently within the environment.

This combined approach offers significant advantages in terms of safety and operational efficiency for AGVs in industrial and logistics environments. The integration of 360-degree lidar and line-tracking technology marks an important step toward optimizing AGV routes and improving the performance of autonomous transport systems.

4. Introduction to the Route Optimization Algorithm

The route optimization algorithm used in this project is designed to guide the Automated Guided Vehicle (AGV) along an optimal path, avoiding obstacles and ensuring high operational efficiency [3]. The algorithm uses data from Lidar sensors, a camera and other environmental variables to determine the best path forward.

Input Variables

- Lidar Sensor Data: Used to detect obstacles and their distance, creating a three-dimensional map of the surrounding environment.
- Camera Data: The high-resolution video feed is processed to detect route markings and other visual cues that can assist in orienting the AGV.
- Destination Coordinates: Predefined destination points along the route, which may vary depending on the cargo being transported.
- Speed and Acceleration Parameters: Used to adjust the vehicle's dynamics based on obstacles and the type of terrain.

Algorithm Stages

- Initialization and Environment Mapping
- Route Planning
- Obstacle Avoidance
- Line Tracking

5. Steps in AGV Development

The AGV was designed for small-scale production and developed with the aim of being used for research and understanding how this type of automated guided vehicle functions.

Components Used in the Development of the Autonomous Vehicle

- Arduino – An open-source microcontroller platform used to control the electronic components.
- Motor Driver Shield – This module is used to control the vehicle's motors. It receives commands from the microcontroller and adjusts the current and voltage needed to move the vehicle's wheels. The shield enables precise and varied movements, such as forward, backward, and turns.
- Raspberry Pi – A mini-computer that provides the processing power for more complex functions, such as image processing and executing route planning algorithms. It also manages the connection to the camera and lidar to analyze the environment and make autonomous decisions.
- 360-degree Lidar – Lidar (Light Detection and Ranging) is a sensor that uses lasers to scan the surrounding environment at 360 degrees, providing a detailed map of obstacles around the vehicle. It is crucial for detecting objects and avoiding collisions, contributing to safe movement.
- 7.4V 5400mAh Battery – Powers the vehicle and its components, providing the necessary energy for the operation of the motors, microcontroller, and other electronic devices. With a capacity of 5400mAh, it ensures an adequate operating time for autonomous travel.

- 1080p Webcam – Offers a 1080p resolution and is used for visual recognition and route tracking. It sends images to the Raspberry Pi, which processes them to keep the vehicle on track and identify elements on the path.
- Chassis – The basic structure of the vehicle, on which all other components are mounted.
- Wheels – The moving components of the vehicle, powered by motors.

6. Conclusions

In conclusion, our project demonstrated the feasibility and effectiveness of using an autonomous AGV equipped with a towing hook in industrial environments. The developed system represented a versatile and adaptable solution, contributing to the optimization of material handling and cargo transport processes [1]. By implementing an efficient route optimization method, we achieved significant results in terms of operational efficiency and cost reduction. This project highlights the potential of AGV technology with a towing hook in improving performance and operational efficiency across various industrial applications.

7. Bibliography

[1] Hasan, M. K., Hossain, M. A., și Rahman, M. A. (2019), "Energy Optimization of Large-Scale AGV Systems"
[2]Stancu, V.-C., și Duțu, C. (2022), "Implementation of Automatic Guided Vehicles in the Operational Production Flow", *Proceedings of the Romanian Academy Series*
[3]Wikipedia (2023), "Vehicle Routing Problem", *Wikipedia*, disponibil online la: https://en.wikipedia.org/wiki/Vehicle_routing_problem
[4]Carlson, J. S., și Pettersson, H. (2022), "Supporting the Design of Automated Guided Vehicle Systems in Internal Logistics"
[5]Hossain, M. A., și Hasan, M. K. (2015), "Optimal Path for AGV System with Intelligent Agents", în: M. Smith și L. Brown (eds.), *Advances in Automation and Robotics*

STRATEGIC EVALUATION AND ORGANIZATIONAL IMPLEMENTATION OF A WMS

CIORNEI Daniel, POPESCU Constantin-Adrian

Faculty: Industrial Engineering and Robotics, Specialization: Industrial Logistics,
Study Year: M1, e-mail: daniel.ciornei@stud.fiir.upb.ro

ABSTRACT: *The primary objective of this work is to evaluate the market for software solutions in the category of digital warehouse management systems and to present key features that define such a software solution. Ultimately, this work aims to present various options available in the market for warehouse management systems and to showcase an own implementation.*

KEYWORDS: *Warehouse Management Systems, Supply Chain Optimization, Digital Integration, Automation Technologies, Cloud-based Solutions.*

1. Introduction

"Warehouse Management Systems" (WMS) provide companies with a significant advantage in maximizing the use of labor and available space, as well as investments in equipment, by coordinating and optimizing the use of resources and material flows. The WMS is a software solution that provides visibility into all of a company's inventory and manages supply chain operations from the entry of goods into the warehouse until they are shipped out [1].

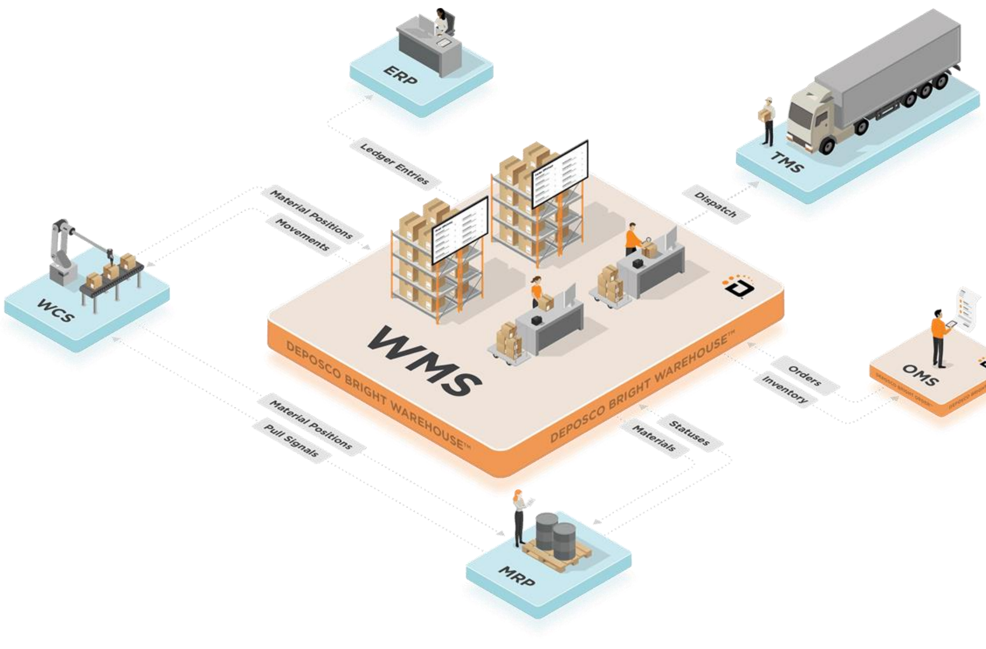

Fig. 1 — Warehouse management systems proposed by the "Deposco" company" [2]

These systems are designed to support the demands of a comprehensive global supply chain, covering distribution, production, intensive asset, and service management activities. By implementing WMS solutions, companies can gain increased visibility into their operations, thereby improving efficiency and reducing operational costs.

Due to advances in digital technology that have fundamentally transformed how customers make purchases, revolutionized supply markets, and altered e-commerce models, the supply chain has become significantly more complex. This increased complexity necessitates that order fulfillment operations be sufficiently flexible and adaptable to respond promptly to rapid market changes. Integrated digital solutions, such as advanced WMS, are essential for managing this complexity and maintaining market competitiveness.

By migrating warehouse management systems to the cloud [3], companies can meet the demands of connected customers through modern order fulfillment solutions that provide real-time visibility, scalability, and market sensitivity. Cloud-based solutions enable real-time data access and better collaboration among various parts of the supply chain. These solutions can quickly scale to meet fluctuating demand and offer advanced analytical capabilities, allowing companies to make informed decisions and continuously improve operational efficiency.

2. Current status

Presently, WMS are essential for companies seeking to efficiently manage and control daily warehouse operations, from the moment goods and materials enter a distribution or fulfillment center until they leave. WMS software represents a critical component of supply chain management, offering real-time visibility into a company's entire inventory, both in warehouses and in transit. In addition to inventory management, a WMS provides advanced tools for picking and packing processes, resource utilization optimization, detailed analytical functions, and more.

In today's context, wholesalers, third-party logistics providers (3PL), and shippers face the pressure to fulfill and deliver orders within a day. Currently, 51% of retailers offer same-day delivery to their customers, and 65% intend to reach this goal within the next two years [4]. The growth of e-commerce sales accentuates this pressure. According to data reported by the "Statista Research Department," the U.S. e-commerce industry is projected to continue growing significantly until 2029, with revenues expected to reach $1.9 trillion, marking an increase of over 53% from 2024 [5]. This sustained growth reflects the continuous expansion of the market, supported by an increase in average revenue per user (ARPU) and the number of users. ARPU is expected to reach $5,639.15 in 2029 [6], indicating greater demand and higher value generated per user. Additionally, the number of users is expected to grow by nearly 22%, reaching 333.5 million in the same period [7]. These trends reflect a development and growth of the e-commerce market.

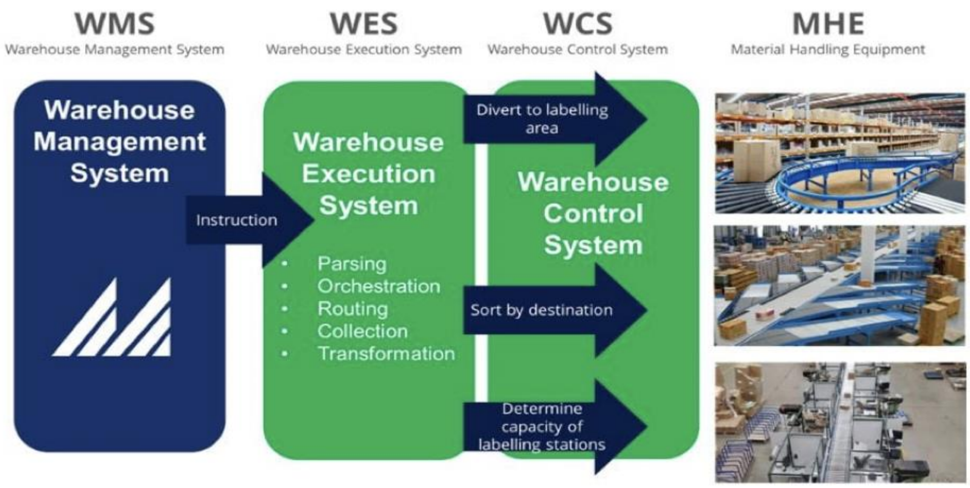

Fig. 2 — Integration of a WMS system within a warehouse [8]

A performant WMS can significantly contribute to optimizing every aspect of warehouse management, from receiving and storage processes to picking, packing, and shipping, as well as inventory tracking and replenishment. These systems organize all these activities through a unified interface. Moreover, WMS integrate with other essential tools, including fundamental technologies such as barcode scanning and RFID labeling, advanced robotics, augmented reality (AR) wearable devices, and mission-critical solutions like transportation management systems (TMS), ERP, and logistics software.

By implementing such integrated systems, companies can significantly improve operational efficiency and the ability to respond quickly to market demands, ensuring optimal management of resources and inventory. This not only contributes to customer satisfaction through fast and accurate deliveries but also maintains competitiveness in an ever-evolving market.

Any warehouse activity, as well as those related to the extended supply chain, can be improved with a WMS —from receiving and storage to picking, packing, and shipping. A WMS facilitates the efficient receipt, processing, and storage of items based on business rules and optimized operational flows. Before the advent of these systems, items were manually recorded with pen and paper to reconcile with procurement orders and physical receipts. In a 2018 Peerless Research survey, 87% of respondents stated that they still handle materials manually during the receiving process.

A modern WMS supporting RFID technology integrates with billing systems and other software, enabling automatic receipt, validation, and reconciliation of items with digital purchase orders through barcode scanning and item labeling for easier storage and retrieval.

WMS software provides real-time visibility into an organization’s inventory across all locations, including items in transit and in stores. A WMS utilizes automatic identification and data capture technologies to ensure accurate inventory tracking. Many systems support cycle counting and demand forecasting using advanced analytical functions, which allow adjusting inventory levels to meet customer demand, whether at points of sale or online.

According to a survey by "Logistics Magazine" [9] the most common packing and fulfillment activities occur in the warehouse, and "ResearchGate" [10] estimates that order picking accounts for 55% of the total warehousing cost. WMS can reduce these costs by optimizing product storage, retrieval, and packing, supporting picking technologies such as RFID, pick-to-light, pick-to-voice, robotics, and algorithms that optimize picking paths.

Voice-picking technology, also known as "voice warehousing" or "pick-by-voice," allows operators to perform tasks and communicate their completion without using paper or relying on their hands and eyes. Operators use a voice-picking device, usually a headset with a microphone or a dedicated terminal, to receive voice instructions from the WMS regarding the location and timing of order picking. For improved accuracy and productivity, a wired or wireless barcode scanner can be included. Simple voice prompts guide operators to their destinations and specify the tasks to be performed. The system allows for multi-modal feedback, offering flexibility through voice responses, barcode scans, or direct text input.

According to the study "Order Picking for the 21st Century" by Tompkins Associates [11], voice-picking solutions significantly improve operations and reduce costs in the supply chain. The voice-managed order picking method has proven to be more accurate and productive than both manual scanning and paper-based label methods.

The intrinsic features of voice management, allowing "hands-free" headset use, contribute to significant and measurable productivity improvements almost immediately after implementation. One notable result is that a company recorded a 50% reduction in returns after implementing the voice management solution, saving nearly $1.3 million in the first year.

Cross-docking is a logistics technique aimed at speeding up the delivery of goods and increasing supply chain efficiency [12]. This involves unloading goods from delivery vehicles to a logistics warehouse and transferring them to outgoing shipment vehicles without the need for storage time between these stages or with minimal storage time. Yard and dock management functionalities allow truck drivers to quickly find the appropriate loading docks. Integration for cross-docking, where incoming goods are immediately placed in outgoing shipments without intermediate storage, is ideal for perishable products. The WMS software checks receipts against current orders and notifies operators if the goods need to be placed in cross-docking locations.

A WMS automatically collects real-time data, eliminating recording errors. This data is integrated with analytical functions to track performance indicators such as on-time shipment, inventory accuracy, distribution costs, order fulfillment rate, and order cycle time. The system can generate shareable visual reports, which can be used to adjust operational processes.

Warehouse workers rely on mobile devices to perform their activities more efficiently. According to the "Warehouse DC Equipment Survey" from 2020 [13], 73% of participants used smartphones and tablets, 55% barcode scanners, and 18% GPS technology, with 28% planning to implement GPS in the next 12 months. A WMS that can integrate these technologies is essential for optimizing warehouse operations.

Artificial intelligence (AI) and the Internet of Things (IoT) are increasingly integrated into warehouse operations, promising to help companies dynamically respond to rapid changes in storage conditions, without being limited to predefined rules. IoT sensors collect data, and artificial intelligence analyzes it and provides advanced predictions that were not previously possible. These collaborative technologies facilitate the transition to a demand-based warehousing model.

IoT data integrates into warehouse management systems from multiple sources, including material handling equipment such as conveyors, smartphones, and portable devices, passive radio signals, and RFID. AI systems process this data and transform it into actionable analyses, identifying trends, predictive models, and other algorithms that allow companies to make decisions based on current conditions.

These technologies can be used to optimize various aspects of warehouse operations. For example, AI and IoT can improve routing and workforce movement management, dynamic inventory allocation, batch order processing, and more. Through these advanced technologies, companies can quickly and efficiently adjust warehouse strategies to adapt to market demands and workflow variations, ensuring increased operational efficiency and a greater ability to respond to customer needs.

These technological integrations not only improve the efficiency and accuracy of warehouse operations but also contribute to creating a more flexible and adaptable working environment. Thus, companies can maintain a high level of performance and competitiveness in a dynamic economic landscape.

3. Implementation

In the intention to develop a proprietary WMS application that includes modern and essential functionalities, the initiative began with the realization of the back-end stage of the application. This application is designed to run exclusively on the web, thus ensuring cross-platform accessibility from any device. Being cloud-based, the application allows for efficient running, testing, and maintenance, also offering the possibility of real-time data interpretation by interconnecting all levels of warehouse management. This approach not only enhances operational efficiency but also provides scalability, enabling the system to grow with the business. Additionally, the web-based nature of the application reduces infrastructure costs and improves ease of access, as it eliminates the need for local installations and extensive IT support.

The project aims to include advanced predictive functionalities based on the analysis of repeatable behaviors of both equipment and human personnel involved. Predictive analytics will be utilized to forecast demand, optimize stock levels, and predict maintenance needs, thereby minimizing downtime and improving productivity. The first stage of this project was the development of a barcode identification application, which facilitates the inventory management process and provides essential real-time information. Thus, the foundations were laid for an application called "Stagetrack." It was developed to allow users to scan and identify products by barcodes, thus facilitating inventory management and providing essential real-time information. The predictive functionalities will enable warehouse managers to anticipate issues before they arise, allowing for proactive management and strategic planning.

The web application "Stagetrack" brings multiple advantages through its accessibility from any internet-connected device, eliminating the need for additional software installation and offering a user-friendly experience. The intuitive design ensures that users can quickly adopt the system with minimal training, which is critical for maintaining productivity during transitions to new systems. The back-end of this application was developed using MuleSoft Anypoint Studio, a platform recognized for its versatility and scalability. MuleSoft facilitates the efficient integration and management of data collected through barcodes, offering a three-layered approach called "API Led-Connectivity": the "Experience" layer, the "Process" layer, and the "System" layer. This structured approach ensures that the application can handle a high volume of transactions while maintaining data integrity and security. Furthermore, the use of MuleSoft ensures that the application can easily integrate with other enterprise systems, providing a seamless flow of information across the organization.

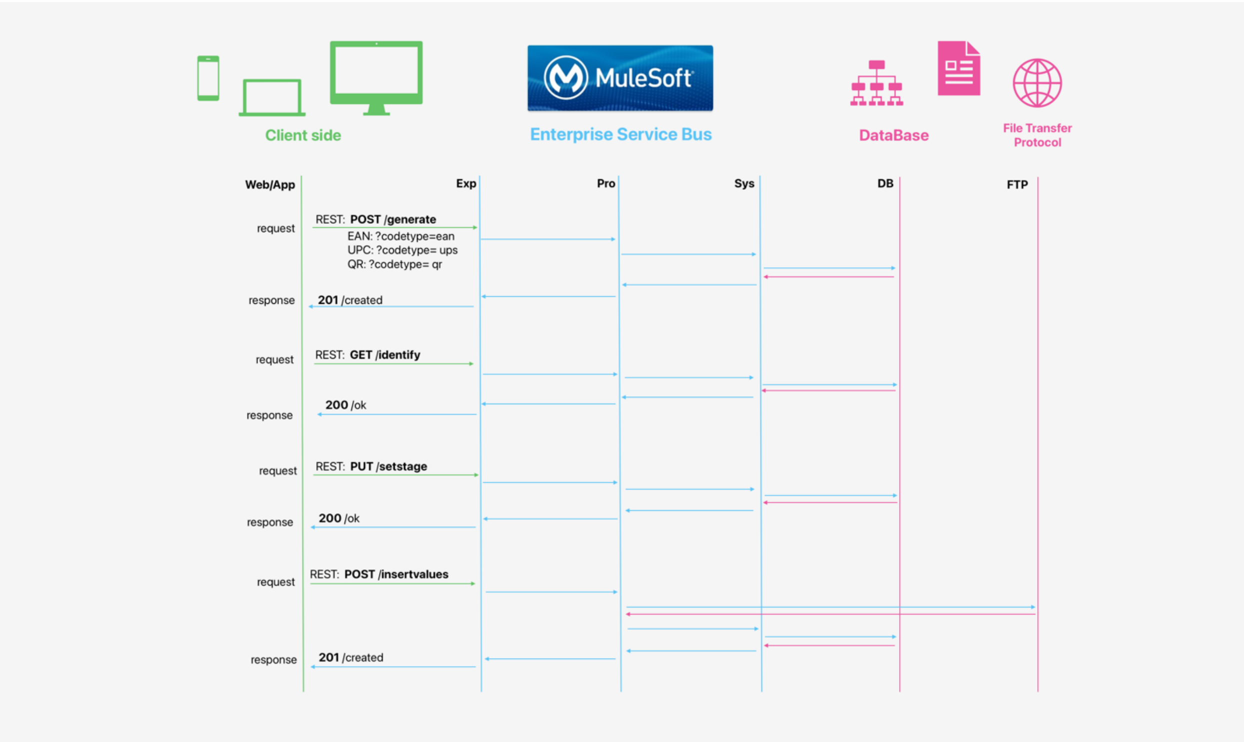

Fig. 3 — Web application architecture of “Stagetrack”

The "Experience" layer manages requests received from web clients, verifying their compliance. This layer ensures that only valid and authorized requests are processed, enhancing the security of the application. The "Process" layer handles data processing and transformation, enabling complex business logic to be applied to the data as it moves through the system. This includes tasks such as data validation, enrichment, and routing. Meanwhile, the "System" layer performs the connection and delivery of processed data to target systems, such as databases or other data management platforms. This three-layered approach allows for a clear separation of responsibilities and streamlines data transfer, ensuring that each layer can be developed and maintained independently. This modularity not only simplifies development but also enhances the system's robustness and flexibility.

For storing generated barcodes, a “MAMP” database was used, organized into tables for three types of barcodes: EAN-13, UPC, and QR code. Each table includes columns for ID, barcode, and the current stage of the product. The "ID" column is auto-incremental, being automatically generated when inserting a new line into the database. The "barcode" column contains the barcode values, and the "stage" column records the current stage of the product in the logistics flow. The data in the "stage" column is updated as products advance in the flow. This structured storage ensures that all relevant information about each product is easily accessible and up-to-date, which is crucial for accurate inventory management and tracking.

"Stagetrack" facilitates database insertions and updates, generating unique codes for new products and updating stage values throughout the logistics process. The application integrates the Postman application used for testing by calling the application through simulating front-end requests, using HTTP requests. This integration allows for comprehensive testing of the application's functionality before deployment, ensuring that it operates as expected under various conditions. The project used the Git version control system, storing the component files of the application on the GitHub platform. This system allows tracking and managing changes, facilitating the rollback of interventions and making changes both locally and remotely. The stages of the application development and its modifications can be followed by accessing the GitHub page at the address: https://github.com/amseiden/stagetrack_monitor. This approach to version control ensures that the development process is transparent and that all changes are well-documented, enabling efficient collaboration among team members.

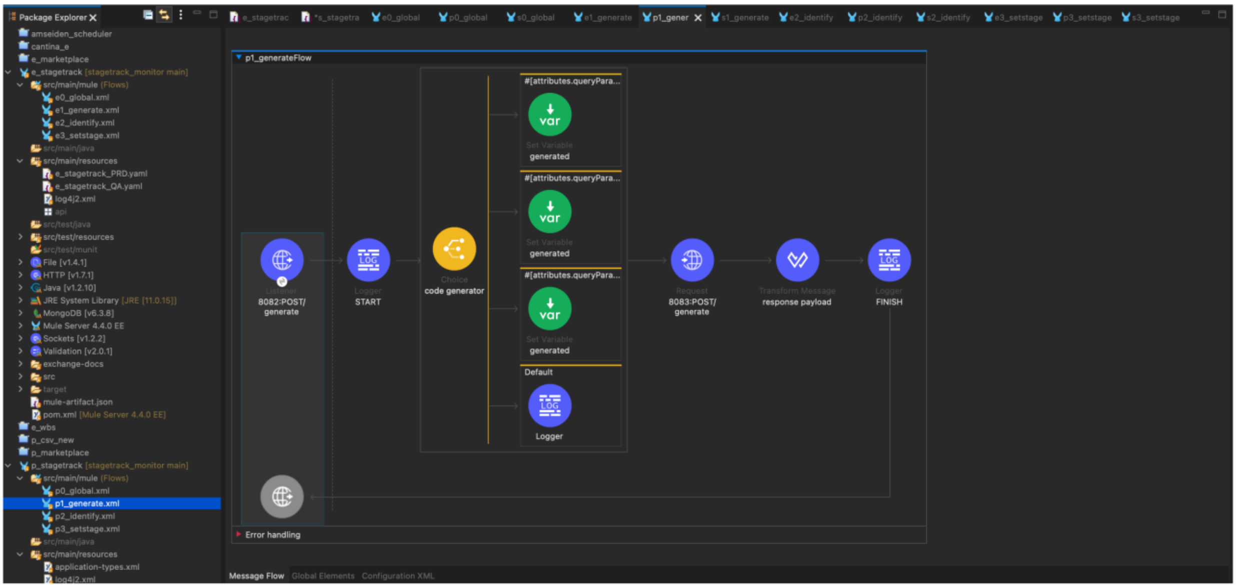

Fig. 4 — Screenshot of "Stagetrack" implementation in Anypoint Studio

These principles drove the design of a modern WMS application, emphasizing web accessibility, cloud functionality, real-time data interpretation, and predictive analytics. This application optimizes warehouse management, streamlining operations and automating processes efficiently. It offers a robust, flexible platform to manage logistical complexities, enhance performance, and adapt to evolving technological and market needs. By leveraging modern technologies and methodologies, the application aims to provide a competitive edge to businesses, helping them to improve their operational efficiency and customer satisfaction. The integration of predictive analytics and real-time data processing positions the application as a cutting-edge solution for modern warehouse management challenges.

4. Results

There are a variety of Warehouse Management System (WMS) solutions, ranging from standardized platforms to customized solutions tailored to specific customer requirements. These solutions vary based on technical characteristics, offered functionalities, scalability, compatibility with other systems and technologies, and the level of automation and integration. Standardized platforms often provide a robust set of features that can cater to a wide range of industries, whereas customized solutions are designed to meet the unique needs of specific businesses, allowing for greater precision and efficiency in warehouse operations. Moreover, the choice between on-premises and cloud-based WMS can significantly impact scalability and integration capabilities. There are a variety of WMS, a few of them were identified as the most frequently used.

“Körber Warehouse Management Systems” offers a comprehensive suite of solutions for warehouse management, designed to optimize operations and meet supply chain demands. These solutions enable the digitalization and automation of warehouses, ensuring efficient inventory management and optimized processes. They are characterized by domain expertise and a focus on operational efficiency, offering flexibility and customization. Körber's systems are known for their ability to handle complex logistics scenarios, supporting businesses in achieving higher throughput and reducing operational costs. The platform also supports integration with various automation technologies such as robotics and IoT devices, enhancing overall warehouse productivity.

Shifting focus, “Luminate Logistics by Blue Yonder” integrates predictive and optimization technologies for supply chain management. The platform uses artificial intelligence and machine learning to identify patterns, anticipate demands, and make real-time decisions. It stands out for its use of advanced technology and offers flexibility and scalability with extended supply chain visibility. Blue Yonder’s solution also emphasizes end-to-end supply chain synchronization, enabling businesses to respond swiftly to market changes and disruptions. Furthermore, the platform’s user-friendly interface and comprehensive reporting tools facilitate better decision-making and strategic planning.

In a similar vein, “Microsoft Dynamics 365 Supply Chain Management” offers deep integration with Microsoft suites, facilitating the implementation and use of the platform. It takes a holistic approach to the supply chain, covering planning, production, distribution, and services. It provides scalable and customizable functionalities with easy integration and robust support from Microsoft. The platform leverages the power of the Microsoft ecosystem, including Azure cloud services, to deliver real-time insights and enhanced collaboration across the supply chain. Additionally, Dynamics 365’s modular architecture allows businesses to adopt the solution incrementally, aligning with their specific growth and operational needs.

Continuing with another strong contender, “Oracle Fusion Cloud Warehouse Management” is natively integrated with other Oracle solutions, offering seamless interoperability. It has advanced analytical and reporting capabilities, allowing a deep understanding of operations and informed decision-making. It is characterized by robust integration and advanced analytics, offering flexibility and scalability. Oracle’s solution also supports a wide range of warehouse functions, from inbound logistics to order fulfillment, ensuring comprehensive management of warehouse activities. The cloud-based nature of Oracle Fusion ensures high availability and security, making it a reliable choice for enterprises aiming for digital transformation.

Lastly, “SAP Extended Warehouse Management” offers complex logistics process management and extensive integration with other SAP solutions. The platform optimizes warehouse space and manages advanced inventory, monitoring operational performance, and identifying trends for process improvement. It stands out for advanced inventory management and space optimization, along with powerful analytical and reporting capabilities. SAP EWM also supports advanced features like labor management and yard logistics, providing a holistic solution for end-to-end warehouse management. The platform's integration with SAP S/4HANA enhances data visibility and operational efficiency, enabling businesses to streamline their supply chain processes effectively.

The WMS solutions market is continuously evolving, driven by technological advancements and the need to adapt to industry changes. A wide range of WMS software solutions is currently available, each tailored to the specific requirements of different industries and types of logistics operations. These solutions not only improve operational efficiency but also enhance accuracy and customer satisfaction. As businesses continue to digitize their supply chains, the demand for innovative and adaptable WMS platforms is expected to grow, further propelling advancements in this critical area of supply chain management.

5. Conclusion

The findings of this work underscore the critical role of modern WMS solutions in enhancing warehouse and supply chain management. Through technological advancements and integrations, these solutions significantly drive efficiency and competitiveness in today's dynamic market. By evaluating existing WMS platforms and detailing the development of the proprietary "Stagetrack" application, this research highlights the substantial benefits of digital solutions in optimizing warehouse operations. The "Stagetrack" application exemplifies the first phase in developing a web-based WMS, featuring real-time data capabilities and user-friendly functionalities, and it establishes a robust foundation for future advancements. This project not only demonstrates immediate operational improvements but also sets the stage for incorporating cutting-edge technologies such as AI and IoT, fostering continuous innovation and enhancement in warehouse management.

6. References

[1] Article "What is a Warehouse Management System (WMS)?" retrieved from the website www.sap.com https://www.sap.com/romania/products/scm/extended-warehouse-management/what-is-a-wms.html

[2] Image retrieved from the company "D e p o s c o", https://deposco.com/blog/what-is-a-warehouse-management-system/

[3] "Factors Influencing the Successful Implementation of the Warehouse Management System (WMS)" Published by Natesan Andiyappillai, International Journal of Applied Information Systems (IJAIS) – ISSN : 2249-0868

Foundation of Computer Science FCS, New York, USA, Volume 12– No.35, December 2020– www.ijais.org

[4] "Data Analytics in Warehouse Management Systems (WMS) Implementations – A Case Study" Proceedings of the 2019 IISE Annual Conference, H.E. Romeijn, A Schaefer, R. Thomas, eds.; Kaan Unnu, Jennifer A. Pazour, Department of Industrial and Systems Engineering, Rensselaer Polytechnic Institute Troy, NY, United States

[5] "Revenue of the e-commerce industry in the U.S. 2019-2029", Statista Research Department, May 22, 2024 https://www.statista.com/statistics/272391/us-retail-e-commerce-sales-forecast/

[6] "Revenue per user of the e-commerce market in the United States from 2020 to 2029", Published by Statista Research Department, May 22, 2024 https://www.statista.com/forecasts/280703/e-commerce-arpu-in-the-united-states

[7] "Number of users of e-commerce in the U.S. 2020-2029" Published by Statista Research Department, May 22, 2024

https://www.statista.com/statistics/273957/number-of-digital-buyers-in-the-united-states/

[8] Image retrieved from "SCJunction", https://www.scjunction.com/blog/warehouse-automation-what-is-the-difference-between-a-wms-wes-and-wcs?utm_content=270673029&utm_medium=social&utm_source=linkedin&hss_channel=lis-jXRDPtdv5m

[9] "2020 Warehouse/DC Equipment Survey: Making the right moves to offset pressures" By Roberto Michel April 15, 2020 https://www.logisticsmgmt.com/article/2020_warehouse_dc_equipment_survey_making_the_right_moves_to_offset_pressur/warehouse_dc

[10] "Improving order-picking process through implementation warehouse management system" By Andjelkovic Aleksandra & Radosavljevic Marija, May 19, 2017 https://www.researchgate.net/publication/317401873_Improving_order-picking_process_through_implementation_warehouse_management_system

[11] "Order Picking for the 21st Century" *By Aaron Miller, Principal Tompkins Associates* www.tompkinsinc.com http://www.baxtek.com/products/vocollect/Voice_v_Scan_White_Paper.pdf

[12] Boysen, N., and Fliedner, M. (2010), "Cross dock scheduling: Classification, literature review and research agenda", Omega, Vol. 38, pp. 413 – 422.

[13] Glock, C. H. et al. (2020) 'Assistive devices for manual materials handling in warehouses: a systematic literature review', International Journal of Production Research, 59(11), pp. 3446–3469. doi: 10.1080/00207543.2020.1853845

STUDY ON THE OPTIMISATION OF BOTTLING FLOWS

SCARLAT Andrei Daniel, COTET Costel Emil

Faculty of Industrial Engineering and Robotics, Study program: Industrial Logistics, Academic year: Master 2, e-mail: nouageneza@gmail.com

ABSTRACT: In this case study I wanted to make a digital twin for a dosing line because the equipment is not so numerous, but the principles and way of thinking remain generally valid for any production line. With this digital twin I will simulate how a virtual production line should behave by collecting and parameterizing the equipment with data from the supplier, so that at the time of purchase everything works exactly as we want it to.

KEYWORDS: Digital Twin, Witness Horizon, optimization, efficiency

1. Introduction

In an era of rapid technological advances and significant changes in the business environment, companies face unprecedented challenges and opportunities. In an age of speed, consumer tastes are constantly changing, and to remain relevant in the marketplace, food companies must constantly understand and meet consumer needs and desires. Consumers are becoming more demanding in the marketplace, creating new challenges for food companies. To avoid losing market share, they need to become flexible to customer needs while maintaining high production standards and building consumer demand and trust.

The use of a Digital Twin helps to understand a change and its impact, for example, they can more quickly identify new recipes, packaging methods or the use of new equipment, identify opportunities by simulating the entire digital process and apply improvement opportunities in the real world.

2. The current stage

Digital twin technology has rapidly evolved, becoming a cornerstone for operational efficiency and resilience in the food and beverage industry. This technology creates a virtual replica of physical systems, allowing real-time monitoring, predictive analytics, and optimization of processes. Recent implementations by industry leaders such as Coca-Cola Icecek (CCI) and an India-based dairy cooperative illustrate the transformative potential of digital twins.

Coca-Cola Icecek, the sixth-largest bottler of Coca-Cola products globally, sought to optimize its clean-in-place (CIP) process to reduce water and energy consumption by 12%. Traditionally, CIP optimization was challenging due to lack of visibility, difficulty in data analysis, and measurement variability. To address these issues, CCI partnered with Amazon Web Services (AWS) to develop a digital twin solution called Twin Sense.

In just two months, CCI implemented Twin Sense, which provided real-time visibility into CIP performance, enabled predictive maintenance, and identified root causes of process failures. The results were significant: within six weeks, CCI reduced energy usage by 1,236 kW, saved 560 cubic meters of water, and decreased cleaning agent consumption by 2,400 liters. Moreover, the digital twin improved process visibility for operators and facilitated the optimization of CIP process time and cost performance. This success led to the development of a commercial model to scale the solution to 30 additional facilities.

An India-based dairy cooperative demonstrated the efficacy of digital twin technology during the COVID-19 lockdowns. According to a Deloitte whitepaper, the cooperative partnered with a technology provider to create a digital twin of their entire supply chain, including supplier locations, plants, and customer/retailer data.

The digital twin provided comprehensive insights into plant operations, truck availability, and idle capacity, allowing the cooperative to monitor and respond to changes in demand efficiently. During the lockdowns, there was a sharp increase in demand for cheese and condensed milk. The digital twin enabled the company to operate at 115% capacity by identifying idle capacity and optimizing load distribution. Additionally, the cooperative leveraged rail transport, partnered with multiple e-commerce retailers, and increased advertising efforts.

As a result, the digital twin facilitated a $98 million revenue increase by helping the company reconfigure its supply chain to sell more products and manage crises more effectively.

These case studies highlight the profound impact of digital twin technology in the food and beverage industry. By providing real-time data insights and predictive capabilities, digital twins enable companies to optimize operations, reduce resource consumption, and enhance their ability to respond to market demands and unforeseen disruptions.

Moving forward, the adoption of digital twin technology is expected to grow, driven by advancements in IoT, machine learning, and cloud computing. As more companies recognize the benefits, digital twins will likely become integral to achieving operational resilience and agility in the industry.

For the case study we chose to model and simulate a bottling line in 330 ml cans. The supplier of the bottling line from which I took inspiration is Krones. It is a system composed of 5 working points, 4 parts, 5 buffers and 4 conveyors.

Thus, based on the data extracted from the equipment datasheets, we extracted the following data: cycle time for the equipment, change-over time and uptime.

To determine the cycle time for each equipment we collected and centralised the nominal speed of each equipment according to the supplier.

The formula used to calculate the cycle time was as follows:

Cycle time = (Number of products)/(Unit of time in which they are produced)

Table 1. Cycle time for equipment

Current number	Equipment	Rated speed	Cycle time
1	Depalletiser	10800 doses/h	3 min
2.	Monoblock Dosing-Capping Machine	7200 dozes/h	2 min
3.	Baxator	8000 boxes/h	2.22 min
4.	Palletiser	8500 rows/h	2.36 min
5.	Flaker	8500 rows/h	2.36 min

The change over has been centralised in the table below according to the manufacturer:

Table 2. Change over for equipment

Current number	Equipment	Change over
1	Depalletiser	0 min
2.	Monoblock Dosing-Capping Machine	60 min
3.	Baxator	30 min
4.	Palletiser	45 min
5.	Flaker	0 min

To determine the uptime we considered an operating time of 24 hours and 6 maintenance shutdowns, each with a 30-minute repair time.

The calculation and data being as follows:

- Time period analysed: 24 hours or 1440 minutes.
- Total time available: 1440 minutes.
- Total downtime: 6 intervals of 30 minutes each, so in total 6 * 30 = 180 minutes of downtime.

Uptime (%)=(((Total available time - Downtime))/(Total available time) *100 = ((1440 minutes-180 minutes))/1440 *100 = 1260/1440 *100 =
0.875 * 100 = 87.5%

For the handover time between work points we took into account the conveyor speeds and the working time required to process each process, setting the handover times as follows:

Table 3. Equipment uptime

Current number	Transfer	Timp
1	Between Depalletizer and Monoblock Doser-Capper	5 min
2.	Between Monoblock Filler-Capper and Baxer	6 min
3.	Between Baxer and Palletizer	5 min
4.	Between Palletizer and Folder	1 min

I used Witness Horizon software to make digital twins.

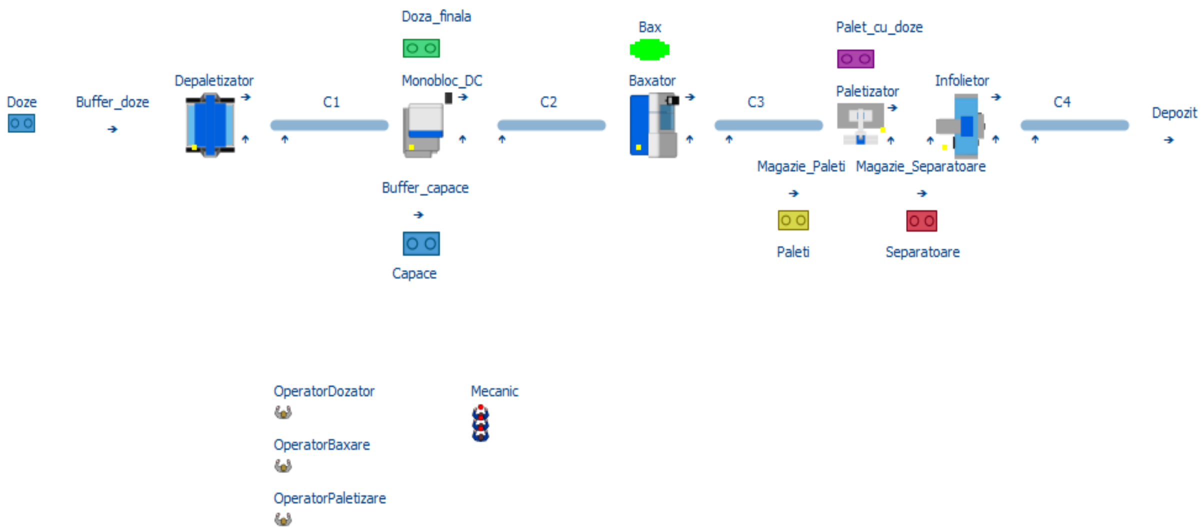

Fig. 1. Shaping the bottling line

The doses are stored in the dose buffer, from where they are taken by the depalletizer and placed on the C1 conveyor, from where they are transferred to the doser-capper monoblock. This is where the final dose is assembled after being dosed with the cap which is taken from the cap buffer and transported to the baxer for grouping of the doses. The baxer takes the filled doses from the C2 conveyor and makes the bax of 6 doses and sends them on to the palletising area. The palletiser stacks the pallet by taking 480 doses from the C3 conveyor to make a stack of 10 rows of 48 doses, one pallet from the pallet magazine and 9 dividers from the divider magazine to place them between the rows of doses and give more stability to the pallet, then sends it to the palletiser. The wrapper applies foil to the pallet so that there are no problems during transport to the customer, then sends the pallet on the C4 conveyor to the warehouse.

I simulated a week of production and then I extracted reports on the efficiency of equipment, conveyors, the number of raw materials entering the line, as well as staff working time (7 working days * 8 hours per day * 60 minutes).

The productivity of the system was 299 pallets in a working week (3360 hours).

The depalletizer depalletizes product layere 45.115% of the time, is idle 0.000% of the time, waits 29.018% of the time for operation and is blocked 24.082% of the time. It is down for maintenance 1.786% of the time.

Monobloc_DC fills and caps bottles 53.274% of the time, is idle 0.274% of the time and waits 44.667% of the time for operation. It is off for maintenance 1.786% of the working time.

The baxer packs bottle packs 9.779% of the time, is idle 89.671% of the time, waits 0.550% of the time and is not blocked at all.

The palletizer palletizes cases of bottles 21.001% of the time, is idle 58.753% of the time and is blocked 20.246% of the time.For maintenance it is off 0.893% of the time.

The bottle labeller labels bottles 21.001% of the time, is idle 78.106% of the time and is blocked 0.893% of the time.For maintenance it is off 0.893% of the working time.

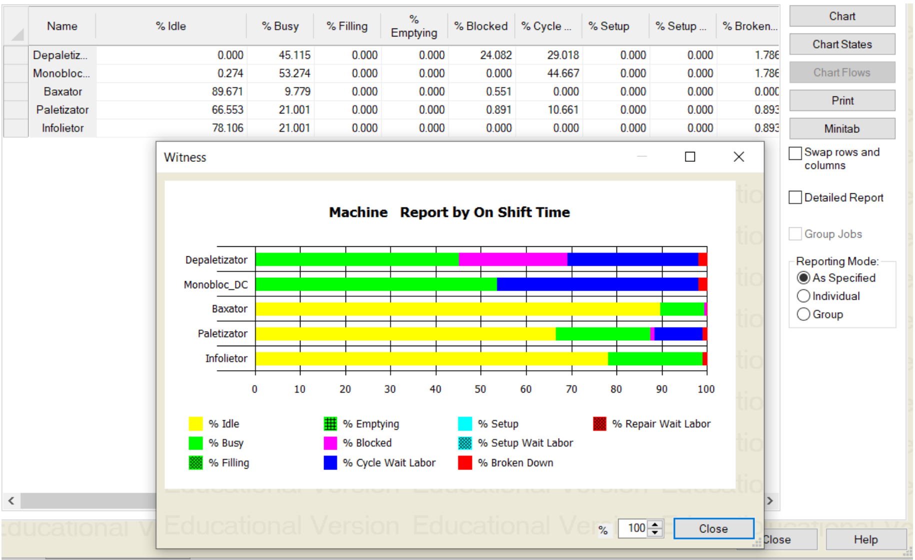

Fig. 2. Equipment Report (Functional Remodelling)

Conveyor C1 moves products 1.518% of the time, is empty 0.089% of the time, has bottlenecks 44.573% of the time, and products are on hold 53.820% of the time.

Conveyor C2 moves products 96.970% of the time, is empty 1.747% of the time, has bottlenecks 0.000% of the time, and products are on hold 1.283% of the time.

Conveyor C3 moves products 8.911% of the time, is empty 69.335% of the time, has bottlenecks 0.000% of the time, and products are on hold 21.754% of the time.

Conveyor C4 moves products 35.546% of the time, is empty 64.454% of the time, has bottlenecks 0.000% of the time, and products are not on hold at all.

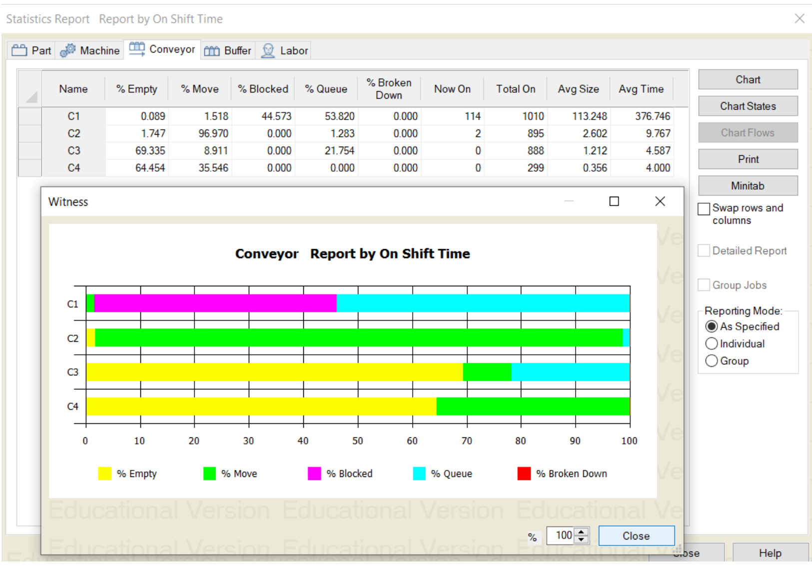

Fig. 3. Report for Conveyors

In order to streamline and optimise the production line, we have resorted to functional remodelling where we have modified some parameters on the flow to reduce bottlenecks.

At the depalletiser we set a cycle time of 5 minutes instead of 3 minutes and we increased the number of operators for the operation and monitoring of the depalletiser and the doser-capper monoblock, respectively the palletiser and the wrapper from 1 to 2; thus each equipment had one operator assigned. The parameterization for the other structural elements has been maintained.

System productivity increased from 299 pallets to 432 pallets produced in one week (3360 hours).

The debugger now works 96.359% of the time compared to 45.115% previously, showing an improvement of 51.244%, with jams decreasing from 24.082% to 0.963%, time to wait decreasing from 29.018% to 2.678%, and time to set decreasing from 1.786% to 0.000%. The operator waiting time decreased to 0% which indicates the correct allocation of staff to monitor and operate the equipment.

Monobloc_Dozer-Capper now works 80.000% of the time compared to 53.274% previously, showing an improvement of 26.726%, with bottlenecks decreasing from 8.636% to 0.963% and waiting time decreasing from 44.667% to 6.226%, but downtime increased from 0.274% to 12.811%. The operator waiting time decreased to 0% which indicates the correct allocation of staff to monitor and operate the equipment.

The Baxator now works 27.193% of the time compared to 9.779% previously, showing an improvement of 17.414%, with idle time decreasing from 89.671% to 65.192%, bottlenecks remaining constant at 0.000%, but waiting time increased from 0.550% to 6.105%.

The palletizer now works 32.245% of the time compared to 21.001% previously, showing an improvement of 11.244%, with bottlenecks decreasing from 20.246% to 1.807%, but downtime has increased from 58.753% to 65.971% and waiting time remains constant at 0.000%.Operator waiting time has decreased to 0% which indicates the correct allocation of staff to monitor and operate the equipment.

The operator now works 32.172% of the time compared to 21.001% previously, showing an improvement of 11.171%, with downtime decreasing from 78.106% to 66.936%, bottlenecks remaining almost constant from 0.893% to 0.892%, and waiting time remaining constant at 0.000%.

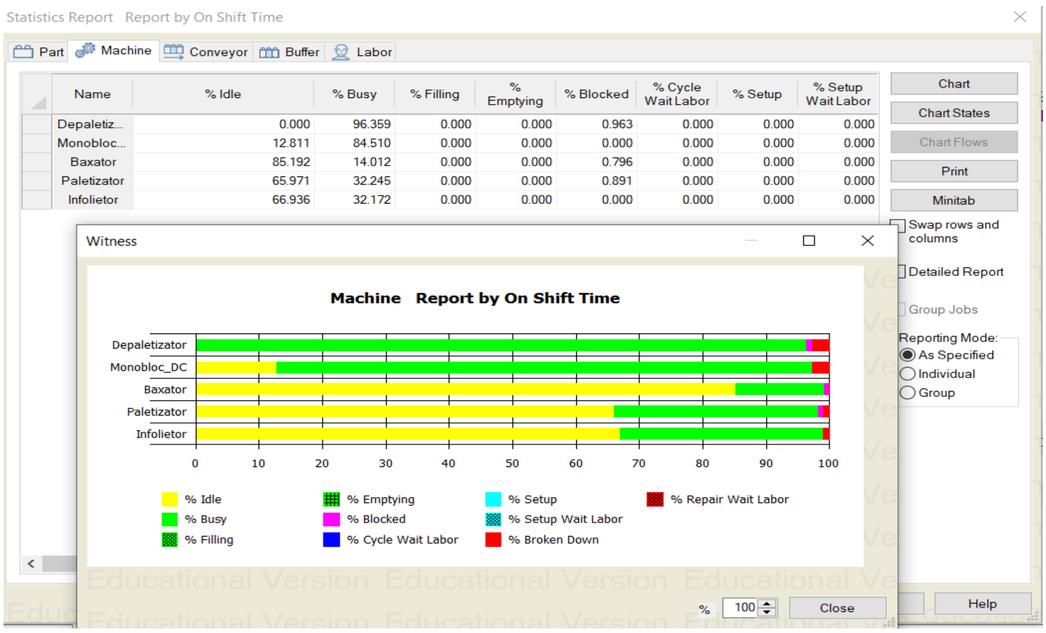

Fig. 4. Equipment Report (Functional Remodelling)

The C1 conveyor now moves product 45.196% of the time versus 1.518% previously, noting a significant improvement of 43.678%, it is empty 2.528% of the time versus 0.089% previously, bottlenecks have decreased from 44.573% to 0.000%, and wait time has decreased from 53.820% to 52.275%.

Conveyor C2 now moves products 95.941% of the time compared to 96.970% previously, noting a slight decrease of 1.029%, it is empty 4.488% of the time compared to 1.747% previously, bottlenecks remain constant at 0.000%, and wait time decreased from 1.283% to 0.171%.

Conveyor C3 now moves products 11.097% of the time compared to 8.911% previously, showing an improvement of 2.186%, is empty 79.580% of the time compared to 69.335% previously, bottlenecks remain constant at 0.000%, and the wait time has increased from 21.754% to 27.377%.

Conveyor C4 now moves products 41.887% of the time compared to 35.546% previously, showing an improvement of 6.341%, is empty 58.113% of the time compared to 64.454% previously, bottlenecks remain constant at 0.000%, and the wait time remains constant at 0.000%.

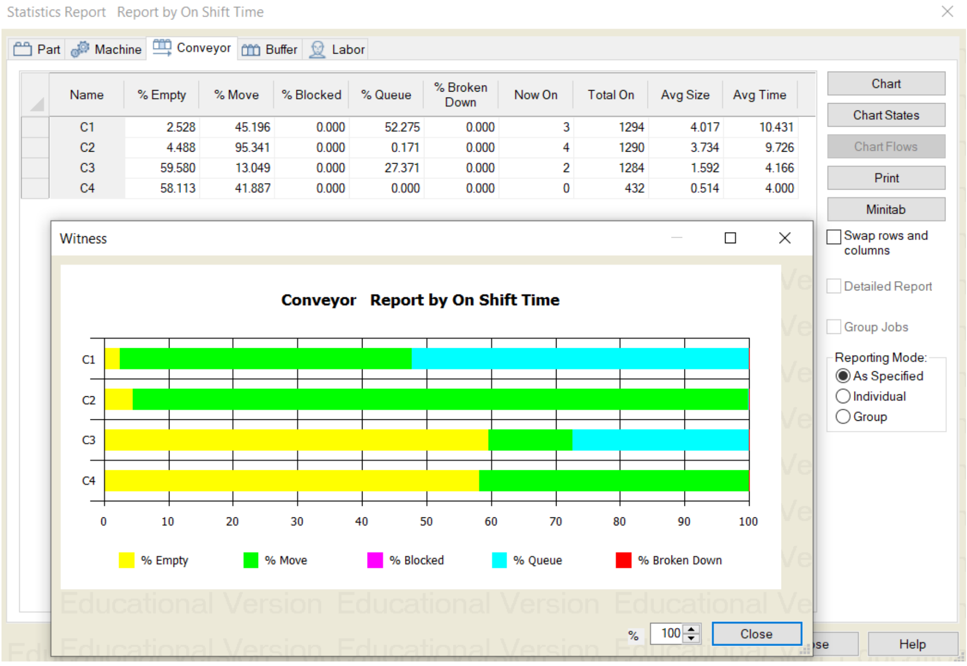

Fig. 5. Report for Conveyors (Functional Remodelling)

3. Conclusions

Implementing a digital twin to optimise a bottling line is essential to ensure efficient, economical and high-quality production. This revolutionary technology enables real-time monitoring, predictive analytics, process optimization and cost reduction, contributing to a company's long-term success and competitiveness in the bottling industry.

4. Bibliography

[1]. https://www.krones.com/media/downloads/Pressant_Universal_de.pdf
[2]. https://www.krones.com/en/products/bottling-lines-for-cans.php#to-top
[3]. https://www.krones.com/media/downloads/Modulfill_Bloc_FS-C_en.pdf
[4]. https://www.digitaltwinconsortium.org
[5].https://foodindustryexecutive.com/2023/05/how-digital-technology-helps-fb-manufacturers-become-more-agile-and-more-resilient/
[6]. https://aws.amazon.com/blogs/industries/digital-twins-and-cpg-manufacturing-transformation/

STUDY ON RFID TAGS POWERED BY SOLAR ENERGY

REZMELIȚĂ Emil, Constantin-Adrian POPESCU

Faculty: Industrial Engineering and Robotics, Specialization: Industrial Logistics, Year of study: VI, Email: emil.rezmelita@stud.fiir.upb.ro

ABSTRACT: Our study investigates the efficiency and benefits of solar-powered RFID tags. We demonstrate their ability to reduce battery dependence and extend device lifespan, providing a sustainable and energy-efficient solution for various RFID applications.

KEYWORDS: solar-powered RFID tags, energy efficiency, battery reliance reduction, device lifespan extension, sustainability.

1. Introduction

The term RFID stands for "Radio-Frequency Identification" and refers to various systems that together enable the automatic identification of objects. The easiest way to imagine the RFID system is to think of a barcode that can transmit information via radio and update it over time [1].

RFID technology has multiple applications in various fields, such as logistics, manufacturing, healthcare, transportation, security, and more. For example, in the retail industry, RFID tags can be used for automatic inventory management of products or to prevent theft through a tag detection system at the store exit.

The advantages of RFID technology include speed and ease in identifying objects, the ability to track and manage product inventory in real-time, the reduction of human errors in identification and tracking processes, and the capability to collect and analyze data in real-time for decision-making. However, there are also certain considerations regarding RFID technology, such as high initial costs, compatibility with existing systems, and issues related to data security and privacy [2].

RFID is a technology that profoundly changes the current way of working and will soon be present in many aspects of everyone's lives. Many believe that RFID is the technology that will enable the realization of the "Internet of Things" (IoT), or rather, a vast network where not only people but also objects will be interconnected.

The potential of this concept has only been partially realized at the moment, and we expect in the coming years to see a large number of innovative applications related to RFID technology.

For individual researchers and universities, RFID poses a challenge because in the coming years, there will be a need to design increasingly sensitive and intelligent tags and readers.

2. Current status

RFID (Radio-Frequency Identification) technology is an automatic identification and tracking method for objects that uses radio waves to transmit data between an RFID tag and an RFID reader. This technology consists of three main components: RFID tags, readers, and data management software.

RFID tags are small devices, either passive or active, that contain information and are attached to objects for identification. They consist of a chip and an antenna that enable wireless communication with the RFID reader. Passive tags do not have a power source and are activated by the radio energy emitted by the reader, while active tags have their own power source and can emit signals over longer distances.

The RFID reader is a device that emits radio signals and reads the information stored on RFID tags. The reader receives and decodes data from the tags within its coverage area and transmits this information to a processing and storage system.

The data management software processes and stores the data read from RFID tags in a database or computer system for managing and monitoring the identified goods or objects.

This software enables monitoring of goods flow, identification of locations, inventory management, and other relevant operations.

Tags do not need power sources (electricity) to function: when "illuminated" by the magnetic field of the antenna to which they are exposed, the tag is actually capable of accumulating the small amount of energy it needs to transmit the information it contains over a short distance. This type of tag is called "passive". If it is necessary to transmit information over a long distance, more energy is needed, and the tag must be powered by a source of electrical energy, such as a battery. In this second case, the tag is called "active" [3].

Solar-powered RFID tags are devices that utilize RFID technology to identify and track objects, with the necessary energy for their operation provided by solar panels. These devices are used in a variety of applications, including in the logistics industry for inventory tracking and management, in agriculture for monitoring animals or crops, in asset management, and in many other fields.

The operating principle of a solar-powered RFID tag is quite simple:

- The solar panels charge the internal battery of the RFID tag using solar light.
- The battery stores the accumulated energy to power the electronic circuit of the RFID tag, which includes the antenna and the RFID microchip.

When the RFID tag is exposed to an RFID reader emitting electromagnetic energy, it activates the tag, allowing it to transmit the stored data to the reader. Due to the use of solar energy, these devices can operate without the need for battery replacement and can be used in environments where access to power sources is limited or nonexistent.

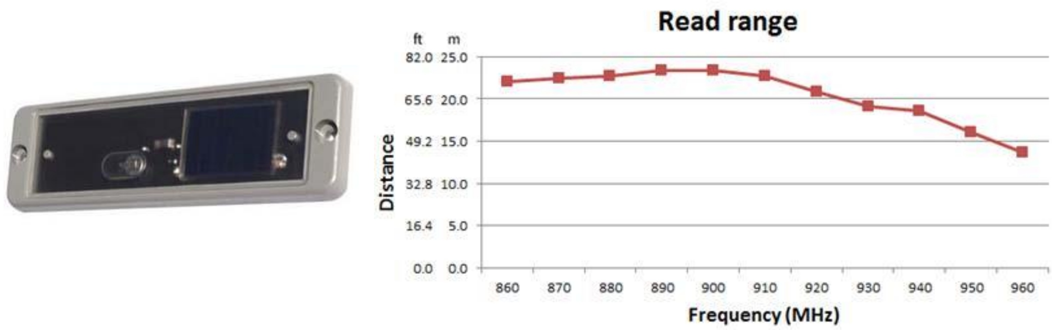

Figure 1. Model of solar-powered UHF RFID tag

Technical specifications:
Frequency range: UHF band, from 860 to 960 MHz (EU: 865-868 MHz; USA: 902-928 MHz)
Reading range: Up to 22 meters
UHF Protocol: ISO 18000-6c compliant, non-volatile memory of 1064 bits, user-accessible memory of 720 bits, EPC numbers on 96 bits accepted
Data retention: 10 years
Tag dimensions: 118 x 35 x 6.6 mm / 4.65 x 1.38 x 0.26 inches
Mounting holes (size): 3.2 mm hole / 6.8 mm recess for head
Placement: distance of 108.5 mm / 4.25 inches
Weight: 32 g / 1.2 oz
Weight: 32 g / 1.2 oz
Operational humidity: 0% to 85% RH
Storage temperature: -40°C to 85°C
Vibration: IEC 60068-2-6
Shock: IEC 60068-2-31
Water resistance: IP-67

This solar-powered UHF RFID tag is a state-of-the-art asset and cargo tag that can be used in multiple applications. It features a unique light panel, a power source combined with an ultra-capacitor, lightweight construction, and high durability, providing reliable performance in both indoor and outdoor applications. It offers a reading range of up to 22 meters depending on the reader, environment, and other factors.

The ultra-high-frequency RFID tag can withstand the harshest outdoor environments and is resistant to shocks, vibrations, dust, water, oil, chemicals, and other hazardous materials. Its special design and durability allow for up to ten years of usage.

The tag does not use batteries. Instead, it utilizes an ultra-capacitor with a practically unlimited lifespan, coupled with a state-of-the-art, high-efficiency solar panel. In light conditions, the solar panel provides energy for a wide reading range, and in extremely low light conditions or total darkness, the ultra-capacitor typically maintains the reading range for up to 48 hours. Note that the tag will continue to operate normally after the ultra-capacitor is completely discharged, albeit with a reduced reading range.

The solar tag continuously charges the capacitor. It takes approximately two minutes to fully charge the capacitor on a sunny day or using direct light from a halogen or sodium lamp. In low light conditions, it will take longer to fully charge the capacitor (Figure 1) [4].

The development of solar-powered RFID tags is increasing due to the advantages this technology offers in various fields. Here are some key aspects of the development of these tags:

Energy efficiency: A major concern in the development of solar-powered RFID tags is increasing energy efficiency. This involves optimizing solar panels to maximize solar energy capture and streamlining charging and battery management circuits to minimize energy losses.

Miniaturization and integration: To facilitate integration into various applications and to enable use in limited space conditions, developers are focusing on miniaturizing RFID tags and associated solar panels. This miniaturization often involves the use of advanced manufacturing and design technologies.

Durability and environmental resistance: Solar-powered RFID tags are often used in outdoor environments and under challenging conditions. The development of these tags includes improving durability and resistance to external factors such as water, dust, extreme temperatures, and mechanical shocks.

Improving autonomy: An important goal of development is extending the autonomy of RFID tags by optimizing energy consumption and maximizing its storage in batteries. This allows the tags to operate for longer periods without being exposed to solar light.

Additional functionalities: Besides the basic functionality of identification and tracking, developers are exploring ways to integrate other sensors and technologies into solar-powered RFID tags. This may include temperature, humidity, pressure sensors, or GPS, thereby expanding the range of possible applications.

In conclusion, the development of solar-powered RFID tags is an active area of research and innovation, with a focus on improving efficiency, durability, and functionality of these devices to meet the diverse requirements of the market.

Advantages of solar-powered RFID tags include:

Sustainability: The use of solar energy reduces dependence on conventional energy sources and contributes to reducing the carbon footprint.

Increased autonomy: Thanks to solar energy, these tags can operate without the need for battery replacement or power from other energy sources, making them suitable for applications in isolated or hard-to-reach locations.

Long-term cost savings: Although the initial costs may be higher than those of regular RFID tags, solar-powered tags can provide significant savings in the long run by eliminating the need for battery replacement and reducing maintenance costs.

Flexibility in implementation: Solar-powered RFID tags are suitable for a variety of outdoor applications or in locations where access to power sources is limited or nonexistent.

These tags are used in various fields, including logistics and supply chain, asset monitoring, agriculture, inventory management, and many others.

3. Materials and methods

To provide a complete example of designing a solar-powered RFID tag, I will detail every aspect of the project, including electronic schematics, PCB design, and necessary materials.

- Project requirements:

Reading distance: The tag must be capable of being read from a distance of at least 5 meters.
Durability: It should be resistant to water, dust, and extreme temperatures.
Autonomy: It must operate autonomously for at least 6 months without additional charging.
Storage capacity: It should be able to store a unique identification code and other relevant information.

- Materials required:

RFID microchip
Solar panel
Lithium-ion battery or lithium-ion polymer battery
Solar charge controller
Printed Circuit Board (PCB)
Electronic components: resistors, capacitors, LEDs, etc.
Waterproof and shock-resistant casing

- Electronic schematic:

RFID microchip: We use a passive RFID microchip with an integrated antenna.
Solar panel: We select a solar panel with efficient photovoltaic cells to charge the battery.
Battery: We integrate a lithium-ion battery or a lithium-ion polymer battery with sufficient capacity to power the RFID tag.
Solar charge controller: We add a solar charge controller to manage and regulate the charging of the battery from the solar panel.
Other components: resistors, capacitors, and other necessary components for the proper operation of the circuit.

- PCB design:

Compact design: We organize the components on the board to minimize the size of the tag.
Optimized traces: We route copper traces on the board to ensure efficient connection between all components.
Component mounting area: We provide enough space to mount and solder the components onto the board.
Connectors: We integrate connectors to allow the connection of the solar panel and other external devices to the board.

- Implementation:

We create the prototype of the RFID tag, assemble the components onto the board, and conduct necessary tests. We integrate the RFID tag into the asset or inventory tracking system, configuring the RFID readers to be compatible with the implemented tags.

This is a general approach to designing and implementing a solar-powered RFID tag. To complete the project, specialized software for electronic schematics and PCB design should be used, along with access to the necessary equipment and materials for assembly. Additionally, it is advisable to work with an electronics and PCB design specialist to ensure the success of the project.

Simplified electronic schematic for a solar-powered RFID tag

To develop an electronic schematic and a printed circuit board (PCB) for a solar-powered RFID tag, following the basic requirements, here is a concrete example:

- Electronic schematic:

Solar panel: We connect a solar panel to a solar charge controller. This regulates the voltage and current from the solar panel to efficiently charge the battery.
Battery: We connect a battery to the solar charge controller. The battery stores solar energy to power the RFID device during periods of darkness or low light.
RFID Microchip and Antenna: The RFID microchip and antenna are connected to a microcontroller, which controls the operation of the RFID device and communication with RFID readers.
Indicator LEDs: We add indicator LEDs to signal the operational status of the device and the battery level.

Printed Circuit Board (PCB):
Compact Design: We arrange the components on the board in a compact manner to minimize the size of the final device.
Optimized Traces: We lay out the copper traces on the board to ensure efficient connections between all components.
Component Mounting Area: We mark the spaces on the board to mount and solder the components, ensuring there is enough room to allow for connections between them.
Connectors: We integrate connectors to allow the connection of the solar panel and other external devices to the board.

This is a simplified example of an electronic schematic and PCB for a solar-powered RFID tag. To complete this project, you will need to use specialized electronic design and PCB software, such as Altium Designer, Eagle, or KiCad, and have access to the necessary equipment and materials for PCB fabrication. Additionally, it is advisable to have knowledge in electronics and PCB design or to work with a specialist in this field (Figure 2) [6].

Figure 2. Simplified electronic schematic for a solar-powered RFID tag

4. Case study

4.1. To provide a concrete example, let's imagine that a logistics company aims to enhance the tracking and management of goods during transportation by implementing a solution of RFID tags with integrated solar panels. They develop and test prototypes in the lab and then successfully implement them across all equipment and packaging used in their transportation and storage operations. The result is a significant increase in the autonomy of RFID tags and a reduction in maintenance costs during long-term usage.

Here's how such a compact design could be envisioned:

Requirement determination and specifications: The company has determined that the RFID tags need to be compact, with dimensions of approximately 5 cm in length and 3 cm in width, to be easily attached to the packaging of goods.

The solar panels must be large enough to provide an adequate power source but still not exceed the dimensions of the tags.

For an RFID tag of the mentioned dimensions (5 cm x 3 cm), we will need to select a solar panel that is small enough to fit on the tag but still efficient enough to provide the necessary energy.

Given the small size of the tag, we'll need to choose a solar panel of similar or smaller dimensions but with high efficiency. An option to consider is that of thin-film flexible solar panels (such as CIGS or amorphous silicon). These solar panels are flexible and can be easily integrated into an RFID tag. They can be cut to desired dimensions and can be quite efficient even in low or indirect lighting conditions.

Material and technology selection: Lightweight and durable materials are chosen for the tag casings, such as durable plastic or fiberglass composites. Manufacturing technology may include 3D printing to create customized casings and efficiently integrate electronic components and solar panels.

Component integration: The solar panels are integrated into the top surface of the RFID tag, with a maximized surface area design to capture as much sunlight as possible.

Lithium-ion batteries and electronic circuits are placed inside the casing, optimizing the available space and ensuring even weight distribution.

Energy efficiency optimization: The charging circuits are designed to maximize the efficiency of battery charging using the solar energy captured by the panels.

Advanced technologies such as MPPT (Maximum Power Point Tracking) are implemented to adjust the efficiency of the solar panels based on the solar light conditions.

Testing and validation: The prototype of the design is tested in the laboratory and in real-world usage environments to evaluate its performance and reliability. Battery capacity, autonomy, and RFID tag functionality are measured under various solar light conditions and usage scenarios.

Continuous optimization: Based on the test results and feedback received, the design is adjusted and improved to optimize performance and energy efficiency. It is ensured that the design remains compact and robust while meeting the requirements and objectives of the logistics company [7].

By following these steps and paying attention to design details and performance, the logistics company can develop a compact and efficient design for RFID tags with integrated solar panels that meet the specific requirements of their cargo tracking operations during transportation.

4.2. Simplified project plan for implementing solar panel integration into RFID tag design for cargo tracking:

Project: integrating solar panels into RFID tags for cargo tracking

- Project objective:

Develop and implement an RFID tag solution that integrates solar panels to extend battery life and make the tags more energy independent.

- Planning phase:

Objectives: Increase the autonomy of RFID tags, reduce maintenance costs.
Requirements: Compact dimensions of the tags, efficient integration of solar panels.
Budget and timeline: Initial budget of €50,000 (EUR), project duration of 6 months.

- Design phase:

Label design: Developing a compact design for RFID tags with integrated solar panels.
Component selection: High-efficiency solar panels, durable lithium-ion batteries.

- Development and testing phase:

Prototyping: Production of prototypes for RFID tags integrated with solar panels.
Prototype testing: Testing in both laboratory and real-world conditions to evaluate performance and reliability.

- Implementation phase:

Mass production: Implementing the solution into mass production according to established specifications.
Staff training: Training the team in the use and handling of the new RFID tags.

- Monitoring and optimization phase:

Performance monitoring: Monitoring the performance of RFID tags during usage.
Continuous improvements: Identifying and implementing necessary adjustments and enhancements.

5. Conclusions and recommendations

Utilizing RFID tags charged with solar energy can bring numerous benefits across various fields and applications:

Sustainability: Solar-powered RFID tags are an environmentally friendly option as they harness renewable solar energy to operate. This can contribute to reducing carbon footprint and adopting a more sustainable model of technology usage.

Improved autonomy: Integrating solar panels allows RFID tags to operate autonomously and be independent of external power sources such as batteries or electric outlets. This can increase flexibility and efficiency in field deployments, especially in areas without access to electrical power.

Redundancy and reliability: Due to the energy storage capacity in the battery, solar-powered RFID tags can continue to operate even in low-light conditions or during the night. This redundancy can ensure continuous and reliable operation of asset tracking and identification systems.

Long-term cost reduction: Although the initial implementation costs may be higher than those of traditional RFID tags, solar energy usage can reduce long-term costs associated with battery replacement and external power supply. Additionally, maintenance costs can be reduced as the tags do not require frequent battery replacements.

Flexibility in deployment: Solar-powered RFID tags can be used in a variety of environments and applications, including outdoor settings, industrial environments, or hard-to-reach areas. They can be quickly and wirelessly mounted in diverse locations, facilitating implementation in different operational contexts.

In conclusion, using solar-powered RFID tags can bring multiple benefits, including sustainability, improved autonomy, increased reliability, reduced costs, and flexibility in implementation. These benefits can make these tags an attractive option for various asset tracking, identification, and management applications in different industries and operational environments.

To increase the autonomy of RFID batteries, the following suggestions could be considered:

Energy consumption optimization: Developing and implementing more efficient algorithms for data processing and communication between RFID readers and tags to reduce the energy consumption of devices.

Solar energy usage: Integrating solar panels into the design of RFID tags to allow battery charging using solar energy, which could significantly extend battery life and make tags more durable over time.

Battery technology innovation: Researching and developing more efficient and durable batteries, such as lithium-ion batteries or wireless battery technologies, which can provide higher autonomy and longer lifespan compared to conventional batteries.

Data transmission optimization: Using more advanced communication technologies, such as Bluetooth Low Energy (BLE) or LoRa (Long Range) technology, which consume less energy during data transmission than traditional RFID communication technologies. [8].

Energy saving mode implementation: Developing and implementing energy-saving modes in RFID tags, such as sleep mode or idle mode, to reduce energy consumption when tags are not actively used.
These suggestions could contribute to improving the autonomy of RFID batteries and expanding the use of this technology in various applications and work environments.

6. Bibliography

[1]. RFID - Radio Frequency Identification, http://ro.wikipedia.org/wiki/RFID
[2]. PESCARU G., DRAGOMIR R., PUŞCOCI S., ”Activities optimization using RFID technologies”, în AGIR Bulletin - Telecommunications, no. 2/2008, pp. 66–78
[3]. LIXANDROIU, R., ”A Model of Traceability for Equipments Using RFID Technologies within an Integrated System”, în Revista Informatica Economică, no. 2(38)/2006, pp. 124 - 128
[4]. site https://gaotek.com/ro/product/gao-tek-solar-powered-uhf-gen-2-rfid-tag/#tab-4
[5]. site ELECTROKITS, https://www.electrokits.ro/identificarea-in-radiofrecventa-rfid-aplicatii-ale-sistemelor-saw-rfid/
[6]. site ELECTRONICĂ APLICATĂ, https://electronicaaplicata.wordpress.com/tag/identificare-automata/
[7]. LAHIRI S., RFID Sourcebook, Prentice Hall PTR, 2005
[8]. BHATT H., GLOVER B., RFID Essentials, O'Reilly, 2006

FUSION TRACKING: AN INNOVATIVE LOW-COST, HIGH-ACCURACY 3D POSE ESTIMATION USING UWB AND IMU TECHNOLOGIES

PĂLĂȘAN Rareș Tudor, PARPALĂ Lidia
Liceul Scoala Europeana București, 11th grade IB
Contact: rares@palasan.ro

ABSTRACT: With the increasing complexity of indoor environments and the limitations of Global Navigation Satellite Systems (GNSS) for indoor localization, there is a growing need for precise 3D pose estimation technologies. This paper introduces a novel approach that combines Ultra-Wideband (UWB) with Inertial Measurement Units (IMU) to address the challenges of cost, accuracy, and operational constraints commonly faced with traditional methods such as laser systems, camera arrays, and RF trilateration. By leveraging a new UWB library optimized for multi-tag tracking and an extended Kalman filter to correct for IMU drift, my system offers a cost-effective and highly accurate alternative to conventional tracking technologies. This research not only demonstrates significant improvements in tracking accuracy and system cost but also integrates the robustness required for dynamic indoor applications. The system's dual approach utilizes the precision of UWB for spatial localization and IMU for motion sensing, effectively mitigating common issues like multipath interference and signal obstruction, thus ensuring reliable 3D pose estimation even in complex indoor settings.

KEYWORDS: 3D Localization, Ultrawideband, Trilateration, IMU, EKF

1. Introduction

The evolution of interactive technologies, particularly in virtual and augmented reality, necessitates more sophisticated tracking systems to create immersive experiences. Traditional systems, such as laser tracking, offer high precision and quick response but are expensive and require an unobstructed line of sight. Camera-based systems reduce costs but compromise on precision and need a clear view. RF trilateration is cost-effective and works through obstacles but suffers from low refresh rates.

My research addresses these deficiencies by developing a hybrid tracking system that leverages the strengths of UWB and IMU technologies. UWB technology is extremely precise and does not require a line of sight, making it superior to optical methods in crowded environments. However, like all radio frequency systems, it can be prone to multipath signal errors and non-line-of-sight issues, which we mitigate using techniques derived from satellite navigation systems.

IMUs provide acceleration and rotation data, ideal for rapid response tracking but susceptible to cumulative errors or drifts over time. By applying an extended Kalman filter, we can integrate absolute position data from UWB with relative motion data from IMU to create a comprehensive tracking solution.

2. Research and Development Process

The development process began with an in-depth analysis of current 3D positioning technologies, identifying key areas where they fail to meet cost-effective and precise tracking needs. We drew inspiration from commercially available technologies, such as Apple Air Tags and VR tracking systems, designed to be inexpensive yet efficient.

Current positioning systems all have their drawbacks. Here are some of the most popular options used in virtual reality applications:

2.1 Laser Tracking (Vive)

Laser tracking systems, like those used in HTC Vive, utilize base stations that emit structured infrared lasers. These lasers traverse the room and are detected by sensors on VR headsets and controllers. The timing of these laser strikes is then calculated to determine the precise position and orientation of the VR devices.

Table 1.

Pros	Cons
High precision and accuracy: Submillimeter precision due to laser measurements.	Setup complexity: Requires careful placement of base stations and calibration.
Low latency: Real-time response essential for immersive VR experiences.	Line of sight requirement: Objects obstructing the line of sight between base stations and the headset can interrupt tracking.
Room-scale tracking: Capable of effectively tracking large areas.	Cost: Generally, more expensive than other tracking methods due to sophisticated hardware.

2.2 Inside-Out Camera Tracking (Vive)

Inside-out tracking uses cameras mounted on the VR headset to constantly scan the surroundings. The system identifies fixed points in the environment and uses changes in these points relative to the user's movement to determine position.

Table 2.

Pros	Cons
Autonomous: No need for external sensors or base stations, making it more portable.	Environmental dependency: Tracking accuracy can decrease in environments without well-defined or dynamically changing features.
Easy setup: Simpler to set up compared to systems requiring external trackers.	Lighting conditions: Performance can vary depending on lighting conditions; low light can reduce tracking efficiency.
Scalable: Easily adapts to different room sizes without additional setup.	Cost: Generally, more expensive than other tracking methods due to sophisticated hardware.

2.3 IMU Tracking (SlimeVR)

IMU (Inertial Measurement Unit) tracking, as used by systems like SlimeVR, involves sensors measuring rotational speed and linear acceleration. These data are used to estimate device orientation and movement through space.

Table 3.

Pros	Cons
Highly responsive: Provides immediate response to movement.	Drift over time: IMUs can accumulate errors (drift) over time, which must be corrected periodically.
Portable and compact: IMUs are small and can be directly embedded into devices, enhancing portability.	Limited position tracking: Without external references, IMUs primarily provide relative motion data, lacking precise position tracking.
Cost-effective: Generally, less expensive than optical tracking solutions.	

2.4 External Camera Localization (April Tags)

This method involves using external cameras to detect visual markers or tags placed in the environment, such as April Tags. The camera captures the tag, and software calculates the position and orientation relative to the tag.

Table 4.

Pros	Cons
Flexibility: Can be set up in various environments with minimal hardware requirements.	Field of view limitations: Only objects within the camera's field of view can be tracked.
Cost-effective: Low-cost cameras and printable tags make this a budget-friendly option.	Setup time: Requires time for placing and potentially recalibrating tags in the environment.
High precision: Provides high accuracy within the visual field of the tags.	Visual condition dependency: Performance can degrade in low light conditions or if tags are obstructed.

2.5 RF Trilateration

RF trilateration uses the timing or power of radio frequency signals between nodes to determine positions. It measures the distance between multiple nodes and calculates positions based on the geometric properties of triangles.

Table 5.

Pros	Cons
Works through obstacles: Can operate in environments where optical methods are obstructed.	Interference sensitivity: RF signals can be distorted by other electronic devices or reflective surfaces, affecting accuracy.
Scalability: Can be scaled to cover large areas.	Setup complexity: Requires precise calibration and multiple nodes for accurate tracking.
Integration with existing networks: Can utilize existing RF infrastructure, such as Wi-Fi.	

We selected a fusion of technologies that complement each other's strengths. My setup involved five ESP32-UWB development boards; two were equipped with ICM-20948 9-DOF IMUs (although only the accelerometer and gyroscope were used) and functioned as mobile tags, while the other three served as stationary anchors, configured in a right-angled triangle to optimize the trilateration process.

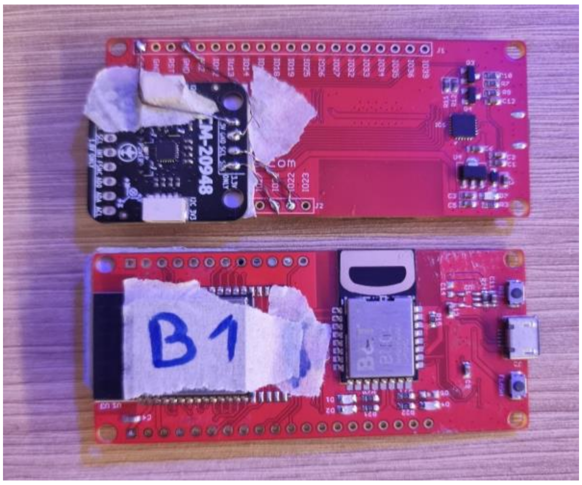

Fig. 1: ESP32-UWB and ICM-20948 IMU assembly

Fig. 2: Anchor assembly made out of two PVC pipes and three ESP32-UWB boards

3. UWB Innovations

3.1 Distance Calculation

To enable simultaneous tracking of multiple tags, I developed a new UWB library that incorporates asymmetric two-way ranging, a method that calculates distance based on the time of flight of radio signals between two points. The asymmetric two-way ranging process works as follows:

1. **Initialization**:

    - Tags emit signals at predetermined intervals.

- When an anchor detects a signal from a tag, it sends a "range initialization" message, pairing the two devices.

2. **Ranging Process:**
    - The tag sends a "POLL" message to the anchor.
    - The anchor responds with a "POLL ACK" (Acknowledgment) message.
    - The tag then sends a "RANGE" message, which includes the timestamps of the previous messages.

3. **Distance Calculation:**
    - Upon receiving the "RANGE" message, the anchor calculates the distance based on the timestamps of the messages exchanged during this sequence. This is done using the formula described below.
    - The anchor then sends a "range report" packet back to the tag. This report includes the calculated distance, so both the anchor and the tag are aware of the range.

4. **Outcome:**
    - This process allows for continuous tracking of the distance between the tag and the anchor, facilitating precise 3D positioning without the need for a direct line of sight. This is particularly beneficial in crowded or indoor environments.

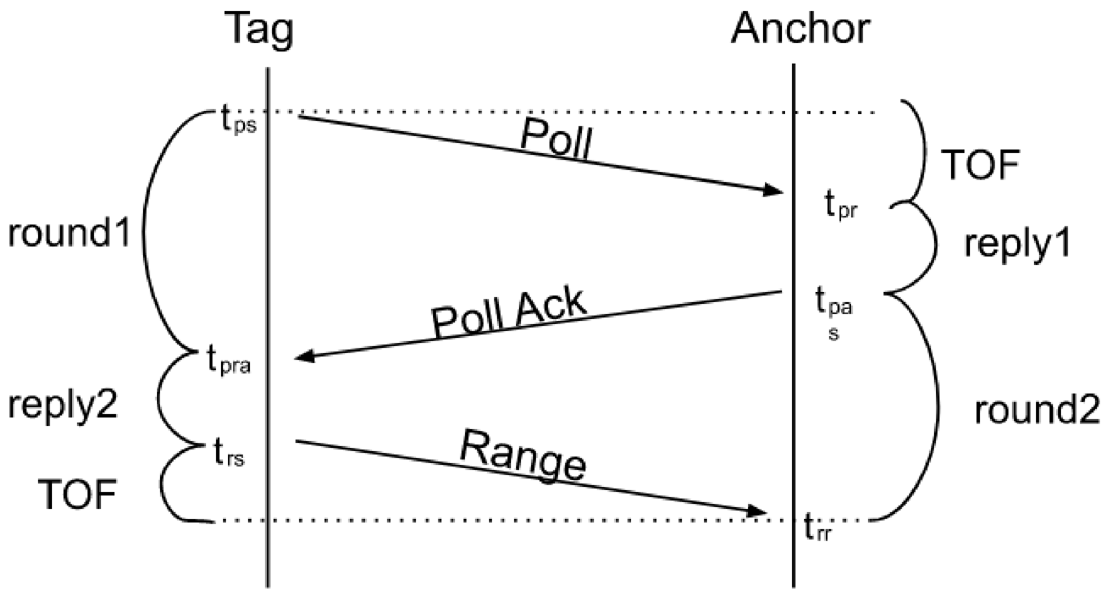

Fig 3: Two-way asymmetric ranging diagram

t_{ps} *represents the time the Poll message is sent by the tag*
t_{pra} *represents the time the Poll Ack message is received by the tag*
t_{pas} *represents the time the Poll Ack message is sent by the anchor*
t_{pr} *represents the time the Poll message is received by the anchor*

t_{rr} *represents the time the Range message is is received by the anchor*
t_{rs} *represents the time the Range message is sent by the tag*

The times set for rounds and responses are calculated as follows:

$$round1 = (t_{pra} - t_{ps}) \quad (1)$$

$$reply1 = (t_{pas} - t_{pr}) \quad (2)$$

$$round2 = (t_{rr} - t_{pas}) \quad (3)$$

$$reply2 = (t_{rs} - t_{pra}) \quad (4)$$

The time of flight (ToF) is calculated as:

$$ToF = \frac{round1 \times round2 - reply1 \times reply2}{round1 + round2 + reply1 + reply2} \quad (5)$$

To ensure accuracy, I performed extensive calibration to correct for the inherent antenna delay in the UWB devices. This process involved taking multiple measurements at a known distance to identify and adjust any distortions in the readings, thus enhancing the system's precision.

After performing this calibration, the intervals showed a consistent error of approximately 2 meters. This error is due to the antenna delay, which is the time it takes for the device's antenna to send a message. To account for this, I conducted several measurements and calculated the distance adjustment needed to obtain an accurate reading. This calibration function must be run on each device, as the antennas of the modules we purchased are not perfect.

```
int getDistanceOffset(int steps, int measuredDistance) {
    long sum = 0;
    while (steps--) {
        int distance = DWM1000.getRange();
        sum += distance;
    }
    int averageDistance = sum / steps;
    return measuredDistance - averageDistance;
}
```

Fig. 4. Function for calibrating the distance reading from the UWB modules

3.2 Position calculation for the tag

Once the distances between the anchors and tags are determined, the next step is to find the position of the tags. Among the numerous indoor positioning techniques (2D and 3D) reported in the literature, the most commonly used and recognized are based on a geometric approach. This approach generally suggests that localization is achieved in two stages. The mobile device first records one or more signal parameters that depend on the user's location from an appropriate number of emitters, and then calculates the coordinates of the relative location in a 2D or 3D plane using standard geometry.

In our technique (Trilateration), the approximate distance to each emitter is calculated by determining the time it takes for the signal to reach the terminal when transmitted from a given access point (Fig. 5.1). The latter technique is based on the terminal's ability to record the angle of arrival of a signal from a specific access point or base station (Triangulation). Modern radio technologies, such as UWB and even millimeter-wave (mmWave) radios, create opportunities for very precise time-of-arrival estimation.

Triangulation involves estimating a 2D or 3D location using unilateral or multilateral measurements (the position is determined from the measured lengths of three sides of a triangle) (Fig. 5.2). Trilateration estimates the location using multiple distance measurements, while angulation uses angles relative to known positions.

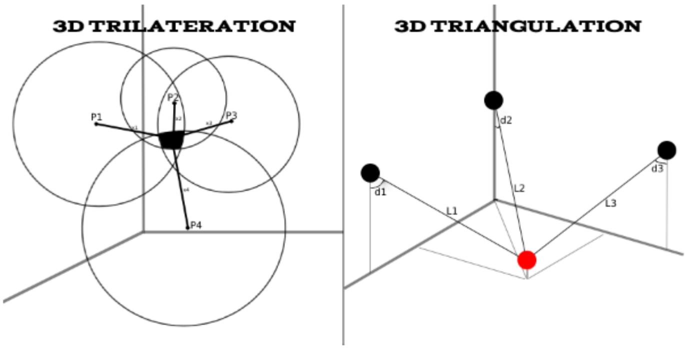

Fig. 5.1. Trilateration and 5.2. Triangulation

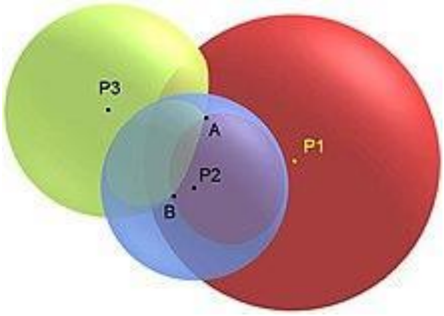

Fig. 6. Trilateration using three anchors

To reduce costs, we decided to use only three anchors for trilateration. The issue with this method is that there are two possible positions where the tag could be. To address this, we can strategically place the antennas to eliminate one of the solutions, such as placing the antenna array on one of the exterior walls of the building.

The geometric basis of trilateration involves forming spheres around each anchor with radii equal to the measured distances. The point where all three spheres intersect is the location PP (Fig. 6). Mathematically, this can be formulated as follows:

The equations of the spheres relative to each anchor are:

$$(x-x_1)^2+(y-y_1)^2+(z-z_1)^2 = r_1^2 \qquad (6)$$

$$(x-x_2)^2+(y-y_2)^2+(z-z_2)^2 = r_2^2 \qquad (7)$$

$$(x-x_3)^2+(y-y_3)^2+(z-z_3)^2 = r_3^2 \qquad (8)$$

Where $(x_1,y_1,z_1),(x_2,y_2,z_2),(x_3,y_3,z_3)$ $A_1.A_2.A_3$

To find the coordinates of point **P**, we simplify the system of equations:

- We first isolate x and y in terms of z from the first two equations.
- Then, we substitute these expressions into the third equation.
- Solving the resulting equation for z, we then calculate x and y using the relations derived in the first step.

This method typically yields two possible solutions for the location of **P**, corresponding to the intersections of the spheres. To select the appropriate solution, additional context or constraints, such as the known orientation or arrangement of the anchors, can be applied.

For a simplified scenario where the anchors are positioned in a standard orientation (e.g., forming a right triangle or on a flat plane), specific formulas can be derived. Assume that **A1** is at the origin, **A2** is on the x-axis, and **A3** is in the xy-plane. The coordinates for **P** can be approximated by:

$$x = \frac{r_1^2-r_2^2+d^2}{2d} \qquad (9)$$

$$y = \frac{r_1^2 - r_3^2 + ix^2 + j^2 - 2ix}{2j} \qquad (10)$$

$$z = \sqrt{r_1^2 - x^2 - y^2} \qquad (11)$$

Where d is the distance between **A1** and **A2**, and i and j are the coordinates of **A3** relative to **A1**. The coordinate **z** will have two solutions, one negative and one positive.

In practice, the anchors may be positioned arbitrarily, requiring a translation and rotation of the coordinate system to align with a simpler and more calculable model. This involves:

Translation: Initially translating the entire configuration so that one anchor, typically **A1**, is at the origin, simplifying distance calculations and reducing the complexity of subsequent rotations.

Rotation: Next, rotating the other two anchors to lie along a coordinate axis or plane that is easier to manage. This involves finding a rotation matrix that aligns **A2** along the x-axis and **A3** in the **xy-plane**.

By transforming the system into this new coordinate space, the previously derived trilateration formulas can be directly used to find the position of P relative to the new axes. Finally, applying the inverse of these transformations (i.e., inverse rotation followed by inverse translation) maps this position back to the original coordinate system of the anchors. This approach allows us to achieve the same result as standard trilateration while using only three anchors instead of four.

.

3.3 Integrating IMU Data with an Extended Kalman Filter (EKF)

IMUs (Inertial Measurement Units) are essential for tracking orientation and motion by measuring linear accelerations and angular velocities. These consist of accelerometers and gyroscopes, each providing critical data about the dynamics of motion. However, these sensors are known for their susceptibility to errors known as "sensor drift," which accumulate over time and can significantly distort measurements.

To counteract inaccuracies caused by drift, this study employs an Extended Kalman Filter (EKF), an algorithm renowned for its effectiveness in aerospace and automotive applications. EKF offers a dynamic method of correcting deviations by continuously predicting and updating estimates based on new data. This process ensures high tracking accuracy even with prolonged use.

The integration of EKF operates through two main stages:

1. Prediction Phase: The filter predicts the future state of the system using a model of the dynamics and previous state estimates. This phase utilizes the physics of motion and initial readings from the IMU to forecast the next position and orientation.

2. Update Phase: When new data from the UWB system is introduced, EKF adjusts the predicted state by calculating a "Kalman gain." This gain optimizes the weighting of new data against predicted data, refining the state estimate with the latest measurements.

The effectiveness of integrating IMU with EKF is demonstrated through simulations that mimic real-world conditions. These simulations help validate theoretical models and provide a foundation for practical implementation. For example, the system was tested in a controlled environment where tags equipped with IMUs were maneuvered along various trajectories, and the corresponding outputs were meticulously analyzed.

Algorithmic Formulation: The basic mathematical framework involves formulating state transition equations that describe the dynamics of motion as perceived by the IMU. These equations are crucial for the prediction phase of EKF:

$$x_{k+1} = Ax_k + Bu_k + w_k \qquad (12)$$

Where **xk** is the state vector at time **k**, **A** is the state transition matrix, **B** is the control input matrix, **uk** represents the control inputs, and **wk** is the process noise.

During the update phase, EKF uses measurements from the UWB system to correct the IMU estimates:

$$y_k = Hx_k + v_k \qquad (13)$$

Where **yk** is the measurement vector, **H** is the measurement matrix, and **vk** is the measurement noise. The Kalman gain **K** is calculated to minimize the estimation error:

$$K_k = P_k H^T (H P_k H^T + R)^{-1} \qquad (14)$$

Here, **Pk** is the prediction error covariance, and R is the measurement noise covariance matrix. Essentially, the Kalman Gain balances the new UWB measurements with the predicted states from the IMU, optimizing the accuracy of position and motion estimates.

Integrating IMU data with UWB inputs through EKF not only improves accuracy but also enhances the reliability of the tracking system, particularly in environments where UWB signals might be obstructed or reflected. This synergistic approach leverages the rapid response of IMU data and the positional precision of UWB measurements to provide a robust solution for 3D position estimation in complex settings.

The extended role of IMUs in this research highlights their critical contribution to overcoming the inherent limitations of each technology when used independently. This holistic integration ensures that the system is not only more precise but also more adaptable to the evolving demands of real-time tracking applications.

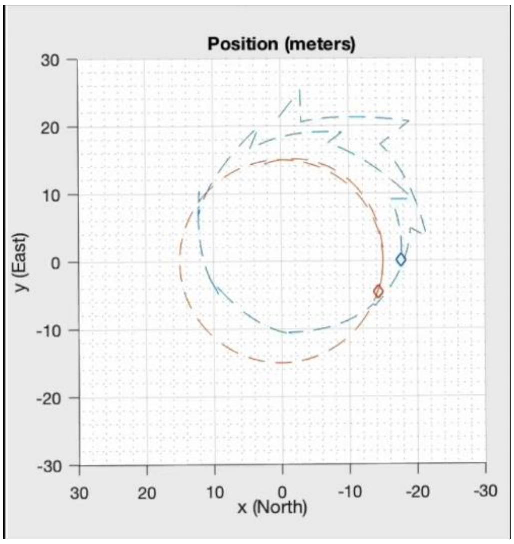

Fig.7. Position estimation only using the GPS UWB system,

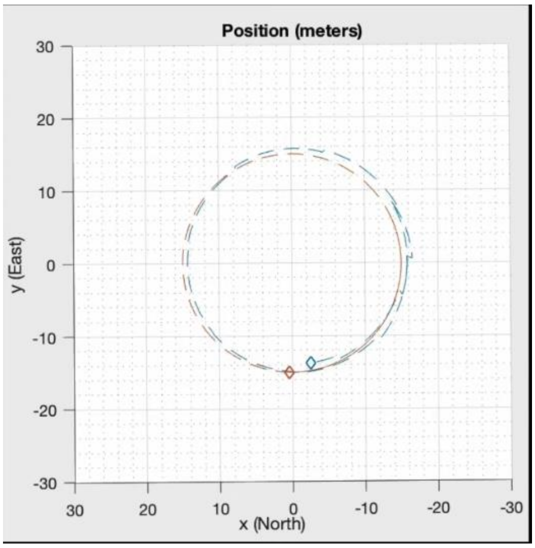

Fig.8. Estimated position after integrating the IMU with the UWB system

To better understand the dynamic interaction between IMU and UWB data, we will simulate IMU and UWB readings based on a virtual tag to test the accuracy of our model (Fig. 9).

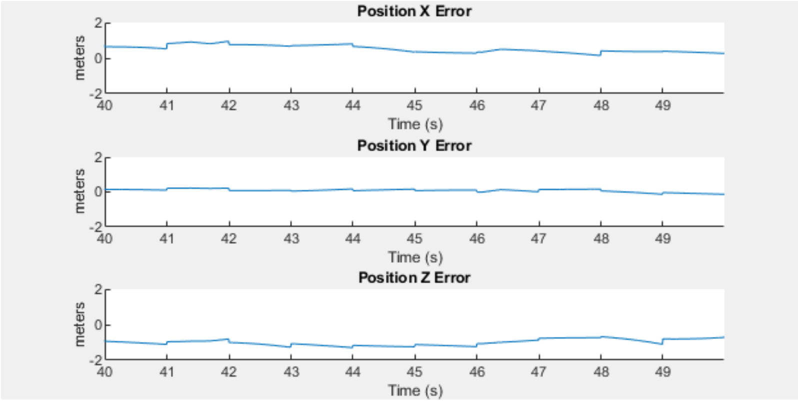

Fig.9. Error after integrating the IMU

Conclusions

This research successfully demonstrates a novel approach to 3D position estimation by integrating Ultra-Wideband (UWB) and Inertial Measurement Unit (IMU) technologies. This fusion addresses significant challenges related to cost, accuracy, and operational constraints in dynamic indoor environments where traditional methods fail. By utilizing a newly developed UWB library optimized for multi-tag tracking and an extended Kalman filter to mitigate IMU drift, the system offers an innovative, cost-effective, and highly accurate alternative for real-time location tracking.

The dual-technology approach ensures robust position estimation capabilities, even in settings prone to multipath interference and signal obstructions. The precision of UWB technology combined with the rapid response of IMU sensors enables efficient tracking without the need for a direct line of sight, distinguishing this system from conventional optical and laser-based methods. Additionally, the scalability and adaptability of this system to complex indoor configurations make it an ideal solution for a wide range of applications, from augmented reality to automated inventory management.

The research results not only reflect substantial improvements in tracking accuracy but also highlight the system's accessibility, making advanced tracking technology more attainable. Future work will focus on refining the integration of technologies, enhancing tracking robustness in more chaotic and unpredictable environments, and extending the system's application to outdoor settings. This innovative approach paves the way for broader adoption and further exploration in both commercial and research domains, ensuring that the fusion tracking system remains at the forefront of 3D position estimation technology.

4 Bibliography

1. Sesyuk, A., Ioannou, S., & Raspopoulos, M. (Year). A Survey of 3D Indoor Localization Systems and Technologies.
2. Zafari, F., Gkelias, A., & Leung, K. K. (Year). A Survey of Indoor Localization Systems and Technologies.
3. Alarifi, A., Al-Salman, A., Alsaleh, M., Alnafessah, A., Al-Hadhrami, S., Al-Ammar, M. A., & Al-Khalifa, H. S. (Year). Ultra Wideband Indoor Positioning Technologies: Analysis and Recent Advances.
4. Yao, L., Yao, L., & Wu, Y. (Year). Analysis and Improvement of Indoor Positioning Accuracy for UWB Sensors.

DESIGNING AND PROTOTYPING A QUADRUPED ROBOT

ION Paula, POPESCU Diana

Faculty: Industrial and Robotics Engineering, Specialization: Management of Virtual Industrial Enterprises, Year of study: master II, e-mail: paula.ion@stud.fiir.upb.ro

ABSTRACT: The design and construction of quadruped robot were focused on the optimization of leg dimensions, movement modes and actuation mechanisms. This study involved a detailed analysis of the robot's components to gain a comprehensive understanding of their functions and interactions. By identifying optimal values for leg dimensions and refining motion strategies, the project seeks to improve the robot's performance for various applications and on different surfaces. The project and reported results are aimed providing useful information that can simplify the design and construction process of a quadruped robot.

KEYWORDS: mobile robot, four-legged ones, robot dog, legs, movement

1. Introduction

Mobile robots are drawing increasing research interest because of their capabilities to help or replace humans in dangerous or challenging environments, as well as for providing human personal assistance and security [1-2]. The adaptability of quadruped robots extends their application across various sectors, including natural disaster response, industrial inspections, and material transportation in challenging environments like battlefields and nuclear sites Tracked, wheeled, and legged are the three categories in which these robots can be classified, each dedicated to a certain type of terrain/application. For instance, wheeled and tracked robots are effective on flat terrain but lose their effectiveness on soft or bumpy ground [1]. In comparison, legged robots, especially four-legged ones, are better suited to a variety of challenging environments, as the footholds allow them to move omnidirectional [1-2]. Four-legged robots of interest in the current study, are especially important because of their simpler architecture and control methods compared to six- or eight-legged robots [1]. With multiple degrees of freedom and different power sources (pneumatic, electric, hydraulic), motion control is based on feedback-based adjustments to achieve the desired motion [2-3]. The legs operate independently of their body that serves as a floating base [3]. Legged robots' multiple Degrees of Freedom (DOF) in their joints allow them to navigate obstacles and uneven terrain efficiently, further expanding their utility compared to wheeled robots. They incorporate advanced perception and cognition systems for autonomous operation, making them versatile tools in various fields of locomotion, cognition, navigation, and perception [4].

A four-legged robot is made of different materials like plastic, carbon fiber, and aluminum alloys, and is equipped with sensors and controls for autonomous functions [2, 4]. Examples of quadruped robots include the TITAN-XIII, a sprawling-type quadruped robot that demonstrates high speed and energy-efficient walking by utilizing a wire-driven mechanism and low center of gravity for stability [4][2]. Mammal-type quadruped robots, such as Boston Dynamics' BigDog, the hydraulic HyQ, and the electric MIT Cheetah, have demonstrated superior performance in rough terrains by leveraging advanced actuation mechanisms and dynamic control strategies [4]. These robots benefit from features like active compliance joints and high torque density motors, enabling energy-efficient walking and dynamic movements [4]. The development and experimentation with all these robots prove their potential to outclass the traditional designs in rough terrains [2, 4]. On the contrary, sprawling-type quadruped robots offer high stability due to their low center of gravity and wide supporting leg polygon. They also allow for versatile foot placements, and are less prone to damage from falling. Designs like the TITAN series, have compact leg mechanisms and innovative sensors to autonomously navigate the complex terrains [4].

The design and construction of a quadruped robot focus on optimizing leg dimensions, movement modes, and actuation mechanisms. This study involved a detailed analysis of the robot's components to gain a comprehensive understanding of their functions and interactions [2, 5-6]. By identifying optimal values for leg dimensions and refining motion strategies, the project aimed to improve the robot's performance for various applications and on different surfaces [7-8]. The project and reported results provide useful information that can simplify the design and construction process of a quadruped robot [2-3].

2. Design and mechanics

The design proposed in this study is based on the following principles:

- It is a quadruped robot;
- One leg will allow 2 movement points;
- No shoulder movement for the initial model;
- Chosen method for movement is electronic servos;
- Controlled with the help of a Raspberry Pi;
- Power will be provided by cable from an external source.

The most challenging part was selecting a proposal set of servos that would correspond with the size and weight of the robot, to allow a fluent movement and actions. Affordability was also considered when selecting the servos since the price/utility for dual shaft servos vs single shaft servos pointed out to select the single shaft and design the leg so that the weight is also distributed on the other side.

MG996R metal gear torque is the selected servo, its position being controlled with a high degree of accuracy. The technical characteristics are the following:

- Weight: 55 g;
- Size: 40.7x19.7x42.9mm;
- Power: 9.4kg / cm (4.8V), 11kg / cm (6V);
- Response time: 0.14s / 60 grade (6V);
- Power consumption: 4.8 - 7.2V;
- Running Current 500 mA – 900mA;
- Stall Current 2.5 A (6V);
- Operating temperature: 0 – 55ºC.

Selecting a single shaft servo has an impact on the shape of the case that holds the servo because it must be able to cope with having an additional shaft, opposing the servo shaft (Fig.1). The opposing shaft required a ball bearing to facilitate movement (Fig.2).

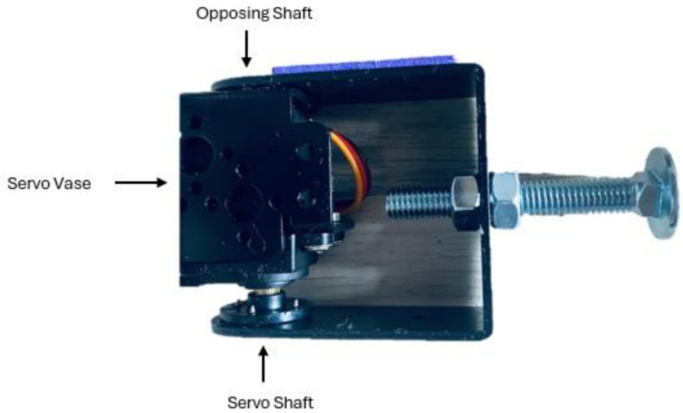

Fig. 1. Servo case connected to moving part.

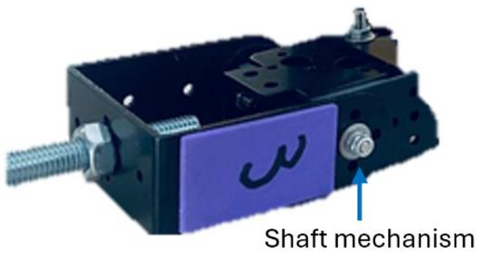

Fig. 2. Shaft mechanism and ball bearing.

The U-shaped aluminum servo mount in the leg structure offers a number of advantages. Designed for standard sized servos, these mounts are lightweight yet strong, and the many mounting holes on these mounts make it easy to create mechanisms and attach various components.

Incorporating these mounts into the leg design has resulted in a more reliable leg, capable of withstanding dynamic loads and maintaining the stability, overall weight and durability of the robot.

The leg setup is designed so that any change can easily be made to the movement allowed by the servo. Calibrating the movement can be done by adjusting the servo wheel position relative to the position of the joint. For maintaining the symmetry of the design (Fig.3), there are left and right legs, depending on the servo position (Fig.4). Initially the default plastic wheels (that were supplied with the servo) have been used. During the initial tests some of the wheels could not cope with the tension, since the servo shaft is made of metal.

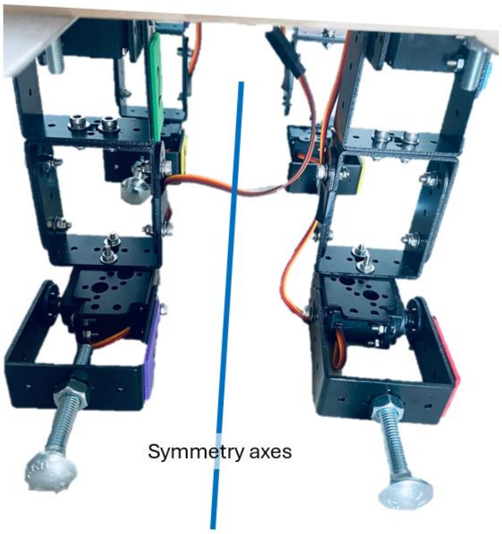

Fig. 3. Left and right legs, view from front

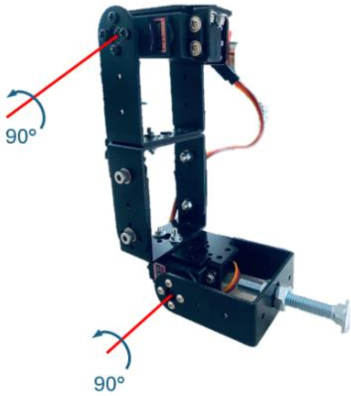

Fig. 4. Left leg.

The design allows for flexibility in terms of feet position (where on the length should the front and rear feet should be connected to the body), length (how long should be the body in relation with the length of the feet) and width (what would be the optimal width for the robot in order to maintain proper balance and provide a "dog like" appearance) of the robot (Fig.5). The controlling unit was placed in the middle for best balance.

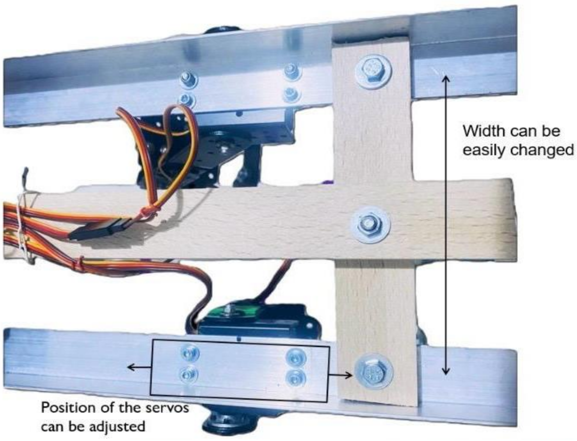

Fig. 5. Top view

3. Control of the robot

The robot is equipped with eight servos, two on each leg. The control of the servos was done by using a Raspberry Pi and a PWM Shield with 16 channels. For the programming of the movements, Python was used, along with the library for controlling the shield.

Two Amps power sources were used to power up the Raspberry Pi and the servo shield.

After the initial assembly was done, the testing stand was built (Fig.6). The stand must be built in such ~~a~~ way that would allow easy calibration of servos (wheel adjustment), movement without any impediments and provide a way to observe movements. To easily work with the servo's, colors were assigned to each of them, and up and down movements were applied for individual keys on the keyboard.

At the beginning each leg was calibrated. For the calibration several steps were required:

- Define the minimum and maximum movement of each servo.
- Identify the position of the wheel related to the desired movement.

- Adjust the wheel position.
- Define direction of movement. Since they were symmetrically set, on one side the movement was from 0 to 90 and on the other from 90 to 0.

After the legs were calibrated initial complex movements (involving more than one leg) were tested. Initial simulations revealed slow response of servos for complex movements. This was traced back to two electrical issues:

- The servo power cables were not long enough to reach the shield so additional cables were added to what could not support the required power consumption.
- Also, the required power~~,~~ while under load, was not enough. At least 1Amp would be required for each of the servos. The used power source was not enough so an addition 10Amp power source had to be used. This power source will also require proper cables to be able to transmit the power towards the shield. The shield is designed to cope with up to 20Amp power consumption, so having this power source was not a problem for the shield.

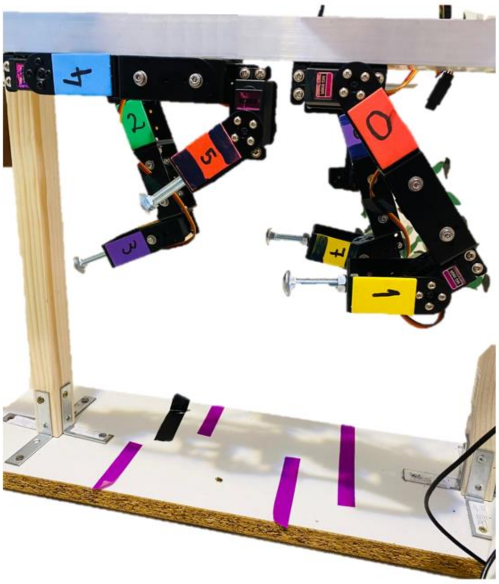

Fig. 6. Testing stand

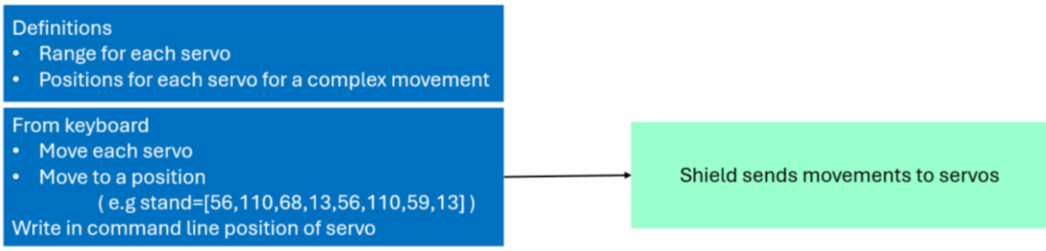

Fig. 7. Python logic blocks

The code was implemented based on 3 logic blocks (Fig.7). Using the keyboard to control each servo allowed a better adjustment for complex movements. After the issues have been fixed, it was ready to be tested without the testing stand.

First test revealed that the weight of the power cable unbalanced the robot and movements were not as expected. The design allowed for compensating weights (in the shape of a book) to be used to re-balance the robot and make the movements as desired. Figures 8-14 shows several movements the robot can perform.

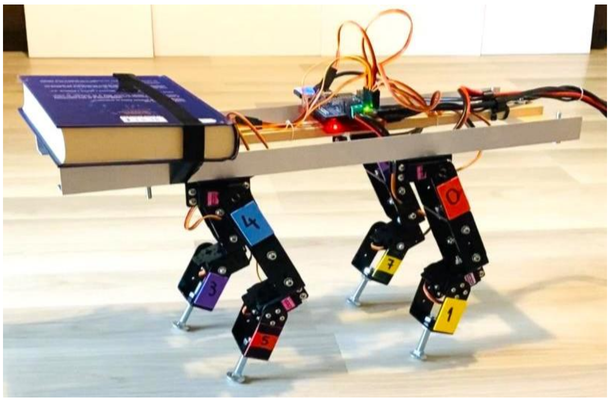

Fig. 8. “Stand”

Fig. 9. “SitDown

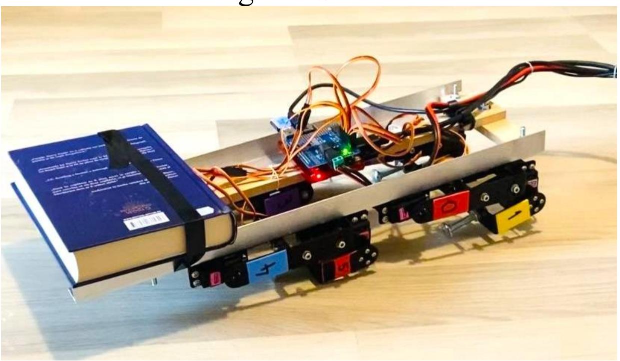

Fig. 10. “LayDown”

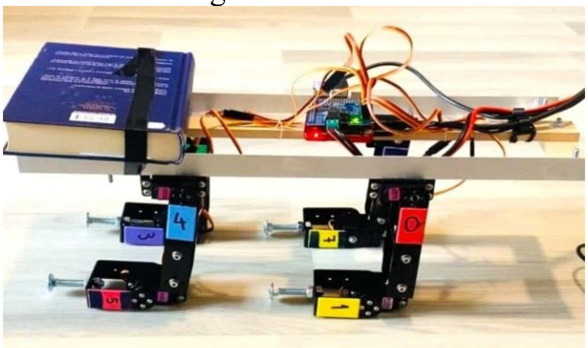

Fig. 11. “KneesDown”

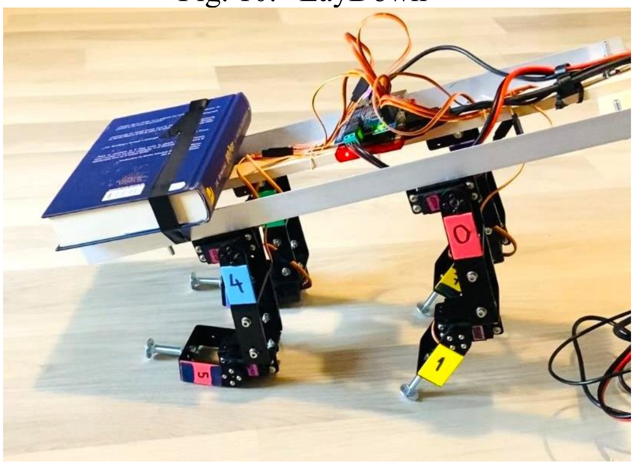

Fig. 12. “UpBack

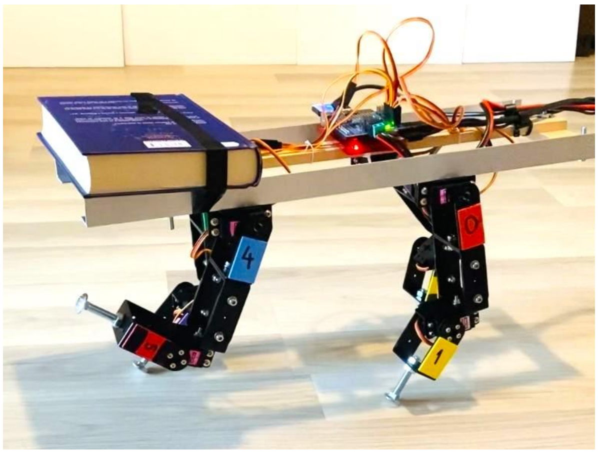

Fig. 13. “SayHey”

The impact on the surface where the robot performs its movements was also studied and from the tests it can be observed that the speed of movement changes when the surface changes. When we have a perfectly flat and hard surface, its movements are much more precise and reliable. When the surface is soft, the robot moves more slowly. As this robot is a "prototype", no weights were made and as the wires from the source impacted the center of gravity, for the tests a weight, more precisely a book, was placed to achieve its balancing in the most correct way. As a result of this first experiment, seven movements were performed, which can be activated individually or together.

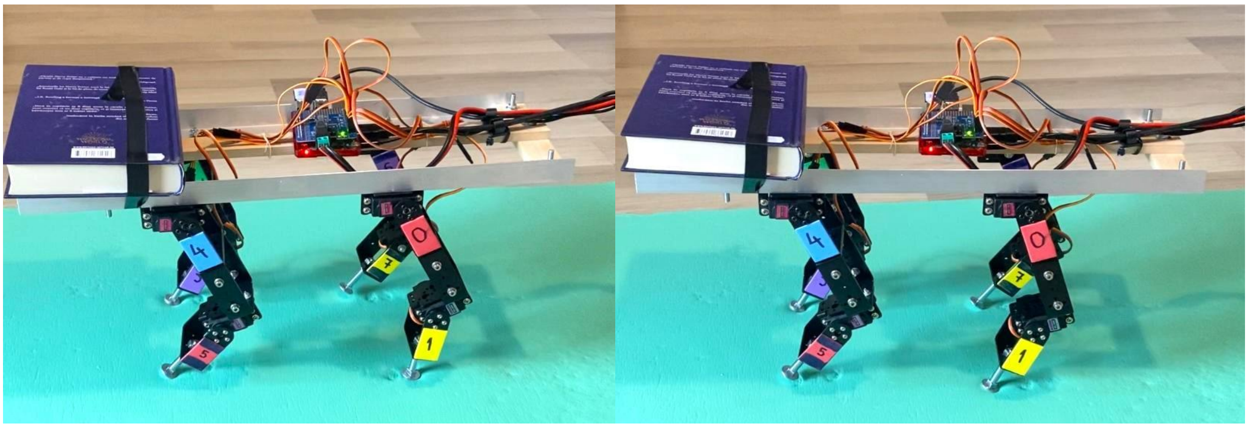

Fig. 14. “Happy”

4. Conclusions and future implementations

The research showed that the speed movement should be adjusted based on some input data. Servos move with their designed speed to the specified position, and it might be required for some complex commands to move much slower. To give it more autonomy and to make sure each command is carried properly, and for the robot stability a gyroscope must be used. This way commands will be sent to perform action and those actions will be stopped or adjusted in case they may cause an unbalance or even make the robot fall down. For the autonomy of the robot, the use of an external battery with high discharge amperage will also be considered, which would greatly help mobility and power.

5. Bibliography

[1] Kitano, S., Hirose, S., Horigome, A., & Endo, G. (2016). TITAN-XIII: sprawling-type quadruped robot with ability of fast and energy-efficient walking. Robomech Journal, 3:8. DOI: 10.1186/s40648-016-0047-1.

[2] Fan, Q., & Huang, Y. (2024). A Review of Quadruped Robots: Structure, Control, and Autonomous Motion. Advanced Intelligent Systems. DOI: 10.1002/aisy.202100200.

[3] Arikawa, K., Hirose, S. (1996). Development of quadruped walking robot TITAN-VIII. Intelligent Robots and Systems, IROS 96. Proceedings of the 1996 IEEE/RSJ International Conference, 1, 208–214. DOI: 10.1109/IROS.1996.570670.

[4] Zhang, D., & Zhang, H. (2016). On the improvement of walking performance in natural environments by a compliant adaptive gait. International Journal of Robotics Research, 22(6), 1240–1253. DOI: 10.1109/TRO.2006.884343.

[5] Semini, C., Tsagarakis, N. G., Guglielmino, E., Focchi, M., Cannella, F., & Caldwell, D. G. (2011). Design of HyQ, a hydraulically and electrically actuated quadruped robot. Proceedings of the Institution of Mechanical Engineers, Part I: Journal of Systems and Control Engineering, 225(6), 831–849. DOI: 10.1177/0959651811402275.

[6] Seok, S., Wang, A., Chuah, M. Y. M., Hyun, D. J., Lee, J., Otten, D. M., Lang, J. H., & Kim, S. (2015). Design principles for energy-efficient legged locomotion and implementation on the MIT Cheetah robot. Mechatronics, IEEE/ASME Transactions on, 20(3), 1117–1129. DOI: 10.1109/TMECH.2014.2339013.

[7] Hutter, M., Gehring, C., & Hopflinger, M. A. (2013). Walking and running with StarlETH. The 6th International Symposium on Adaptive Motion of Animals and Machines (AMAM), 5–9. URL: http://publications.asl.ethz.ch/files/hutter13dynamic.pdf.

[8] Poulakakis, I., Smith, J. A., & Buehler, M. (2005). Modeling and experiments of untethered quadrupedal running with a bounding gait: The Scout II robot. International Journal of Robotics Research, 24(4), 239–256. DOI: 10.1177/0278364904050917.

VIDEO IDENTIFICATION AND POSITIONING SYSTEM USING 2D/3D CAMERAS

MACOVEI Flavius Daniel, PARPALA Radu-Constantin

Facultatea de Inginerie Insutriala si Robotica, Specializarea MIIV, Anul de studii I, e-mail: flavius.daniel.macovei@gmail.com

ABSTRACT: This paper aims to develop a video identification and positioning system using 2D and 3D cameras. Video recognition technology has diverse applications, ranging from surveillance and security to industrial process automation. Implementing this system involves using image processing algorithms and machine learning to ensure accurate identification and precise positioning.

1. Introduction

In recent years, video-based identification and positioning technologies have advanced rapidly, finding applications in diverse fields such as security, surveillance, industrial automation, and autonomous navigation. These systems utilize 2D and 3D cameras to capture detailed images of the environment, enabling precise object identification and spatial positioning.

This paper aims to explore and develop an integrated identification and positioning system using 2D and 3D cameras. The primary objectives are to analyze existing technologies, develop an efficient image processing algorithm, and evaluate the system's performance in real-world scenarios.

2. Current Stage

For the project it was used OpenCV, or Open-Source Computer Vision Library, it is a library open software specialized source in processing and image analysis and videos real time. Here are some of the KEy functionalities of OpenCV:

Fig. 1. Utility of OpenCV

▪ Image processing:
OpenCV provides a wide range of functions and algorithms for image manipulation and transformation. These include filtering operations, geometric transformations, color conversions, edge detection, and more.
▪ Object detection:
The library includes algorithms for object detection and recognition in images and videos. This can be used for tasks like face detection, eye detection, vehicle detection.
▪ Video stabilization:
The library provides tools for stabilizing videos, reducing shaking and unwanted camera movements.

▪ Camera calibration:

OpenCV includes functionality for camera calibration, which is the process of adjusting camera parameters to obtain an accurate representation of the scene.

NumPy, is not specifically used for object detection itself, but is frequently used in conjunction with other libraries and frameworks to facilitate image and data processing during object detection, some reasons why NumPy is often used in this context:

Efficient data handling: NumPy provides efficient data structures such as arrays multidimensional arrays, which allow efficient storage and manipulation of image data. This is essential in image processing tasks where performance is crucial.

Fast numerical calculation: NumPy is optimized for fast numerical calculations, having a efficient implementation in the C language. This is useful in object detection tasks, which often involve computationally intensive operations such as mathematical operations on images.

Integration with other libraries: NumPy integrates well with other Python libraries used in object detection, such as OpenCV, which provides image processing functionality and detection algorithms. Using NumPy together with these libraries, developers can perform complex image processing and numerical calculations with ease.

Manipulation of image data: NumPy provides powerful functionality for manipulation image data, including cropping and resizing images, extracting regions of interest, applying filters, and more. These operations are essential in the object detection process.

Although NumPy is not directly used for object detection, it is an essential tool in the image and data processing that underlies this task.[1]

CODE ANALYSIS:

This code is an example of using OpenCV and NumPy to create a simple application to detect geometric shapes based on color in a video stream from a camera.

Test > Shape&Color > Cerc Stiintific > ...

```
import cv2
import numpy as np

def empty(img):
    pass

video=cv2.VideoCapture(0)
cv2.namedWindow("TrackBar")
cv2.resizeWindow ("TrackBar",600, 300)
cv2.createTrackbar("hue_min", "TrackBar",0,179, empty)
cv2.createTrackbar("hue_max", "TrackBar",179,179, empty)
cv2.createTrackbar("sat_min", "TrackBar",0,255, empty)
cv2.createTrackbar("sat_max", "TrackBar",255,255, empty)
cv2.createTrackbar("val_min", "TrackBar",0,255, empty)
cv2.createTrackbar("val_max", "TrackBar",255,255, empty)

while True:
    ret,img=video.read()
    hsv=cv2.cvtColor(img, cv2.COLOR_BGR2HSV)
    hue_min=cv2.getTrackbarPos("hue_min","TrackBar")
    hue_max=cv2.getTrackbarPos("hue_max","TrackBar")
    sat_min=cv2.getTrackbarPos("sat_min","TrackBar")
    sat_max=cv2.getTrackbarPos("sat_max","TrackBar")
    val_min=cv2.getTrackbarPos("val_min","TrackBar")
    val_max=cv2.getTrackbarPos("val_max","TrackBar")

    lower=np.array([hue_min, sat_min, val_min])
    upper=np.array([hue_max, sat_max, val_max])
    mask=cv2.inRange(hsv, lower, upper)
    cnts,hei=cv2.findContours(mask, cv2.RETR_EXTERNAL, cv2.CHAIN_APPROX_NONE)
    for c in cnts:
        area=cv2.contourArea(c)
        if area>300:
            peri=cv2.arcLength(c, True)
```

Fig. 2. Code Example

```
            peri=cv2.arcLength(c, True)
            approx=cv2.approxPolyDP(c, 0.02*peri, True)
            x,y,w,h=cv2.boundingRect(c)
            cv2.rectangle(img, (x,y), (x+w, y+h), (0,255,0), 2)
            cv2.putText(img, "Points:"+str(len(approx)), (x+w+20, y+h+20), cv2.FONT_HERSHEY_COMPLEX, 0.7, (0,255,0), 2)
        if len(approx)==4:
            cv2.putText(img,"Rectangle" , (x+w+20, y+h+45), cv2.FONT_HERSHEY_COMPLEX, 0.7, (0,255,255), 2)
        elif len(approx)==3:
            cv2.putText(img, "Traiangle", (x+w+20, y+h+45), cv2.FONT_HERSHEY_COMPLEX, 0.7, (255,255,0), 2)
        else:
            cv2.putText(img, "Circle", (x+w+20, y+h+45), cv2.FONT_HERSHEY_COMPLEX, 0.7, (255,255,255), 2)
    cv2.imshow("Frame",img)
    cv2.imshow("hsv",hsv)
    cv2.imshow("Mask",mask)
    k=cv2.waitKey(1)
    if k==ord('q'):
        break
video.release()
cv2.destroyAllWindows()
```

Fig. 3. Code Example

Code explanations:

- Imports the necessary libraries, cv2 (OpenCV) and NumPy (NumPy).
- An empty function is defined, which is used as a callback function for trackbars created later.
- The video capture from the camera (potentially the first available camera) opens.
- A window and trackbars are created for setting the HSV color range we want to detect. HSV is a color model used in digital imaging that represents colors according to three main components: Hue, Saturation, and Value.
- During the while loop, the video frames are read.
- Converts each frame to the HSV color space to facilitate color detection.
- Gets the trackbar values for setting the HSV color range.
- A mask is applied to the HSV image to extract only areas with colors in the specified range.
- Find the contours of the objects in the mask using cv2.findContours().
- For each contour, the geometric shape is determined, and a rectangle is drawn around it. The number of points for each contour is also added.
- The original image, HSV image and mask, as well as the detected geometric shapes are displayed.
- The program runs until the user presses the 'q' key to end the application.[2]

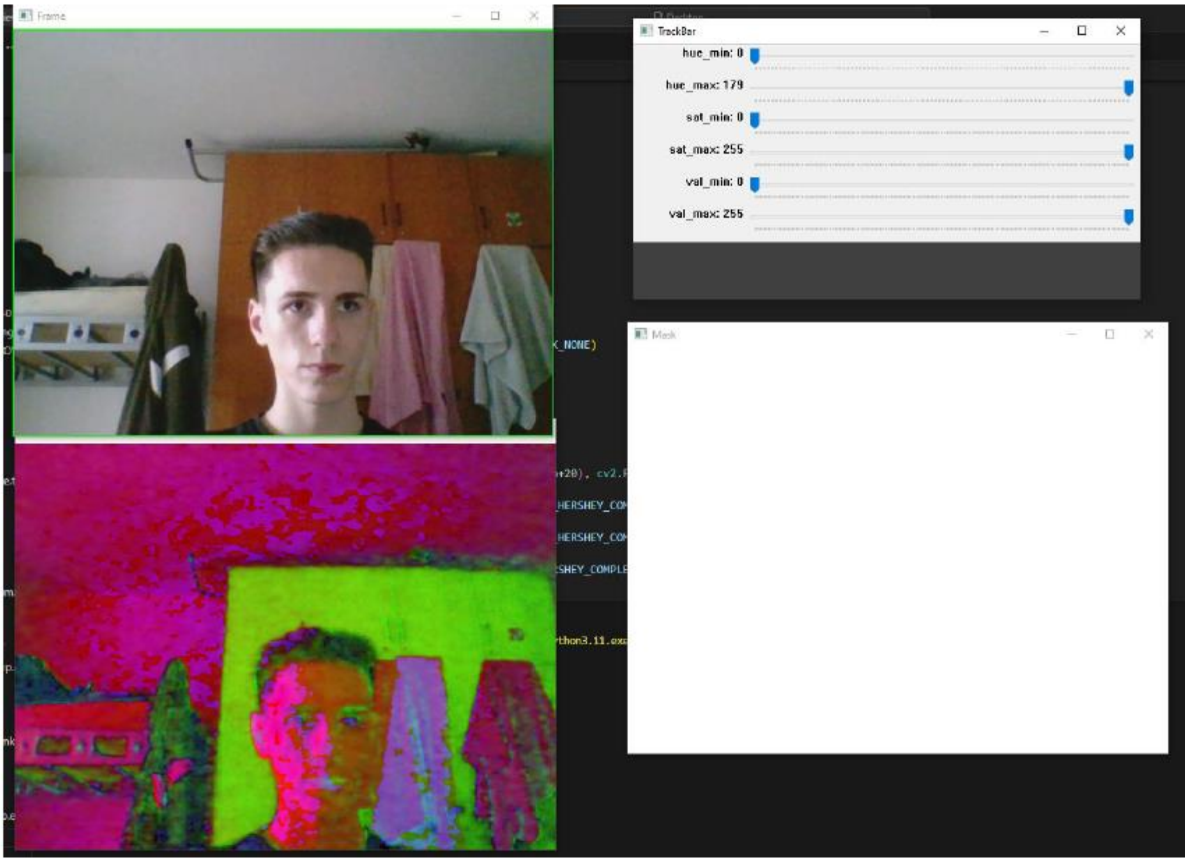

Fig. 4. Trackbars

These are the trackbars created to be able to detect objects and their color. Trackbars are graphical interface elements used in the OpenCV library to allow users to adjust parameters for object detection, such as color. These interactive controls are useful in the development process of object recognition algorithms, enabling real-time adjustments of settings to achieve optimal results in object detection and tracking in an image or video stream. Through trackbars, users can experiment with different values and configurations to optimize the performance of the recognition algorithm.

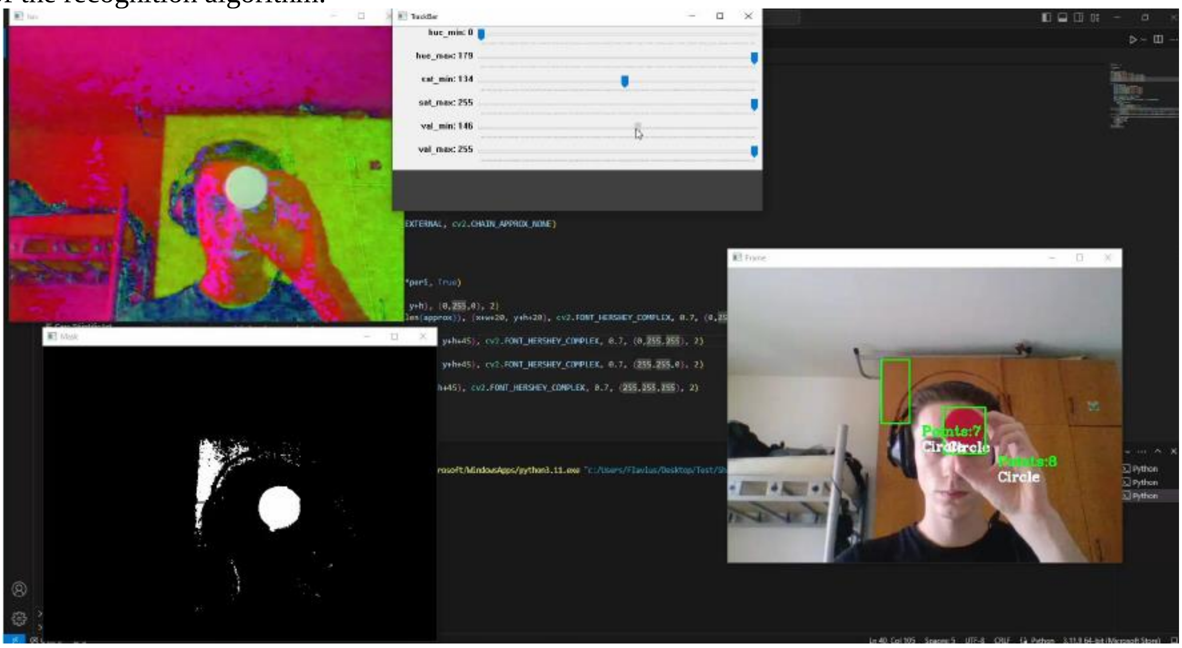

Fig. 5. Presentation of results for a circle

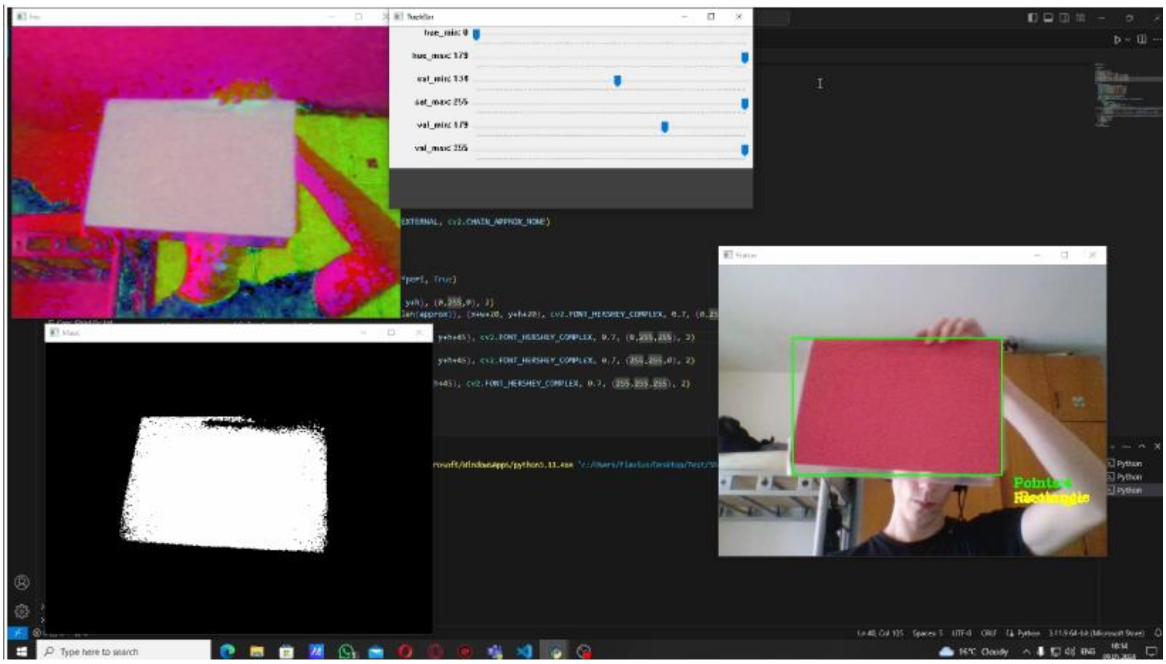

Fig. 6. Presentation of results for a rectangle

3. Conclusions

It shows how OpenCV and NumPy are used for image manipulation and for efficient numerical operations.
Presentation of the process of detecting geometric shapes by displaying the original image, the HSV and the mask, together with the detected geometric shapes.
We can emphasize the usefulness and versatility of OpenCV and NumPy in the field of image processing and highlight the way in which they can be used to implement applications for detecting objects and analyzing images in real time.

Bibliography

[1]. Bradski, G (2000), "The OpenCV Library", Dr. Dobb's Journal of Software Tools.
[2]. Rosebrock, A (2017), "Deep Learning for Computer Vision with Python", PyImgeSearch

DESIGN AND CREATION OF A CUSTOM PROSTHETIC DEVICE WITH 3D PRINTING AND 3D SCANNING

PESCARU Radu-Vlad, POPESCU Diana

Facultatea: FIIR, Specializarea: Managementul Întreprinderilor Industriale Virtuale, Anul de studii: 2, e-mail: radu_vlad.pescaru@stud.fiir.upb.ro

ABSTRACT: The primary focus of this research was the development and manufacturing, using 3D printing, of a prosthetic device for individuals who have lost one or more fingers. Designing such a device is a complex task due to the inherent diversity in hand anatomies and pathologies among patients. Consequently, creating a universally fitting prosthetic is challenging. However, the use of additive manufacturing, a technology known for its suitability for prototyping and customization, represents a feasible solution as it facilitates the production of tailored objects while enabling iterative refinements. The upper limb prosthesis includes a mechanical solution for the movement of each segment, which represents the main benefit of the proposed design, as users can easily 3D print and assemble the device at home.

KEYWORDS: 3D printing; reverse engineering; assistive device; medical engineering; design

1. Introduction

The integration of advanced engineering technologies in the design and manufacturing of prosthetic devices has revolutionized the field of medical engineering. The increasing availability and feedstock diversity for 3D printing (3DP) processes determined a significant shift towards creating customized, patient-specific assistive devices [1]. The additive manufacturing technology (AM), the standardized name for 3DP, not only enhances functionality and comfort of the prostheses by customization, but also reduces production costs and time [2], making the prosthetics more accessible to a wider range of users.

3DP allows for the fabrication of complex geometries, difficult to obtain otherwise, and this aspect is particularly advantageous in the medical field where personalized solutions are often required to meet the unique anatomical and functional needs of each patient [2]. According to Thorsen et al. [3], the digital fabrication techniques, such as 3DP, enable the involvement of patients in the co-design and creation of personalized assistive devices, thus empowering them and improving the overall user experience. The customization capabilities of 3DP have been demonstrated in various medical applications, including the creation of prosthetic limbs and orthotic devices [4]. A cost-effective analysis by Hunzeker et al. [54] highlighted the benefits of 3DP in occupational therapy, emphasizing its ability to produce low-cost, customizable, and replicable items. These advantages are particularly important in the context of assistive devices, where individualized adjustments are often necessary to ensure optimal fit and function. 3DP has also been shown to significantly improve the quality and performance of medical devices. For instance, studies have demonstrated that 3D-printed prosthetics can be tailored to better match the user's anatomy, leading to improved comfort and functionality [6]. This is a relevant aspect for applications requiring accuracy and personalization, such as craniofacial reconstruction and orthopedic implants [7].

Moreover, the use of advanced materials like PLA+ (Polylactic Acid Plus) enhances the durability and flexibility of the prosthetics, essential characteristics for medical applications [8-9].

Materials and method

Generating the 3D CAD model of the prosthesis

The design process of the prosthesis began with creating a CAD model using NX software. The primary focus was on developing a closed quadrilateral guiding mechanism to ensure the functionality and stability of the prosthesis. This mechanism was aimed to control the movement of the prosthesis, closely replicating the natural movements of fingers (fig.1). The design had involved multiple iterations to optimize the dimensions and shape of the components, making them compatible with the specific anatomy of the patient’s hand.

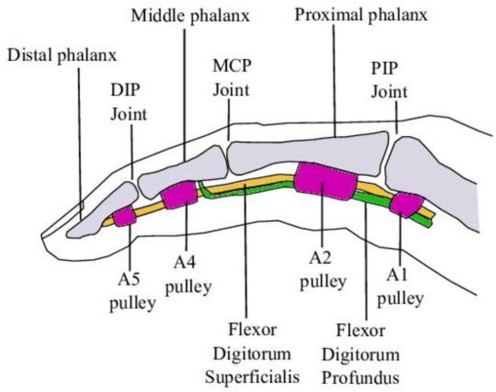

Fig. 1 Anatomy of a human finger [10]

Another critical aspect of the prosthesis design was creating a support that could be securely and comfortably mounted on the patient’s hand (fig.2). Initially, the support was designed as a sleeve made from TPU (Thermoplastic Polyurethane), known for its flexibility and shock absorption capabilities. However, this solution proved ineffective as the holes in the support failed during use/testing, compromising the rigidity of the assembly. Then, PLA + filament was selected as build material, more details being presented in the next sub-section.


Fig. 2. First prototype of a support to be placed on hand

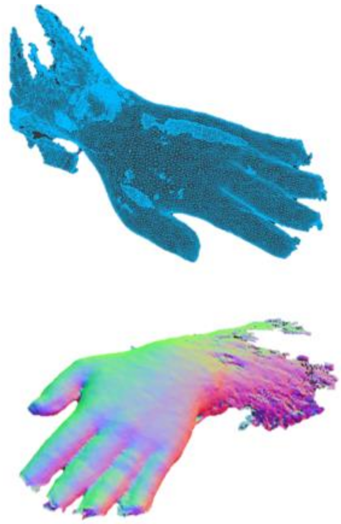
Fig. 3 Patient hand data generated by the 3D scanner app

The generation of the customized support involved 3D scanning the patient’s hand with 3D Scanner App, which utilizes the infrared sensor of a smartphone camera to create a point cloud of the hand’s surface (fig.3). This point cloud was imported into Ansys SpaceClaim for further cleaning and processing. The cleaning process involved removing noise and other imperfections, ensuring that the digital model was as accurate as possible. After cleaning the point cloud, the geometry of the support was generated by printing the nodes of the discretization network on two parallel planes corresponding to the joint and the beginning of the finger phalanges.

The connection between the prosthesis and the support was achieved through a quick-release coupling inspired by the mechanism used in paint guns. The fit between the boss pins and the smaller diameter step was 0.03 mm, ensuring a firm and stable connection. This design allows easy assembly and disassembly of the prosthesis while providing a secure attachment. The quick coupling functions by deforming the boss to pass through the bore and lock into the larger diameter step (Fig. 4).

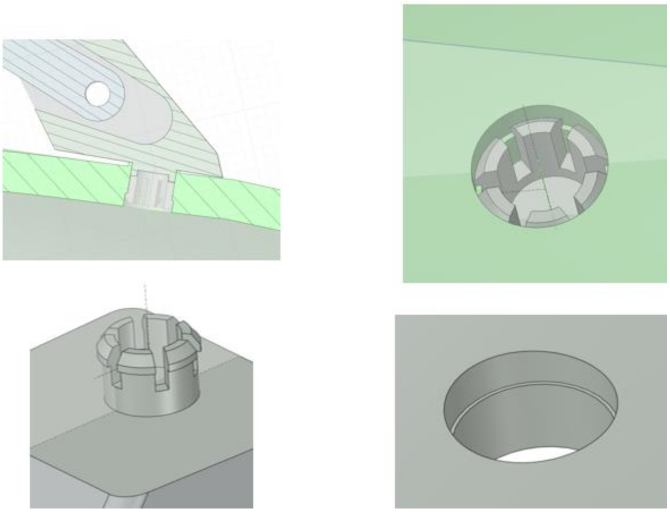

Fig. 4 The assembly solution used for the prosthetic

During the conception of the prosthesis, several design approaches were considered (fig.5). Initially, the focus was on generating an anthropomorphic model similar to a glove covering the finger and including a grip part for the palmar area. Later, due to the complexity of the geometry, a simpler model focused on functionality was chosen.

Fig. 5 The anatomical variant of the product (left) and the functional design (right)

After generating a complete CAD model containing both the active part and the support, the prosthesis was printed and tested. It was concluded that the index finger no longer touched the thumb of the patient's hand. This required redesigning the last segment and the connection areas. To correctly generate the movement, the intermediate segments were resized as well (fig.6).

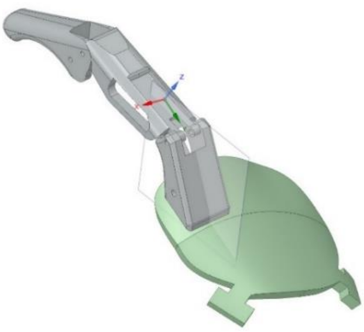

Fig. 6 Preliminary design solution

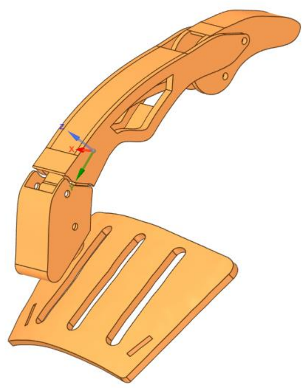

Fig. 7 The final solution

The support was also refined while retaining the assembly variant. The modifications included creating splits to allow cooling of the area where the prosthesis is mounted, and designing grip zones where elastics will be mounted.

Fig. 8 The 3D printed object

3D Printing the prosthetic

The design and 3D printing process of the prosthesis involves a series of well-defined steps and the use of essential technical specifications and parameters to ensure the quality and functionality of the final product. This section details each step of the process, from the initial model conception to the actual printing, and discusses the technical specifications and 3D printing parameters used.

The design process began with the creation of a CAD model using NX software. The CAD model was based on the anatomical shape of the patient's hand and fingers, which were previously 3D scanned. The CAD model was developed iteratively using the Realize Shape module in NX for organic modeling. The modeling started with a primitive shape, usually a sphere, which was then elongated and flattened until the desired shape was achieved. This modeling method allows fine and precise adjustments, ensuring that the prosthesis fits perfectly to the contour of the patient's hand.

Integrating the actuation mechanism represented a crucial step in the design. To ensure optimal functionality, a closed quadrilateral mechanism was chosen, which allows controlled movement of the prosthesis, replicating the natural movements of the fingers. This choice was based on kinematic studies and simulations conducted in the Rigid Body Dynamics workshop in the Ansys suite. After finalizing the CAD model, the prototype was fabricated using a Creality Ender 3 V2 3D printer. The material chosen for printing was TPU (Thermoplastic Polyurethane) due to its flexibility and mechanical strength. TPU is ideal for applications requiring a high degree of flexibility and durability, being preferred over PLA or ABS in this context.

The 3DP of the prototype required setting specific parameters to ensure the quality and precision: Layer height: 0.1 mm; Print speed: 30 mm/s; Nozzle temperature: 235°C; Bed temperature: 60°C; Infill density: 20%; Infill pattern: Gyroid; Wall thickness: 0.8 mm.

These parameters were chosen to optimize layer adhesion and prevent delamination during the use of the prosthesis. Additionally, glue stick was used on the print bed to improve the adhesion of the pieces during fabrication.

The prototype was subjected to a series of tests to evaluate functionality and durability. These tests included gripping and manipulating objects of various sizes and weights, simulating real-life usage scenarios. After these tests, PLA+ was chosen as build material and printing with: ayer height: 0.1 mm; Print speed: 70 mm/s; Nozzle temperature: 210°C; bed temperature: 65°C; Infill density: 20%; Infill pattern: Gyroid; Wall thickness: 0.8 mm.

PLA+ (Polylactic Acid Plus) is an improved version of the PLA (Polylactic Acid) material frequently used in 3D printing. This material was selected for the prosthesis prototype due to its availability, low cost and printability. Additionally, PLA+ has higher mechanical strength than PLA, making it more durable and resistant to mechanical stress [11], which makes it more suitable for certain uses, including customized prosthetics. PLA+ offers a better balance between flexibility and hardness, reducing the risk of cracking or breaking during use [12], making it more suitable for objects that may be subjected to shocks or accidental drops. One important advantage of PLA+ is its better layer adhesion, thus reducing the risk of delamination or layers detachment from the printing bed. Moreover, PLA+ provides a better surface finish, with a finer texture and fewer imperfections. This aspect is important not only for the aesthetic appearance of the prosthesis but also for user comfort, as a smooth surface reduces the risk of skin irritation.

3. Results

Testing the functionality of the customized prosthesis was essential to ensure its performance and safety for end users. The process began with an initial assessment of the comfort and fit of the prosthesis on a healthy user's hand. This involved placing the prosthesis on the hand and observing its use, focusing on its adaptation to the hand's contour, the pressure exerted on the skin, and the ease of mounting and dismounting. Feedback was crucial for identifying potential issues and making adjustments to improve comfort. After initial adjustments, the prosthesis underwent a set of functional tests to evaluate its ability to perform daily activities. These tests included gripping and manipulating objects of various sizes and weights, simulating real-life usage scenarios. The prosthesis was tested with items such as cutlery, toothbrushes, pens, and other daily-use instruments, documenting the stability of the grip, the force required for manipulation, and user feedback. Durability testing involved subjecting the prosthesis to repeated cycles of use for simulating the long-term wear. It was used intensively in a controlled environment to observe any defects over time. The materials and design were tested for resistance to mechanical stress and impact.

Furthermore, the tests (Fig. 9) included evaluating the quick coupling mechanism. The prosthesis underwent repeated mounting and dismounting tests to ensure the quick coupling functioned efficiently. These tests demonstrated that the quick coupling mechanism is robust and easy to use, providing a secure and stable attachment.

Fig. 9 Testing the functionality of the prosthetic

4. Conclusions and discussions

The design and manufacturing process of the prosthesis highlighted the complexity and importance of integrating advanced technologies. 3D scanning enabled the creation of a precise digital model of the patient's hand, which was essential for customizing the prosthesis. Iterative CAD modeling ensured a perfect fit and optimal functionality. The PLA+ material used for the prosthesis offered durability and flexibility, essential characteristics for medical applications. Rigorous durability and functionality tests confirmed that the prosthesis can withstand intense daily use and various environmental conditions. User feedback was crucial for final design adjustments, ensuring that the prosthesis not only meets technical requirements but also provides a high level of comfort and reliability.

The projects for creating the customized handle and prosthesis demonstrated the vast potential of additive manufacturing in medical engineering. 3D scanning and printing technologies allow the creation of medical devices perfectly tailored to the specific needs of each patient, offering a high level of personalization and comfort. The use of advanced materials, such as PLA+, ensures the durability and strength required for medical applications. Additive manufacturing reduces costs and production time, allowing rapid prototyping and continuous iteration, which facilitates innovation and adaptation to individual patient needs. These technologies not only improve the quality of life for patients by creating customized prosthetics and other assistive devices but also open new perspectives for the development and application of innovative solutions in modern medicine.

5. References

[1] J. Ten Kate, F. S. Smit, and S. A. Breedveld (2017), "3D-printed upper limb prostheses: a review," Disability and Rehabilitation: Assistive Technology, vol. 12, no. 3, pp. 300-314.

[2] R. Thorsen, F. Bortot, and A. Caracciolo (2019), "From Patient to Maker - A Case Study of Co-Designing an Assistive Device Using 3D Printing," Assistive Technology, vol. 31, no. 3, pp. 142-150.

[3] M. Hunzeker and R. Ozelie (2021), "A Cost-Effective Analysis of 3D Printing Applications in Occupational Therapy Practice," The Open Journal of Occupational Therapy, vol. 9, no. 1, pp. 1-12.

[4] Y. Bozkurt and E. Karayel (2021), "3D printing technology; methods, biomedical applications, future opportunities and trends," Journal of Materials Research and Technology, vol. 14, pp. 1430-1450.

[5] J. G. Lee, M. Y. Huh, H. R. Kim, J. J. Shin, and W. Y. Han (2018), "Development of 3D printed assistive device for hand functions of patients with hemiparesis," Geriatrics, vol. 3, no. 4, pp. 89-99.

[6] M. Hunzeker and R. Ozelie (2021), "A Cost-Effective Analysis of 3D Printing Applications in Occupational Therapy Practice," The Open Journal of Occupational Therapy, vol. 9, no. 1, pp. 1-12.

[7] J. B. Matthews-Brownell and M. A. Hall (2019), "Replicability of 3D printed orthoses: a study of veterans with hand conditions," Assistive Technology, vol. 31, no. 3, pp. 187-194.

[8] D. Schwartz, C. Firmat, and A. D. Beltran (2018), "Standardizing 3D printing interventions in occupational therapy: a research methodology," Journal of Occupational Therapy Research, vol. 4, no. 1, pp. 45-60.

[9] D. A. Grames (2020), "The feasibility of using 3D printing in occupational therapy for adaptive equipment," Occupational Therapy International, vol. 27, no. 1, pp. 66-74.

[10] A. Bajaj, V. Jain, P. Kumar, A. Unal, and A. Saxena (2021), "Soft Hand Exoskeleton for Adaptive Grasping Using a Compact Differential Mechanism," in Mechanism and Machine Science. Lecture Notes in Mechanical Engineering, D. Sen, S. Mohan, and G. Ananthasuresh, Eds. Springer, Singapore.

[11] https://www.xometry.com/resources/pla-vs-pla-plus/ (accessed June 11th 2024)

[12] https://all3dp.com/2/pla-vs-pla-3d-printer-filament-compared/ (accessed June 09th 2024)

DESIGN AND ADDITIVE MANUFACTURING OF FLEXIBLE FINGER GRIPPERS

ROTARU Dragoș, POPESCU Diana
Facultatea: IIR, Specializarea: MIIV, Anul de studii: I, e-mail: dragosrotaru89@gmail.com

ABSTRACT - Fin ray soft grippers are a type of soft robotics end-effector that emulate the flexible fins of fish. Compared to traditional rigid grippers, these grippers offer several advantages, including enhanced flexibility and adaptability to objects of various shapes and sizes. Fin ray soft grippers excel in dynamically changing or unstructured environments, particularly when handling soft and delicate objects. The selected design parameters for optimization include rib structure, rib thickness, and rib orientation. By adjusting these parameters, two different fingers were designed, analyzed and optimized. Fingertip deformation and deformation were tested under real conditions. The results demonstrated that the grips are effective in both wrap and pinch grips.

KEYWORDS: Fin ray grippers, End-Effector, Tip deflection, 3D printing

1. Introduction

Robotic end-effectors are devices attached at the end of a robot's arm, designed as the interface between the robot and the workpiece. These can be classified based on several criteria: type of actuation (pneumatic, electrical), functionality (mechanical grippers, welding torches, magnetic grippers, vacuum grippers, paint guns, drills, etc.), and adaptability (standard end-effectors, adaptive end-effectors), etc . [1]. Advances in engineering continuously enhance their functionality, improving aspects such as precision, wear resistance, versatility and modularity [2], as proved by different reviews in this field [3].

The design of an end-effector is customized based on its role in the automation process and the geometry of the workpiece, particularly if a gripping function is targeted. In this context, the adaptation of the gripper to the workpiece is a critical design criterion. Therefore, soft grippers, which conform to the objects' shapes, have recently been developed using 3D printing technology [4]. The soft grippers are made from flexible materials which allow adaptation to the objects they are gripping, which make them useful for tasks that suppose manipulating fragile or irregularly shaped items. From this category of grippers, one can distinguish fingers grippers [5], Fin-ray grippers [6], tendon-driven grippers [7], octopus-like grippers [8], jamming grippers [9], etc. Fin-ray grippers of interest in this paper mimic the shape and physiology of fish fins (two bones arranged in a V shape with connective tissue between them [10]). Their design includes connected beams that form a triangular compliant mechanism, which buckles and deforms, thus conforming around the objects [11]. A force applied on the surface determine the sides of the structure to bend (Fig.1), resulting in the base and tip deforming toward the applied load.

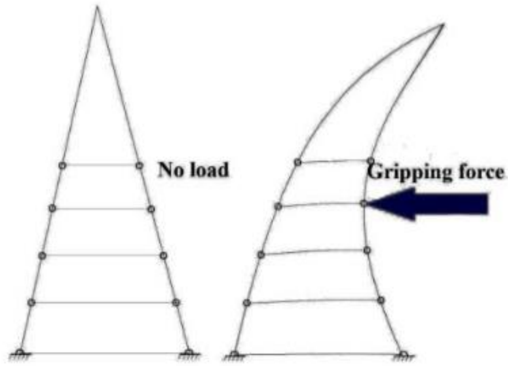

Fig. 1 Fin-ray effect working principle [12]

This paper addresses a specific type of soft gripper with three fingers, aiming to comparatively analyze three materials suitable for 3D printing such devices. The materials considered are ABS and PLA, commonly used as feedstock filaments for the Material Extrusion (MEX) process. In this process, thermoplastic material is extruded through a nozzle and selectively deposited in layers, as determined by the settings in slicing software. This comparison focuses on the printability of each material, particularly considering the requirements of the fin-ray structure which is designed for direct assembly (clearance values, printing parameters, etc.). The suitability of each material is evaluated through gripping tests using a benchmark object. The gripper's three fin-ray fingers are attached to a device equipped with gears and electrical actuation for repeatedly opening and closing of the fingers. This part of the device is also made by MEX, from ABS due to its superior mechanical properties in comparison with PLA considering the durability of the gears condition. Therefore, the evaluation of the optimal material for the fingers also considers the combination with the actuation device.

2. Material and Method

2.1. Design of the fin-ray and the gripper

The construction of the fingers based on the fins of the fish makes it more stable and more adaptable in the handling of objects of a greater variety. For our application, the gripper will be mounted on a robotic arm that will take the bulbs on a conveyor, test their functionality, and then place them in a box for storage and delivery. The gripper will be electrically actuated with the help of an electric motor supplied with a voltage of 5 volts DC, equipped with a reducer with a transmission ratio of 127:1, the actuation of the bins, which are arranged at an angle of 120 degrees, will be done by a pinion worm gear mechanism. All the parts are 3D printed, and the housing and the worm wheel are printed simultaneously, the assembly being removable. The three pins that secure the gears have an octagonal profile to facilitate sliding and reduce friction. Fin Ray fins are secured by a dovetail guide.

Further improvement in force response can be achieved by tilting the ribs from their default orientation. If the ribs are thinner and more flexible, this will increase the distribution of the contact force along the entire length of the finger, being effective for handling delicate objects. If the ribs are thinner and more flexible, they will improve the distribution of contact force along the length of the finger, making it more effective for handling delicate objects. As the flexible ribs deform, they jam together, increasing the finger's overall stiffness due to friction between the layers. This results in a higher rate of force generation in fingers with tilted ribs. This behavior is responsible for the enhanced rate of force generation observed in these fingers. The gripper can be operated in either jammed or relaxed mode, depending on the finger's placement relative to the target. The flexible ribs lock as they deform, increasing the overall stiffness of the finger due to friction between the layers. This leads to a higher rate of force generation in fingers with inclined ribs. This behavior is what causes inclined ribbed fingers to have an increased rate of force generation. The gripper can be operated in locked or relaxed mode, depending on the positioning of the finger in relation to the target. The flexible ribs lock as they deform, increasing the overall stiffness of the finger due to friction between the layers. This leads to a higher rate of force generation in fingers with inclined ribs. This behavior is what causes inclined ribbed fingers to have an increased rate of force generation. The gripper can be operated in locked or relaxed mode, depending on the positioning of the finger in relation to the target. A finger with thin and flexible ribs possesses remarkable softness, allowing for the even distribution of forces and easy deformation upon contact. This type of finger can gently adapt to the shape of the target object. However, reducing the thickness of both the ribs and the outer shell is expected to decrease the force generation capacity. While this is advantageous for handling delicate objects, it limits the maximum weight the fingers can support and restricts their use in tasks that require exerting force against rigid targets.

It is important to note that as the rib thickness decreases, the flexibility of the fastener increases, but its load capacity decreases. This creates a trade-off between flexibility and load capacity. Of the three geometric parameters considered in finger design, the number of ribs significantly influences finger displacement. Increasing the number of ribs results in greater tension on the object and a reduction in fingertip travel. Rib distribution is crucial to determining gripper performance, as ribs are key components influencing finger stiffness. Therefore, the arrangement and number of ribs must be carefully considered to optimize the performance of the gripper. In addition, the slope of the outer wall has a significant impact on the stress, while the wall thickness plays a major role in the deformation of the fixture

.

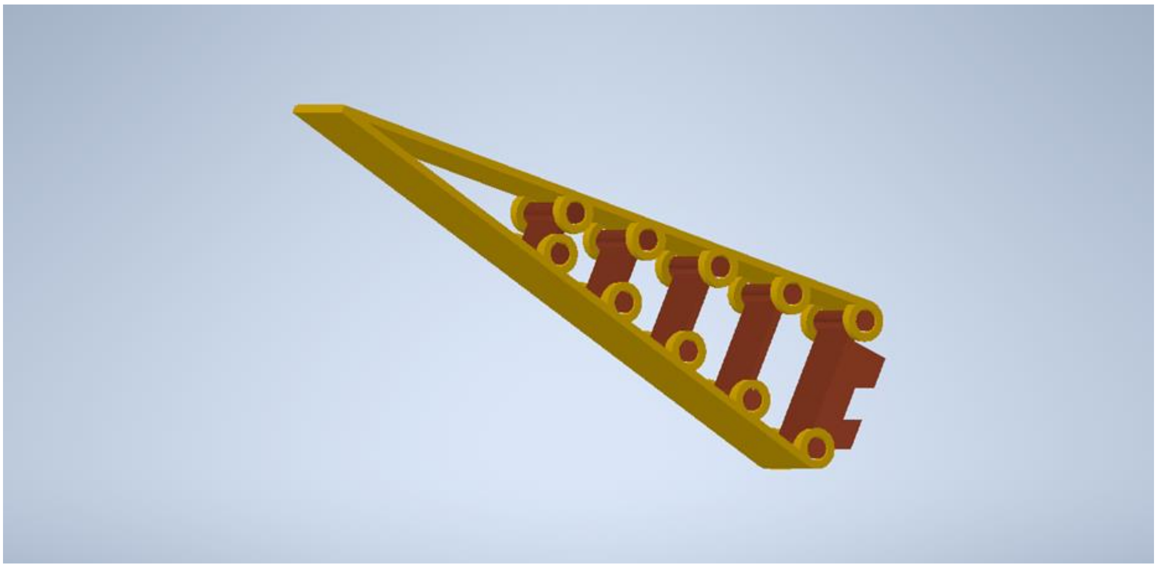

Fig. 2. Design made

2.2. 3D printing fin-ray fingers from ABS

ABS (Acrylonitrile Butadiene Styrene) filament is one of the most used materials in 3D printing. It is a thermoplastic polymer composed of three monomers: acrylonitrile, butadiene and styrene. This material was first patented in the 1940s and quickly gained popularity. ABS is used in many industries today because of its flexibility, malleability and strength. You can find it in a variety of products, from Lego toys to household appliances to pipe systems. Compared to most cheap polymers, ABS is quite flexible, withstands high temperatures and can be easily processed. In the field of 3D printing, it is valued for being quick to print and more durable than many other options. ABS solidifies uniformly and hardens without post-processing. Users tend to choose it for its relative high temperature resistance and flexibility. However, it should be noted that printing with ABS filament may require a heated print bed and good ventilation, as the gas emitted during melting can be harmful.

Tab.1. Recommended printing conditions

RECOMMENDED PRINTING CONDITIONS

Parameter	
Nozzle temperature	245 – 265 (°C)
Build surface material	BuildTak®
Build surface treatment	Glue, Magigoo
Build plate temperature	90 - 100 (˚C)
Cooling fan	OFF
Printing speed	30-50 (mm/s)
Raft separation distance	0.2 (mm)
Retraction distance	1 (mm)
Retraction speed	20 (mm/s)
Environmental temperature	Room temperature - 90 (˚C)
Threshold overhang angle	50 (˚)
Recommended support material	PolyDissolve™ S2

Gripper soft Fin Ray is manufactured by 3D printing (FDM) due to its complex design, non-removable and from several components printed at the same time. The Ultimaker S5 is the printer I used to print both the fingers and the body of the gripper using ABS.

The fingers of the Gripper are printed from ABS, which offers an efficient manufacturing method due to advantageous properties such as flexibility and adaptability that allows adaptation to the shape of the object it grips, this being possible due to the unique geometries of the fingers that curve and mold on object offering a secure and delicate grip.

Another property is that of absorbing shocks, which is essential for the handling of fragile objects, and it can withstand high temperatures of up to 105 degrees C.

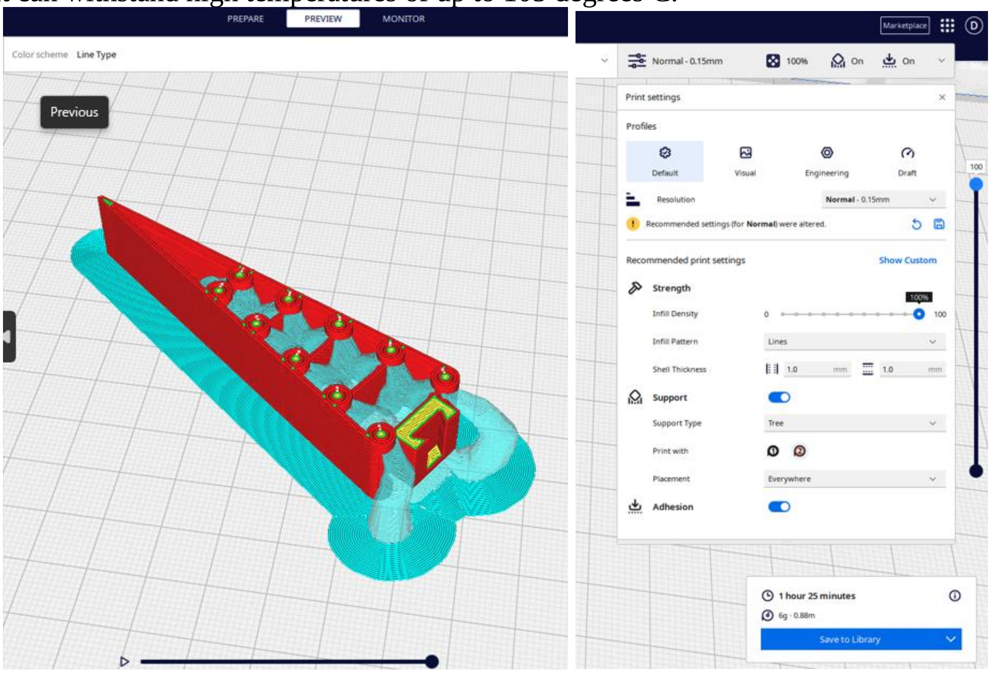

Fig. 3. ABS printing parameters

2.3. 3D printing fin-ray fingers from TPU

Gripper soft Fin Ray is manufactured by 3D printing (FDM) due to its complex design, non-removable and from several components printed at the same time. The Ultimaker S5 is the printer I used to print both the fingers and the body of the gripper using TPU and respectively ABS for the body of the gripper.

Gripper's fingers are printed from TPU 95 A. It is a thermoplastic elastomer designed from the combination of rubber and plastic. The TPU material is hard enough, flexible, durable, resistant to abrasion and oily substances.

The unique mixture of rubber and plastic makes it ideal for our application of handling spherical objects and more specifically LED bulbs and those with filament and glass globe which are quite fragile and slippery.

TPU offers some extraordinary benefits due to its thermoplastic nature such as high load capacity, high tear and tensile strength.

Tab. 2. Properties of TPU

Properties	Typical Value
Shore Hardness	95
Density	1230 kg/m3
Ultimate Tensile Strength	45 MPa
Elongation at Break	450 %

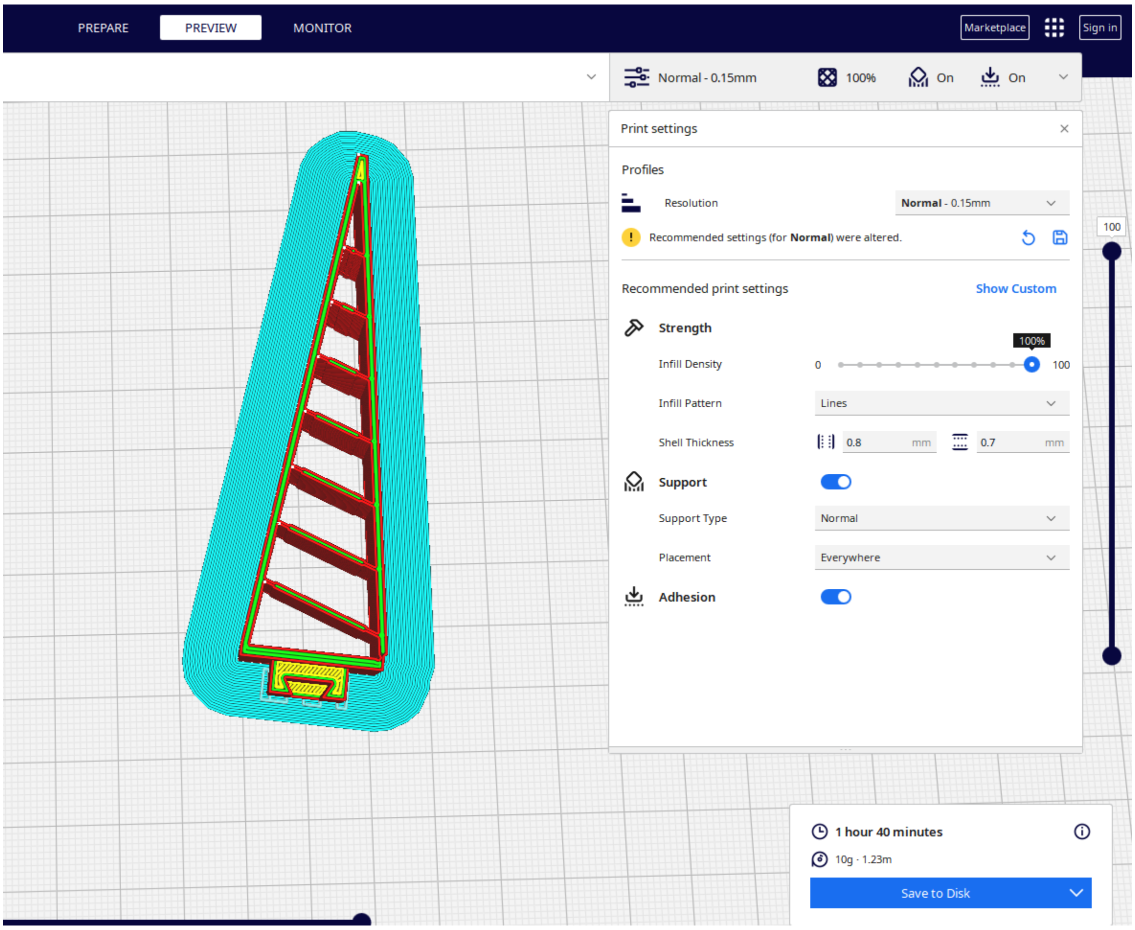

Fig. 3. TPU printing parameters

3. The final design

Fig. 3. The final design

It is a clamping device with 3 jaws arranged circularly at 120 degrees with electric drive, the rotational movement of the motor is transmitted further through a worm gear transmission system. All the parts are 3D printed and the casing and the worm wheel are printed at the same time, the assembly being removable. The three pins that secure the gears have an octagonal profile to facilitate sliding and reduce friction. The barges are attached to the 3 wheels by a dovetail guide.

4. Conclusions

- In this research, the potential of a new approach based on simulation and the design of soft grippers was demonstrated.
- Thanks to the simulation, the gripper can be adapted in advance to the handled product and its variations by scaling or optimization. The design approach allows new grip variations to be validated very easily and cost-effectively adapted as needed.
- Also, the production cycle is now much shorter than before, as parts can be printed directly from the CAD model
- A 3D printer is mobile and can be placed anywhere, but it does not only have its positive sides.
- It should also be considered that mass production is not yet possible with 3D printing.
- Another problem now is the tolerance of the printers which are not yet suitable for some industries
- All things considered, it's safe to say that 3D printing will shape the future of many industries when it comes to the manufacturing process. The flexibility of this technique has already influenced technology in the fields of the medical sector for example. Many prostheses are now produced by 3D printers to precisely fit the needs of customers.

- With all these advantages of this technology, it is only a matter of time before 3D printing will be found in many other areas of business.

8. Bibliografie

[1]. Monkman, G. J., Hesse, S., Steinmann, R., Schunk, H.- Robot Grippers. WILEY-VCH Verlag GmbH & Co. KGaA, Weinheim, 2007

[2]. Stano, G., Ovy, S.M.A.I., Edwards, J.R. et al. One-shot additive manufacturing of robotic finger with embedded sensing and actuation. Int J Adv Manuf Technol 124, 467–485 (2023). https://doi.org/10.1007/s00170-022-10556-x Tawk, C., Mutlu, R., & Alici, G. (2020). A3D Printed Modular Soft Gripper for Conformal Grasping. 2020 IEEE/ASME International Conference on Advanced Intelligent Mechatronics (AIM), 583-588.

[3]. F. Oliveira, V. Tinoco, S. Magalhães, F. N. Santos and M. F. Silva, "End-Effectors for Harvesting Manipulators - State Of The Art Review," 2022 IEEE International Conference on Autonomous Robot Systems and Competitions (ICARSC), Santa Maria da Feira, Portugal, 2022, pp. 98-103, doi: 10.1109/ICARSC55462.2022.9784809.

Dai, Y.; Xiang, C.; Qu, W.; Zhang, Q. A Review of End-Effector Research Based on Compliance Control. Machines 2022, 10, 100. https://doi.org/10.3390/machines10020100

Tang, Q.R.; Lai, J.; Zhang, L.K.; Zhao, Q.Y.; Li, N.; Zou, H.W. A review on the research of flexible grasping technology based on space robotic arm. Shanghai Space 2019, 36, 111–119

[4]. K. Blanco, E. Navas, L. Emmi and R. Fernandez, "Manufacturing of 3D Printed Soft Grippers: A Review," in IEEE Access, vol. 12, pp. 30434-30451, 2024, doi: 10.1109/ACCESS.2024.3369493

Stano, G., Ovy, S.M.A.I., Edwards, J.R. et al. One-shot additive manufacturing of robotic finger with embedded sensing and actuation. Int J Adv Manuf Technol 124, 467–485 (2023). https://doi.org/10.1007/s00170-022-10556-x

Subramaniam V, Jain S, Agarwal J, Valdivia y Alvarado P. Design and characterization of a hybrid soft gripper with active palm pose control. The International Journal of Robotics Research. 2020;39(14):1668-1685. doi:10.1177/0278364920918918

[5]. R. Truby, R. Katzschmann, J. Lewis, D. Rus, "Soft Robotic Fingers with Embedded Ionogel Sensors and Discrete Actuation Modes for Somatosensitive Manipulation." IEEE RoboSoft, Apr 2019

[6]. Crooks, W., Vukasin, G., O'Sullivan, M., Messner, W., & Rogers, C. (2016). Fin Ray® Effect Inspired Soft Robotic Gripper: From the RoboSoft Grand Challenge toward Optimization. Frontiers in Robotics and AI, 3. https://doi.org/10.3389/frobt.2016.00070

Yang Y, Jin K, Zhu H, Song G, Lu H, Kang L. A 3D-Printed Fin Ray Effect Inspired Soft Robotic Gripper with Force Feedback. Micromachines (Basel). 2021 Sep 23;12(10):1141. doi: 10.3390/mi12101141.

Shan, X., & Birglen, L. (2020). Modeling and analysis of soft robotic fingers using the fin ray effect. The International Journal of Robotics Research, 39, 1686 - 1705.

[7]. Do, P.T.; Le, Q.N.; Luong, Q.V.; Kim, H.-H.; Park, H.-M.; Kim, Y.-J. Tendon-Driven Gripper with Variable Stiffness Joint and Water-Cooled SMA Springs. Actuators 2023, 12, 160. https://doi.org/10.3390/act12040160

[8]. Song, J., Feng, Y., Hong, Z., Zeng, S., Brannan, A. C., Song, X., & Tan, J. (2023). Octopus-Inspired adaptable soft grippers based on 4D printing: numerical modeling, inverse design, and experimental validation. Advanced Intelligent Systems, 5(8). https://doi.org/10.1002/aisy.202200384

[9]. Brown, E., Rodenberg, N., Amend, J., Mozeika, A., Steltz, E., Zakin, M. R., Lipson, H., & Jaeger, H. M. (2010). Universal robotic gripper based on the jamming of granular material. Proceedings of the National Academy of Sciences of the United States of America, 107(44), 18809–18814. https://doi.org/10.1073/pnas.1003250107

[10]. Festo (2009).BionicTripod with FinGripper. Available at: https://www.festo.com/rep/en_corp/assets/pdf/Tripod_en.pdf

[11]. Zapciu, ICmas

IMPROVING THE PERFORMANCE OF THE ORGANIZATION BY ANALYZING THE NONCONFORMITIES IN THE FIELD OF PLASTIC INJECTION

IORDACHE (MIHALCEA) Monica Ionica , Ghinea Mihalache

Faculty of Industrial Engineering and Robotics,
Specialization: Conception and Management in Productics,
Anul de studii: I,
e-mail: monica.mihalcea@stud.fiir.upb.ro; (Numai pentru autorul corespondent)

ABSTRACT: The paper addresses the structure of the process of continuous improvement and the implementation of a system of control, analysis and correction for all incidents recorded in the organization as nonconformities.
Starting from the injection process, presenting the description of the manufacturing stages, the improvement system, the optimization solutions chosen to adapt to the current market requirements, and, we have identified a management system that can be implemented in an organization to ensure continuous improvement of the core process and related ones.
I have detailed how to approach and implement a system based on collecting information on incidents, incident analysis and root cause identification, establishing preventive and corrective actions, tracking their implementation, and, monitor and evaluate the effectiveness of the improvements applied and manage and track the entire process so that it ensures the treatment of all incidents, without exception..

KEYWORDS: Plastics materials, analysis, causes, improvement, nonconformity.

1. Introduction

Plastics injection is a manufacturing process of parts, obtained by injecting molten granules into a mold. The melt cools and by solidification takes the form of the cavity in which it was injected.

In recent years, products made of plastic have grown due to the high productivity of the process, the versatility and potential to replace metal in many applications.

Plastic appeared as raw material at the end of the IX century (ebonite and celluloid). Technology developed slowly until the middle of the XX century when it began to grow. In 1944 the worldwide production of polymer resins, being used mainly in electrical applications, for insulation. The main groups of materials used today (polystyrene, PVC, polyolefin and polymethacrylate) were developed at industrial level before 1950.

Since the middle of the XX century, the development of plastics has taken a large scale, penetrating the majority of industries.

Plastics injection is used to produce goods such as packaging, auto parts and components, toys, storage containers, mechanical parts, components of medical installations and appliances, in electronics, and in medical devices, consumer goods, and even military applications.

The use of plastics in the automotive industry (industry whose development has driven the development of the entire world economy) has led to a decrease in vehicle mass, an increase in active and passive safety, the decrease in fuel consumption and emissions and major aesthetic improvements allowing for the flexible technology to shorten the development time of new models.

The plastic injection industry is in a constant evolution and improvement, this aspect assuming the fulfillment of the quality conditions and the specific requirements of the products made.

Although the injection process is apparently simpler than other processes based on other technologies, keeping product quality under control is a complex activity that requires staff involvement at all levels.

Achieving a high level of quality is a desideratum of all companies in the automotive industry being one of the fundamental conditions to novel on the market. The decrease in quality costs is also very important because it is related to the overall decrease in costs and thus to the increase in competitiveness.

The automotive industry is highly competitive. The demands of end customers are constantly growing and carmakers are struggling to attract customers through ever better offers materialized by reasonable prices, high-level characteristics of the products and the quality that the customer perceives by the reliability manifested by the vehicle and the degree to which he feels satisfied with the characteristics of the products.

In this context, the continuous improvement activity has a central place in any company in the automotive industry, its objectives are to permanently improve the quality of products and the overall results of the activity measured in the end by profitability and market share.

The process of continuous improvement achieved through the QRQC (Quick Response Quality Control) tool, has as starting point the identification of all nonconformities, the analysis, the realization, the implementation of a corrective/preventive action plan, the application of measures, the, monitoring results, getting improvements and using lessons learned.

In this paper I will present a way in which a system of continuous improvement is implemented to contribute to the achievement of the above mentioned objectives.

2. The current state of knowledge in the field

2.1. Plastics - introductory notions and areas of use [2], [3]

In recent years, products made from plastics have registered an important evolution in several industrial areas.

DEX defines plastic as a “synthetic product of organic, inorganic or mixed nature that can be easily processed into various objects, hot or cold, with or without pressure”. [1]

Plastics are materials that have the basic components of polymers. Apart from polymers, plastics also contain:

- Filling materials: fiberglass, wood flour, asbestos, talc;
- Plastics: high-boiling esters, increasing elasticity and reducing fragility.
- Stabilizers: antioxidants, photostabilizers to preserve properties during processing.

Masele plastice se pot utiliza în industrii precum:

- Automotive construction, for the realization of the appearance and technical parts of the car – dashboard, fence bars, filters, pipes, shields, interior panels, supports, shock absorbers, etc, handles, mirror housing, dashboard housing. A large part of these components have the role of Security
- Food industry, for packaging, boxes, cutlery, cylinders, jars
- Medico industry – pharmaceutical: syringes, sterile packaging, capsules, protective panels and components, appearance and functional medical equipment
- Consumer goods industry - toys, tables, chairs and other items, furniture
- Building materials - pipes, plates, gutters, insulating materials, sanitary products

There are a number of issues for which automotive manufacturers have adopted plastics processing technologies and products obtained through them and have designed and applied many plastic elements in the design and automobile structure:

- long service life of the vehicle,
- eliminating the risk of corrosion;
- reduction of the mass of motor vehicles;
- reducing fuel consumption and emissions
- the freedom to design the parts in different shapes and with varied textures,
- the potential for innovation and change,

- versatility in the integration of components,
- consistency, flexibility and recyclability,
- increase the level of safety
- increased comfort.

Current economic and environmental concerns make the production of fuel-efficient vehicles a high priority in the automotive industry.

Plastics of industrial importance are based on 30 – 40 different types of polymers, which are put on the market in about 13000 variants below about 25000 trade names.

Plastics used today form three large groups in terms of type of uses:

- plastics ("reachine") for general use, manufactured in large quantities (commodities): PVC, PE, PP, polymers based on styrene (PS, PS-HI)
- technical resins that have improved mechanical, electrical and thermal properties compared to resins for general use, in applications that require increased resistance to various stresses: PA, POM, PC, PET, PBT, PBT, ABS, ASA, PC+ABS, PBT+PC.
- high-performance resins that have very high resistance characteristics, especially in terms of behavior at very high temperatures or in the context of high mechanical stress: PPS, PSU, PEK. These materials successfully replace metal in applications that require very high resistance to mechanical, physico-chemical and thermal stresses.

From the point of view of the behavior of the chemical structure of the material, plastics fall into two categories:

- thermo-rigids, in which the chemistry of the material changes during processing, due to the application of pressure and temperature, so that the finished product is chemically different from the raw material and can no longer return to its original state from this point of view. This category includes bakelites, melamines, alkyds, artificial tires, etc
- thermoplastics are materials that have basically the same chemistry after and before processing. By grinding, regranulating and re-melting they can be reused, even if some of the properties are no longer the same. Examples of thermoplastics are: PS, Nylon, PE, PP, PVC, PC, PET and high-performance resins.

2.2. Injection into the mold

Injection into the mold (classical injection using plasticizing screw machines) is today the most widespread technology.

The plastic in the form of granules is inserted into a bowl and from there it reaches a heating cylinder where it is compressed, malaxed and heated by means of a screw.

This mechanical and thermal process provides a homogeneous paste that is driven by the rotating screw (screw) to the feeding point of the mold. The material injected under pressure passes through the machine's diuse and the mold's diuse and comes into contact with the closed mold and thermostat. The molten plastic material in contact with the mold walls takes its shape by cooling and solidification. The removal of the plastic product from the mold is carried out with the help of an ejector system (thrower package).

Phases of an injection cycle

1) The process begins with the mold closing phase, which has as parameters the mold closing pressures, the mold closing speeds and the mold closing strokes;

2) The advance phase of the injection unit, in which the material is pushed through the cylinder towards the mold, is characterized by the following parameters: the pressure of the injection unit, the, the

speed of advancement of the injection unit, the setting of the contact point the injection unit nozzle with the die nozzle;

3) The injection phase is the most important phase as it directly influences the quality level of the injected parts. The parameters initially set are not constant but evolve throughout the process. The injection pressure gradually increases from the zero point to the maximum set value (it is limited between 100-200 bar), the injection speed is set depending on the type of material used, the complexity of the part, and, thickness of the walls of the workpiece and the required level of quality of the workpiece surfaces. The control parameter of the injection phase is the injection time;

4) Maintaining phase. It is also an important phase as it directly influences the quality of the injected parts. This phase occurs from the moment the material filled the mold cavities until the cooling phase begins, preparing to expel the injected parts. The parameters characterizing this phase are the holding pressure and holding pressure time and switching point. These two parameters are set so as to ensure dimensional stability and uniform compaction of the injected parts. The control parameter is the material cushion and represents the volume of material left in front of the snail at the end of the maintenance phase. The material cushion is a constant parameter during the injection and maintenance phases.

5) Cooling phase. The control parameters of this phase are the mold temperatures and the cooling temperatures of the parts, which are set according to the plastic material used, the complexity of the part, and, quality requirements relating to the appearance of the surfaces of the workpiece;

6) Dosing and decompression phase. In this phase the snail of the injection unit performs the rotation movement. The control parameter is the dosage speed [rot/min] and is the parameter responsible for the quality of the plasticizing process. Decompression has as a control parameter the dosing time and represents the withdrawal of the snail to reduce the pressure in front of it after dosing;

7) Injection unit withdrawal phase up to adjusted position. The set-up parameters are the retracement stroke [mm], the retracement speed [s] and the withdrawal pressure [bar];

8) The opening phase of the mold. The first opening step is recommended to be slow, the second opening step is recommended to be fast to gain time and the last step is recommended to be done with a slow speed;

9) The last phase is the extraction phase of the injected part from the mold. In this cycle the parts are pushed out of the mold using the removal plate and the throwers (ejectors). The remaining pieces on the pitchers are automatically picked up by the gripper, with the help of the robot and are positioned on a moving conveyor that has the role of transporting the parts to the operator's area, depending on the degree of automation, directly into the packaging.. Upon completion of this last injection cycle, the mold closes and resumes the next cycle from phase one.

2.3. Complexity of the activity

In a company that has as main activity the production of plastic parts by injection, there are many activities in many fields, grouped by processes.

Customers require products that meet the technical requirements and have the required quality, low prices and short delivery times.

The company wants to meet customer requirements in terms of profitability, being interested in increasing sales and lowering costs. In this sea of complexity (see figure 1) there are always opportunities both positive (to improve performance and results) and negative (defective products, malfunctions in activities):

Defects can have different causes that need to be identified and eliminated by specific actions.

Dysfunctionalities can lead to unjustified machine and equipment stoppages or activities, or they can be directly fault-generating. And these must be observed, the causes must be identified and eliminated.

Before the occurrence of defects and malfunctions, preventive actions can be taken to reduce the damage due to defects and stationers.

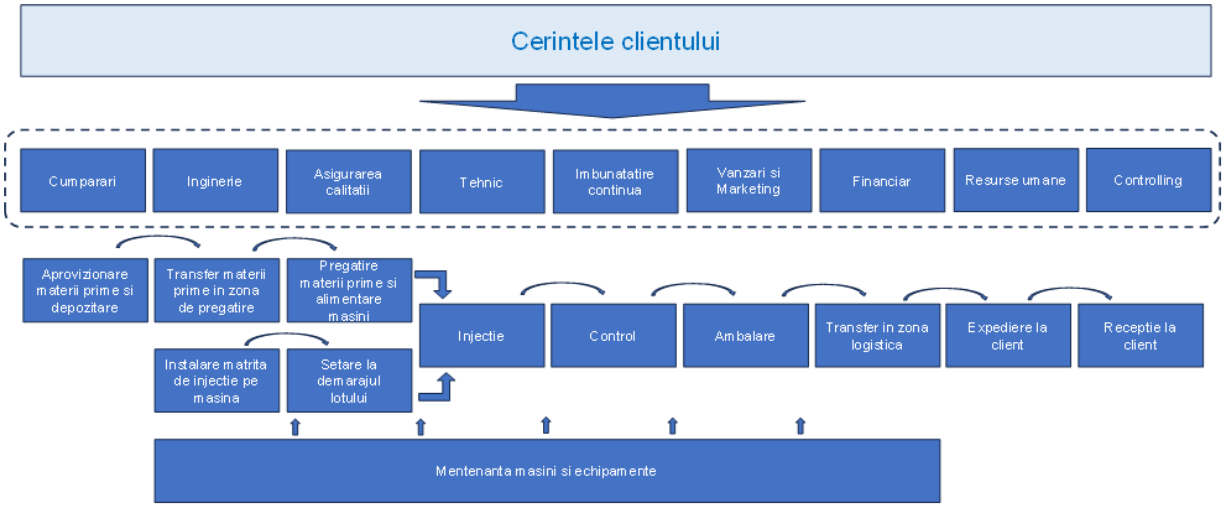

Fig.1 General structure of activities

Also, any factual situation, expressed by indicators such as: number of defects, percentage of defective parts, degree of loading of cars, the degree of availability of machinery, the rate of implementation of preventive maintenance, the ratio between preventive maintenance and corrective maintenance, the time of change of manufacture, etc – can be improved. In fact, any situation must be improved because competition in the field is constantly growing and customer requirements are also increasing.

In this context, the continuous improvement activity is positioned as a central mechanism for improving the performance in a company, through specific actions aimed at preventing the occurrence of defects and malfunctions, fast and definitive correction of defects and malfunctions, finding solutions to improve the situation and collecting and applying employee improvement ideas.

2.4. Description of the improvement process

The Continuous Improvement process according to IATF 16949:2016 and ISO 9001:2015 standards is carried out in the organization with the purpose of identifying all the weak points, loss and waste and aims to analyze and take actions that eliminate weaknesses and losses and improve performance for the benefit of the customer.

The improvement process procedure covers all non-conformities registered in the enterprise until the improvement study is carried out and minimized.

The stages of the improvement process are as follows:

1) The first phase integrated in the improvement process is the management analysis. In the Management Analysis carried out at the beginning of each year, the results of the performance objectives for the entire management system are presented, the objectives for the current year are set, the strategy and policy and quality objectives of the organization are presented. During this meeting, there are established actions with the role of improving the activity in each process integrated in the organization, as well as, and also are established actions that have the role of achieving the performances set by Top Management. As input data in the management analysis activity are considered the result of the global indicator on the degree of customer satisfaction, the stage of the actions from the previous analyses, and, results of performance objectives and indicators /each process per organization, nonconformities and corrective actions, results of audits, performance of suppliers, opportunities for improvement, Requirements IATF 16949. [5]. The conclusions of the Management Analysis are input data into the process of Continuous improvement. 2)

The second phase integrated in the process of continuous improvement is called Nonconformity and corrective action. [5]. During this phase, nonconformities are identified, are analyzed and corrective actions, immediate actions to eliminate or minimize nonconformity are established. The conclusions of this analysis are input data into the improvement process.

3) The third phase integrated in the improvement process Problem solving and Prevention/error removal.[5] In this phase, the corrective actions referred to in point two are evaluated from a technical and economic point of view, improvement opportunities are identified, optimization actions are established, preventive actions and anti-error solutions. The conclusions of this phase are input into the improvement process.

4) The fourth phase integrated in the process of continuous improvement are the results of internal audits. Internal audits are conducted according to the annual internal audit program Quality management system processes and Manufacturing Processes. In the audit process, a number of non-conformities classified by the auditor minor or major are identified, an action plan is drawn up to eliminate the identified non-conformities. The action plan is the entry into the process of continuous improvement.

5) Phase five integrated in the improvement process consists in issuing and implementing company employee suggestions. Each proposal is registered, analyzed in terms of applicability, technical and economic. The conclusion of the analysis is the entry date in the process of continuous improvement with the role of applying and monitoring the effectiveness after their implementation.

6) Phase number six integrated in the process of continuous improvement are Customer complaints and analysis of checks of falls in use. [5]. In this phase, customer reports are analyzed, corrective-preventive actions are identified, anti-error measures are identified, optimization measures are applied. The conclusions of this analysis are input data into the process of continuous improvement.

7) Phase Seven integrated into the process of continuous improvement [6] Improvement of products and services to meet requirements as well as address future needs and expectations. [6]. In this phase, possible actions to optimize internal processes are identified in order to identify solutions for customer satisfaction. The conclusions of this process are input data into the process of continuous improvement in order to monitor the improvement of the performance and effectiveness of the quality management system. [6]

3. Conclusions

Continuous improvement is a sure way to increase the competitiveness of companies. A company that does not rely on continuous improvement can only achieve success temporarily, followed by the degradation of results over time.

Factors – key success for implementing a system from the quest-end of castor, which is a constituency a solid base to be able to implement for the implementation of a high-quality castor system to implement a high-quality system:

- Commitment of organization management at all levels
- Changing the organizational culture to determine an appropriate organizational behavior that can perpetuate indefinitely the efforts of continuous improvement
- involvement of all employees in continuous improvement efforts
- Implementation of a simple but rigorous analysis system and integration of all departments in efforts to identify solutions
- Implementation of a rigorous system of tracking the way in which actions are implemented and the results obtained from this implementation.

4. Bibliography

[1] DEX online- https://dexonline.ro

[2] Ehrenstein, Gottfried W. – Polymeric Materials: Structure, Properties, Applications - Hanser Publications Inc. Cincinatti, 2001

[3] Michaeli Walter, Greif Helmut, Kretzshmar Gernot, Ehrig Frank - Training in Injection Molding - Hanser Gardner Publications Inc. Cincinatti, 2001

[4] Rees Herbert – Understanding Injection Molding Technology - Hanser Gardner Publications Inc. Cincinatti, 1994

[5] Cerinte IATF 16949:2016 – Standard al sistemelor de management al calității aplicabile sectorului automobile
[6] ISO 9001:2015 - Sisteme de management al calității – cerinte
[7] https://tervene.com/blog/quick-response-quality-control-qrqc;
[8] Cachon, Gerard si Terwiesch, Christian – Matching Supply With Demand, McGraw-Hill 2020
[9] David Rizzardo – How to Build a Culture of Continous Improvement – Chapter 6, Resistance, Demotivation and Motivation
[10] Robbins, Stephen P. and Judge, Timothy, A. – Essential of Organizational Behavior 14th Edition, Pearson
[11] Aoudia, Hakim and Testa, Quintin – Perfect QRQC Les Fondations – Maxima, Paris, 2011
[12] Stoica, Costin – Curs Kaizen – Document intern Delta Invest, 2024
[13] Imai, Masaaki – Kaizen, The Key To Japan's Competitive Success – McGraw Hill Publishing Company 1986.

AUTOMATING A GREENHOUSE USING AN ARDUINO PROGRAMMABLE CONTROLLER

NICOLAE Andrei-Ionut, IONESCU Paul-Iosif, Catalin Gheorghe AMZA

University: Facultatea de Inginerie Industriala si Robotica, Specialization: Industrial Engineering, Student Year: 1st, e-mail: paul_iosif.ionescu@stud.fiir.upb.ro

ABSTRACT: Our project was created to address a few main concerns regarding documentation, and assistance with the growth of different plant life. The main concerns our installation aims to correct are, addressing the issues that come with actively or automatically managing different crops, such as fruits or vegetables, medicinal plants, and flowering plants, monitoring the environmental conditions of development for any designated subject, and accommodating these factors in accordance with the user input. Said input is collected by our own, provided, Bluetooth-paired, MIT App Inventor application, which not only allows for adjustable metrics of light, temperature and soil moisture but provides regular measurements displayed in real time of temperature and moisture, which adds the benefit of constant monitoring through its associated user interface.

KEYWORDS: plant, Arduino, monitoring, Bluetooth, application.

1. Introduction:

Greenhouses play a vital role in modern agriculture, providing controlled environments for optimal plant growth regardless of external weather conditions. These enclosed structures allow farmers and gardeners to cultivate crops year-round, extending growing seasons and improving yield and quality. Central to the success of a greenhouse is its ability to maintain specific environmental conditions, including temperature, humidity, light levels, and ventilation. Effective control of these parameters is essential for maximizing plant health, growth, and productivity.

One accessible and cost-effective solution for greenhouse control is the use of programmable controllers, such as the Arduino Uno, an open-source microcontroller board based on the ATmega328P microcontroller. It features digital and analog input/output pins that can be easily programmed to interact with various sensors, actuators, and other electronic components. Arduino Uno boards are affordable, widely available, and user-friendly, making them an excellent choice for DIY greenhouse automation projects. With an Arduino Uno and various sensors and actuators, growers can develop custom control systems tailored to their specific needs.

Our plant monitoring system is a simple and efficient piece of technology, comprised of an Arduino UNO, breadboard (170x55mm / 400 holes), a few sensors (ultrasonic range finder, temperature sensor, humidity sensor, light sensor) a water pump, a light [1], a fan [2], an LCD monitor, 3 relays, and a Bluetooth transmitter, all working together to aid the plant in growing in a safe and harmonious environment.

2. Implementation of the project:

Thanks to its Bluetooth capabilities, the system can communicate with a smartphone app (see Fig. 1), through which the user can control its actions. The user can switch between an automatic and manual mode coded in our Arduino Software while also being able to see the temperature and soil moisture in real-time, calculated given the range detector of the water level (Eq. 1), and the dampness of the soil (Eq. 2).

$$W = h - (ts * 0.034 / 2) \tag{1}$$

$$mp = (1023 - x) / (1023 - 280) * 100 \tag{2}$$

Annotations and their meanings:

W – water level [cm];

h – the height of the water container [cm];

ts – window of time when the sensor is measuring the distance [ms];

mp – moisture percentage [%];

x – the registered resistance [Ω];

Fig. 1 MIT App Simulation

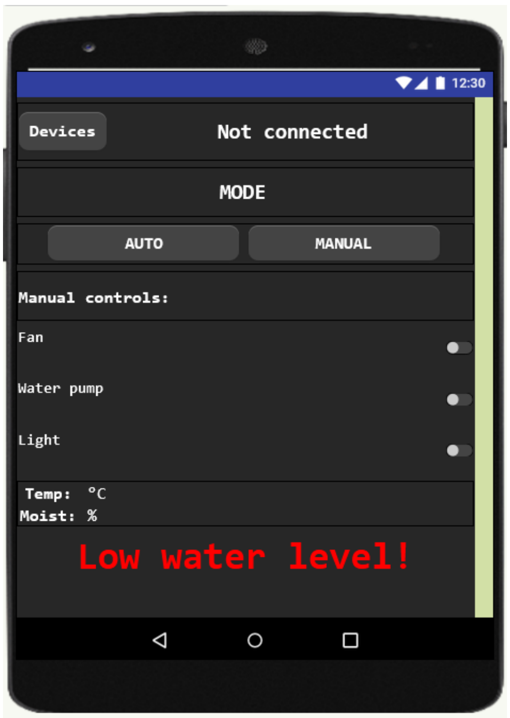

The Arduino UNO was programmed using its designated software, Arduino IDE 2.3.2 [3], while the smartphone application was constructed using MIT App Inventor [4], a high-level block-based visual programming language.

The code first checks if the boolean variable "case_auto" is false and the distance between the ultrasonic range finder and the water within the container in which the pump is submerged is less than 10 cm, indicating an optimal water level (see Fig. 2).

```
while(case_auto==false && distance<=10)
{
  Incoming_value=Serial.read();
 digitalWrite(trigPin,LOW);
  delayMicroseconds(2);
  digitalWrite(trigPin,HIGH);
  delayMicroseconds(10);
  digitalWrite(trigPin,LOW);
  duration = pulseIn(echoPin,HIGH);
  distance = duration * 0.034 / 2;
  lcd.setCursor(10,0);
  lcd.print("       ");
  Temperature();
  lcd.setCursor(0,1);
  lcd.print("M: ");
  lcd.print(Moisture_Percentage(moisture),1);
  lcd.setCursor(8,1);
  lcd.print(" %");
  float temp = DHT.temperature;

  Serial.print(temp);
  Serial.print("|");
  Serial.print(Moisture_Percentage(moisture));
  Serial.print("|");
  Serial.println(distance);
```

```
Serial.print(temp);
Serial.print("|");
Serial.print(Moisture_Percentage(moisture));
Serial.print("|");
Serial.println(distance);

if(Incoming_value == '0')
  digitalWrite(fan_relay, HIGH);
else if(Incoming_value == '1')
  digitalWrite(fan_relay, LOW);
else if(Incoming_value == '2')
  digitalWrite(light_relay, LOW);
else if(Incoming_value == '3')
  digitalWrite(light_relay, HIGH);
else if(Incoming_value == '4')
  digitalWrite(wpump_relay, HIGH);
else if(Incoming_value == '5')
  digitalWrite(wpump_relay, LOW);

  if(Incoming_value=='6')
  case_auto=true;

  delay(1000);
```

Fig. 2. Arduino code for Manual Mode

The code then calculates the distance once again through its distance equation (see Eq. 1), along with reading and printing the temperature and moisture values on the LCD monitor. It then sends to the receiving Bluetooth client (see Fig. 3).

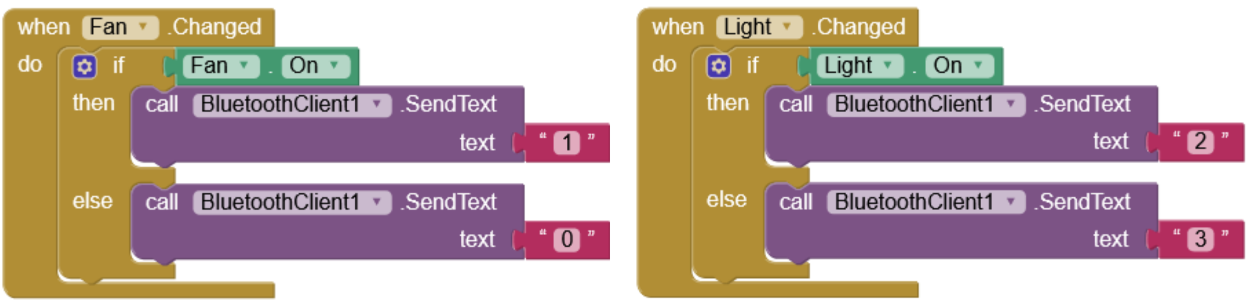

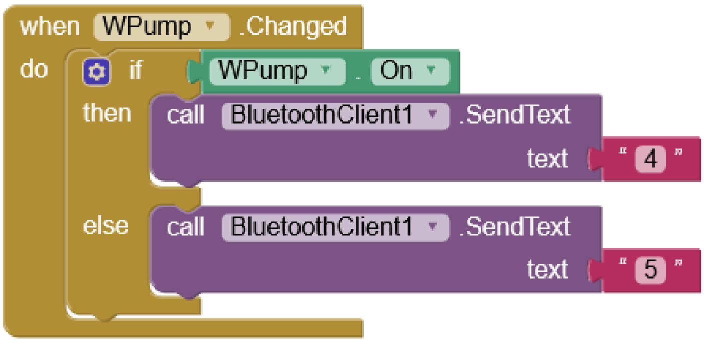

Fig. 3. MIT Bluetooth caller Block Diagram

The values of the smartphone app are to be displayed. In manual mode, the user has switches for manual control of the fan, light and water pump. Each switch sends a specific value for its on/off positions. The code checks for the received values and turns the relays connected to these components on or off. If the user switches to auto mode, the app will send the value 6 to the Arduino, making the boolean variable "case_auto" true. Thus, the logical condition for the manual mode is no longer valid, and the system will go into automatic mode.

This block of code within the MIT app displays the temperature, and moisture, and enables and disables the "Low water level!" warning message (see Fig. 4). First, a global list and a blank global input are created. Then, the code runs a loop that executes itself every other second. The code checks if the device is connected to the Arduino via Bluetooth and if it's receiving data then starts constructing the list, the elements of it being separated by the character "|", as shown in the provided block of code from the Arduino IDE app (see Fig. 1).

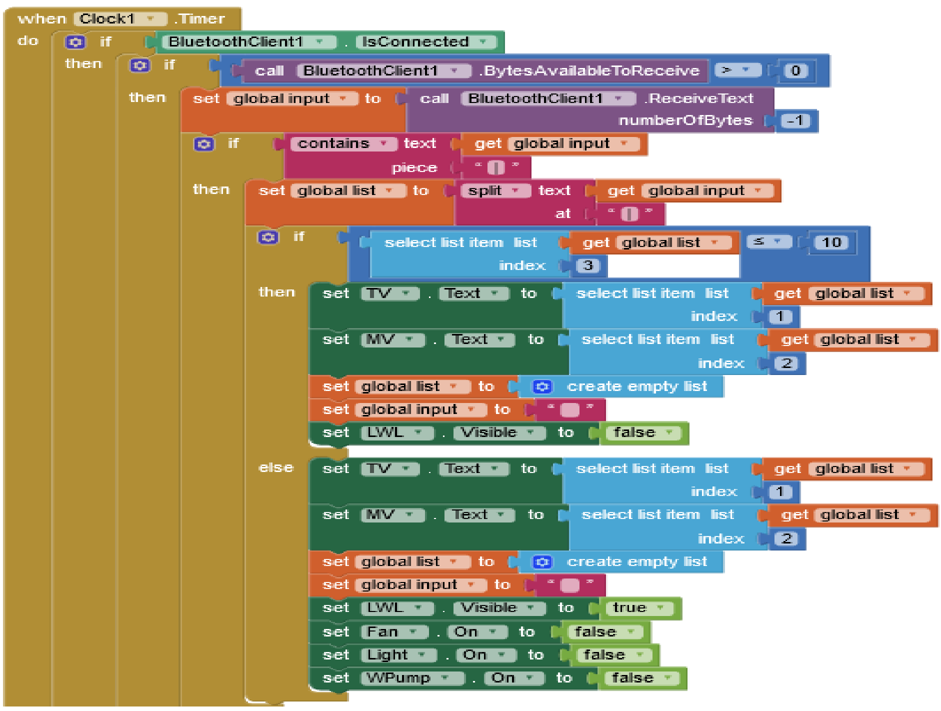

Fig. 4. MIT Info-Reciever/Announcer Block Diagram

The Arduino then sends 3 values that are included in the list (temperature, moisture, and distance between the ultrasonic range finder and water), the third one will not be displayed within the app, but it will be used to determine whether or not the water level is low by comparing it with a specified value. If the value of the distance is low, that means that the water's surface is close to the sensor, indicating optimal levels. In that case, the program will only display the temperature and moisture. If the value of the distance is high that means that the water level is low, in which case, apart from displaying the temperature and moisture, the app will also show a "Low water level!" warning and will not allow the user to operate the switches in any capacity.

3. Discussions and conclusions:

Currently, the project is in functional condition (see Fig. 5). The Arduino module and the breadboard are mounted on a plastic dish. The other components are contained in a box in which the plant sits. The code and app function accordingly, with little to no bugs or errors.

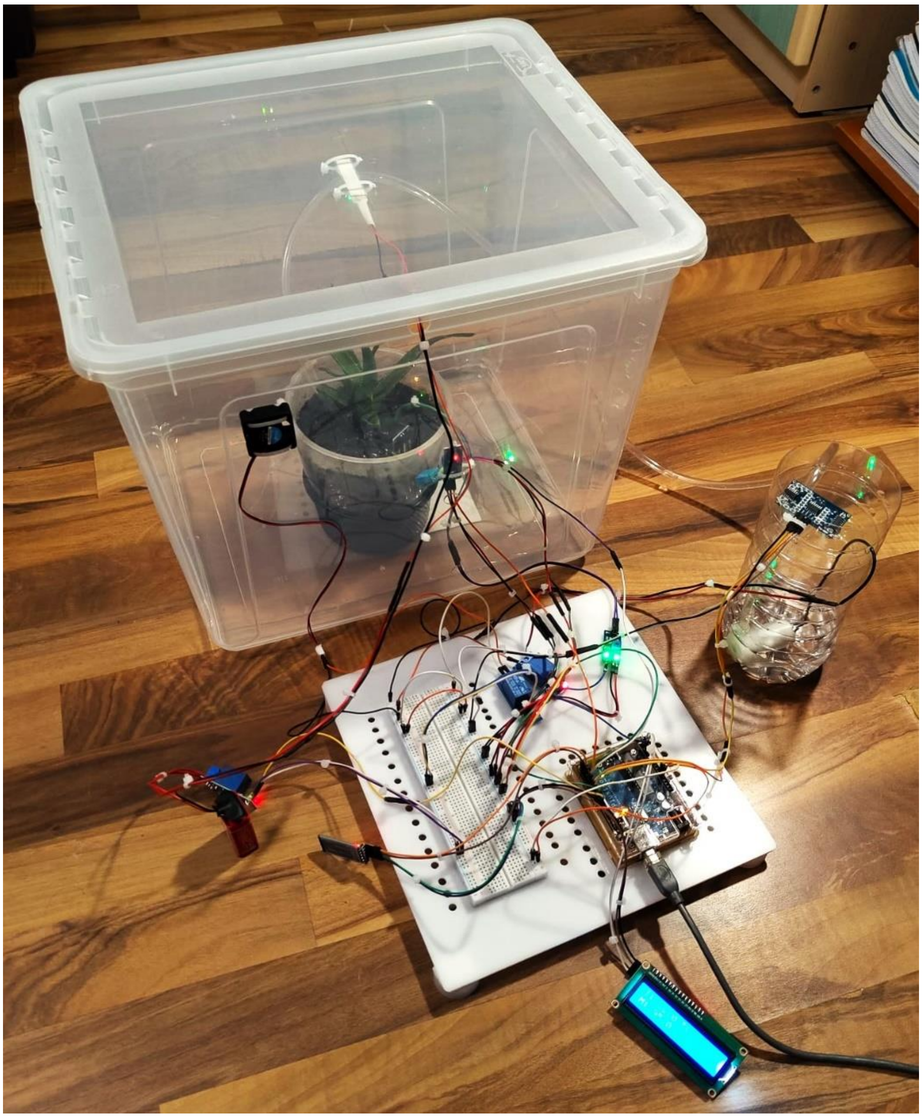

Fig. 5. Our physical prototype system

With regard to our project and research, we can conclude that our prototype could accommodate a plethora of different horticultural subjects, namely crops and gymnosperms, providing useful data as well as automatic maintenance through its Arduino code.

Even though the system functions adequately, it does suffer from a certain limitation: namely, the Arduino UNO's ability to provide adequate power to all the connected and consuming components. To solve this issue, we would need to use a separate power source for each element, which will solve the issue, whilst decentralizing the power distribution and complicating the system maintenance process.

Another improvement that can be brought to the system, is the integration of a database that contains the optimum parameters for different types of plants. With the help of this database, the user would be able to easily connect the system to a different plant and specify the new type of subject in the smartphone application, which automatically would fine-tune the humidity, temperature, and light level thresholds, so that the new plant can have a proper or even accelerated growth.

4. Bibliography:

[1]. Paradiso, R., and Proietti, S. (2022). Light-Quality Manipulation to Control Plant Growth and Photomorphogenesis in Greenhouse Horticulture: The State of the Art and the Opportunities of Modern LED Systems, J Plant Growth Regul 41, 742–780, ISSN 1435-8107;

[2]. Gijzen, H., Heuvelink, E., Challa, H., Marcelis, L.F.M., Dayan, E., Cohen, S. and Fuchs, M. (1998). HORTISIM: A MODEL FOR GREENHOUSE CROPS AND GREENHOUSE CLIMATE, Acta Hortic. 456, 441-450, ISSN 0567-7572;

[3]. Mark, G., (2016). Arduino Project Handbook: 25 Practical Projects to Get You Started, No Starch Press, ISBN-10 1593276907;

[4]. Karen, L., and Selim, T. (2022). Become an App Inventor: The Official Guide from MIT App Inventor: Your Guide to Designing, Building, and Sharing Apps, MITeen Press, ISBN-10 1536224081;

SMART DONOR BLOOD MIXING DEVICE

SÎRBULESCU Maria-Denisa, ȘELARU Carmen Cristina Ioana, STAN-IACOB Adrian, POMOHACI Bogdan, Marinela Nicoleta MARINESCU , Larisa BUȚU

Faculty of Industrial Engineering and Robotics, Specialization Robotics, Year of study: II, e-mail: denisa.srbulescu@yahoo.com

ABSTRACT: This article aims to present the designing an intelligent blood stirring device for donation centers. A donor blood mixing device is an essential device used during blood transfusions to ensure the proper handling of collected blood. This device measures and agitates the blood bag, preventing blood clot formation. By continuously mixing the blood with the anticoagulant solution within the bag, the device ensures that the anticoagulant is evenly distributed, maintaining the blood's viability and quality for transfusion.

KEYWORDS: blood, blood mixing device, blood coagulation, 3d printing, Arduino

1. Introduction

In the modern medical era, technological innovations play a crucial role in improving the efficiency and safety of medical procedures, with a significant impact on the field of blood donation. A key aspect of this process is the blood mixer, an innovative technology that plays a crucial role in the preparation and processing of donated blood. In Romania, only 1.7% of the population regularly donates blood, compared to a European average of 10%.

Blood transfusion is the process of transferring blood from one person (donor) into another person's blood vessels [1] Donated blood and its components (red blood cells, platelets, and plasma) enable a variety of important treatments that often make the difference between life and death. Blood transfusions are essential in the event of a serious accident or major surgery involving significant blood loss and are often necessary for cancer patients. Donated plasma, a component of blood, is also used to produce drugs such as immunoglobulins and clotting factors, which are essential for the treatment of certain serious inherited blood disorders such as hemophilia. Donated blood is used in many ways other than whole blood transfusions. Processing produces plasma, red blood cell concentrates, platelet concentrates, etc., each of which is used in specific cases in the provision of medical services.

Donating blood requires the collection of 450 ml of blood. This volume will be replenished in 24-36 hours and red cells in 6-8 weeks. [2] Blood is collected at body temperature, i.e. +37 °C. But to maintain its vital properties, it must be cooled to below +10 °C for transport and stored at refrigeration temperatures of about +4 °C until use. If blood is stored or transported outside these temperatures for a long period of time, it loses its ability to transport oxygen or carbon dioxide to and from tissues, respectively, at the time of transfusion. Other serious concerns include the risk of bacterial contamination if blood is exposed to high temperatures. Conversely, blood exposed to temperatures below freezing can suffer hemolysis and lead to a fatal transfusion reaction [3].

The blood mixing device is a device used to assist blood donors in avoiding blood clotting or clots in donor blood bags by placing blood bags in blood bag containers. The container containing the blood bag is then shaken using a motor found in the device. The blood bag shaking function is for the anticoagulant solution in the blood bag to mix with the blood from the donor. The solution in the bag is "Citrate Phosphate Dextrose Adenine Anticoagulant Solution (CPDA-1)". This solution is used to prevent blood clots or clotting from the donor while the blood is in the bag [1].

There are a variety of capacities available for bags used in donation: 250 ml, 350 ml, and 450 ml. The device developed by our team is designed for use with bags having a capacity of 450 ml. The device is equipped with an LCD screen that displays the weight of the bag, and when the optimal weight is reached, it signals by lighting up an LED.

The device is made using 3D printing technology and its components are fully engineered. 3D printing of devices has become an increasingly popular method in prototyping and manufacturing due to its flexibility and versatility. The 3D printing process enables the fast and efficient manufacture of complex parts, including custom medical devices. Using 3D printing technology, devices can be designed and manufactured quickly without the need for special tools or molds. This provides opportunities to tailor devices to specific user needs or individual application requirements. In addition, 3D printing also enables the design and functionality of devices to be optimized by rapidly iterating prototypes and testing concepts in an efficient and cost-effective way. Thus, 3D printing is a promising solution for device development and manufacturing, offering significant benefits in terms of time, cost, and product customization.

1.1 Blood mixer design

At the initial stage of designing the blood mixing device, our main objective was to create a simple but effective device that would facilitate the blood donation process. To achieve this goal, we started by making preliminary sketches of the blood-mixing device to outline the overall concept and structure of the device. Once we defined the desired designs, we moved on to 3D design of the parts using the Onshape app. This step allowed us to create detailed three-dimensional models to ensure the device would function correctly and identify any design issues before manufacturing.

Next, we generated complete 2D drawings, including dimensions, for use in the manufacturing process. This step was essential to ensure consistency and accuracy in the construction of each component of the device.

The blood mixing device is composed of multiple designed components, and one of the most important is its housing. The housing houses the tray drive system, which consists of a servo motor featuring a cam that moves the tray in a controlled and precise manner, allowing for efficient blood mixing. A scale consisting of a 1 kg load cell with an HX711 amplifier is used to monitor the blood quantity. The load cell is made of an aluminum alloy and can measure the change in electrical resistance as a function of strain (such as pressure or force) applied to the load bar, relating to it proportionally.
The tray is formed in two pieces to facilitate the printing process, it is also connected to the housing by a spindle and two grsc 607RS type bearings with dimensions 7x19x6 (dxDxB; inner diameter x outer diameter x width).

Fig. 1 Bearing type grsc 607RS

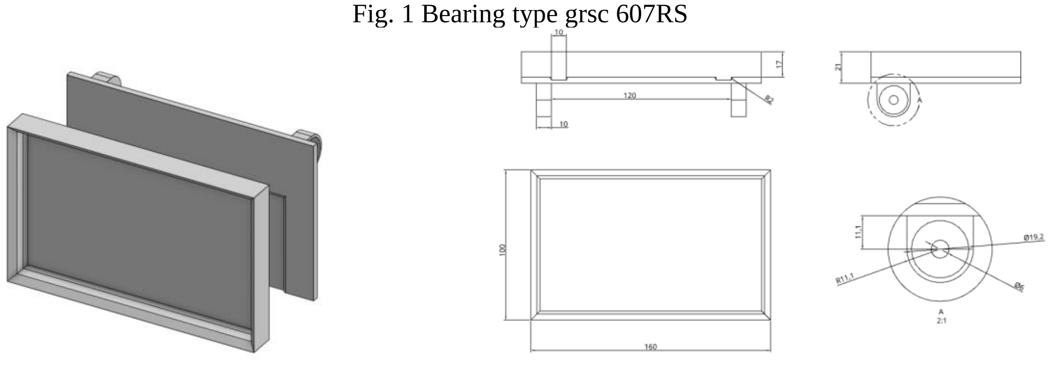

Fig. 2. 3D image (a.) and schematic diagram of the medical device tray (b.)

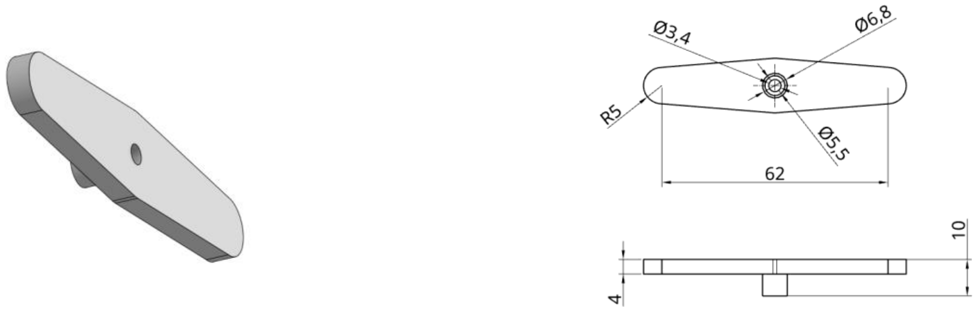

Fig. 3. 3D image (a.) and schematic diagram of the medical device cam (b.)

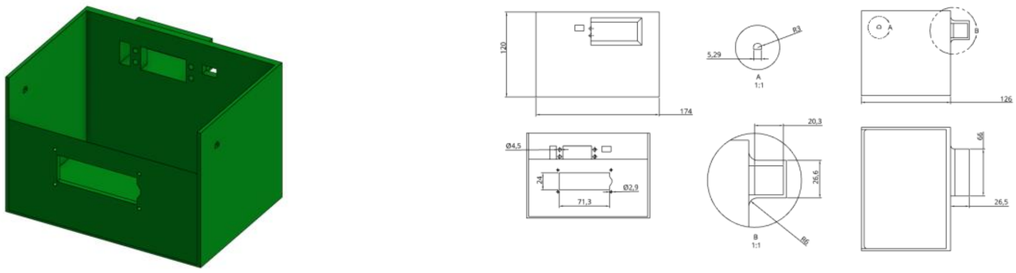

Fig. 4. 3D image (a.) and schematic diagram of the medical device case (b.)

Fig. 5. 3D image (a.) and schematic diagram of the main axis of the medical device (b).

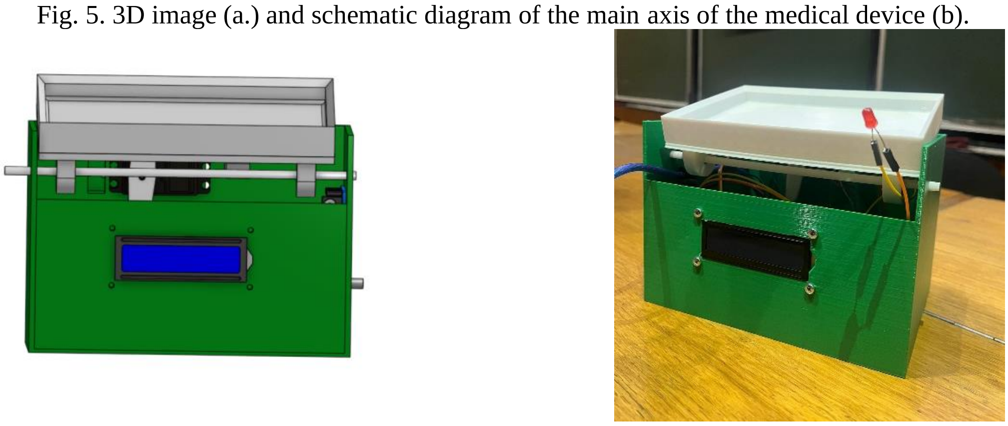

Fig. 6. Assembled blood mixing device.

1.2 3D printing of blood mixing device

To make the blood mixing device, we opted for 3D printing technology, which gave us the possibility to make a detailed three-dimensional model of the device.

To realize our concept, we used the Sovol SV06 3D printer, known for its reliable performance and print quality. This printer uses molten plastic filament, building the object layer-by-layer. With a generous printing area of 300mm x 300mm x 340mm, the printer was able to produce the necessary components for our device.

For materials, we chose PLA+ filament, known for its durability and resistance to impact and abrasion. PLA+ is a PLA-based product, modified to have better adhesion between layers, thus providing a stronger structure. [4] We set the extrusion temperature at 210°C, with a bed temperature of 60°C and a printing speed of 200 mm/s to ensure both quality and efficiency of the process. The total printing time was approximately 72 hours, and the result was a series of high-quality components with sufficient accuracy to assemble the prototype blood-mixing device.

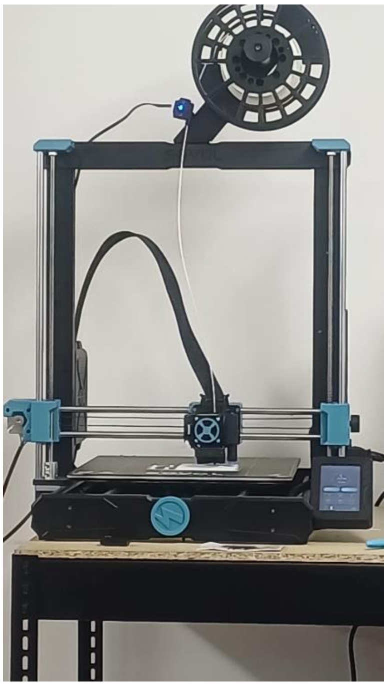

Fig. 7. Sovol SV06 3D printer used to print the component parts of the blood mixing device

These printed components were then assembled and tested to verify the correct operation of the device.

Fig. 8. Printing process of blood mixing device parts

1.3 Programming the blood mixing device

To operate the device, we opted to use an Arduino Uno board, known for its ease of use. This Arduino board is connected to an MG996R servo motor and a 1kg load cell equipped with an HX711 amplifier. Thus, we have the ability to effectively control and monitor motion and weight within the device.
User interaction and information display is via an LCD screen, which provides an intuitive and easy-to-understand interface. This configuration allows the user to observe and monitor the amount of blood collected in real-time.

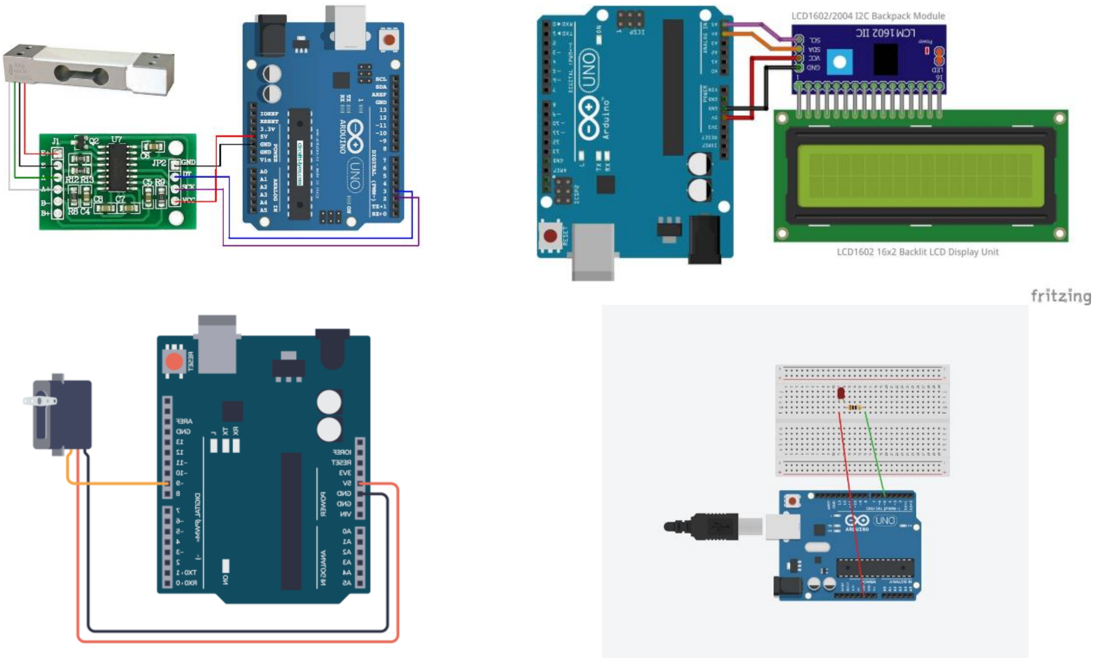

Fig. 9. Making electrical schematics for the blood mixing device

The code was made in Arduino IDE, a special software for programming Arduino boards. This code makes the tray loaded with a bag of blood move at a constant speed until it reaches a weight of 450 ml. At this point, the movement of the motor stops, and the user will be informed by signaling that this preset weight has been reached, which is done by lighting an LED. The weight is constantly displayed on the LCD screen, providing real-time monitoring of the process.

```
sketch_may09a §
#include <Wire.h>
#include <LiquidCrystal_I2C.h>
#include "HX711.h"
#include <Servo.h>

#define DOUT_PIN  3
#define CLK_PIN   2

#define I2C_ADDR    0x27
#define LCD_COLUMNS 16
#define LCD_ROWS    2

LiquidCrystal_I2C lcd(I2C_ADDR, LCD_COLUMNS, LCD_ROWS);
HX711 scale;
Servo motorServo;

void setup() {

  lcd.init();
  lcd.backlight();

  scale.begin(DOUT_PIN, CLK_PIN);

  scale.set_scale(1000.0);
  scale.tare();

  lcd.setCursor(0, 0);
  lcd.print("Greutate: ");
  pinMode(7,OUTPUT);
  motorServo.attach(9);

}
void loop() {
  motorServo.write(90);
  delay (3000);

  float weight = scale.get_units(10);
  weight=abs(weight);

  lcd.setCursor(0, 1);
  lcd.print("          ");
  lcd.setCursor(0, 1);
  lcd.print(weight);
  lcd.print(" g");
  if (weight > 150)
  {
    digitalWrite(7,HIGH);
```

```
sketch_may09a §
LiquidCrystal_I2C lcd(I2C_ADDR, LCD_COLUMNS, LCD_ROWS);
HX711 scale;
Servo motorServo;

void setup() {

  lcd.init();
  lcd.backlight();

  scale.begin(DOUT_PIN, CLK_PIN);

  scale.set_scale(1000.0);
  scale.tare();

  lcd.setCursor(0, 0);
  lcd.print("Greutate: ");
  pinMode(7,OUTPUT);
  motorServo.attach(9);

}
void loop() {
  motorServo.write(90);
  delay (3000);

  float weight = scale.get_units(10);
  weight=abs(weight);

  lcd.setCursor(0, 1);
  lcd.print("          ");
  lcd.setCursor(0, 1);
  lcd.print(weight);
  lcd.print(" g");
  if (weight > 150)
  {
    digitalWrite(7,HIGH);
    motorServo.detach();
  }
  else
  digitalWrite (7,LOW);
  delay(1000);


  motorServo.write(50);
  delay(3000);

}
```

Fig. 10. Blood mixing device program

1.4 Conclusions

The blood mixing device is a precise solution to ensure constant agitation of blood bags and prevent clotting. This device facilitates the blood donation process by providing continuous monitoring of the amount of blood in the bag. Useful in hospitals and blood donation centers, this device provides valuable support to nurses.

Potential improvements could include the implementation of a blood flow monitoring solution to prevent blockages or other abnormalities. Monitoring pulse, heart rate, and glucose levels could also bring additional benefits. A second change could be the implementation of an interactive interface allowing users to choose the type of blood bag (250 ml, 350 ml, 450 ml), blood group, and Rh

2. Bibliography

[1]. C.B Putra, H. G. Ariswati, S. Sumber, M. Zahar (2020) ”*Automatic Blood Collection and Mixer in a Blood Transfusion System Equipped with Barrier Indicators* ”, volum 2, pages 60-67 https://doi.org/10.35882/ijeeemi.v2i2.1 (accessed on 21.04.2024)

[2]. https://www.reginamaria.ro/articole-medicale/donarea-de-sange-tot-ce-trebuie-sa-stii (accessed on 21.04.2024)

[3]. http://nbtc.naco.gov.in/assets/resources/training/8.pdf (accessed on 21.04.2024)

[4]. https://zyx3d.ro/produs/esun-pla-1-75-green-1kg/ (accessed on 21.04.2024)

[5]. *** *Bearing type grsc 607RS* https://www.emag.ro/rulment-premium-607-2rs-fag-607-2rs-fag/pd/DQ8V1DMBM/?cmpid=101317&utm_source=google&utm_medium=cpc&utm_campaign=DSA_Electrocasnice_mari_MDA__Desktop&utm_content=118943336809&gad_source=1&gclid=EAIaIQobChMIvK30xeuyhgMVRZGDBx3_DjDAEAAYASAAEgKeuPD_BwE (accessed on 21.04.2024)

[6]. *** *Making electrical schematics for the blood mixing device* https://www.build-electronic-circuits.com/arduino-servo-motor/ (accessed on 21.04.2024)

[7].*** *Making electrical schematics for the blood mixing device* https://images.app.goo.gl/Rk4RKTRbcAHjFbYG7 (accessed on 21.04.2024)

[8].*** *Making electrical schematics for the blood mixing device* https://images.app.goo.gl/MUik5AfCXuwkLekM6 (accessed on 21.04.2024)